Downloaded from orbit.dtu.dk on: May 03, 2024

DTU Library

Interspecies between Bacillus subtilis and Pseudomonas

Lyng, Mark

Publication date:
2023

Document Version
Publisher's PDF, also known as Version of record

Link back to DTU Orbit

Citation (APA):
Lyng, M. (2023). *Interspecies between Bacillus subtilis and Pseudomonas*. DTU Bioengineering.

General rights
Copyright and moral rights for the publications made accessible in the public portal are retained by the authors and/or other copyright owners and it is a condition of accessing publications that users recognise and abide by the legal requirements associated with these rights.

- Users may download and print one copy of any publication from the public portal for the purpose of private study or research.
- You may not further distribute the material or use it for any profit-making activity or commercial gain
- You may freely distribute the URL identifying the publication in the public portal

If you believe that this document breaches copyright please contact us providing details, and we will remove access to the work immediately and investigate your claim.

Interspecies interactions between *Bacillus subtilis* and *Pseudomonas*

Mark Lyng

PhD thesis
July 2023

Bacterial Interactions and Evolution group
Department of Biotechnology and Biomedicine
Technical University of Denmark

Main academic supervisor
Professor Ákos T. KOVÁCS
Technical University of Denmark
Department of Biotechnology and Biomedicine

Co-academic supervisor
Professor Lars JELSBAK
Technical University of Denmark
Department of Biotechnology and Biomedicine

Chair of Assessment committee
Senior Scientist Claus STERNBERG
Technical University of Denmark, DK
Department of Biotechnology and Biomedicine

Assessment committee member
Associate Professor Mette BURMØLLE
University of Copenhagen, DK
Department of Biology

Assessment committee member
Research Director Marc ONGENA
Liége University, BE
Gembloux Agro-Bio Tech

Table of Contents

Preface

This PhD thesis was submitted as partial fulfilment of the requirements to obtain a PhD degree from the Technical University of Denmark (DTU). The work described in this thesis was carried out from August 2020 to August 2023 in the Bacterial Interactions and Evolution group at the Department of Biotechnology and Biomedicine, DTU.

The project also included a five-month external stay supervised by Associate Professor Scott Rice at the Singapore Centre for Environmental Life Sciences Engineering, Nanyang Technological University, Singapore.

The Ph.D. project was supervised by Professor Ákos T. Kovács, co-supervised by Professor Lars Jelsbak and funded by a DTU Alliance Strategic Partnership PhD fellowship.

Mark Lyng
Kgs. Lyngby, July 2023

Acknowledgements

With a project like a PhD, one stands on the shoulders of giants.
Not only because science is advanced by the combined effort of all scientists, but also because it is near impossible to undertake a journey, like the Ph.D., alone. Therefore, I would like to start this thesis by expressing my gratitude to the giants whose shoulders I have stood on.

My deepest gratitude to my supervisor Ákos T. Kovács for giving me the opportunity to do this Ph.D. and to develop scientifically, professionally, and personally. The last three years have taught me so much, and I now feel just a little farther to the right on the Dunning-Kruger curve.

Thank you to everyone who has participated in the scientific work performed as part of my project. Your insights have helped dramatically increase the robustness of our shared publications. Special thanks go to Morten Schostag, Morten Hansen, and Carlos Lozano-Andrade who have continuously made themselves available for discussions and helped reassure me about my science.

Thank you to current and former members of the BIE group. For providing a solid work environment with plenty of room to have fun, and to my students for being willing to learn and for teaching me heaps in return. Have a great time in Leiden.

Thank you to the Hacker Crew from Odense for loving my plots and (probably, secretly) hating my coding. You are all responsible for at least one third of my thesis.

Thank you to Flemming, Nikolaj, and ”Videnskabeligt Udfordret” for providing me with a breath of fresh air at least once a week, and letting me deep-dive into subjects completely outside of my usual sphere of interests. Eel testicles, radioactive humans, unethical primate experiments, and a good dose of accordion are largely the reason why I was able to keep going when times were tough.

The biggest thank you in the entire world to my family. Your support has been so extremely important, and I am eternally grateful, also that most of you have stopped asking what a Ph.D. is, and why I would want to keep studying after having finished my studies. Thank you to Katja and Mikkel for ice cream and champagne, to Dan and Tenna for beer and late-night discussions, to Heidi and Bram for homemade meals and a spot on your bench, to Maria, Line, and Mikkel for quips and banter, and to mom, Mogens, dad, and Anni for warmth and hospitality.

But most of all to Helene, the love of my life and the coming mother of my child. What you have had to endure for me to finish my degree, I would not wish upon my worst enemy. Still, you have been a rock and your encouragement has been invaluable. I cannot wait to start the next chapter of our lives together.

Abstract

Most of the biomass on Earth is comprised of microorganisms which shape ecology as we know it. Bacteria literally form mountains and determine the fates of living beings. But they also lend themselves to biotechnological exploitation. Particularly plant-growth promoting rhizobacteria carry the potential to alleviate hunger and environmental pollution from synthetic fertilizer and pesticides. Strains from the *Bacillus* and *Pseudomonas* genera have shown great promise in this field, and there is an increased interest in developing mixed-species consortia to attain synergistic biostimulation. However, the information on intermicrobial interactions between *Bacillus* spp. and *Pseudomonas* spp. is currently sporadic and unstructured, and despite both genera being environmentally ubiquitous and often co-isolated, there is no clear consensus on their compatibility. The purpose of this PhD has been to bridge this gap. We wanted to better understand what happens when members of these two genera come into contact and whether their interactions can be predicted from their taxonomy.

To structure the current information on *Bacillus* and *Pseudomonas* ecology, we conducted a review of the available literature on pairwise interactions. Most often interactions were found reported as negative, mediated by the production of bioactive secondary metabolites. We also concluded that the available information is too sporadic to infer interactions patterns from. Therefore, we screened a collection of 720 *Pseudomonas* soil isolates for their impact on *Bacillus subtilis* pellicle formation. With this study, we found that interactions between *B. subtilis* and fluorescent pseudomonads followed similar ecological rules as for other organisms. Interactions became negative as medium richness was reduced. However, we also demonstrated that we could predict the fate of *B. subtilis* in coculture from *Pseudomonas* taxonomy. *Pseudomonas protegens* proved a strong inhibitor of *B. subtilis* due to the production of the antimicrobial 2,4-diacetylphloroglucinol, while *Pseudomonas lini* could increase pellicle production in dilute medium.

We found a conserved negative interaction mediated by the presence of the *B. subtilis* siderophore bacillibactin, and thus investigated the molecular mechanism behind this interaction. We found that *B. subtilis* could restrict the growth of phytopathogenic *Pseudomonas marginalis* and cause a down regulation of secondary metabolism but only when producing its primary siderophore. The loss of bacillibactin production conferred an advantage to *P. marginalis* and

reversed the interaction. We hypothesized this interaction to be an iron tug-of-war between bacillibactin and the *Pseudomonas* siderophore pyoverdine.

This thesis provides a structured collection of interactions between bacilli and pseudomonads and contributes novel insight to how *B. subtilis* interacts with plant-associated pseudomonads. I present several interactions that are conserved intraspecifically, but also interspecifically across *Pseudomonas* species. Future work could build further on these findings and determine the degree of conservation and their implications for applied agricultural consortia.

Resumé

Det meste af jordens biomasse består af mikroorganismer, der danner økologi som vi kender det. Bakterier bygger bogstaveligt talt bjerge og bestemmer levende væseners skæbner. Men de repræsenterer også et stort bioteknologisk potentiale. Særligt plantefremmende rodbakterier bærer på muligheden for at afhjælpe sult og miljøforurening fra syntetiske gødninger og pesticider. Stammer fra slægterne *Bacillus* og *Pseudomonas* har vist stort potentiale inden for dette felt, og der er en øget interesse i at udvikle blandede artskonsortier for at opnå synergetisk biostimulering. Informationen om intermikrobielle interaktioner mellem *Bacillus* spp. og *Pseudomonas* spp. er dog i øjeblikket spredt og ustruktureret, og selvom begge slægter er miljømæssigt almindelige og ofte isoleres sammen, er der ikke en klar konsensus om deres kompatibilitet. Formålet med denne ph.d. har været at bedre forstå denne kompatibilitet. Vi ville vide, hvad der sker, når medlemmer af disse slægter kommer i kontakt, og om deres interaktioner kan forudsiges ud fra deres taksonomi.

For at strukturere den nuværende information om deres økologi gennemgik vi den tilgængelige litteratur om parvise *Bacillus*-*Pseudomonas*-interaktioner og fandt, at de fleste rapporterede interaktioner er negative, medieret af produktion af bioaktive sekundære metabolitter. Vi konkluderede også, at den tilgængelige information er for ustruktureret til at udlede interaktionsmønstre fra. Derfor screenede vi en samling af 720 *Pseudomonas*-jordisolater for deres indvirkning på *Bacillus subtilis*-pellikeldannelse. Med denne undersøgelse fandt vi, at interaktioner mellem *B. subtilis* og fluorescerende pseudomonader fulgte lignende økologiske regler som andre organismer. Interaktioner blev negative, som mediets koncentration blev reduceret. Vi demonstrerede også, at vi kunne forudsige *B. subtilis* skæbne i blandet kultur ud fra taksonomien af *Pseudomonas*. *Pseudomonas protegens* viste sig at være en stærk hæmmer af *B. subtilis* på grund af produktionen af det antimikrobielle 2,4-diacetylphloroglucinol, mens *Pseudomonas lini* kunne øge pellikelproduktionen i fortyndet medie.

Vi fandt en konserveret negativ interaktion medieret af tilstedeværelsen af *B. subtilis*-sideroforen bacillibactin, og undersøgte derfor den molekylære mekanisme bag denne interaktion. Vi fandt, at *B. subtilis* kunne begrænse væksten af en plantepatogen *Pseudomonas marginalis* og forårsage en nedregulering af sekundær metabolisme, men kun når den producerede sin primære siderofor. Tabet af bacillibactin-produktion gav *P. marginalis* en fordel og vendte

interaktionen. Vi hypoteserede, at denne interaktion er en jern-tovtrækning mellem bacillibactin og *Pseudomonas*-sideroforen pyoverdin.

Denne afhandling leverer en struktureret samling af interaktioner mellem baciller og pseudomonader og bidrager med ny indsigt i, hvordan *B. subtilis* interagerer med planteassocierede pseudomonader. Jeg præsenterer adskillige interaktioner, der er konserveret intraspecifikt, men også interspecifikt på tværs af *Pseudomonas*-arter. Fremtidige studier kunne bygge videre på disse fund og bestemme graden af bevarelse og deres implikationer for anvendte landbrugskonsortier.

Scientific work included in this thesis

Study 1 – Mark Lyng, Ákos T. Kovács, Microbial ecology: Metabolic heterogeneity and the division of labor in multicellular structures, *Current Biology* 2022; 32:14, R771-R773, https://doi.org/10.1016/j.cub.2022.06.008

Study 2 – Mark Lyng, Ákos T. Kovács, Frenemies of the soil: *Bacillus* and *Pseudomonas* interspecies interactions, *Trends in Microbiology* 2023; 31:8, 845-857, https://doi.org/10.1016/j.tim.2023.02.003

Study 3 – Mark Lyng, Birta Þórisdóttir, Sigrún H. Sveinsdóttir, Morten L. Hansen, Gergely Maróti, Lars Jelsbak, Ákos T. Kovács, Taxonomy of *Pseudomonas* spp determines interactions with *Bacillus subtilis*, to be submitted 2023; deposited to *bioRxiv* https://doi.org/10.1101/2023.07.18.549276

Study 4 – Mark Lyng, Johan P. B. Jørgensen, Morten D. Schostag, Scott A. Jarmusch, Diana K. C. Aguilar, Carlos N. Lozano-Andrade, Ákos T. Kovács, Competition for iron shapes metabolic antagonism between *Bacillus subtilis* and *Pseudomonas*, *in review at ISME Journal* 2023; deposited to *bioRxiv* https://doi.org/10.1101/2023.06.12.544649

Scientific work not included in this thesis

Jonathan Joseph-Spaulding, Thøger J. Krogh, Hannah C. Rettig, **Mark Lyng**, Mariam Chkonia, Silvio Waschina, Simon Graspeuntner, Jan Rupp, Jakob Møller-Jensen, Christoph Kaleta, Recurrent Urinary Tract Infections: Unraveling the Complicated Environment of Uncomplicated rUTIs, *Frontiers in Cellular Infection Microbiology* 2021; 11:562525, https://doi.org/10.3389/fcimb.2021.562525

List of Abbreviations

ABC	ATP-binding cassette
ACP	Acyl carrier protein
AT	Acyl transferase
BB	Bacillibactin
BGC	Biosynthetic gene cluster
BSM	Bioactive secondary metabolites
CLP	Cyclic lipopeptide
DAPG	2,4-diacetylphloroglucinol
DH	Dehydrogenase
DHB	2,3-dihydrobenzoic acid
EPS	Exopolysaccharide
ER	Enoyl reductase
KB	King's B
KR	Ketoreductase
KS	Ketosynthase
MS	Mass spectrometry
NRP	Non-ribosomal peptide
NRPS	Non-ribosomal peptide synthetase
PCP	Peptidyl carrier protein
PGPR	Plant-growth promoting rhizobacteria
PK	Polyketide
PKS	Polyketide synthase
TE	Thioesterase
WT	Wild Type

Chapter 1 – General Introduction

Earth houses an incredible variety of living organisms. And while it may seem like large, complex animals make up most of this variety, their numbers pale in comparison to microbes [1]. Though the actual abundance is debated [2, 3], there is no doubt that an enormous part of the biomass of our planet is made up of fungi, bacteria, archaea, and protists. Quite early after the discovery of microbes and the acknowledgement of their diversity, it became clear that many natural processes are driven by their metabolism. Cyanobacteria terraformed the early Earth by converting carbon dioxide to oxygen [4], plants require nitrogen fixed by bacteria [5], and in recent years, the role of microbes in human development has expanded drastically [6]. Thus, all organisms on the planet are undeniably affected by the functional outcomes of microbial interactions. Intraspecific, interspecific, and interkingdom interactions are the foundations of ecology, driven by genetics and physiology as well as abiotic environmental factors [7]. Understanding these interactions allows us to link microbial community composition to function and provides a framework for predictions.

In this thesis, I specifically concentrate on plant-growth promoting rhizobacteria (PGPR) which are involved in biocontrol and biostimulation of plant species through interactions with their host and with neighboring microbes in the rhizosphere (i.e., the soil surrounding plant roots) [8]. These microbes have the potential to aid human efforts to sustainably feed our growing population, by acting as biofertilizers and biopesticides. With synthetic fertilizers, nitrogen and phosphorous are not efficiently fixed in the soil [9], but are washed away with agricultural runoff, accumulating in water bodies, and reducing biodiversity [10]. Similarly, the current generation of pesticides persist in the environment, reaching drinking water storages and eventually households [11]. Pesticide exposure has been associated with reduced fertility in both men and women [12, 13] in addition to several molecules being regarded as carcinogenic to humans [14]. Still, bacterial products are encountering significant challenges in substituting conventional products due to legislations and ineffective marketing, but also product efficacy and consistency [15].

As with other functional outcomes, efficacy here is tightly related to microbial interactions. Microbes may be outcompeted when applied to soil [16], their target molecule may be degraded through higher-order interactions [17], and signal molecules may alter their metabolic profile [18]. To address some of these problems, this PhD thesis has investigated the intermicrobial interactions between two widely studied PGPR genera: *Bacillus* and *Pseudomonas*. Members

of these genera are strongly associated with the plant rhizosphere and are often co-isolated [19, 20]. They are also the basis for many marketed PGPR products [21] and interspecies combinations have been tested on multiple occasions for their influence on plant health and growth [20]. Still, little consensus exists on the relationship between bacilli and pseudomonads, and thus, it is currently difficult to predict outcomes of cocultures based on these organisms.

Aim of study

The purpose of this PhD has been **to elucidate interspecific interactions between members of the genera *Bacillus* and *Pseudomonas* in a pairwise context**. Emphasis has been placed on plant-associated fluorescent pseudomonads and *Bacillus subtilis*. Some microbial systems develop emerging properties from their associated proto multicellularity resulting in metabolic heterogeneity, and we initially speculated if this could be the case for co-existing bacilli and pseudomonads. Thus, in **Study 1**, we discuss a recent paper in the context of metabolic heterogeneity in biofilms. With this discussion, I gained insight into complex net-positive interactions, providing a basis for the first scientific question of the PhD:

What is currently known about Bacillus-Pseudomonas interactions?

This question was investigated in **Study 2**, a literature review of studies coculturing members of *Bacillus* and *Pseudomonas* together either pairwise or in communities under varying conditions. Here, I revealed that most reported interactions are negative and driven by the potential of each participant to produce bioactive secondary metabolites (BSMs) through amensalism or competition.

However, though some high-quality manuscripts of *Bacillus-Pseudomonas* interactions do exist, they are performed with emphasis on one or a few species pairs. We believed the literature to contain too few interactions to resolve interaction context-dependency and were unable to define a general phylogenetic pattern. Thus, a clear question emerged from this literature review:

Can taxonomy predict Bacillus-Pseudomonas interactions?

Study 3 addresses this question through a medium-throughput screening of pairwise interactions between *B. subtilis* and 720 soil-isolated fluorescent pseudomonads. We did find a

predictor in taxonomy and identified a molecular determinant for *Pseudomonas*-mediated inhibition of *B. subtilis*. **Study 3** also established several negative interactions, for which the mechanisms are unclear. In **Study 4**, one such interaction between *B. subtilis* and potentially phytopathogenic *Pseudomonas marginalis* was investigated thoroughly and discovered to be caused by competition for iron which ultimately results in inhibition of *P. marginalis* secondary metabolism.

Thesis outline

The thesis is divided into in five chapters, where the opening **Chapter 1** – General Introduction provided a general introduction to microbial ecology and *Bacillus* and *Pseudomonas* in plant biocontrol, as well as outlining the scientific questions investigated in this thesis. **Chapter 2** – Interactions in microbial ecology discusses interactions in microbial ecology in general, without a species-specific emphasis. **Chapter 3** – *Bacillus subtilis* and fluorescent pseudomonads, directs the discussion to *B. subtilis* and fluorescent pseudomonads, starting with a description of each group of organisms, before investigating their relations with other microbes and with each other. The literature **Study 2** acts as a framework for reviewing *Bacillus-Pseudomonas* interactions in this chapter. In **Chapter 4** – Predicting microbial interactions, I discuss if and how microbial interactions can be predicted from phylogeny or other descriptors. Here, I put the results from **Study 3** in context of the field, by attempting to map interactions between *B. subtilis* and fluorescent pseudomonas to d in the context of colony and pellicle biofilm. In the final **Chapter 5** – The sociomicrobiology of iron, I investigate the impact of iron and siderophores on microbial ecology and add the results from **Study 4** to the growing body of literature describing iron in bacterial interactions. The studies mentioned in the thesis can be found in full after the concluding remarks.

Chapter 2 – Interactions in microbial ecology

Ecological interactions can generally be divided into three main categories: Beneficial, neutral, or detrimental. Interactions are used to describe a relationship between one pair of organisms, where each participant experiences some influence from the other. Considering the three main outcomes, each interaction can be described by the fitness-influence on both participants, resulting in six classes (Fig. 1) [22]. Additional definitions exist for interactions based on their timescale (e.g., antagonism can be predation in the short term or parasitism in the long term).

Biological interactions have historically been essential for understanding ecosystem stability. However, herein lies a complication; an ecosystem is not a pairwise interaction. Rather, it is a network of many interactions, pairwise or larger, affecting each other directly and indirectly [23]. For example, food chains describe linear predator/prey relationships and can be combined into a food web network with information on the transfer of trophic energy within a system. Thus, food webs are interaction networks built on short-term trophic interactions, and by understanding the food web and how influential each predator/prey relationship is, it becomes possible to predict the consequence of losing a node of the network [23].

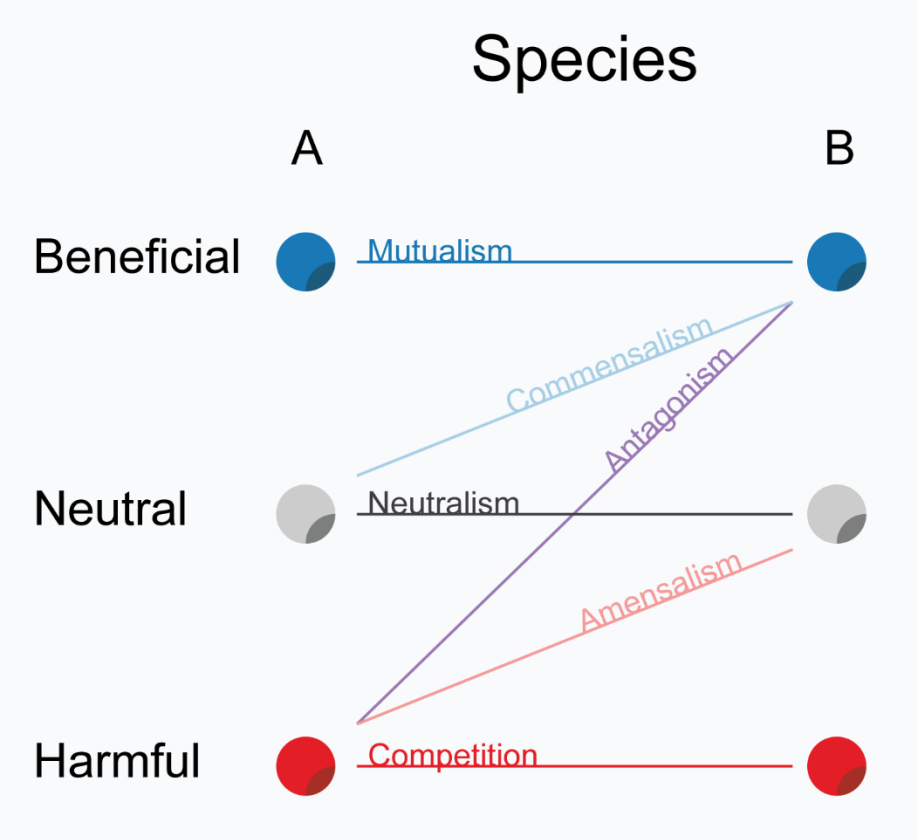

Figure 1 – Ecological interactions. The fitness effect conferred by one organism (left column) on another (right column) contributes to the determination of an interaction (lines connecting columns). Positive fitness effects (blue) result in increased reproductive ability, while negative effects (red) do the opposite, and neutral have no effect (gray). An interaction is named by the combined signs of the two organisms.

This all translates to microbial ecology, though, at the microbial scale it is exceedingly difficult to map entire networks, particularly as most natural microbes currently cannot be cultivated in a laboratory [24, 25]. So, studies in microbial ecology either describe microbiome composition and consequential outcome (the top-down approach) or interactions between small subsets of microbiome members in synthetic communities (the bottom-up approach). Both types of studies attempt to uncover information about how interactions influence the function of the microbiome, though, as we mention in **Study 2**, debate is heavy on whether pairwise interactions translate to community interactions.

The studies presented in this thesis investigate interactions in cocultures with few members. Such systems provide simplicity, increasing the reproducibility of results at the expense of complexity. Later in this chapter, I will also discuss the aforementioned debate and whether pairwise interactions scale to a community context.

Positive interactions

When microbes confer beneficial fitness effects on interaction partners, it happens through either mutualism (+/+) or commensalism (0/+). I choose to group antagonism (+/-) with negative interactions, because of the inherent selfishness in exploiting an interaction partner for self-interests.

Commensalism is the less ambiguous of the two. Theoretically, commensal interactions are quite intuitive; the commensal gains a benefit without incurring a cost to its interaction partner. However, as outlined in the excellent review by Mathis and Bronstein (2020), commensalism has rarely been adequately investigated [26]. Many studies fail to consider the reciprocity of the interaction, and instead assume a neutral outcome, when negative or positive effects are inconceivable. Even when neutral outcomes are rigorously documented, they can be overturned with additional research due to oversight. This has historically meant that many commensalisms have been reassigned when the positive or negative effect was identified (e.g., "commensal" *Escherichia coli* residing in the human gut engages in a mutualistic relationship with its human host, by modulating pathogen colonization and immune system homeostasis [27, 28]). On these grounds, Zapalski (2011) dismisses the notion of commensalism entirely describing it as: "*a concept that cannot be proven, as the absence of proof cannot be regarded as a proof of absence*" [29]. In contrast, Mathis and Bronstein (2020) do not dismiss commensalism, rather, dividing it into "no-effects" and "balanced-costs-and-benefits" interactions [26]. Thus, commensalism can either incur a completely neutral effect or costs and benefits can

cancel out exactly to a net-neutral effect. Between microbes, true commensalism has been described only rarely. Andrade-Domínguez *et al.* (2014) cocultured the budding yeast *Saccharomyces cerevisiae* with the nitrogen-fixing bacterium *Rhizobium etli* and found that the bacterium benefited from growth with the yeast to create a commensal interaction [30]. Commensalism was short-lived, however, as the interaction depended on simultaneous fungal secretion of bacterial growth inhibitors and promoters, the latter eventually depleting from the medium. Upon lack of growth promotion, *R. etli* growth diminished, and the interaction developed into amensalism. Eventually, the selection pressure on *R. etli* from the growth inhibitors led to phenotypic differentiation with emerging phenotypes being able to outcompete *S. cerevisiae* in an antagonism. Though this commensalism changed over time, constant replenishment of growth promoting molecules may have been able to sustain it for prolonged periods.

Mutualism is particularly known from eukaryote-prokaryote interactions such as the gut microbiota. Some animals are dependent on microbes residing in their intestinal system for accessing non-digestible nutrient sources, providing microbes with substrate, and receiving digestible metabolic byproducts in return [31]. This type of symbiosis is also known as syntrophy or cross-feeding, where one organism utilizes a nutrient and converts it to a nutrient for another organism [32]. Famous examples include human and ruminant microbiotas as well as the microalgal endosymbionts of coral [33, 34].

Syntrophy has also been described for several interbacterial relations. Clear examples were presented by Dolfing *et al.* (2008), who established two separate cocultures of either a *Moorella* sp. and a *Methanothermobacter* sp. or a *Desulfovibrio* sp. and a *Methanobrevibacter arboriphilus* capable of growing on formate; but only in cocultures [35]. Sun *et al.* (2022) employed the PGPR type strain *Bacillus velezensis* SQR9 to recruit a *Pseudomonas stutzeri* (now *Stutzerimonas degradans*) from the cucumber rhizosphere and demonstrated how *S. degradans* produced branched-chain amino acids in minimal medium rescuing auxotrophic *B. velezensis* [36].

Syntrophy is strictly metabolic, but not all mutualistic interactions relate to metabolism. With a broader term, such interactions can be described by cooperation [32], often between specialized organisms that have traded off utilization of one resource for utilization of another. Non-producers can be complemented by neighbors in ecological niches they would otherwise be unable to inhabit. One-sided complementation is known as facilitation, and when facilitation is mutual, it fulfills at least one of the four requirements for division of labor (Fig. 2):

1. Functional complementarity

2. Synergistic advantage
3. Negative frequency-dependent selection
4. Positive assortment

Thus, if interacting partners 1) complement a function of each other, 2) gain a larger-than-additive fitness advantage in coculture, 3) display lower fitness as the abundance of a partner is low, and 4) frequently encounter a partner, they are undergoing division of labor [37]. Per definition, linear interactions are then excluded from being division of labor, as they violate the first requirement. Cooperative interactions can develop into such linear interactions, through the spontaneous evolution of non-producing exploiters in a behavior known as "cheating" [38], which will be discussed more in the section **Negative interactions** below.

In **Study 1**, we discussed the results of a publication by Schwartzman *et al.* (2022), who described how *Vibrio splendidus* temporally differentiate into metabolic heterogeneity, creating bacterial aggregates five times larger in diameter than predicted by mathematical modelling [39, 40]. The clustering of *V. splendidus* cells facilitated positive assortment, while metabolic differentiation during the development of the aggregates yielded alginate-utilizers and carbon-storers complementing each other to ensure collective synergy. With the exception of frequency dependency (which was not investigated), these aggregates fulfilled the requirements of division of labor when grown on alginate. The growth conditions used in the studies mimicked the natural environment of *V. splendidus* well, but it is unknown whether the behavior exists in the marine environment.

The division of labor presented by Schwartzman *et al.* (2022) provides an example of intraspecific division of labor through metabolic differentiation, a phenomenon that has been observed on multiple occasions [41–44]. In **Study 1**, we additionally discussed examples of intraspecific genetic division of labor as well as interspecific division of labor. When each interacting partner carries only the genetic machinery for their own specialist task, division of labor is said to be genetic rather than phenotypic. Such interactions would appear over evolutionary time scales where the specialization in one task results in the genetic loss of specialization in the complementary task. An example is found with *B. subtilis* producing biofilm matrix components. To establish an air-liquid pellicle biofilm, *B. subtilis* must produce both exopolysaccharides (EPS) and the amyloid protein TasA. Respectively disrupting each operon removes

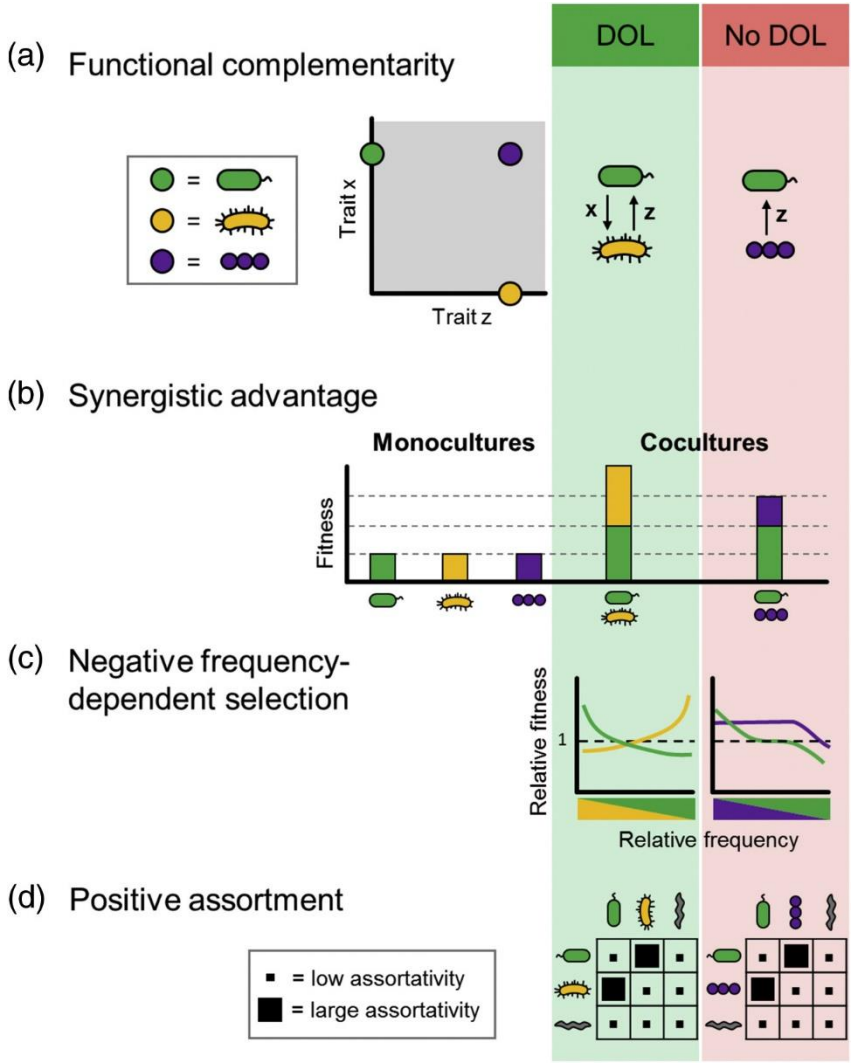

Figure 2 – Division of labor require four criteria. When microbes engage in mutualistic interactions, they may be classified as division of labor (DOL) if they fulfill four requirements: a) The interaction must be between organisms which are oppositely specialized such that they functionally complement each other. b) The complementation must provide a fitness advantage to both organisms that is larger than the sum of each partner individually. c) The fitness of each organism must positively correlate with the abundance of the interaction partner, such that the fitness of each partner is highest, when the abundance of the companion is highest. d) The interaction partners must be able to come into contact relateively easily. Reprinted from [37] with permission.

pellicle formation, but cocultivation of mutants results in synergistic pellicle formation [45]. The interaction displays negative frequency dependency and has built-in positive assortment, making it a clear case of division of labor. Genetic division of labor can also occur spontaneously, suggesting that such evolution can arise in natural systems [46]. However, the long-term stability of genetic division of labor seems to be dependent on the subsequent selection pressure established in the population [47]. If selection favors mass-producers, they can be exploited by other emerging genotypes that gain fitness advantages from not having to produce while still obtaining the resource themselves [48].

Naturally occurring interspecies division of labor presents a paradox. On one hand, distantly related organisms are more likely to harbor different (and thereby potentially complementary) pathways, yet ecology and evolution predicts that higher relatedness favors division of labor because it benefits kin selection [49]. This could explain why many reported interspecific divisions of labor involve synthetic rather than naturally occurring cocultures [50–53]; evolution favors division of labor between closely related organisms, negatively impacting assortment of distantly related microbes. However, interspecies division of labor does exist in nature. A well-known example is lichen; a fungal, algal, and bacterial mutualism. In certain lichen, the fungal partner has evolved to lose mitochondrial energy production (an otherwise essential function) but is likely complemented by the algal partner releasing ATP for the benefit of the community [54]. Lichen represents an example of low-relatedness division of labor, possibly emerging through co-evolution. The *B. velezensis* - *S. degradans* interaction described by Sun *et al.* (2022) was not identified as division of labor, because of the lack of information on frequency dependency and complementation [36], but the results of the study do not rule out division of labor. Bacilli and pseudomonads certainly have the potential to come in contact [20], and the large genetic diversity within each genus potentiates functional complementation.

Negative interactions

As the publication title by Palmer and Foster (2022) states: “Bacterial species rarely work together” [55]. Pairwise microbial interactions are mostly negative, with microbes engaging in amensalism (0/-), antagonism (+/-), or competition (-/-).

Competition presents itself in two forms: Indirect exploitative competition and direct interference competition. The goal of most organisms is to further the genetic line in a process that requires space and nutrients. With many relatively distantly related species occupying similar nutritional niches, selection favors microbes that establish and divide faster by utilizing

resources more efficiently. Thus, in an environment where two interactants are equally suited for a resource, the fastest growing microbe wins [56, 57]. Specifics depend on the nature of the niche, in whether it is well mixed or not. When resources are not uniformly distributed in an environment, interactants become spatially segregated into microcompartments [58]. Even in such cases, fitness (approximated by the proportion of the niche occupied by an interactant) strongly correlates with growth rate. The growth kinetics of each interactant on their own explain much of the fitness effect in pairwise interactions, but not everything [57]. When microbes invest in offensive molecules, they gain a competitive advantage even if they grow slower than their interaction partner and therefore, many microbial interactions revolve around the production of antimicrobial metabolites or even cellular weapons. These negative interactions were recently revealed to not be additive, but instead follow a "strongest effect" model, where the effect of the strongest antagonistic molecule decides the fitness effect irrespective of the presence of other antagonistic molecules [59]. Additionally, microbes have evolved complex mechanisms to deprive competitors of essential resources, but in response, countermeasures have evolved against these mechanisms as well, such as with siderophore piracy (see **Chapter 5** – The sociomicrobiology of iron**)**. All in all, negative interactions span nutritional, spatial and antimicrobial competition.

Amensalism is the negative complement to commensalism, where the amensal interactant reduces fitness of a partner. For instance, *Lactobacillus* spp. in the vaginal microbiota produce lactic acid under anaerobic conditions, independent of neighboring microbes [60]. The decrease in pH inhibits opportunistically pathogenic yeasts from the *Candida* genus, without conferring additional fitness cost to *Lactobacillus*. The neutral aspect of amensalism provides similar problems as with commensalism, due to the difficulty of documenting a net neutral interaction outcome.

Antagonism is much more widespread, encompassing interactions such as predation and parasitism, which are well-known from microbiology. Microbiological predation also exists, but it can be more difficult to correctly classify when microbes specifically kill other cells for nutrition as opposed to competitive killing with subsequent nutrient uptake. A classic example is found with *Myxococcus xanthus*. This species "hunts" and kills other microbes with a range of secondary metabolites and secretion systems, lysing prey cells and taking up the expelled cellular components as nutrients [61]. However, studies have shown that *M. xanthus* is not chemotactic towards prey [62], and that most killed *E. coli* cells are left unconsumed [63]. *Bdellovibrio* spp. on the other hand, are described as obligate predators, based on their initial

characterization in 1966 and subsequent host-dependence when cultured in the lab [64]. *Bdellovibrio* spp. cannot be grown in typical lab media unless supplemented with protein extracts from non-kin cells [65]. Predation is genetically encoded, allowing for spontaneous occurrence of facultative predators that can grow axenically [66]. Bacterial predation is otherwise rare, possibly owing to the inability of some species to grow on typical growth medium.

An interesting interaction type that somewhat crosses the line between commensalism and antagonism is cheating. Producing a common good renders the population vulnerable to exploitation by individuals who opt out of production and conserve energy for other processes. These "cheating" individuals gain a fitness advantage and can outcompete producers, which eventually leads to the collapse of the system when no producers are left [47]. Interestingly, Leinweber *et al.* (2017) demonstrated how competitive cocultures of *Pseudomonas aeruginosa* and *Burkholderia cenocepacia* stabilize when intraspecific competition (in the form of cheating) is higher than interspecific competition [67], and in general, when cheaters experience a negative fitness effect, cooperation seems to be stable [68].

Translatability of Pairwise Interactions

Because of the enormous diversity of microbial communities, understanding community assembly poses a challenge. An intuitive approach to determine species co-existence could be to infer pairwise interactions community structure from pairwise interactions. One could then expect that a pair with competitive exclusion would also exclude the less fit organism in community settings. This is known as the reductionistic view. However, microbial interactions are always context-dependent and often develop temporally [30, 69, 70]. Thus, pairwise interactions observed in a laboratory environment rarely translate to natural contexts. Context-dependency pertains to the influence that nutrient composition as well as temperature and other abiotic factors have on cell growth and metabolism [71–73]. Context dependency does not necessarily refute a reductionistic view. However, an alternative hypothesis argues that community assembly is complex and derived from emergent properties. Additional interactants contribute with their own metabolisms which are also context-dependent and may modulate

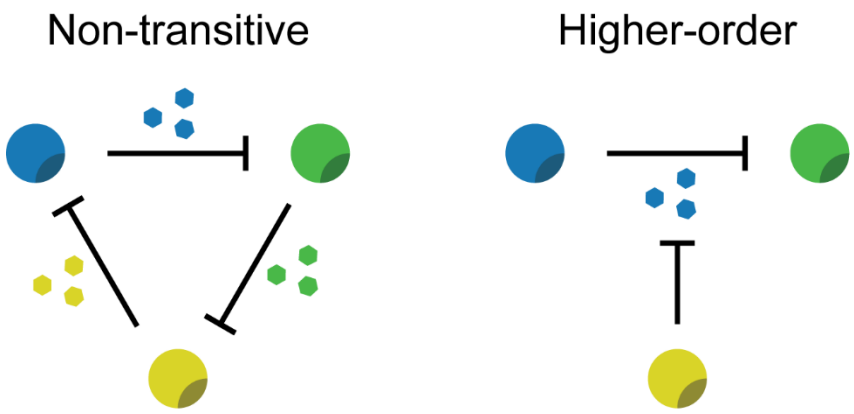

Figure 3 – Higher order interactions are emergent. The addition of other participants to an interaction can result in novel distributions that may not be apparent from the collection of pairwise interactions. When three participants inhibit each other cyclically, they engage in non-transitive interactions, also known as "rock-paper-scissors" (left). However, when a third participant influences the interaction between to partners without directly interacting with either, the interaction is known as a higher-order interaction. Such interactions cannot be inferred from pairwise cocultures.

what has already been observed in the pairwise interaction. Even so, modeling interaction networks of communities through a bottom-up approach (inferring knowledge from pairwise interactions) has been common practice [74]. Often, models require an abundance of genomic, metabolic, and empirical data that may be hard to obtain. As an alternative, Friedman, Higgins, and Gore (2017) attempted to infer community structure of species trios using information on pairwise interactions. Structure outcomes were simplified to two outcomes: competitive exclusion or stable coexistence [75]. Thus, three species A, B, and C, all of which are pairwise compatible with each other, are expected to participate in a stable trio under similar conditions. However, this prediction only held for half of the examined communities, and the authors argue that higher-order interactions (interactions that are only present with additional interactants) could explain some, but not all unexpected outcomes. Still, using their assembly rules based on pairwise interactions, the authors were able to predict trio assembly more accurately than simulations based on general Lotka-Volterra models, and when predicting the outcome of a mixture of eight species, pairwise interaction information was an equally good predictor of community structure as Lotka-Volterra simulations. Adding information about the trio outcomes increased prediction accuracy from 62% to 86%.

The bane of predicting community assemblies also comes from one of their most attractive assets: Emergence. Combining microbes into communities can result in novel properties undetectable in mono- or even pairwise cultures. When one species modulates the interaction between other species without directly affecting them, they are said to perform higher-order interactions (Fig. 3) [76, 77]. These properties can be present immediately or develop over time due to the relatively low evolutionary scale for microbes [58]. In a recent preprint, Hansen *et*

al. (2023) demonstrated how antimicrobial orfamide A produced by *Pseudomonas protegens* was degraded serially by two members of a four-species community [17]. Orfamide A concentrations in *P. protegens* monoculture exceeded the minimal inhibitory concentration for *Rhodococcus globerulus* almost two-fold but did not inhibit in the five-species community due to the degradation of the metabolite. Others have identified novel metabolites from polymicrobial communities undetectable in mono- or pairwise cocultures [72]. The degradation and possible differential regulation of metabolism in community assemblies likely leads to natural concentrations of antimicrobials that are much lower than those employed in laboratories. At such concentrations, metabolites may not explicitly be deadly, but could instead function as regulators and signal molecules [18, 78, 79].

Friedman, Higgins, and Gore (2017) provided evidence for the reductionistic hypothesis, but their pairwise and trio interactions were not able to predict all community assemblies. So, can pairwise interactions infer community assemblies? This question was recently investigated in a study comparing pairwise interaction outcomes to community outcomes in 12 separate stable microbial communities with 5-13 members [80]. Though the communities were experimentally validated as stable (each member invaded its community in a negative frequency-dependent pattern), a majority of the 144 pairwise interactions (71.5%) resulted in competitive exclusion, suggesting that community assembly is governed by complex interaction networks that cannot be predicted from pairs. The authors themselves, however, discuss how the applicability of the two hypotheses is context-dependent, similarly to the interactions themselves, but there is still no evidence for when community assembly is reductionistic and when it is emergent.

Pairwise interactions can hold some predictive power, but context-dependency and higher-order interactions are likely to explain the difficulty in translating simple interactions to more complex community settings. Control and awareness of these caveats is essential when inferring function from bottom-up experiments, which are superior to top-down approaches in simplicity and experimental control and allow for gradual mapping of mechanisms in bacterial interactions. Hopefully, a deeper understanding of individual microbial interactions will translate into a better comprehension of how higher-order interactions emerge and communities assemble.

Chapter 3 – *Bacillus subtilis* and fluorescent pseudomonads

Bacillus subtilis

B. subtilis is a Gram-positive, endospore forming bacterium which has historically been essential as a model organism for biofilm formation, secondary metabolite production, and plant growth promotion [81]. It is rod-shaped and motile with peritrichous flagella, which the bacterium uses for aerotaxis and plant root colonization, and it has been isolated from many diverse sites, rendering it environmentally ubiquitous [20]. Biofilm formation, sporulation and secondary metabolite production are all important characteristics of *B. subtilis* that also come into play in intermicrobial interactions.

Biofilm formation by *B. subtilis* mainly presents itself in two forms: a solid/air interface colony or a liquid/air interface pellicle [82]. The macroscopic physical properties and secreted metabolites from each of these biofilms are quite similar. EPSs are secreted along with an amyloid protein component, TasA, which are thought to interact and strengthen the matrix

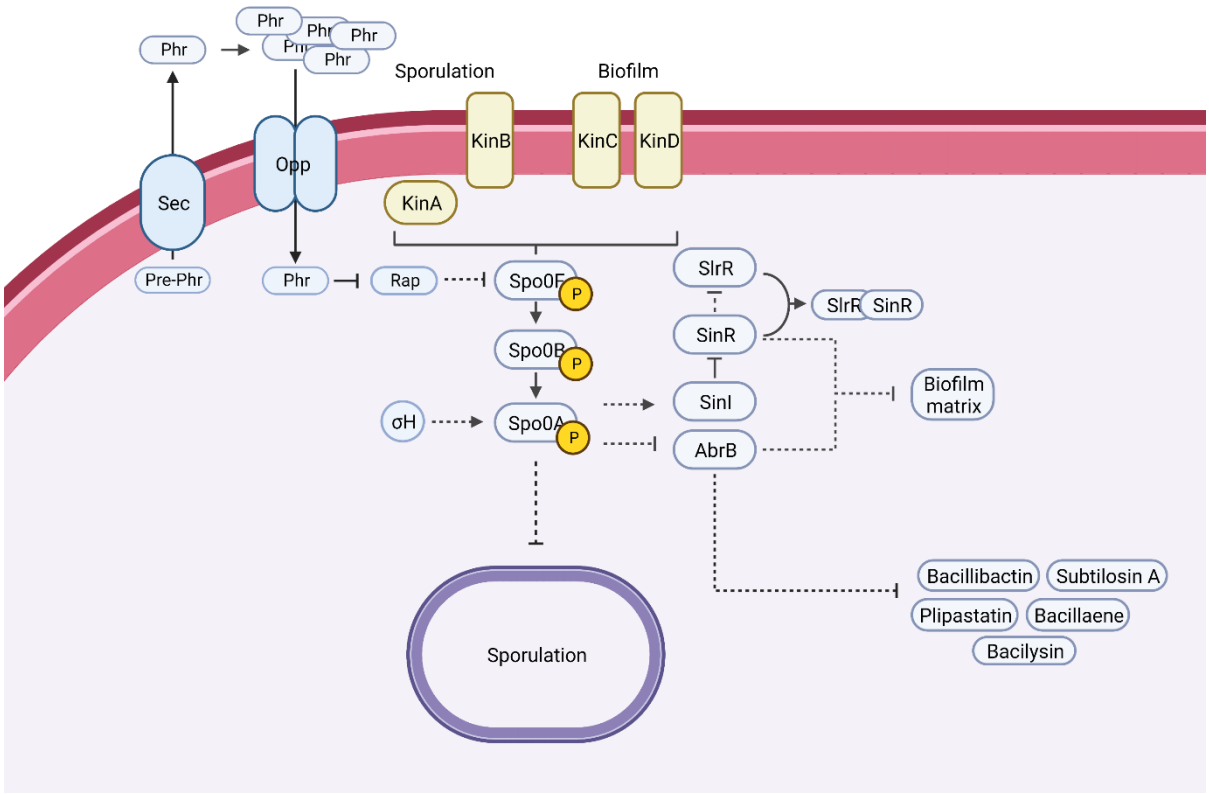

Figure 4 – *Bacillus subtilis* lifestyle is regulated by the Spo0A pathway. Upon recognition of environmental signal molecules, the histidine kinases KinABCD become activated and initiate the phosphorylation cascade starting with Spo0F and ending with Spo0A. Spo0A is a master regulator controlling sporulation, biofilm formation, and likely secondary metabolite production via AbrB. Lifestyle regulation is mediated by a concentration gradient. High concentration of phosphorylated Spo0A result in sporulation, while intermediate levels signal for biofilm formation. Spo0A phosphorylation and transcription is additionally controlled via Sigma H (σH) and the Rap/Phr quorum sensing system. Dashed lines indicate trasncriptional regulation. Solid lines indicate protein interactions. Arrowheads indicate positive regulation, bar-heads indicate negative regulation. Created with Biorender.

resulting in the formation of wrinkles [83]. These wrinkles, in turn, are hypothesized to increase surface area to facilitate oxygen diffusion [84] and nutrient transfer [85]. Additionally, the production of a hydrophobin BslA contributes to a highly hydrophobic surface [86]. Biofilm formation and the physicochemical properties of a biofilm likely confer an advantage for *Bacillus* in colonizing specific niches and indeed, pellicle productivity of *B. subtilis* has been shown to correlate positively with plant root colonization [87, 88].

Regulation of biofilm-related gene expression happens through the global regulator, Spo0A, which controls expression of more than 140 genes in *B. subtilis* [89]. Other than biofilm, Spo0A regulates genes with roles in sporulation, motility, and competence (Fig. 4). Activation of sensor kinases initiates the phospho-relay comprised of Spo0F and Spo0B which serially transfer phosphoryl groups from one to the other and finally to the ultimate target, Spo0A. Upon phosphorylation, Spo0A is activated and changes conformation to allow DNA binding which acts as the control mechanism [90]. Interestingly, the lifestyle of *B. subtilis* depends on the intracellular level of phosphorylated Spo0A (Spo0A~P), with low concentrations leading to a planktonic lifestyle, intermediate concentrations initiating biofilm formation, and high concentrations initiating sporulation [91]. This concentration gradient is managed through the stimulation of the histidine kinases KinABCDE [92, 93], where KinA and KinB are spatially confined to the center of a colony biofilm and KinC and KinD to the outer edges. Under laboratory conditions, KinC and KinD increase Spo0A~P levels enough for differentiation into biofilm-forming cells [92], while KinA and KinB can raise the concentration even higher to initiate sporulation [93].

Endospores are vital for the survival of many Gram-positive bacteria, and there has been some speculation that spore-forming bacteria isolated from soil are not in fact metabolically active in natural environments [94]. However, experimental evidence refutes this claim, demonstrating the ability of bacilli to sporulate, germinate, and divide in soil [95, 96]. Endospores are incredibly tough, enduring ultraviolet radiation, extreme temperature, chemical disinfection, and prolonged desiccation [97]. In truth, the viable time frame of endospores is still not known, with reports outcompeting each other for the record of oldest viable endospore. In 1995, a publication in Science claimed to have germinated a 25-40 million-year-old endospore of a close relative to *Bacillus sphaericus* (now *Lysinibacillus sphaericus*) [98]. Sporulation is initiated by nutrient depletion that causes cells to undergo asymmetric cell division into a prespore and the mother cell. The mother cell engulfs the prespore and synthesizes spore coat

components. Once the inner spore is mature, the mother cell lyses and the spore is released [97].

Both biofilm formation and sporulation strongly depend on iron availability [99–101]. *B. subtilis* grown in the biofilm-inducing medium MSgg cannot form a pellicle biofilm when iron homeostasis is disrupted [102]. To acquire Fe(III) (ferric iron) from the environment, *B. subtilis* utilizes the catecholate siderophore bacillibactin (BB) [103]. BB synthesis is encoded in the *dhbA-F* operon, which is translated into a non-ribosomal peptide synthetase pathway. Upon synthesis, BB is exported out of the cell, where it binds Fe(III) with high affinity before being taken up again by the FeuABC-YusV ABC transporter system [104–107]. Ferri-BB is hydrolyzed by BesA and iron is released for use in enzymatic reactions in a homeostasis that is controlled by the Ferric Uptake Regulator, Fur [106]. A *ΔdhbA* mutant is unable to synthesize 2,3-dihydroxybenzoate (DHB) and its inability to form a pellicle in MSgg suggests that both DHB and BB are implicated in iron uptake in pellicle formation [108]. In **Study 4**, we found that a *ΔdhbA* mutant was reduced in its transcription of many sporulation-related genes compared to a wild-type *B. subtilis*, which coincided with reduced wrinkle formation on the surface of colonies [101].

Fluorescent pseudomonads

Pseudomonas is a genus of Gram-negative gamma-proteobacteria with incredible diversity and environmental universality [109]. Many *Pseudomonas* spp. function as model organisms for a wide range of fields. *P. protegens* and *Pseudomonas fluorescens* in biocontrol [79, 110], *Pseudomonas syringae* in plant pathogenicity [111], *Pseudomonas putida* in fermentation and remediation [112], and *P. aeruginosa* in human pathogenicity [113]. Most pseudomonads encode high biosynthetic potential in their genomes [114], and one metabolite especially has allowed for phenotypically driven taxonomy. The siderophore pyoverdine (Pvd) contains a structurally conserved chromophore which can be excited by ultraviolet/violet light (340 nm – 420 nm) and emits blue/green light (440 nm – 520 nm) [115, 116], allowing for easy identification of Pvd-producing strains [117]. These strains were historically grouped together as fluorescent pseudomonads irrespective of additional phenotypic traits [109, 118]. Herein lies a problem. *P. aeruginosa*, *P. fluorescens*, *P. putida*, and *P. syringae* are all fluorescent, even though their genomes, environmental presence, and phenotypic characteristics are quite dissimilar (some

strains that do not produce Pvd instead produce pyocyanin that also fluoresces). In fact, the entire *Pseudomonas* genus has continuously been under scrutiny ever since its foundation, and many have attempted to 'clear up' *Pseudomonas* taxonomy. A breakthrough came from using rRNA hybridization to separate "wrong" pseudomonads (*Pseudomonas senu lato*) from "real" pseudomonads *(Pseudomonas sensu stricto*) [109]. Additional reclarification has divided *Pseudomonas sensu stricto* into 13-14 groups (depending on methodology), and the diverse *P. fluorescens* group further into 10 subgroups (Fig. 5) [110, 119, 120]. Though reclassifications are

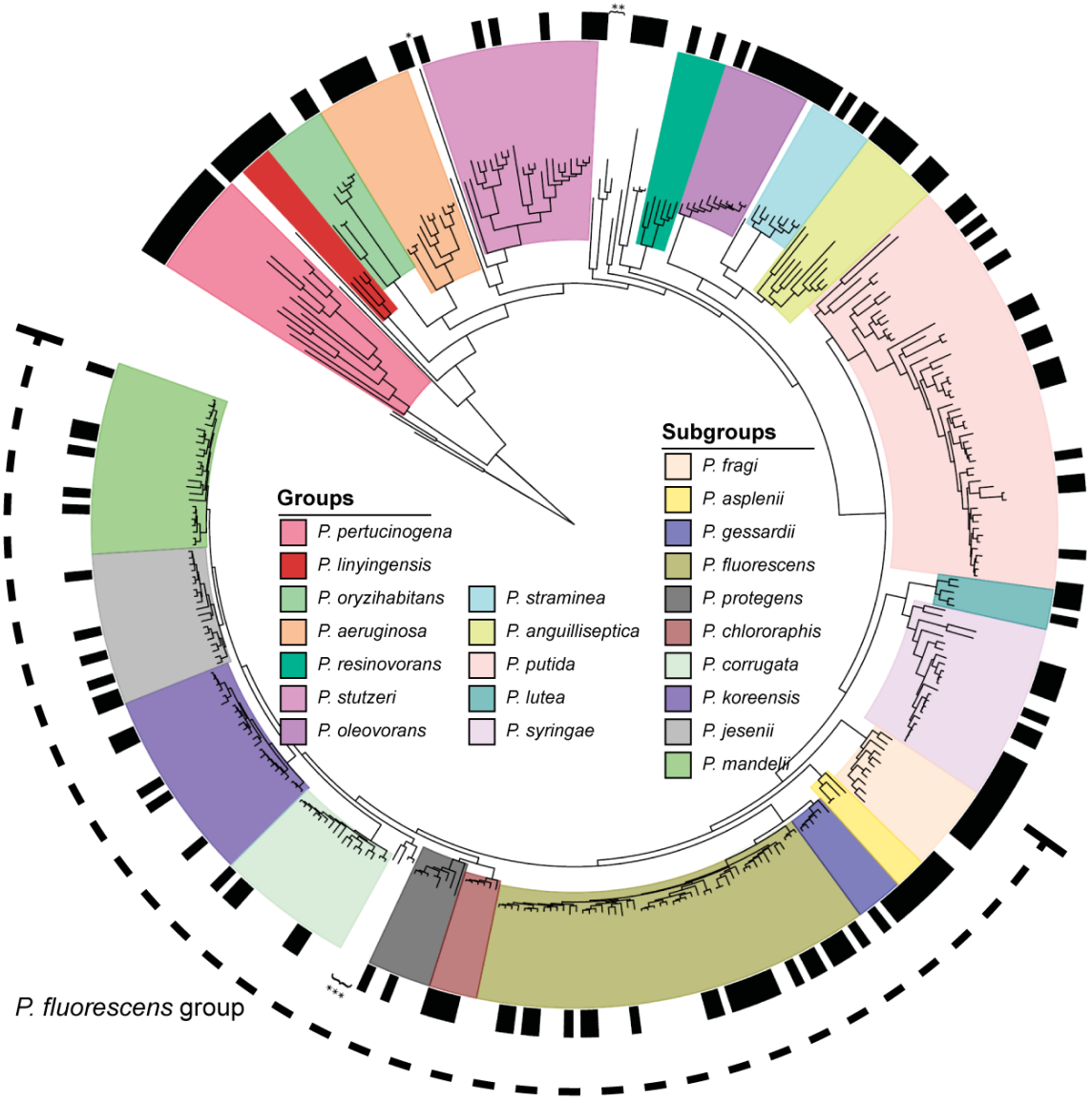

Figure 5 – *Pseudomonas* phylogenetic tree. Maximum likelihood phylogeny based on protein sequence alignments of 100 single-copy orthologous genes from 355 strains of *Pseudomonas* spp., three strains of *Azotobacter* spp., and one strain of *Azomonas agilis*. Three genomes of *Cellvibrio* spp. were included as an outgroup with the branch truncated to improve visualization of the tree topology. Outer circle: genomes of type strains for each species are indicated with a black box. *Placement of *Azomonas agilis*. **Clade composed of ten genomes of *Azotobacter* spp. ***Clade representing a new subgroup within the *P. fluorescens* group. Dashed line denotes the tree dedicated to the *P. fluorescens* group. Adapted from [119] with permission.

ongoing [121]. Studies investigating the *Pseudomonas* pangenome have indicated that accessory genomes have evolved with their respective core genomes, suggesting a relatively low rate of horizontal gene transfer [110, 114, 122]. Thereby, phenotypic traits seem to be conserved across certain taxonomic levels allowing for fairly accurate functional prediction based on taxonomy alone.

In the current paradigm, the *P. fluorescens* group is comprised of the subgroups *fragi, asplenii, gesaardii, fluorescens, chlororaphis, protegens, corrugata, koreensis, jessenii, and mandelii*, phylogenetically associated in that order. All subgroups contain species that have been associated with plants, either as PGPR or as phytopathogens, and some subgroups contain species that are both (e.g., *P. fluorescens* and *Pseudomonas marginalis* from the *fluorescens* subgroup). *P. fluorescens* species are not alone in associating with plants. *P. putida*, *P. stutzeri*, and *P. syringae* also all engage in interactions with plants or with other microbes in the plant environment [36, 123, 124]. Thus, fluorescent pseudomonads, irrespective of taxonomic group, carry large potential within agricultural science as biostimulants and biocontrol agents.

Secondary metabolism

Contrary to their name, secondary metabolites have tremendous implications in microbial physiology and ecology. Separate from basic metabolic processes, required for cell viability, secondary metabolites are produced under specialized circumstances. Terminology therefore now also includes “specialized metabolites”, appreciating the significant, but context-dependent, roles of these metabolites. Chemically, secondary metabolites are immensely diverse, encompassing virtually all known organic functional groups into molecules able to sequester iron, degrade host tissue, facilitate communication, and antagonize rival organisms among many other functions. They are often produced from enzymes encoded in biosynthetic gene clusters (BGCs) closely associated in the genome [125].

Bacillus and *Pseudomonas* are well-known for their biosynthetic potential. *B. subtilis* allocates approximately 5% of its genome to genes participating in the secondary metabolism [126], while fluorescent pseudomonads are particularly well-known for their siderophore, cyclic lipopeptides, and phloroglucinols [127]. These metabolites are categorized into groups

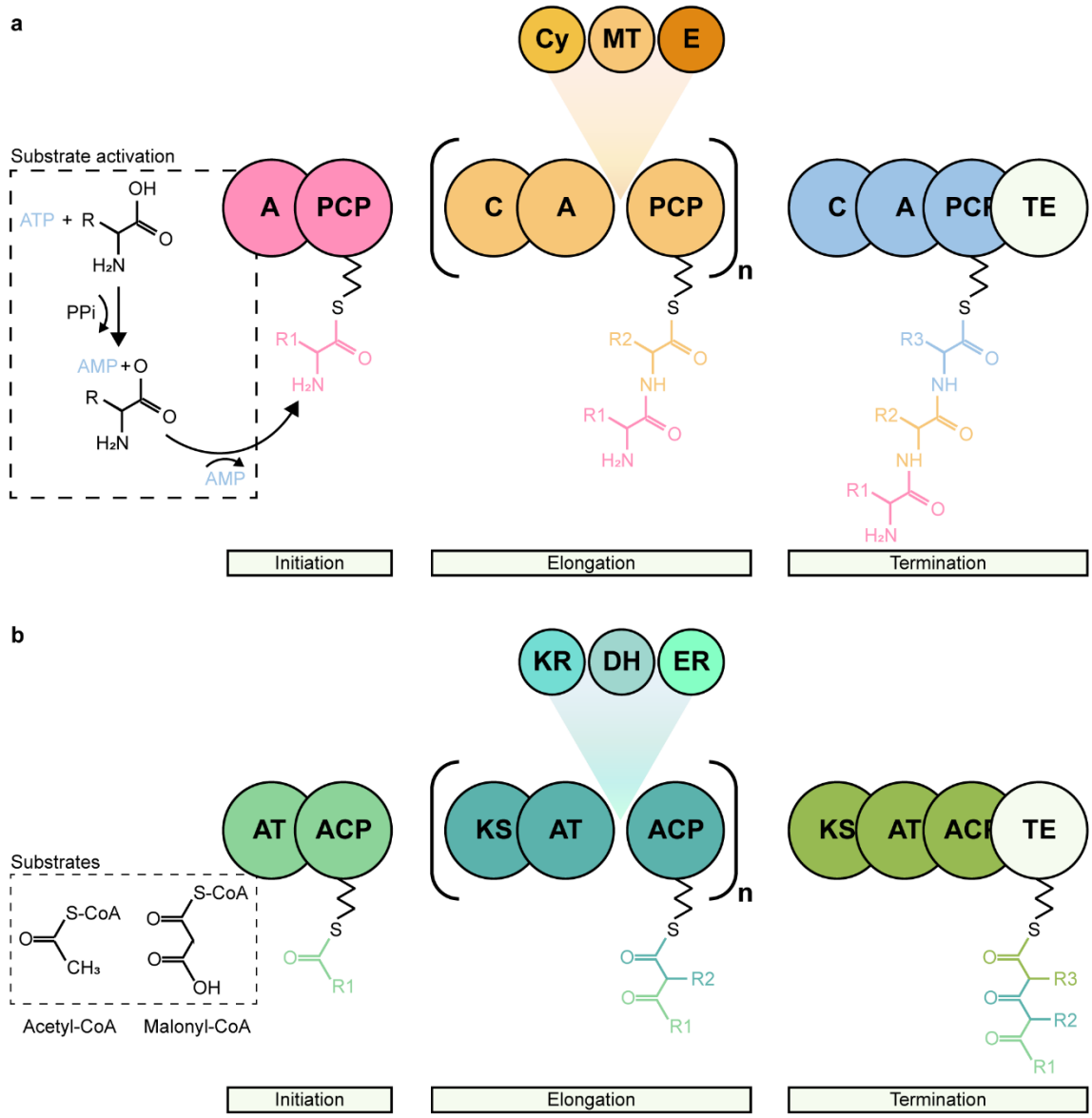

Figure 6 – Non-ribosomal peptide and polyketide synthesis. (a) Non-ribosomal peptides are synthesized by modular synthetases with initiation, elongation, and termination modules. The substrates are activated by the adenylation (A) domain via ATP and bound to the peptidyl carrier protein (PCP) domain. The molecule is synthesized from N- to C-terminal by the condensation (C) domain and can obtain structural diversity through the modification by cyclization (Cy), methylation (Me) and epimerization (E) domains. The molecule is completed when it is cleaved from the synthetase by a thioesterase (TE) domain. (b) Modular polyketides are synthesized much like non-ribosomal peptides, though with no expenditure of energy and using acetyl-CoA or malonyl-CoA as substrates. The acyltransferase (AT) domain selects a substrate and loads it onto the acyl-carrier protein (ACP) domain. The ketosynthease (KS) domain elongates the molecule by catalyzing the condensation of extender units to the growing chain. Structural diversity is achieved by ketoreductions via the ketoreductase (KR), dehydrogenase (DH) or the enoyl reductase (ER) domains. Synthesis is terminated when the molecule is cleaved from the synthase by a TE domain.

characterized by chemical structure or biosynthetic pathway, the largest groups of which are non-ribosomal peptides and polyketides (Fig. 6).

Non-ribosomal peptides (NRPs) are chains of amino acids that are not translated from mRNA via the Central Dogma [128]. Rather, they are synthesized by modular enzymatic complexes termed non-ribosomal peptide synthetases (NRPSs), each module elongating the NRP with a single unit in an "assembly line" (Fig. 6a). The units are generally amino acids, but alternative substrates, such as hydroxy acids and aminobenzoic acids can be incorporated as well. Each module carries (at least) three enzymatic domains: The adenylation (A) domains are responsible for activating the correct substrate via ATP utilization, transferring it to the peptidyl carrier protein (PCP) domain by catalyzing the formation of a thioester bond. The condensation (C) domain catalyzes the formation of a peptide bond between the new unit and the growing peptide chain, elongating the molecule linearly from N-terminus to C-terminus. The final module in the complex also carries a thioesterase (TE) domain which cleaves the thioester bond between peptide and PCP, releasing the final metabolite. Each module can contain additional domains such as methylation, oxidation, and epimerization domains.

Cyclic lipopeptides (CLPs) comprise a class of NRPs that incorporate an acyl chain in a cyclized peptide. They function as surfactants and antimicrobials against bacteria and fungi [129, 130]. In **Study 3**, we found that *Pseudomonas* CLPs are particularly deadly and specific. CLPs from the viscosin, tolaasin, and syringopeptin groups have demonstrated antagonistic effects against *Bacillus* spp., though variation in CLP structure even within groups results in a range of antagonistic strengths and in target specificity to the species level [131, 132]. Fewer CLP groups have been identified from *B. subtilis*. Surfactins, plipastatins, and iturins share similar group-specific functions with *Pseudomonas* CLPs. Surfactin is a multifunctional surfactant essential for *Bacillus* motility, colonization, and intermicrobial antagonism [133, 134]. Interestingly, surfactin and sessilin (from the tolaasin group) interact molecularly, forming a white precipitate visible to the naked eye [135]. In this regard, surfactin functions as a chemical shield against the antimicrobial sessilin.

Siderophores are NRPs named for their iron-chelating function. They are further subdivided based on their Fe(III)-binding functional group, into hydroxamates, catecholates, phenolates, carboxylates or a mixture of the groups (Fig. 7) [136]. The catecholate structure of BB from *Bacillus* is conserved by the Dhb biosynthesis (Fig. 7a). The siderophore consists only of three repeating NRP subunits produced from DHB, glycine, and threonine, and the functional implication of substituting even one amino acid moiety for a different one, likely contributes

to the structural conservation of BB [137, 138]. In contrast, Pvd from *Pseudomonas* is constructed like a CLP with a cyclized or linear peptide of 6-14 variable amino acid constituents, bound to a conserved chromophore deriving from dihydroxyquinoline (a modified peptide), and a variable acyl tail (Fig. 7b) [139, 140]. The variability in peptide sequence and acyl chain structure provides pyoverdines with structural diversity that is strain- and context-dependent [116]. Additionally, Pvd biosynthesis genes are arranged on *Pseudomonas* genomes without well-defined structure and with no apparent pattern (Fig. 7c) [141]. Consequently, studies disagree on the affinity of Pvd other than the fact that it is indeed "high". Though BB and Pvd both are multifunctional in their capacity to bind multiple metal ions, Pvd function is not limited to metal chelation, but additionally entails intermicrobial signaling [18]. It is interesting to speculate if this additional functionality derives from the variable structure of Pvd as well as the likely production of secondary siderophores, decreasing the selection pressure for Pvd to evolve into ever-increasing iron affinity. Secondary functions have not yet been identified for BB, even though bacilli similarly harbor multiple iron-uptake systems [106, 142].

In **Study 4**, we described an iron-dependent mutual antagonism between *B. subtilis* and Pvd-producing *P. marginalis*, and found that WT *B. subtilis* with functional BB, could restrict the growth of the *P. marginalis* colony and surround it on King's B (KB) agar. When the *dhb* operon was disrupted, the interaction inverted and *P. marginalis* instead antagonized *B. subtilis*, also restricting colony expansion. In our manuscript, we hypothesized that BB possesses the higher Fe(III) binding affinity of the two siderophores, winning an iron tug-of-war. However, we did not explicitly test this hypothesis, and current published estimations of Fe(III) binding affinities for BB and Pvd do not come to a clear consensus, likely due to non-uniform experimental conditions. We additionally found that the restriction of colony expansion by BB was conserved across fluorescent *Pseudomonas* isolates of different species, and so, if our

hypothesis is true, this would indicate that different pyoverdines all possess lower Fe(III) binding affinities than BB from *B. subtilis*. If this translates to natural systems, it suggests that *B. subtilis* harbors an advantage against *Pseudomonas* in ecological competition for iron.

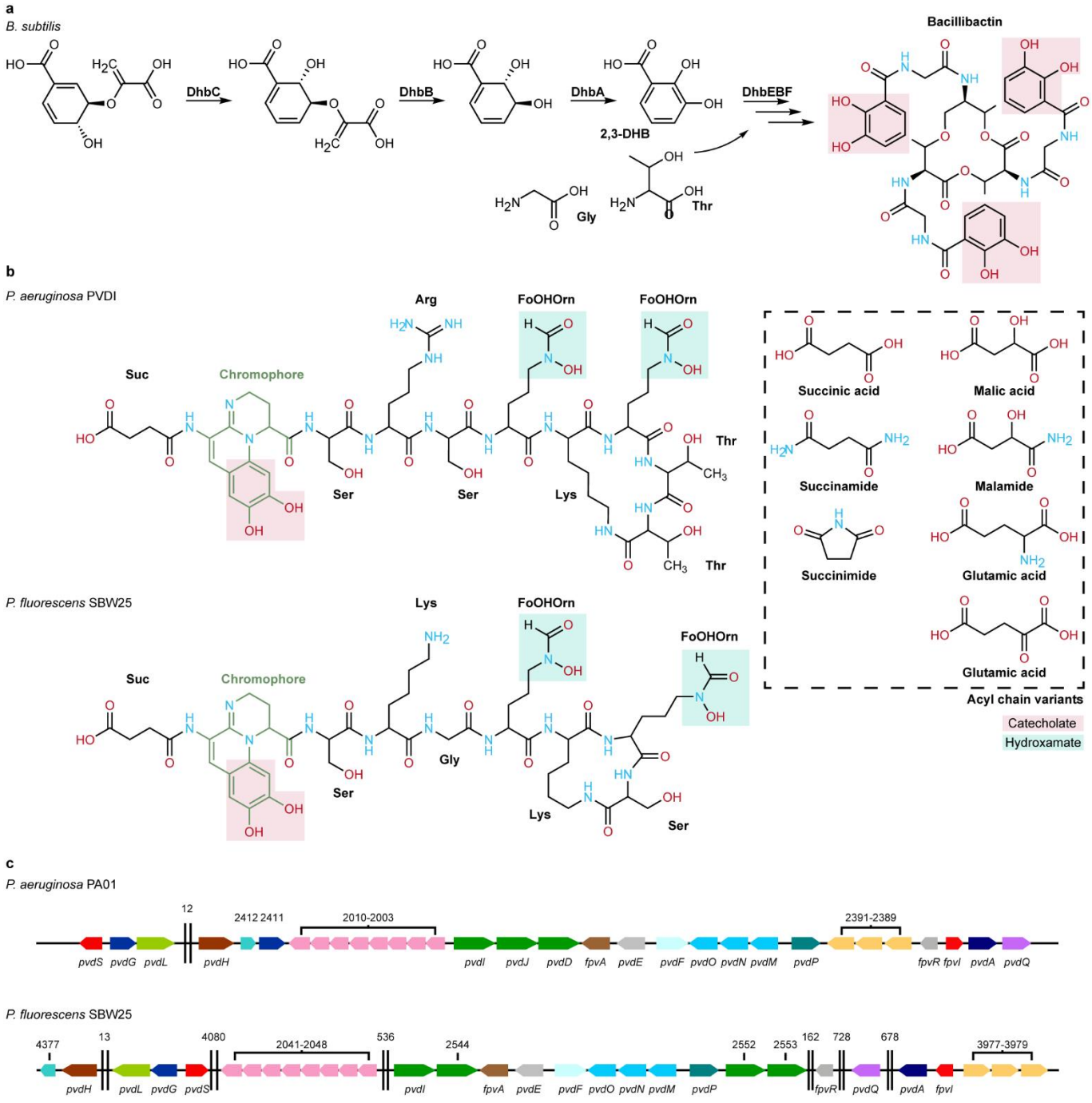

Figure 7 – The siderophores of *Bacillus* and *Pseudomonas*. (a) Bacillibactin is a non-ribosomal peptide synthesized in a multienzymatic pathway to produce 2,3-dihydroxybenzoic acid (2,3-DHB), which is combined with glycine and threonine by the synthetase DhbEBF to yield the chatecolate-carrying (red square) bacillibactin. (b) Pyoverdine (PVD) is structurally different between pseudomonads. It is produced as a cyclic lipopeptide with an acyl moiety of which seven variants are currently known. The acyl chain is bound to a conserved chromophore (green) which is linked to a variable peptide moiety of 6-14 amino acids. The chromophore incorporates a catecholate group (red squares), while the peptide chain carries one or more formyl-hydroxylornithines which have hydroxamate groups (HO-N-COH) on their side chain (blue squares). (c) The genomic arrangement of pyoverdine-synthesizing genes similarly differ between *Pseudomonas* spp. in no apparent pattern. Genes are often spread across the genome with larger spacers between regions resembling mobile genetic elements. (a) recreated from [101], (b) recreated from [139], and (c) recreated from [141].

Polyketides (PKs) are produced similarly to NRPs (Fig. 6b). They are chains of acetate and/or malonate synthesized by polyketide synthases (PKS) which can be modular (commonly associated with bacteria) or iterative (commonly associated with fungi) [143]. The acyltransferase (AT) domain selects, activates, and catalyzes the loading of the starter unit coupled to Coenzyme A (CoA) onto the acyl carrier protein (ACP) domain. The ketosynthase (KS) domain elongates the molecule by catalyzing the condensation of extender units to the growing chain. As with NRPSs, PK synthesis is terminated by a TE domain. Structural diversification is achieved through the implementation of modifying domains such as ketoreductase (KR), dehydratase (DH), and enoyl reductase (ER) domains.

DAPG (2,4-diacetylphloroglucinol) is an important *Pseudomonas* polyketide. Produced mainly by a few species within the *Pseudomonas corrugata* and *P. protegens* subgroups [144], it is widely known for its antimicrobial activity, and has been strongly associated with disease-suppressive soils [145]. DAPG is an instigator of plant exudation of amino acids, providing plant-associated pseudomonads with nutrients [146]. Its biosynthesis is encoded in the *phl* BGC with eight conserved genes, of which *phlDACB* encode the main biosynthetic enzymes. Biosynthesis is initiated by the Type III PKS, PhlD, catalyzing the condensation of three monomers of malonyl-CoA into phloroglucinol. An enzyme complex consisting of PhlACB then acetylates phloroglucinol into monoacetylated phloroglucinol and then DAPG.

Transcriptional regulation of secondary metabolism differs significantly between *Bacillus* and *Pseudomonas*. In *B. subtilis*, regulation is decentralized but likely happens via the switching between lifestyles (Fig. 4). Most BGCs are expressed by distinct cells providing phenotypic heterogeneity, but some are homogeneously regulated by all cells in a population [147]. As mentioned previously, lifestyle in *B. subtilis* is under control of the KinA-E and Spo0ABF phosphorylation cascade. But other systems contribute additionally to this regulation. The DegSU and ComPA two-component systems control natural competence, sessility, and surfactin production [148–150]. All three systems function through phosphorylation of transcription factors, which can be further regulated by response regulator aspartyl-phosphate phosphatases (Rap) and their corresponding phosphatase regulator (Phr) proteins. *B. subtilis* encode many Rap/Phr systems (an average of 11 pairs per strain [151]), each of which are specific in their dephosphorylation target (i.e., RapG is specific to DegU, RapABEHIJP to Spo0F, and RapCDFHKP to ComA) [152, 153]. Rap enzymes and their cognate Phr regulators are transcriptionally coupled [154]. Rap remains intracellular, while Phr is exported to the environment and simultaneously cleaved from its signal peptide [155]. Phr is internalized by an

oligopermase protein (Opp) where it binds and sequesters Rap. When cell density is low, Rap-levels are high and phosphorylated response regulators are dephosphorylated, resulting in a motile, non-surfactin producing, and non-competent cell. Increasing levels of Phr lead to a sessile biofilm lifestyle with surfactin production. Though this system has only been coupled to surfactin, several other antimicrobials are known to be regulated by the biofilm master regulator AbrB. Bacilysin, bacillibactin, plipastatin, bacillaene, and subtilosin A BGCs are all repressed by AbrB [102, 156–159], suggesting that sessile, biofilm-forming cells are also more likely to transcribe the biosynthetic genes involved in antimicrobial production. AbrB is an inhibitor of biofilm formation as it restricts the transcription of genes involved in matrix production and the double negative regulator SinI, and *abrB* itself is repressed by Spo0A~P [160]. NRPSs of *B. subtilis* require activation of the PCP domains by 4-phosphopantetheinyl transferase (Sfp), and the domesticated strain 168, which carries an inactive version of *sfp* is unable to produce surfactin, bacillibactin, plipastatin, and bacillaene [161–163]. Interestingly, *sfp* regulation has not yet been subject to experimental analysis.

In *Pseudomonas*, secondary metabolism is controlled by the regulator of secondary metabolism (Rsm) through the Gac/Rsm system (Fig. 8) [164–167]. Activation of Gac/Rsm induces a lifestyle switch to sessility similar to *Bacillus*, and controls approximately 10% of *P. fluorescens* SBW25, *P. protegens* Pf-5, and *P. chlororaphis* 30-84 genomes [164]. The histidine kinase GacS activates the response regulator GacA, which is a transcription factor for the species-specific Rsm sRNA transcripts. Rsm sRNAs are double negative regulators that bind and sequester Rsm RNA-binding proteins. When not inhibited, the RNA-binding proteins repress transcription of target genes, including secondary metabolite BGCs and alternative sigma factors such as RpoS, AlgU, and PvdS. The activating ligand for GacS has not yet been identified but is expected to happen (at least partly) via self-secreted metabolites, and the GacA response regulator of a specific *P. fluorescens* isolate has been demonstrated to be positively regulated by plant-associated molecules [168]. The two transmembrane receptors RetS and LadS are involved in GacS signal modulation by respectively inhibiting or activating GacS. Stimulation of the activating receptor, LadS, can occur with Ca^{2+}-ions [169].

Of note, BGCs involved in production of DAPG, Pvd, multiple CLPs, pyoluteorin, pectin lyase as well as nitrogen fixation are all under control of Gac/Rsm. Understanding and controlling this system therefore potentiates the control of *Pseudomonas* pathogenicity, biostimulation, and biocontrol activity [170, 171]. Interestingly, GacS/GacA seem to be influenced by *Bacillus*-produced molecules. Zhang *et al.* (2019) found a strong repressor of *P. syringae* pv. *Tomato gacS* transcription in the extract of *Bacillus* sp. BR3 with no effect on cell growth [172]. This downregulation was enough to abolish plant pathogenicity at exposure to 16 µg/mL. In

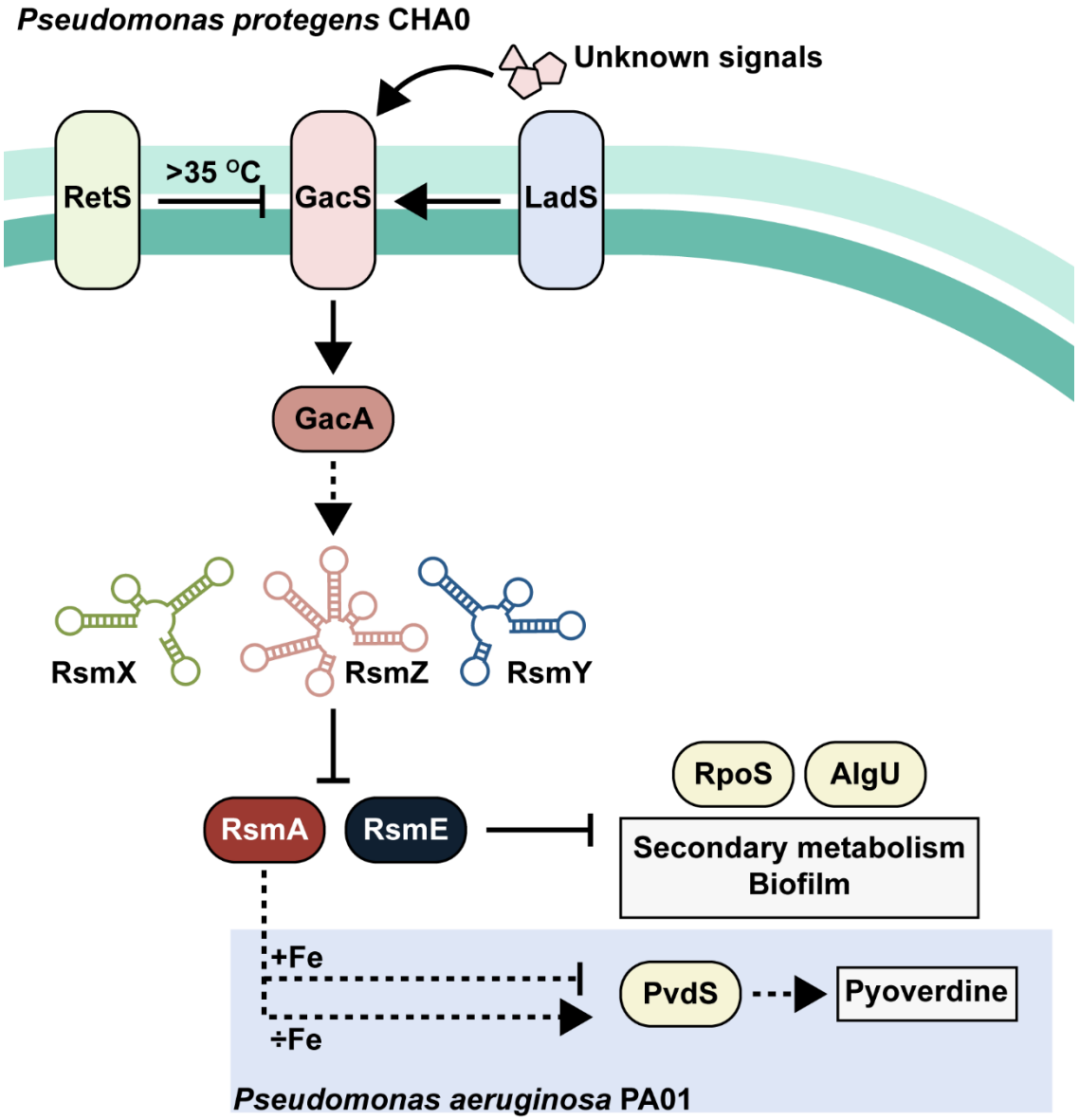

Figure 8 – The Gac pathway of *Pseudomonas.* The Gac/Rsm pathway is a master regulon of lifestyle in many gammaproteobacteria. In pseudomonads, GacS responds to still unknown signal molecules and phosphorylates GacA. Phosphorylated GacA acts as a transcriptional activator for the small RNAs RsmXYZ. The presence of RsmXYZ is species-specific and can include any combination of them. These sRNAs bind and sequester the Rsm proteins which regulate alternative sigma factors RpoS, AlgU, and PvdS thus controlling biofilm lifestyle and secondary metabolism. In *P. aeruginosa*, PvdS-regulation by RsmA is iron-dependent. GacS is further regulated by two transmembrane receptors, RetS and LadS. In *P. protegens* CHA0, RetS is initiated by temperature, which likely is the reason for temperature sensitivity in soil pseudomonads. Recreated from [167, 173, 174].

Study 4 we found a similar result when analyzing the transcriptome of *P. marginalis* where coculture with WT *B. subtilis* reduced *gacS* transcription 2-fold compared to monoculture growth and coculture with a Δ*dhbA* mutant. Whether this downregulation is due to iron starvation has yet to be examined, but we observed that transcription of the iron-starvation alternative sigma factor *pvdS* was upregulated, when *gacS* was repressed. In *P. aeruginosa*, the RNA-binding protein RsmA was demonstrated to impose alternate effects on *pvdS*-expression dependent on iron concentrations, such that excess iron led to negative regulation of *pvdS* while limited iron had the opposite effect (Fig. 8) [173]. Since GacS stimulation results in inhibition of RsmA, the interaction outcome presented in **Study 4** resembles the iron-deplete conditions presented by Peng *et al.* (2020). However, while *pvdS* was upregulated in *P. marginalis*, almost all other *pvd*-genes were downregulated suggesting a secondary regulation of pyoverdine. This hypothesis is corroborated by the findings of Frangipani *et al*. (2013) who found that a Δ*rsmA* mutant of PA01 produced more pyoverdine than the WT under iron-limited conditions [174], where RsmA is expected to positively regulate *pvdS* (and thereby pyoverdine biosynthetic genes) [173]. Additionally, disruption of *gacA* or sRNAs *rsmZ* and *rsmY* resulted in diminished levels of pyoverdine under conditions where PvdS is expected to be present in low abundance. The RsmA-mediated regulation of pyoverdine was found to be independent of Fur, indicating a redundancy in regulation of pyoverdine biosynthetic gene transcription [174].

Ecological roles in the rhizosphere

Plant growth promotion is one of the key properties of *Bacillus* and *Pseudomonas* from a technological perspective. Crops require nutrients in the form of nitrogen, phosphorous, and iron which are often present in forms that are inaccessible. PGPR make inorganic metals bioavailable with nitrogenase, phosphorous solubilization, and siderophores, respectively. Atmospheric nitrogen (N_2) is converted to ammonia (NH_3) via the ATP-consuming nitrogenase encoded in the *nif* gene cluster [175]. Nitrogenase activity is not conserved in bacilli or pseudomonads but has been demonstrated both in the *Bacillus cereus* and *B. subtilis* groups as well as in the *P. stutzeri* group and the *P. koreensis* and *P. entomophila* subgroups [176–179]. Members of both genera are also able to solubilize inorganic phosphate by incorporating phosphoryl into organic acids [180, 181]. Plants can perform this process themselves but delegating it to symbiotic microbes would allow for specialization into other traits. BB and Pvd have been shown to alleviate iron deficiency by modulating plant iron uptake systems, and possibly by functioning as exosiderophores [182, 183].

Bacteria can also directly alter plant physiology, similarly to human gut microbes. *Arabidopsis thaliana* produces larger leaves, when exposed to the volatile compounds, acetoin and 2,3-butanediol by changing the homeostasis of cytokinins (cell division promoters) and ethylene (growth and senescence regulator) [184]. A blend of *B. subtilis* volatiles causes *A. thaliana* to redistribute auxins from leaves to roots, alleviating negative regulation of leaf size, and promoting root formation [185]. *Pseudomonas* similarly produce both auxins, cytokinins, and volatile signal molecules, stimulating root branching and stress tolerance [181, 186, 187].

Plants attract PGPR to their root systems because roots secrete a collection of exudates. Exudates are species specific in their composition of macromolecules and secondary metabolites and act as nutrient reservoirs, toxins, and signaling molecules for microbes [87, 188, 189]. *Bacillus* and *Pseudomonas* are chemotactic towards exudates from a variety of plants, and the association with plants create a mutualistic relationship where the bacteria gain carbon-based nutrients while protecting the plant and providing the plant with growth stimulating molecules. When nutrients are not automatically provided, the bacteria may acquire those themselves. *B. velezensis* secretes the type seven secretion system effector protein YukE which inserts in the plant root to create a pore-like structure that specifically leaked iron [190], while *Pseudomonas*-produced DAPG and phenazine has been shown to increase amino acid efflux from plants 16-fold [146]. The nutrients supplied by the plant are important for proper differentiation of PGPR. When *B. subtilis* reaches the root, it starts producing biofilm. *Bacillus* mutants deficient in matrix production have been demonstrated to be unable to efficiently colonize the roots of tomato and *A. thaliana* [45] and when evolved in the presence of Arabidopsis or tomato, mutations preferentially establish in the *sinR* gene, creating a biofilm hyper-producing phenotype [87, 191]. Recently, biofilm production was additionally demonstrated to be selected for when *B. subtilis* was evolved in the presence of a competing *Pseudomonas fluorescens* on tomato roots [191]. The mutations in biofilm repressors provided *B. subtilis* with an advantage in subsequent root colonization against *P. fluorescens*, *P. protegens*, *P. capeferrum*, and *P. stutzeri*. Biofilm as protection against *Pseudomonas* has been demonstrated on multiple occasions, both *in vitro* and *in situ* [192–194], and in **Study 2**, we established biofilm formation and sporulation as defensive features for *Bacillus* when in contact with *Pseudomonas* spp.

In addition to their mutually beneficial interaction with plants, *Bacillus* and *Pseudomonas* also seem to preferentially recruit each other, once established. The addition of *B. velezensis* to cucumber roots enriched the rhizosphere microbiota for *Pseudomonas* and *Pseudoxanthomonas* resulting in increased cucumber plant growth [36], while the addition of *B.*

amyloliquefaciens to banana plants mobilized the residing pseudomonads increasing the ability to fight off plant-pathogenic *Fusarium oxysporium* [195]. Synthetic addition of *Bacillus-Pseudomonas* consortia has also resulted in alleviation of drought and salt stress [36, 123]. Importantly, strains that are incompatible *in vitro* can be combined *in situ* and even result in trait synergy [196].

Biocontrol activity is a hallmark of bacilli and pseudomonads. Their arsenals of secondary metabolites have been shown to harbor antimicrobial properties against both fungal and bacterial pathogens. Biocontrol can occur either passively in a competition for space or nutrients or actively with the production of specific antimicrobials, and finally indirectly by inducing the plant systemic resistance [197]. Passive biocontrol is probably a major reason for bacteria associating with plants due to the evolutionary selection for species that do not cause harm to the plant [198]. Siderophores are largely thought to confer passive competition by sequestering iron from pathogens, restricting their growth. Both BB and Pvd have been reported on multiple occasions to reduce disease incidence and pathogen colonization [199–201]. Surfactin has been shown to create pores in membranes of some (but not all) competitors [126, 202]. With the role that surfactin plays in plant root colonization, there is a chance that some reported biocontrol studies where surfactin is essential actually show how surfactin mediates passive biocontrol by providing *Bacillus* with a colonization advantage [192, 203].

Both *Pseudomonas* spp. and *Bacillus* spp. are well known for eliciting systemic resistance against pathogens in plants, *Bacillus* mainly through 2,3-butanediol, surfactin, and fengycin [197] and *Pseudomonas* through flagella, siderophores, and DAPG [204], though, very few examples exist of either priming plant defenses against the other. *B. cereus* has been shown to instigate *Arabidopsis thaliana* systemic resistance against *P. syringae* pv. *tomato* both dependent and independently of salicylic acid, jasmonic acid, and ethylene signaling [205–207].

Bacillus and *Pseudomonas* generally engage in active biocontrol. In **Study 2**, we found that most pairwise interactions between bacilli and pseudomonads are negative and classified many of them as amensalistic owing to the lack of documented effects on the killing strain. In most instances, *Pseudomonas* conferred a negative fitness effect on its *Bacillus* partner, with *Bacillus* biofilm formation and sporulation acting as defensive measures keeping a subset of the population alive. However, it is likely that hidden fitness effects were simply never identified, and that these interactions instead are antagonistic or competitive. Killing neighboring cells frees up space and nutrients establishing a positive effect on the killing strain. In several studies, the negatively affected strain was not outcompeted, possibly because of defensive measures, but

also potentially because of opposing offensive measures resulting in competition. Indeed, several studies did document negative effects on both interactants.

Phytopathogenicity is another trademark of fluorescent pseudomonads. A variety of pathogens are phylogenetically nestled in between fluorescent PGPR pseudomonads, underpinning the thin line between plant pathogen and PGPR. These organisms are threatening the agricultural economy as they infect virtually all modern crop species. Interestingly, taxonomy is not a clear indicator of pathogenicity and species heavily associated with pathogenicity have repeatedly also included non-pathogenic isolates. With *Pseudomonas* spp., pathogens are particularly prevalent in the *P. syringae* group but also in the *P. fluorescens, P. corrugata,* and *P. asplenii* subgroups of *P. fluorescens* [111, 208–212]. The *P. syringae* group has been studied extensively and is one of the best understood phytopathogens today [111]. Its pathogenicity stems from a tripartite pathogenicity island which includes a type three secretion system (T3SS) and several conserved and variable T3SS effector molecules (T3E). It is also able to cause host cell death (termed "hypersensitivity"), ice nucleation, and inactivate auxins. This results in an opportunistic pathogen that can sustain itself on the phylloplane with no symptoms before it breaches the surface and enters the plant tissue. Other than T3SS, *P. syringae* strains produce the lipodepsipeptide CLPs syringopeptin and syringomycin. While they are not essential for pathogenicity in *P. syringae,* they do contribute substantially to virulence, and other species that produce structurally similar metabolites are similarly pathogenic [124, 213]. In fact, many virulence factors of plant pathogenic pseudomonads are secondary metabolites that are controlled by the Gac/Rsm regulon, along with plant-beneficial metabolites [214]. *P. marginalis* pathogenicity originates from its pectate lyase and protease activity, which is essential for plant pathogenicity [209], *Pseudomonas tolaasii* produces the tolaasin CLPs which causes brown blotch on edible mushrooms [215], and *P. corrugata* produces corpeptin A and B [216]. Thus, it seems that *Pseudomonas* plant pathogenicity is strongly associated with secondary metabolomes and that pathogenicity can be controlled via the Gac/Rsm system. The evolution of pseudomonads to become pathogenic or plant growth promotional is yet to be elucidated, and more research is needed to understand if pathogenicity generally stems from vertical or horizontal evolution. However, the association of specific lipodepsipeptides with pathogenicity is intriguing: Did pathogenicity cause CLP function or is the reverse true?

Chapter 4 – Predicting microbial interactions

Phylogeny is the study of evolutionary relationships between organisms. Originally proposed by Ernst Haeckel in the late 19th century, phylogeny was inferred from morphological traits in a similar manner to how Charles Darwin examined the beaks of Galapagos finches [217]. In "The Origin of Species", Darwin described how he expected closely related organisms to be more likely to compete due to potential niche overlap which would be less prevalent in organisms that were distantly related [218]. In the same century, Thomas Huxley observed how similar traits can evolve independently in convergent evolution [219], explaining the low phylogenetic accuracy that morphology provides. Once nucleotides were discovered to encode the genetics of organisms, conserved DNA elements were rapidly adopted as novel tools of phylogenetic inference, sparking a revolution in phylogenetics and taxonomy. At this point, phylogeny became quantifiable and phylogenetic trees, describing the evolutionary relatedness between organisms, progressed from visualizations to analytical tools. Taxonomy (the classification of organisms into hierarchical levels) followed the development of phylogeny and organisms were divided into genera and species based on specific DNA sequences. For decades, the gene encoding the small ribosomal subunit has been the gold standard for phylogenetic analysis of bacteria as well as for taxonomic classification [220]. Decades of 16S analysis have revealed its strengths and weaknesses. To this day, sequencing of genes encoding the 16S subunit remains favorable due to low cost and high speed, but with their limited length, 16S-encoding genes carry only a portion of available phylogenetic information. Additionally, some organisms have been found to be polyallelic for ribosomal subunit genes, with distinct information on each allele, complicating both phylogenetic analysis and taxonomic classification (*Bacillus* is polyallelic for 16S) [221]. With the exponential developments in whole-genome sequencing, phylogeny is now often inferred from entire genomes increasing the available nucleotide information several thousand-fold [222, 223]. Even still, accurate prediction from bacterial phylogenetics proves difficult. In addition to vertical evolution, bacteria also undergo a significant amount of horizontal evolution. Naturally competent cells can take up DNA and incorporate it on their own genomes or as transferable genetic elements. Pathogenicity islands and bacteriophage elements can have sequence lengths of hundreds of thousands of base pairs and comprise a substantial part of the bacterial genome [111, 224]. Thus, an otherwise clonal population can diverge enormously with a single horizontal gene transfer event.

Darwin's hypothesis of relatedness sparking competition later became, together with the Environmental Filtering hypothesis (differences in environmental tolerances increase with

phylogenetic distance), the focus of understanding ecology using phylogenetics. These studies investigate the role of "relatedness" in interactions between organisms. Relatedness here is a broad term. Two phylogenetically distant organisms can converge on similar spatial and nutritional niches. Therefore, microbiologists often describe both phylogenetic and metabolic relatedness [57]. Indeed, close metabolic relatedness has on multiple occasions followed the competition-relatedness hypothesis [225, 226], but close phylogenetic relatedness can result in non-competitive kin recognition [227]. Some studies find an antagonistic "peak" at an intermediate phylogenetic relatedness that is distant enough to not outcompete kin, yet not so distant that the two organisms have nothing in common [225, 228]. Interestingly, this peak is present both with resource and interference competition, suggesting that interference competition is a mechanism of resource competition (i.e., organisms competing for resources utilize antimicrobials to outcompete each other). However, some argue that the interplay between exploitative and interference competition is evidence that the theorized relationship between phylogeny and competition should be put under scrutiny. Naughton *et al.* (2015) cocultured eight species of green algae and found no correlation between phylogenetic and competitiveness, arguing that most studies concurring with the competition-relatedness investigate pairwise interactions, which do not translate to communities (see Translatability of Pairwise Interactions) [229]. A large-scale study on prediction of pairwise interactions did demonstrate that phylogenetic distance correlated positively with predictive ability, and interactions proved conserved within a taxonomic unit but vary between units [57]. Additionally, phylogenetic and metabolic distance were found to be equally good predictors, and both were outperformed by information on monoculture growth which proved a superior predictor (i.e., a fast-growing organism outcompetes a slow-growing organism irrespective of relatedness). Others have found that the (lack of) phylogenetic accuracy has obscured interaction patterns, solidifying the necessity of well-defined taxonomy or accurate measures of phylogeny [230].

An alternative explanation could be that phylogenetics cannot explain patterns of interactions and community assembly. When coculturing closely related *Streptomyces* soil isolates from a single grain of soil, interactions were demonstrated to be broadly and bimodally distributed and an isolate either inhibited or facilitated most other isolates [231]. These interactions were, however, dramatically different even across isolates with almost identical 16S rDNA sequences, demonstrating a low correspondence between phylogeny and interaction sign and strength. A comparison of *Streptomyces* interactions between three soil sites, found interaction network distributions to differ significantly, such that each site displayed a separate preference

for triad interactions despite the high phylogenetic relatedness between samples [232]. The authors of these studies assert that rapid co-evolution contributes to the development of interaction networks and that a continuous co-evolutionary arms race is responsible for inhibitory interactions. In a recent preprint, Pomerleau *et al.* (2023) subjected *B. subtilis* to adaptive laboratory evolution with three strains of fluorescent pseudomonads and found that rapid evolution increased the competitive potential of *B. subtilis* [191]. With the distant phylogenetic relatedness between *Bacillus* and *Pseudomonas*, members of these genera are not expected to compete under the competition-relatedness hypothesis. However, if local co-evolution is a stronger determinant for intermicrobial interactions than phylogeny, it could explain the prevalence of antagonistic interactions among bacilli and pseudomonads. It does not, however, explain the taxonomic conservation of interactions.

Taxonomy of *Pseudomonas* spp. predicts interactions with *B. subtilis*

In place of phylogeny, many microbiologists turn to taxonomy. In zoology, traits can often be inferred from morphology and reveal much information about the lifestyle of an animal. Microbes are too small for rapid morphological analysis, and elucidating their traits requires specialized equipment. Thus, traits are often inferred from homology. When an organism is found to exhibit some phenotype, organisms of the same taxon are expected to present a similar phenotype. Taxonomic classification is often a first step in describing a microbiological isolate, and once placed in a genus or species, much can be deduced about its metabolism and physiology without requiring high phylogenetic accuracy. This does require a certain degree of trait conservation within taxa. As interactions between *Bacillus* and *Pseudomonas* are mediated by their secondary metabolites [20], BGCs represent traits that must be taxonomically conserved to be useful for interaction predictions. Indeed, as noted previously, *Pseudomonas* accessory genomes have evolved with their core genomes [110, 114], suggesting little horizontal gene transfer, and consequently high species-specific BGC conservation. In contrast, a key property of bacilli is their natural competence, which can cause divergent phylogeny between *B. subtilis* isolates. Even so, BGCs have been demonstrated to be conserved across *B. subtilis* isolates [126].

In **Study 3**, we attempted to predict interaction outcomes between *B. subtilis* and fluorescent pseudomonads from taxonomy. A fluorescently labeled *B. subtilis* strain was cocultured with 720 soil isolates revealing a context-dependent taxonomic conservation of interactions. Interaction signs and strengths were quantified in one direction (isolate affecting *Bacillus*). We

chose the *B. subtilis* pellicle as our model system as pellicle formation has been shown to correlate positively with plant root colonization [88]. With a medium-throughput screen based on a spinning disc confocal microscope, the pellicle biovolume could be determined in monoculture and coculture and interaction strength could be expressed as the fold change in pellicle biovolume (Fig. 9). The isolate library was screened in two types of media either rich (tryptic soy broth - TSB) or diluted (LB supplemented with glycerol and manganese - 0.1 × LBGM). Context dependency was immediately apparent from the stark difference in interaction distributions in the two types of media. In rich media, interactions were predominantly neutral, while diluted media yielded equally many neutral and negative interactions. Based on their interaction with *Bacillus* in dilute media, we categorized each isolate either as neutral, negative, or positive and used an amplicon sequencing approach to taxonomically classify the isolates at the species-level (Fig. 10).

The taxonomy of the soil isolates revealed a statistically significant enrichment for specific taxa in each screening category suggesting that *P. protegens* and *P. capeferrum* are likely to harbor strains that negatively affect *B. subtilis*, while *Pseudomonas trivialis* and *P. lini* likely comprise strains that positively affect *B. subtilis*. Intriguingly, we confirmed our taxonomic predictions by coculturing *B. subtilis* with closely related reference strains from separate isolation sites. Thus, we demonstrated the ability to predict *B. subtilis* fates from *Pseudomonas* taxonomy. However, these predictions are (like the interactions themselves) context dependent. For instance, *P. capeferrum* was able to inhibit *B. subtilis* in pellicle regardless of medium concentration, but it was unable to inhibit on agar surfaces. Still, the fact that most interactions between *B. subtilis* and fluorescent pseudomonads are negative contrasts the competition-relatedness hypothesis. One explanation could be that their metabolic relatedness is high due to convergent evolution. A systematic investigation of *Bacillus* and *Pseudomonas* metabolomes

have yet to be performed. Metabolic simulation of communities with up to 40 members have revealed interaction polarization into cooperative and competitive communities, diverging in genome size, metabolic potential, and antimicrobial production. Competitive isolates feature larger genomes and are mainly present in soils, both of which are characteristics of bacilli and pseudomonads.

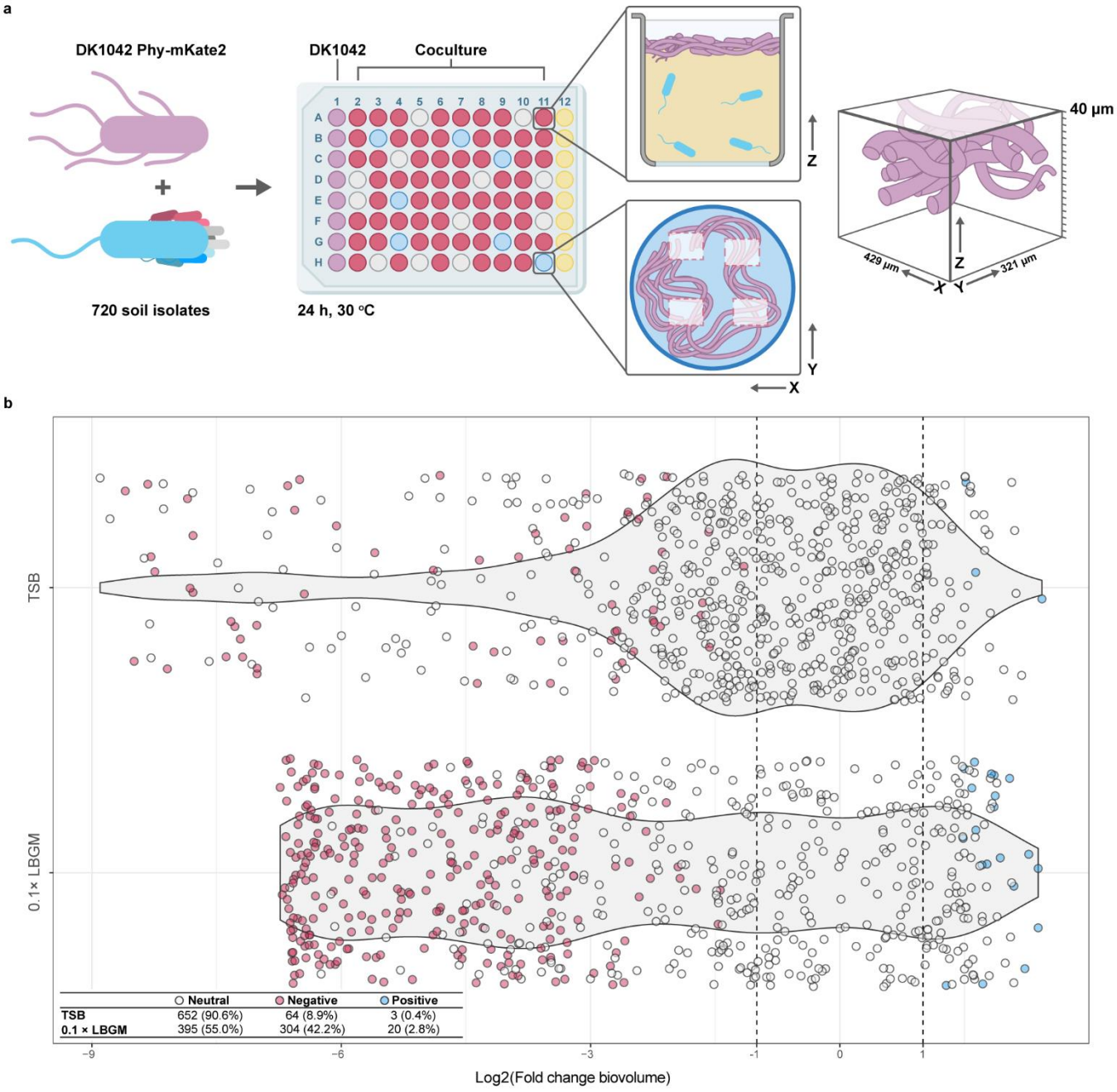

Figure 9 - Pseudomonads negatively affect *B. subtilis*. a: *B. subtilis* DK1042 constitutively expressing mKate2 was mixed pairwise with 720 fluorescent soil isolates and grown statically for 24 h at 30 ºC in a microplate format. Monocultures of DK1042 (purple wells) were used for comparison of pellicle formation, and wells with non-inoculated medium (yellow wells) were used to control for contamination. Each well was imaged in four positions with a Perkin Elmer Opera QEHS, acquiring images in the Z-direction every 2 µm to obtain a cube with height 40 µm. Media was removed prior to microscopy. **b:** DK1042 biovolumes were compared between co- and monoculture to yield a $\log_2$(Fold Change). Points represent median of three replicates. Neutral, negative, and positive categories were assigned based on median and interquartile range. Figure from **Study 3.**

Thus, the prevalence of competition between these two genera may stem from their large genomes and high potential for secondary metabolite production, and these may have evolved due to a continuous arms race, that does not depend on phylogeny. Were this to be the case, it would be rather remarkable that the interactions are conserved on a taxonomic level. This suggests that bioactive secondary metabolites (in these genera) are highly conserved and can be

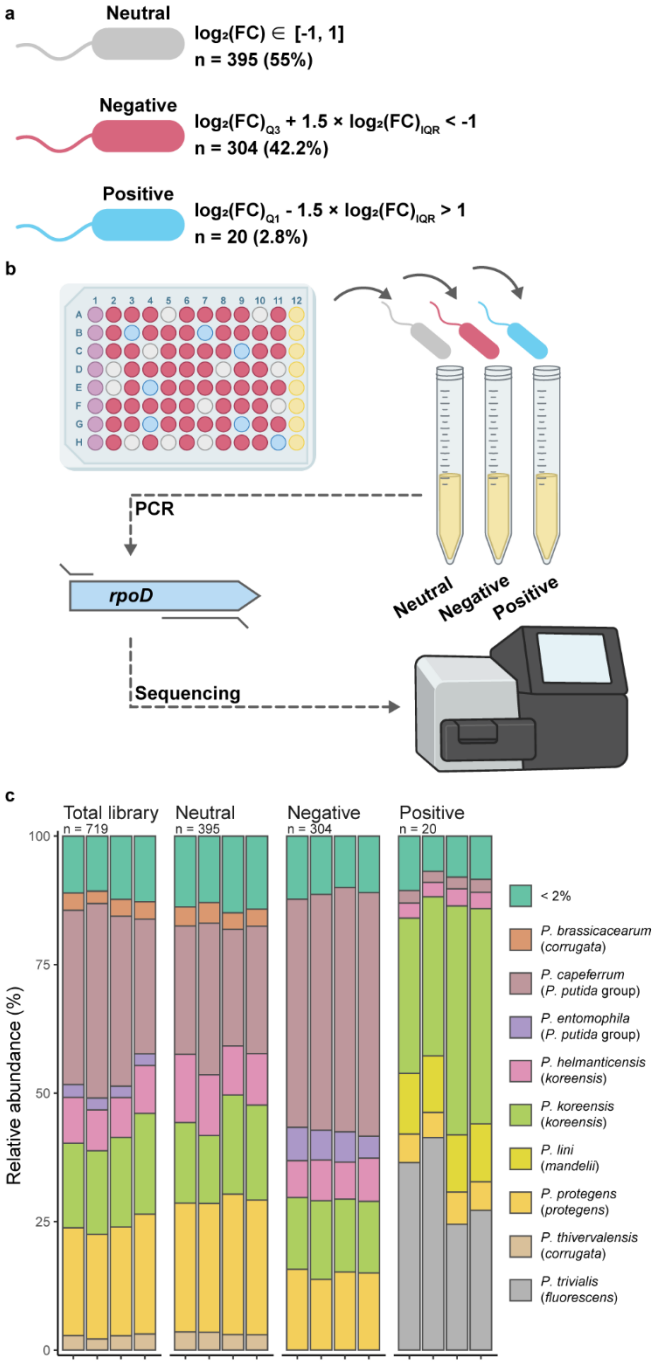

Figure 10 - Screen categories are enriched for species-specific taxa. a: Fluorescent isolates were assigned a category based on median and interquartile range, such that negatives resulted in *Bacillus subtilis* DK1042 $\log_2(FC) < -1$ and positives in $\log_2(FC) > 1$. n and percentages are from screen in 0.1× LBGM. **b:** Isolates were grown in precultures and pooled in equal cell numbers according to their categorization, to taxonomically characterize each category on a species level with *rpoD* amplicon sequencing. **c:** Relative abundance of *Pseudomonas* spp. in each category. Parentheses indicate group or *P. fluorescens* subgroup. Taxons comprising less than 2% of a pool has been merged. Figure from **Study 3.**

inferred from taxonomy. With the effort in coculturing PGPR for emergent traits, there may be value in determining taxon-specific interaction outcomes under relevant conditions. Once the molecular mechanism of the interaction is identified, the presence of that specific trait can be used as a biomarker. As others before us, we found that the antagonistic activity of *P. protegens* was likely conferred by DAPG production [78, 201] and were able to use the biosynthetic gene *phlD* as a biomarker for *B. subtilis* inhibition. We did not identify effector molecules for *P. capeferrum* inhibition or for *P. trivialis* and *P. lini* pellicle promotion but once identified, such molecules could potentially be used for future screenings of *Bacillus*-compatible pseudomonads.

An important caveat of our study continues to be the translatability of pairwise interactions. The interactions in our setup depended on both nutrient composition and cultivation lifestyle, and it is very probable that an increase in complexity (via the addition of microbes) will alter the interaction outcome. It would be interesting to expand our screen and test how the presence of *Pseudomonas* spp. affects *B. subtilis* in a community.

Chapter 5 – The sociomicrobiology of iron

Iron is one of the most abundant metals in the soil. However, most iron is oxidized into the insoluble ferric state that precipitates into particles too large for cells to take up. The propensity of iron to undergo redox reactions renders it essential to many biological processes. Thus, organisms need to scavenge iron in fierce competition with each other often utilizing siderophores [136]. The physiological consequences of iron competition have been studied ever since desferrioxamine was discovered in 1949 and are very well understood. Less rigorously studied is the ecological impact of siderophore- and iron competition.

Siderophores are not the only iron uptake mechanisms in bacteria. Many organisms additionally possess the EfeOUB system for uptake of soluble Fe(II) (ferrous iron) and systems for uptake of Fe(III) bound in organic molecules such as citrate and heme [233]. But it is arguably siderophores that drive most of iron-mediated microbial ecology. Most species have a primary siderophore (i.e., the siderophore with the highest affinity for iron) and can have secondary siderophores as well[108, 139]. When the molecules are secreted to the surroundings, they dissolve Fe(III) bound in <10 nm hematite (Fe_2O_3) and ferrihydroxide ($Fe_x(OH)_y$) particles, by displacing oxygen bonds with those located in the siderophore functional groups [234, 235]. The amino acid backbones facilitate dissolution of the ferri-siderophore complex, and the insoluble mineral deposits are converted into Fe(III) that can be taken up by a cell. Uptake of ferri-siderophore complexes occurs through specialized systems specific to the siderophore. Gram-negative species typically utilize membrane-bound receptors to recognize the iron-loaded siderophore and transport it across the outer membrane [136]. Much of Pvd post-synthetic modification happens in this periplasmic space, and it is here that iron dissociates from Pvd before it is transported into the cytosol [140]. Pvd, however, is not present in the cytosol. When Pvd is synthesized, the initial NRPS product is a non-fluorescent ferribactin. This is transported into the periplasmic space where it matures to functional Pvd. When Pvd has collected iron extracellularly, it can be recycled in the periplasmic space for additional use. Gram-positives do not possess an outer membrane and therefore transport their siderophore directly into the cytosol via ATP-binding cassette transporters [106].

In addition to their own primary siderophore, bacteria can utilize secondary siderophores and even foreign siderophores from other species [236, 237]. Thus, siderophores can be common resources, which potentiates their involvement in all resource-based interactions described in **Chapter 2** – Interactions in microbial ecology and indeed, siderophores have been the subject of syntrophy, division of labor, cheating, and competitive exclusion [136]. Pyoverdines,

are often shared among *Pseudomonas* spp. In Gram-negative bacteria, siderophores are taken up by TonB-dependent receptors, and though they are quite specific and bind molecules other than siderophores [238], the abundance of receptors encoded in the genome roughly correlates with the number of foreign pyoverdines a strain can internalize [239]. As such, pseudomonads can cross-feed on pyoverdines that are structurally dissimilar from their own cognate pyoverdine. *P. thivervalensis* LMG21626^T has been shown to utilize 13/31 foreign pyoverdines with 6-10 amino acids [240], *P. protegens* Pf-5 can utilize 17 distinct pyoverdine structures [241], and *P. entomophila* L48 16/24 [242] (pyoverdine structures differ across studies and cross-feeding capability cannot be directly compared between strains). Interestingly, pyoverdine cross-utilization is not shared between closely related strains [242], suggesting horizontal gene transfer. Indeed, Cornelis and Bodilis (2009) found that 11 genomes from the *P. aeruginosa*, *P. putida*, and *P. syringae* groups shared only a single core TonB-dependent receptor, while the rest were accessory genes, some of which were strongly orthologous between phylogenetically distinct genomes [243]. Some receptor-encoding genes were duplicated or even triplicated, and others clustered on "receptor islands". In *P. aeruginosa*, it has been demonstrated that adaptation to the cystic fibrosis lung involves deletion of TonB-dependent receptor genes, illustrating that such rearrangement is possible [244]. Butaité *et al.* (2017) examined a collection of 315 *Pseudomonas* isolates from soil and freshwater sources and found that 9% were pyoverdine non-producers that were facilitated in low-iron environments by pyoverdine producers [245]. Thus, pyoverdine cross-utilization is a major influence on shaping the ecology of pseudomonads.

A similar structural diversity is not present with BB, and thus *B. subtilis* ecology does not seem to depend on the acquisition of different bacillibactin receptors. It is, however, capable of taking up xenosiderophores from distantly related genera in a process known as siderophore piracy. Enterobactin (Ent) is structurally similar to BB and both are internalized by FeuABC-YusV, but in the cytoplasm, each siderophore is hydrolyzed by a distinct esterase (BesA for BB and YbbA for Ent) [237]. Transporters have also been found for petrobactin (produced by *B. cereus*), ferrioxamine E (*Streptomyces olivaceus*), ferrichrome (*Ustilago maydis*), arthrobactin (*Arthrobacter pascens*), and ferri-dicitrate (*Bradyrhizobium japonicum*) [246]. Interestingly, reports of siderophore piracy by *Bacillus* describe induction of differentiation. Upon hydrolyzation of exogenous and endogenous siderophores, sporulation is induced, likely by an iron-mediated regulation [237]. In contrast, perception of enantio-pyochelin from *P. sessilinigenes* stimulates the production of bioactive secondary metabolites in *B. velezensis* [18]. The small

structural similarity between BB and Ent is expected to stem from divergent evolution, though the order of appearance is unknown [247].

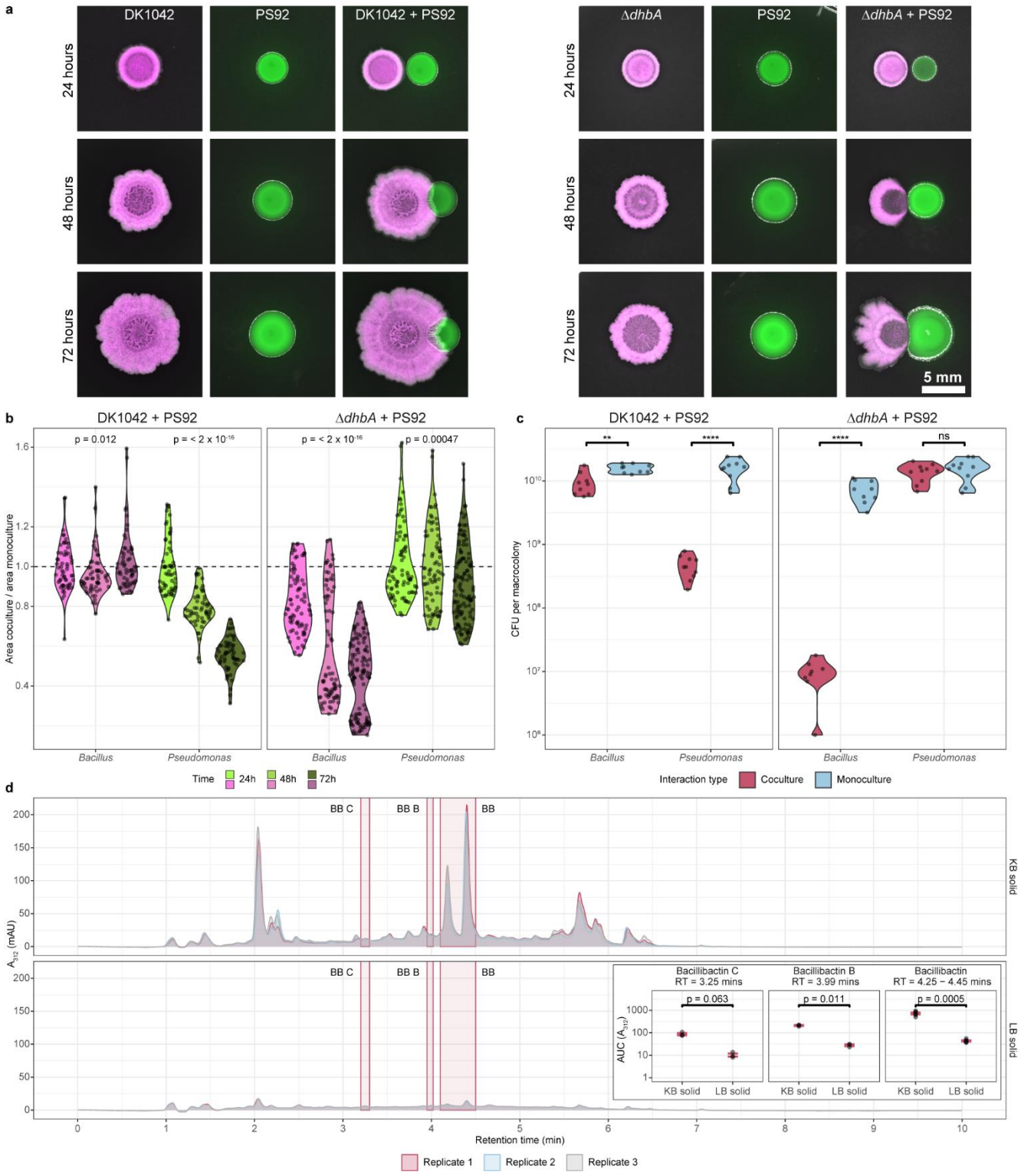

Figure 11 – Bacillibactin-dependent antagonism. a: *B. subtilis* DK1042 (mKate2, magenta) and *P. marginalis* PS92 (msfGFP, green) were cocultured on KB agar with 5 mm between colony centers and imaged every 24 h. Scale = 5 mm. b: Coculture colony area was normalized against monoculture colony area and plotted for each partner (x-axis) in the two interactions (facets). The dashed line indicates coculture = monoculture. The p-value was calculated by analysis of variance (ANOVA) within groups (n = 40 colonies from two independent experiments). c: Colony-forming units were determined from the macrocolonies in co-culture and monoculture. Significance stars are from Student's t-tests (n = 10 colonies from two in-dependent experiments; **p <0.01, ****p <0.0001; ns: not significant. d: Ultra-violet quantification of LC-MS on DK1042 monocultures at λ = 312 nm. Bacillibactin and isomers in KB (above) and LB (below). BB, Bacillibactin; BB B, Bacillibactin B; BB C, Bacillibactin C. Inset: Peak area under the curve (AUC) of bacillibactin and isomers in KB and LB. Labels are p-values from Student's t-test (n = 3 independent experiments). Figure from **Study 4.**

The presence of Ent-utilizing mechanisms in *B. subtilis* suggests that BB evolved from Ent, and the associated sporulation response would therefore be part of the typical regulatory framework in *Bacillus*. The secondary metabolite-mobilizing response to *P. sessilinigenes* siderophores was found to be stronger in the presence of enantio-pyochelin than pyoverdine, suggesting that iron is not the mediator of this response [18]. Thus, it seems that *Bacillus* can use iron from siderophores when their uptake systems have been evolutionarily preserved but that siderophores that are not evolutionarily related to *Bacillus* instead may function as signal molecules for perceiving competitors.

B. subtilis and *Pseudomonas* compete for iron

The competition for iron between *Bacillus* and *Pseudomonas* is largely understudied. With **Study 4**, we investigated the implication of BB in pairwise interactions between *B. subtilis* and *P. marginalis*. We found that BB is essential for proper inhibition of *P. marginalis* by *B. subtilis* (Fig. 11). This inhibition was context dependent, such that only growth on solidified siderophore-inducing KB medium produced the phenotype. Growth in liquid media or in lysogeny broth (LB) did not reproduce the bacillibactin-mediated antagonism. Liquid chromatography mass spectrometry (LC-MS) suggested this to be a consequence of a strong reduction in BB production on all media types other than solidified KB. We confirmed that BB and not DHB was the mediator of antagonism by coculturing single gene deletion mutants each disrupted in a gene of the *dhbA-F*-operon next to *P. marginalis* and demonstrating that no mutant (regardless of gene disruption) was able to antagonize *Pseudomonas*. Interestingly, we found that intermediates of the Dhb pathway could be secreted and utilized as common resources by the mutants. Specifically, a mixture of Δ*dhbA* and Δ*dhbF* mutants were able to complement each other to antagonize *P. marginalis* to a similar degree as the wild type. The Δ*dhbA* mutant was severely reduced in biofilm formation, to a stronger degree than the other Δ*dhb* mutants. Correspondingly, Δ*dhbCEF* were less inhibited than Δ*dhbA*, corroborating the hypothesis that *Bacillus* biofilm formation is important for protection against pseudomonads.

The mutual inhibition was determined to be dependent on iron, and any addition of iron regardless of source and concentration restored Δ*dhbA* fitness. The antagonism of a Δ*feuA* mutant, unable to internalize ferri-BB, could not be restored by $FeCl_3$ but was restored in a concentration-dependent manner by ferric citrate (which is not taken up by BB), suggesting that antagonism is mediated by an antibiotic that is regulated through iron homeostasis. However, transcriptomic and metabolomic analysis of the cocultures did not identify any well-known

secondary metabolite to be differentially expressed in the *B. subtilis* WT compared to Δ*dhbA* (Fig. 12). Rather, genes involved in sporulation and germination were generally downregulated in Δ*dhbA*, but when testing a sporulation-deficient Δ*sigF* mutant, antagonism was not abolished. Mass spectrometry imaging additionally revealed that *P. marginalis* pyoverdine production was repressed in coculture with *B. subtilis* WT compared to Δ*dhbA*. From the transcriptomic data, we found that most of the Gac/Rsm regulon was downregulated in the WT interaction, including pyoverdine, type six secretion system, and alginate. The increase in *pvdS* transcription defied our expectations, and as explained in **Chapter 3**, is indicative of a negative regulation by GacA, under the conditions outlined by Peng *et al.* (2020) [173], though it contrasts the findings of Frangipani *et al.* (2013) [174].

Whether iron starvation or repression of Gac (or both) is the antagonizing factor is yet to be studied. Experimentally, this could be determined via competitive culturing with heterologous apo-siderophores or single-gene deletion mutants. Both outcomes have interesting implications in biocontrol and in the use of coculture formulations of *Bacillus* and *Pseudomonas*. We cocultured *B. subtilis* with a collection of local *Pseudomonas* soil isolates and found the surrounding and restriction of the *Pseudomonas* colony on KB to be conserved across species. These pseudomonads belong to the *P. fluorescens* group and comprise both PGPR and phytopathogens. Understanding the ecology between them and *Bacillus* allows for a more efficient formulation of cocultures and a better comprehension of the consequences of applying each bacterium to agriculture. However, to fully understand the implications of BB on *Pseudomonas* soil ecology, these hypotheses should be tested *in situ*. As explained in **Chapter 2**, microbial interactions are always context-dependent, and the medium-dependency of this interaction underpins this notion. Thus, additional experimentation will be needed to determine if these results can be translated to applied settings.

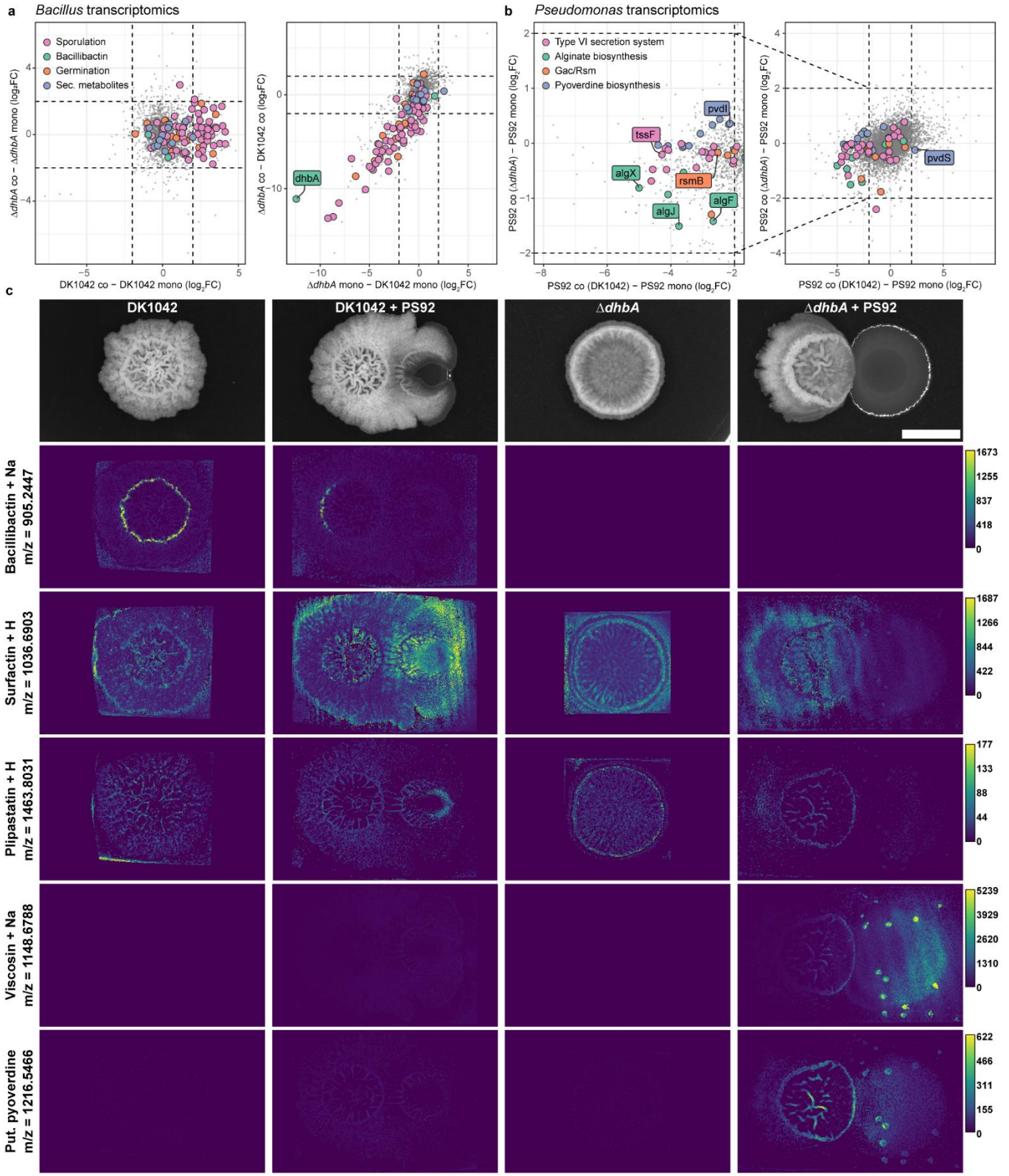

Figure 12 – *B. subtilis* alters *P. marginalis* transcriptome and metabolome via *gacS* a: Δ*dhbA* downregulates genes related to sporulation and germination independently of having PS92 as its interaction partner. DK1042-upregulated genes of the same category only when in coculture with PS92. Dashed lines indicate log2(FC) = |2|. **b:** Several biosynthetic pathways related to the Gac/Rsm two-component system were significantly downregulated (log_2(FC) <-2 and adjusted *p*-value <0.01) in coculture with DK1042, except for the alternative sigma factor *pvdS*. **c:** Mass spectrometry imaging reveals the presence/absence of select metabolites as well as their spatial localization in the interactions. Scale bar = 5 mm. Grey values are root mean squared intensity across all samples, and lookup tables were scaled identically across each metabolite. NaN pixels were set to zero. Metabolites were annotated with metaspace using the 2019 Natural Product Atlas database. m/z = 1216.5466 was manually annotated as a pyoverdine structure.

Still, the potential for an iron tug-of-war between *Bacillus* and *Pseudomonas* presents an interesting hypothesis. Our results suggest that in the event of a BB-Pvd iron competition, BB is the stronger chelator and *Pseudomonas* does not possess a xenosiderophore uptake system for BB. When *Bacillus* does not produce BB, the tides turn, and *Pseudomonas* gains the advantage, additionally suggesting that *Bacillus* is unable to take up *Pseudomonas* siderophores. Both bacilli and pseudomonads have previously been shown to take up xenosiderophores, but only if they are structurally similar to their own primary siderophore [237, 248]. The Gram status of the xenosiderophore producer is not important, with *Bacillus* and *Pseudomonas* pirating siderophores from *E. coli* and *Streptomyces ambofaciens*, respectively. Thus, the fact that bacilli and pseudomonads do not pirate each other leaves one wondering about their co-evolutionary status. Are pirated siderophores the product of co-evolution or simply a stochastic coincidence? Have bacilli and pseudomonads co-evolved in soil environments or do they actually not associate?

Chapter 6 – Concluding remarks

The world is made up of microbial interactions. Positive or negative, there is no denying the influence of microbial interactions. Much research has been dedicated to understanding how microbes interact and what the impact of their interactions are. Be it top-down approaches investigating the community diversity responses to environmental flux or bottom-up approaches elucidating community assembly structures via combinatorial pairwise interactions.

In this thesis, I have discussed microbial interactions with an emphasis on plant-growth promoting bacilli and pseudomonads. Strains in these genera represent enormous biotechnological potential in their biocontrol and biostimulation properties, that may supplement or even replace current synthetic pesticides and fertilizers. Replacing synthetic products will not only alleviate the environmental strain they pose, but it will also continue to provide high agricultural yields necessary for sustaining the growing human population.

We have found that both bacilli and pseudomonads are bacteria with complex lifestyles, capable of growing in virtually any environment due to their large metabolic capacity. They are also powerful producers of bioactive secondary metabolites that contribute to their competitive capacity and their biocontrol abilities. When microbes from these genera meet, they generally engage in negative interactions, mediated by their antimicrobial molecules, possibly evolved by consistent encounters. As such, antagonisms have countermeasures, and offenses are opposed by defenses. Most interactions are species-specific, owing to a high degree of conservation of biosynthetic gene clusters. This allows for predictions of interaction outcomes based on taxonomy. With our studies, we found that *P. protegens* and *P. capeferrum* inhibited *B. subtilis* regardless of isolation source. For *P. protegens*, a biomarker was identified in 2,4-diacetylphloroglucinol, and we hypothesize that additional biomarkers exist for other taxonomically conserved interactions, though, they have yet to be found.

Though interactions are taxonomically conserved, they are also context dependent and likely change as community complexity increases. Future studies should investigate how *Bacillus-Pseudomonas* interactions develop as phylogenetic richness increases. This would also increase our understanding of the impact of mixed-species consortia in agricultural settings.

Bacillus and *Pseudomonas* also compete for iron. Using their respective high affinity siderophores, they restrict iron from each other in a tug-of-war to gain a competitive advantage. Bacillibactin seems to be the stronger siderophore, and *B. subtilis* restricts the growth of many species of *Pseudomonas* when it can produce its primary siderophore. Cocultivation of *B.*

subtilis with *P. marginalis* on King's B agar yields a negative regulation of the *Pseudomonas* regulator of secondary metabolism, GacS.

Organisms that carry large genomes and metabolic potential are likely the seen minority. These species have adapted to wide ranges nutritional niches and lend themselves well to laboratory cultivation. Their ubiquity and prevalence must signify some impact on their surrounding ecology. But they are not alone. They appear in communities mainly composed of the unseen majority; species that cannot be cultivated in laboratory conditions. The nutritional needs and metabolic potentials of unculturable organisms are still a complete unknown, rendering predictions of community interactions challenging if not (currently) impossible. While much valuable information can still be garnered with known unknowns, understanding the full ecological potential of microbial communities is likely to revolutionize our view on their functional properties. Such understanding requires the unified effort of top-down and bottom-up approaches. My goal for this thesis has been to make a small contribution to this effort.

Bibliography

1. Bar-On YM, Phillips R, Milo R. The biomass distribution on Earth. *PNAS* 2018; **115**: 6506–6511.
2. Whitman WB, Coleman DC, Wiebe WJ. Perspective Prokaryotes: The unseen majority. *PNAS* 1998; **95**: 6578–6583.
3. Magnabosco C, Lin LH, Dong H, Bomberg M, Ghiorse W, Stan-Lotter H, et al. The biomass and biodiversity of the continental subsurface. *Nat Geosci* 2018; **11**: 707–717.
4. Sánchez-Baracaldo P, Bianchini G, Wilson JD, Knoll AH. Cyanobacteria and biogeochemical cycles through Earth history. *Trends Microbiol* 2022; **30**: 143–157.
5. Franche C, Lindström K, Elmerich C. Nitrogen-fixing bacteria associated with leguminous and non-leguminous plants. *Plant Soil* 2009; **321**: 35–59.
6. Johnson KVA. Gut microbiome composition and diversity are related to human personality traits. *Hum Microb J* 2020; **15**: 100069.
7. Begon M, Townsend CR. Ecology: From Individuals to Ecosystems, 5th ed. 2021. Wiley, Oxford.
8. Trivedi P, Leach JE, Tringe SG, Sa T, Singh BK. Plant–microbiome interactions: from community assembly to plant health. *Nat Rev Microbiol* 2020; **18**: 607–621.
9. Hepperly P, Lotter D, Ulsh CZ, Seidel R, Reider C. Compost, Manure and Synthetic Fertilizer Influences Crop Yields, Soil Properties, Nitrate Leaching and Crop Nutrient Content. *Compost Sci Util* 2009; **17**: 117–126.
10. Rouse JD, Bishop CA, Struger J. Nitrogen Pollution: An Assessment of Its Threat to Amphibian Survival. *Environ Health Perspect* 1999; **107**: 799–803.
11. Voutchkova DD, Schullehner J, Skaarup C, Wodschow K, Ersbøll AK, Hansen B. Estimating pesticides in public drinking water at the household level in Denmark. *GEUS Bulletin* 2021; **47**.
12. Chiu YH, Williams PL, Gillman MW, Gaskins AJ, Mínguez-Alarcón L, Souter I, et al. Association between pesticide residue intake from consumption of fruits and vegetables and pregnancy outcomes among women undergoing infertility treatment with assisted reproductive technology. *JAMA Intern Med* 2018; **178**: 17–26.
13. Giulioni C, Maurizi V, Castellani D, Scarcella S, Skrami E, Balercia G, et al. The environmental and occupational influence of pesticides on male fertility: A systematic review of human studies. *Andrology* 2022; **10**: 1250–1271.
14. Wallace DR, Buha Djordjevic A. Heavy metal and pesticide exposure: A mixture of potential toxicity and carcinogenicity. *Curr Opin Toxicol* 2020; **19**: 72–79.
15. Velivelli SLS, De Vos P, Kromann P, Declerck S, Prestwich BD. Biological control agents: From field to market, problems, and challenges. *Trends Biotechnol* 2014; **32**: 493–496.

16. Van Elsas JD, Chiurazzi M, Mallon CA, Elhottova D, Krištůfek V, Salles JF. Microbial diversity determines the invasion of soil by a bacterial pathogen. *Proc Natl Acad Sci U S A* 2012; **109**: 1159–1164.
17. Hansen ML, Dénes Z, Jarmusch SA, Wibowo M, Lozano-Andrade CN, Kovács T, et al. Resistance towards and biotransformation of *Pseudomonas*-produced secondary metabolites during community invasion. *BioRxiv* 2023.
18. Andrić S, Rigolet A, Argüelles Arias A, Steels S, Hoff G, Balleux G, et al. Plant-associated *Bacillus* mobilizes its secondary metabolites upon perception of the siderophore pyochelin produced by a *Pseudomonas* competitor. *ISME J* 2022; **17**: 263–275.
19. Mendes R, Garbeva P, Raaijmakers JM. The rhizosphere microbiome: Significance of plant beneficial, plant pathogenic, and human pathogenic microorganisms. *FEMS Microbiol Rev* 2013; **37**: 634–663.
20. Lyng M, Kovács ÁT. Frenemies of the soil: *Bacillus* and *Pseudomonas* interspecies interactions. *Trends Microbiol* 2023; TIMI2204.
21. Figueiredo M do VB, Bonifacio A, Rodrigues AC, de Araujo FF, Stamford NP. Beneficial Microorganisms: Current Challenge to Increase Crop Performance. In: Arora NK, Mehnaz S, Balestrini R (eds). *Bioformulations: for Sustainable Agriculture*. 2016. Springer India, New Delhi, pp 53–71.
22. Wootton JT, Emmerson M. MEASUREMENT OF INTERACTION STRENGTH IN NATURE. *Annu Rev Ecol Evol Syst* 2005; **36**: 419–444.
23. Skusa A, Rüegg A, Köhler J. Extraction of biological interaction networks from scientific literature. *Brief Bioinform* 2005; **6**: 263–276.
24. Hall EK, Bernhardt ES, Bier RL, Bradford MA, Boot CM, Cotner JB, et al. Understanding how microbiomes influence the systems they inhabit. *Nat Microbiol* 2018; **3**: 977–982.
25. Rinke C, Schwientek P, Sczyrba A, Ivanova NN, Anderson IJ, Cheng JF, et al. Insights into the phylogeny and coding potential of microbial dark matter. *Nature* 2013; **499**: 431–437.
26. Mathis KA, Bronstein JL. Our Current Understanding of Commensalism. *Annu Rev Ecol Evol Syst* 2020; **51**: 167–189.
27. Reissbrodt R, Hammes WP, Dal Bello F, Prager R, Fruth A, Hantke K, et al. Inhibition of growth of Shiga toxin-producing *Escherichia coli* by nonpathogenic *Escherichia coli*. *FEMS Microbiol Lett* 2009; **290**: 62–69.
28. Kelly D, Conway S, Aminov R. Commensal gut bacteria: Mechanisms of immune modulation. *Trends Immunol* 2005; **26**: 326–333.
29. Zapalski MK. Is absence of proof a proof of absence? Comments on commensalism. *Palaeogeogr Palaeoclimatol Palaeoecol* 2011; **302**: 484–488.
30. Andrade-Domínguez A, Salazar E, Del Carmen Vargas-Lagunas M, Kolter R, Encarnación S. Eco-evolutionary feedbacks drive species interactions. *ISME Journal* 2014; **8**: 1041–1054.

31. Hammer TJ, Sanders JG, Fierer N. Not all animals need a microbiome. *FEMS Microbiol Lett* 2019; **366**: fnz117.
32. Morris BEL, Henneberger R, Huber H, Moissl-Eichinger C. Microbial syntrophy: Interaction for the common good. *FEMS Microbiol Rev* 2013; **37**: 384–406.
33. Kwong WK, del Campo J, Mathur V, Vermeij MJA, Keeling PJ. A widespread coral-infecting apicomplexan with chlorophyll biosynthesis genes. *Nature* 2019; **568**: 103–107.
34. Cammack KM, Austin KJ, Lamberson WR, Conant GC, Cunningham HC. Ruminnat nutrition symposium: Tiny but mighty: The role of the rumen microbes in livestock production. *J Anim Sci* 2018; **96**: 752–770.
35. Dolfing J, Jiang B, Henstra AM, Stams AJM, Plugge CM. Syntrophic growth on formate: A new microbial niche in anoxic environments. *Appl Environ Microbiol* 2008; **74**: 6126–6131.
36. Sun X, Xu Z, Xie J, Hesselberg-Thomsen V, Tan T, Zheng D, et al. *Bacillus velezensis* stimulates resident rhizosphere *Pseudomonas stutzeri* for plant health through metabolic interactions. *ISME Journal* 2022; **16**: 774–787.
37. Giri S, Waschina S, Kaleta C, Kost C. Defining Division of Labor in Microbial Communities. *J Mol Biol* 2019; **431**: 4712–4731.
38. West SA, Griffin AS, Gardner A, Diggle SP. Social evolution theory for microorganisms. *Nat Rev Microbiol* 2006; **4**: 597–607.
39. Ebrahimi A, Schwartzman J, Cordero OX. Multicellular behaviour enables cooperation in microbial cell aggregates. *Philosophical Transactions of the Royal Society B* 2019; **374**: 1–7.
40. Schwartzman JA, Ebrahimi A, Chadwick G, Sato Y, Orphan V, Cordero OX. Bacterial growth in multicellular aggregates leads to the emergence of complex lifecycles. *Current Biology* 2022; **32**: 3059–3069.
41. Dar D, Dar N, Cai L, Newman DK. Spatial transcriptomics of planktonic and sessile bacterial populations at single-cell resolution. *Science (1979)* 2021; **373**: 1–16.
42. Liu J, Prindle A, Humphries J, Gabalda-Sagarra M, Asally M, Lee DYD, et al. Metabolic co-dependence gives rise to collective oscillations within biofilms. *Nature* 2015; **523**: 550–554.
43. Liu J, Martinez-Corral R, Prindle A, Lee D-YD, Larkin J, Gabalda-Sagarra M, et al. Coupling between distant biofilms and emergence of nutrient time-sharing. *Science (1979)* 2017; **356**: 638–642.
44. Brameyer S, Schumacher K, Kuppermann S, Jung K. Division of labor and collective functionality in *Escherichia coli* under acid stress. *Commun Biol* 2022; **5**: 327.
45. Dragoš A, Kiesewalter H, Martin M, Hsu CY, Hartmann R, Wechsler T, et al. Division of Labor during Biofilm Matrix Production. *Current Biology* 2018; **28**: 1903-1913.e5.
46. Kim W, Levy SB, Foster KR. Rapid radiation in bacteria leads to a division of labour. *Nat Commun* 2016; **7**: 10508.

47. Dragoš A, Martin M, Garcia CF, Kricks L, Pausch P, Heimerl T, et al. Collapse of genetic division of labour and evolution of autonomy in pellicle biofilms. *Nat Microbiol* 2018; **3**: 1451–1460.
48. Dragoš A, Lakshmanan N, Martin M, Horváth B, Maróti G, García CF, et al. Evolution of exploitative interactions during diversification in Bacillus subtilis biofilms. *FEMS Microbiol Ecol* 2018; **94**: fix155.
49. Cooper GA, West SA. Division of labour and the evolution of extreme specialization. *Nat Ecol Evol* 2018; **2**: 1161–1167.
50. Zhou K, Qiao K, Edgar S, Stephanopoulos G. Distributing a metabolic pathway among a microbial consortium enhances production of natural products. *Nat Biotechnol* 2015; **33**: 377–383.
51. Minami H, Kim J-S, Ikezawa N, Takemura T, Katayama T, Kumagai H, et al. Microbial production of plant benzylisoquinoline alkaloids. *PNAS* 2008; **105**: 7393–7398.
52. Dean-Raymond D, Alexander M. Bacterial Metabolism of Quaternary Ammonium Compounds. *Appl Environ Microbiol* 1977; **33**: 1037–1041.
53. Zuroff TR, Xiques SB, Curtis WR. Consortia-mediated bioprocessing of cellulose to ethanol with a symbiotic *Clostridium phytofermentans*/yeast co-culture. *Biotechnol Biofuels* 2013; **6**: 59.
54. Pogoda CS, Keepers KG, Lendemer JC, Kane NC, Tripp EA. Reductions in complexity of mitochondrial genomes in lichen-forming fungi shed light on genome architecture of obligate symbioses. *Mol Ecol* 2018; **27**: 1155–1169.
55. Palmer JD, Foster KR. Bacterial species rarely work together. *Science (1979)* 2022; **376**: 581–582.
56. Ram Y, Dellus-Gur E, Bibi M, Karkare K, Obolski U, Feldman MW, et al. Predicting microbial growth in a mixed culture from growth curve data. *PNAS* 2019; **116**: 14698–14707.
57. Nestor E, Toledano G, Friedman J. Interactions between Culturable Bacteria Are Predicted by Individual Species' Growth. *mSystems* 2023; **8**: e00836-22.
58. Swain A, Fussell L, Fagan WF. Higher-order effects, continuous species interactions, and trait evolution shape microbial spatial dynamics. *PNAS* 2022; **119**: e2020956119.
59. Baichman-Kass A, Song T, Friedman J. Competitive interactions between culturable bacteria are highly non-additive. *Elife* 2023; **12**: e83398.
60. Zangl I, Pap IJ, Aspöck C, Schüller C. The role of *Lactobacillus* species in the control of *Candida* via biotrophic interactions. *Microbial Cell* 2020; **7**: 1–14.
61. Thiery S, Kaimer C. The Predation Strategy of *Myxococcus xanthus*. *Front Microbiol* 2020; **11**: 2.
62. Shi W, Zusman DR. Fatal attraction. *Nature* 1993; **366**: 414–415.
63. Zhang W, Wang Y, Lu H, Liu Q, Wang C, Hu W, et al. Dynamics of solitary predation by *Myxococcus xanthus* on *Escherichia coli* observed at the single-cell level. *Appl Environ Microbiol* 2020; **86**: e02286-19.

64. Rotema O, Pasternak Z, Shimoni E, Belausov E, Porat Z, Pietrokovski S, et al. Cell-cycle progress in obligate predatory bacteria is dependent upon sequential sensing of prey recognition and prey quality cues. *PNAS* 2015; **112**: E6028–E6037.
65. Lambert C, Socket RE. Laboratory maintenance of *Bdellovibrio*. *Curr Protoc Microbiol* . 2008. , **9**: 7B.2.1-7B.2.13
66. Gordon RF, Stein MA, Diedrich DL. Heat Shock-Induced Axenic Growth of *Bdellovibrio bacteriovorus*. *J Bacteriol* 1993; **175**: 2157–2161.
67. Leinweber A, Fredrik Inglis R, Kümmerli R. Cheating fosters species co-existence in well-mixed bacterial communities. *ISME Journal* 2017; **11**: 1179–1188.
68. Özkaya Ö, Balbontín R, Gordo I, Xavier KB. Cheating on Cheaters Stabilizes Cooperation in *Pseudomonas aeruginosa*. *Current Biology* 2018; **28**: 2070-2080.e6.
69. Chamberlain SA, Bronstein JL, Rudgers JA. How context dependent are species interactions? *Ecol Lett* 2014; **17**: 881–890.
70. Zhou X, Leite MFA, Zhang Z, Tian L, Chang J, Ma L, et al. Facilitation in the soil microbiome does not necessarily lead to niche expansion. *Environmental Microbiomes* 2021; **16**: 4.
71. Burman E, Bengtsson-Palme J. Microbial Community Interactions Are Sensitive to Small Changes in Temperature. *Front Microbiol* 2021; **12**: 672910.
72. Chevrette MG, Thomas CS, Hurley A, Rosario-Mel Endez N, Sankaran K, Tu Y, et al. Microbiome composition modulates secondary metabolism in a multispecies bacterial community. *PNAS* 2022; **119**: e2212930119.
73. Baliarda A, Winkler M, Tournier L, Tinsley CR, Aymerich S. Dynamic interspecies interactions and robustness in a four-species model biofilm. *Microbiologyopen* 2021; **10**: e1254.
74. San León D, Nogales J. Toward merging bottom–up and top–down model-based designing of synthetic microbial communities. *Curr Opin Microbiol* 2022; **69**: 102169.
75. Friedman J, Higgins LM, Gore J. Community structure follows simple assembly rules in microbial microcosms. *Nat Ecol Evol* 2017; **1**: 1–7.
76. Ludington WB. Higher-order microbiome interactions and how to find them. *Trends Microbiol* 2022; **30**: 618–621.
77. Kelsic ED, Zhao J, Vetsigian K, Kishony R. Counteraction of antibiotic production and degradation stabilizes microbial communities. *Nature* 2015; **521**: 516–519.
78. Powers MJ, Sanabria-Valentín E, Bowers AA, Shank EA. Inhibition of cell differentiation in *Bacillus subtilis* by *Pseudomonas protegens*. *J Bacteriol* 2015; **197**: 2129–2138.
79. Vick SHW, Fabian BK, Dawson CJ, Foster C, Asher A, Hassan KA, et al. Delving into defence: identifying the *Pseudomonas protegens* Pf-5 gene suite involved in defence against secreted products of fungal, oomycete and bacterial rhizosphere competitors. *Microb Genom* 2021; **7**: 000671.
80. Chang C-Y, Bajić D, Vila JCC, Estrela S, Sanchez A. Emergent coexistence in multispecies microbial communities. *Science (1979)* 2023; **381**: 343–348.

81. Khurana H, Sharma M, Verma H, Lopes BS, Lal R, Negi RK. Genomic insights into the phylogeny of *Bacillus* strains and elucidation of their secondary metabolic potential. *Genomics* 2020; **112**: 3191–3200.
82. Arnaouteli S, Bamford NC, Stanley-Wall NR, Kovács ÁT. *Bacillus subtilis* biofilm formation and social interactions. *Nat Rev Microbiol* 2021; **19**: 600–614.
83. Mielich-Süss B, Lopez D. Molecular mechanisms involved in *Bacillus subtilis* biofilm formation. *Environ Microbiol* 2015; **17**: 555–565.
84. Kolodkin-Gal I, Elsholz AKW, Muth C, Girguis PR, Kolter R, Losick R. Respiration control of multicellularity in *Bacillus subtilis* by a complex of the cytochrome chain with a membrane-embedded histidine kinase. *Genes Dev* 2013; **27**: 887–899.
85. Wilking JN, Zaburdaev V, De Volder M, Losick R, Brenner MP, Weitz DA. Liquid transport facilitated by channels in *Bacillus subtilis* biofilms. *PNAS* 2013; **110**: 848–852.
86. Kobayashi K, Iwano M. BslA (YuaB) forms a hydrophobic layer on the surface of *Bacillus subtilis* biofilms. *Mol Microbiol* 2012; **85**: 51–66.
87. Nordgaard M, Blake C, Maróti G, Hu G, Wang Y, Strube ML, et al. Experimental evolution of *Bacillus subtilis* on *Arabidopsis thaliana* roots reveals fast adaptation and improved root colonization. *iScience* 2022; **25**.
88. Chen Y, Yan F, Chai Y, Liu H, Kolter R, Losick R, et al. Biocontrol of tomato wilt disease by *Bacillus subtilis* isolates from natural environments depends on conserved genes mediating biofilm formation. *Environ Microbiol* 2013; **15**: 848–864.
89. Bzhu. Subtiwiki: The Spo0A Regulon. *http://www.subtiwiki.uni-goettingen.de/v4/regulon?id=protein:2C54FE2ADC82FF414D732018C90649D477A925AD*. .
90. Molle V, Fujita M, Jensen ST, Eichenberger P, González-Pastor JE, Liu JS, et al. The Spo0A regulon of *Bacillus subtilis*. *Mol Microbiol* 2003; **50**: 1683–1701.
91. Fujita M, González-Pastor JE, Losick R. High- and low-threshold genes in the Spo0A regulon of *Bacillus subtilis*. *J Bacteriol* 2005; **187**: 1357–1368.
92. McLoon AL, Kolodkin-Gal I, Rubinstein SM, Kolter R, Losick R. Spatial regulation of histidine kinases governing biofilm formation in *Bacillus subtilis*. *J Bacteriol* 2011; **193**: 679–685.
93. Jiang M, Shao W, Perego M, Hoch JA. Multiple histidine kinases regulate entry into stationary phase and sporulation in *Bacillus subtilis*. *Mol Microbiol* 2000; **38**: 535–542.
94. Earl AM, Losick R, Kolter R. Ecology and genomics of *Bacillus subtilis*. *Trends Microbiol* 2008; **16**: 269–275.
95. Siala A, Hill IR, Gray TRG. Populations of Spore-forming Bacteria in an Acid Forest Soil, with Special Reference to *Bacillus subtilis*. *J Gen Microbiol* 1974; **81**: 183–190.
96. Vilain S, Luo Y, Hildreth MB, Brözel VS. Analysis of the life cycle of the soil Saprophyte *Bacillus cereus* in liquid soil extract and in soil. *Appl Environ Microbiol* 2006; **72**: 4970–4977.

97. Riley EP, Schwarz C, Derman AI, Lopez-Garrido J. Milestones in *Bacillus subtilis* sporulation research. *Microbial Cell* 2021; **8**: 1–16.

98. Cano RJ, Borucki MK. Revival and Identification of Bacterial Spores in 25- to 40-Million-Year-Old Dominican Amber. *Science (1979)* 1995; **268**: 1060–1064.

99. Pelchovich G, Omer-Bendori S, Gophna U. Menaquinone and iron are essential for complex colony development in *Bacillus subtilis*. *PLoS One* 2013; **8**: e79488.

100. Randazzo P, Aubert-Frambourg A, Guillot A, Auger S. The MarR-like protein PchR (YvmB) regulates expression of genes involved in pulcherriminic acid biosynthesis and in the initiation of sporulation in *Bacillus subtilis*. *BMC Microbiol* 2016; **16**: 190.

101. Lyng M, Jørgensen JPB, Schostag MD, Jarmusch SA, Aguilar DKC, Lozano-Andrade C-LN, et al. Competition for iron shapes metabolic antagonism between *Bacillus subtilis* and *Pseudomonas*. *BioRxiv* 2023.

102. Qin Y, He Y, She Q, Larese-Casanova P, Li P, Chai Y. Heterogeneity in respiratory electron transfer and adaptive iron utilization in a bacterial biofilm. *Nat Commun* 2019; **10**: 1–12.

103. Dertz EA, Stintzi A, Raymond KN. Siderophore-mediated iron transport in *Bacillus subtilis* and *Corynebacterium glutamicum*. *Journal of Biological Inorganic Chemistry* 2006; **11**: 1087–1097.

104. Miethke M, Schmidt S, Marahiel MA. The major facilitator superfamily-type transporter YmfE and the multidrug-efflux activator Mta mediate bacillibactin secretion in *Bacillus subtilis*. *J Bacteriol* 2008; **190**: 5143–5152.

105. Ollinger J, Song KB, Antelmann H, Hecker M, Helmann JD. Role of the Fur regulon in iron transport in *Bacillus subtilis*. *J Bacteriol* 2006; **188**: 3664–3673.

106. Miethke M, Klotz O, Linne U, May JJ, Beckering CL, Marahiel MA. Ferri-bacillibactin uptake and hydrolysis in *Bacillus subtilis*. *Mol Microbiol* 2006; **61**: 1413–1427.

107. May JJ, Wendrich TM, Marahiel MA. The *dhb* Operon of *Bacillus subtilis* Encodes the Biosynthetic Template for the Catecholic Siderophore 2,3-Dihydroxybenzoate-Glycine-Threonine Trimeric Ester Bacillibactin. *Journal of Biological Chemistry* 2001; **276**: 7209–7217.

108. Rizzi A, Roy S, Bellenger J-P, Beauregard PB. Iron Homeostasis in *Bacillus subtilis* Requires Siderophore Production and Biofilm Formation. *Appl Environ Microbiol* 2019; **85**: 1–10.

109. Palleroni NJ. The *Pseudomonas* story. *Environ Microbiol* 2010; **12**: 1377–1383.

110. Garrido-Sanz D, Meier-Kolthoff JP, Göker M, Martín M, Rivilla R, Redondo-Nieto M. Genomic and genetic diversity within the *Pseudomonas fluorescens* complex. *PLoS One* 2016; **11**: e0150183.

111. Xin XF, Kvitko B, He SY. *Pseudomonas syringae*: What it takes to be a pathogen. *Nat Rev Microbiol* 2018; **16**: 316–328.

112. Zobel S, Benedetti I, Eisenbach L, De Lorenzo V, Wierckx N, Blank LM. Tn7-Based Device for Calibrated Heterologous Gene Expression in *Pseudomonas putida*. *ACS Synth Biol* 2015; **4**: 1341–1351.
113. Qin S, Xiao W, Zhou C, Pu Q, Deng X, Lan L, et al. *Pseudomonas aeruginosa*: pathogenesis, virulence factors, antibiotic resistance, interaction with host, technology advances and emerging therapeutics. *Signal Transduct Target Ther* 2022; **7**: 1–27.
114. Pacheco-Moreno A, Stefanato FL, Ford JJ, Trippel C, Uszkoreit S, Ferrafiat L, et al. Pan-genome analysis identifies intersecting roles for *Pseudomonas* specialized metabolites in potato pathogen inhibition. *Elife* 2021; **10**: e71900.
115. Chen WJ, Kuo TY, Hsieh FC, Chen PY, Wang CS, Shih YL, et al. Involvement of type VI secretion system in secretion of iron chelator pyoverdine in *Pseudomonas taiwanensis*. *Sci Rep* 2016; **6**: 32950.
116. Cézard C, Sonnet P, Bouvier B. Ironing out pyoverdine's chromophore structure: serendipity or design? *Journal of Biological Inorganic Chemistry* 2019; **24**: 659–673.
117. Turfitt GE. BACTERIOLOGICAL AND BIOCHEMICAL RELATIONSHIPS IN THE PYOCYANEUS-FLUORESCENS GROUP. *Bacterial Classification* 1936; **189**: 1323–1328.
118. Meyer JM, Abdallah MA. The Fluorescent Pigment of *Pseudomonas fluorescens*: Biosynthesis, Purification and Physicochemical Properties. *J Gen Microbiol* 1978; **107**: 319–328.
119. Hesse C, Schulz F, Bull CT, Shaffer BT, Yan Q, Shapiro N, et al. Genome-based evolutionary history of *Pseudomonas* spp. *Environ Microbiol* 2018; **20**: 2142–2159.
120. Silby MW, Cerdeño-Tárraga AM, Vernikos GS, Giddens SR, Jackson RW, Preston GM, et al. Genomic and genetic analyses of diversity and plant interactions of *Pseudomonas fluorescens*. *Genome Biol* 2009; **10**: R51.
121. Gomila M, Mulet M, García-Valdés E, Lalucat J. Genome-Based Taxonomy of the Genus *Stutzerimonas* and Proposal of *S. frequens* sp. nov. and *S. degradans* sp. nov. and Emended Descriptions of *S. perfectomarina* and *S. chloritidismutans*. *Microorganisms* 2022; **10**: 1363.
122. Frapolli M, Pothier JF, Défago G, Moënne-Loccoz Y. Evolutionary history of synthesis pathway genes for phloroglucinol and cyanide antimicrobials in plant-associated fluorescent pseudomonads. *Mol Phylogenet Evol* 2012; **63**: 877–890.
123. Kumar M, Mishra S, Dixit V, Kumar M, Agarwal L, Chauhan PS, et al. Synergistic effect of *Pseudomonas putida* and *Bacillus amyloliquefaciens* ameliorates drought stress in chickpea (*Cicer arietinum L.*). *Plant Signal Behav* 2016; **11**: e1071004.
124. Grgurina I, Mariotti F, Fogliano V, Gallo M, Scaloni A, Iacobellis NS, et al. A new syringopeptin produced by bean strains of *Pseudomonas syringae* pv. *syringae*. *Biochemica et Biophysica Acta* 2002; **1597**: 81–89.

125. Blin K, Shaw S, Augustijn HE, Reitz ZL, Biermann F, Alanjary M, et al. antiSMASH 7.0: new and improved predictions for detection, regulation, chemical structures and visualisation. *Nucleic Acids Res* 2023; **gkad344**.
126. Kiesewalter HT, Lozano-Andrade CN, Wibowo M, Strube ML, Maróti G, Snyder D, et al. Genomic and Chemical Diversity of Bacillus subtilis Secondary Metabolites against Plant Pathogenic Fungi. *mSystems* 2021; **6**: e00770-20.
127. Gross H, Loper JE. Genomics of secondary metabolite production by *Pseudomonas* spp. *Nat Prod Rep* 2009; **26**: 1408–1446.
128. Finking R, Marahiel MA. Biosynthesis of nonribosomal peptides. *Annu Rev Microbiol* 2004; **58**: 453–488.
129. Geudens N, Martins JC. Cyclic lipodepsipeptides from *Pseudomonas* spp. - Biological Swiss-Army knives. *Front Microbiol* 2018; **9**: 1867.
130. Raaijmakers JM, De Bruijn I, De Kock MJD. Cyclic Lipopeptide Production by Plant-Associated *Pseudomonas* spp.: Diversity, Activity, Biosynthesis, and Regulation. *MPMI* 2006; **19**: 699–710.
131. Geudens N, Nasir MN, Crowet JM, Raaijmakers JM, Fehér K, Coenye T, et al. Membrane Interactions of Natural Cyclic Lipodepsipeptides of the Viscosin Group. *Biochim Biophys Acta* 2016; **1859**: 331–339.
132. Reder-Christ K, Schmidt Y, Dörr M, Sahl HG, Josten M, Raaijmakers JM, et al. Model membrane studies for characterization of different antibiotic activities of lipopeptides from *Pseudomonas*. *Biochim Biophys Acta Biomembr* 2012; **1818**: 566–573.
133. Chen X, Lu Y, Shan M, Zhao H, Lu Z, Lu Y. A mini-review: mechanism of antimicrobial action and application of surfactin. *World J Microbiol Biotechnol* 2022; **38**: 143.
134. Rahman F Bin, Sarkar B, Moni R, Rahman MS. Molecular genetics of surfactin and its effects on different sub-populations of *Bacillus subtilis*. *Biotechnology Reports* . 2021. Elsevier B.V. , **32**: e00686
135. Andrić S, Meyer T, Rigolet A, Prigent-Combaret C, Höfte M, Balleux G, et al. Lipopeptide Interplay Mediates Molecular Interactions between Soil *Bacilli* and *Pseudomonads*. *Microbiol Spectr* 2021; **9**: e02038-21.
136. Kramer J, Özkaya Ö, Kümmerli R. Bacterial siderophores in community and host interactions. *Nat Rev Microbiol* 2020; **18**: 152–163.
137. Abergel RJ, Zawadzka AM, Hoette TM, Raymond KN. Enzymatic hydrolysis of trilactone siderophores: Where chiral recognition occurs in enterobactin and bacillibactin iron transport. *J Am Chem Soc* 2009; **131**: 12682–12692.
138. Dertz EA, Xu J, Raymond KN. Tren-based analogues of bacillibactin: Structure and stability. *Inorg Chem* 2006; **45**: 5465–5478.
139. Kümmerli R. Iron acquisition strategies in pseudomonads: mechanisms, ecology, and evolution. *BioMetals* 2022.
140. Ringel MT, Brüser T. The biosynthesis of pyoverdines. *Microbial Cell* 2018; **5**: 424–437.

141. Moon CD, Zhang XX, Matthijs S, Schäfer M, Budzikiewicz H, Rainey PB. Genomic, genetic and structural analysis of pyoverdine-mediated iron acquisition in the plant growth-promoting bacterium *Pseudomonas fluorescens* SBW25. *BMC Microbiol* 2008; **8**: 7.

142. Moore CM, Helmann JD. Metal ion homeostasis in *Bacillus subtilis*. *Curr Opin Microbiol* 2005; **8**: 188–195.

143. Robbins T, Liu YC, Cane DE, Khosla C. Structure and mechanism of assembly line polyketide synthases. *Curr Opin Struct Biol* 2016; **41**: 10–18.

144. Almario J, Bruto M, Vacheron J, Prigent-Combaret C, Moënne-Loccoz Y, Muller D. Distribution of 2,4-diacetylphloroglucinol biosynthetic genes among the *Pseudomonas* spp. Reveals unexpected Polyphyletism. *Front Microbiol* 2017; **8**: 1–9.

145. Raaijmakers JM, Weller DM. Natural Plant Protection by 2,4-Diacetylphloroglucinol-Producing *Pseudomonas* spp. in Take-All Decline Soils. *Mol Plant Microbe Interact* 1998; **11**: 144–152.

146. Phillips DA, Fox TC, King MD, Bhuvaneswari T V., Teuber LR. Microbial products trigger amino acid exudation from plant roots. *Plant Physiol* 2004; **136**: 2887–2894.

147. Yannarell SM, Beaudoin ES, Talley HS, Schoenborn AA, Orr G, Anderton CR, et al. Extensive cellular multitasking within *Bacillus subtilis* biofilms. *BioRxiv* 2022.

148. Ogura M, Shimane K, Asai K, Ogasawara N, Tanaka T. Binding of response regulator DegU to the *aprE* promoter is inhibited by RapG, which is counteracted by extracellular PhrG in *Bacillus subtilis*. *Mol Microbiol* 2003; **49**: 1685–1697.

149. Parashar V, Konkol MA, Kearns DB, Neiditch MB. A plasmid-encoded phosphatase regulates bacillus subtilis biofilm architecture, sporulation, and genetic competence. *J Bacteriol* 2013; **195**: 2437–2448.

150. Auchtung JM, Lee CA, Grossman AD. Modulation of the ComA-dependent quorum response in *Bacillus subtilis* by multiple rap proteins and Phr peptides. *J Bacteriol* 2006; **188**: 5273–5285.

151. Even-Tov E, Bendori SO, Pollak S, Eldar A. Transient Duplication-Dependent Divergence and Horizontal Transfer Underlie the Evolutionary Dynamics of Bacterial Cell–Cell Signaling. *PLoS Biol* 2016; **14**: e2000330.

152. Perego M. Forty Years in the Making: Understanding the Molecular Mechanism of Peptide Regulation in Bacterial Development. *PLoS Biol* 2013; **11**: e1001516.

153. Gallegos-Monterrosa R, Christensen MN, Barchewitz T, Koppenhöfer S, Priyadarshini B, Bálint B, et al. Impact of Rap-Phr system abundance on adaptation of *Bacillus subtilis*. *Commun Biol* 2021; **4**: 468.

154. Pottathil M, Lazazzera BA. The Extracellular Phr Peptide-Rap Phosphatase Signaling Circuit of *Bacillus subtilis*. *Frontiers in Bioscience* 2003; **8**: 32–45.

155. Perego M, Brannigan JA. Pentapeptide regulation of aspartyl-phosphate phosphatases. *Peptides (NY)* 2001; **22**: 1541–1547.

156. Karataş AY, Çetin S, Özcengiz G. The effects of insertional mutations in *comQ, comP, srfA, spo0H, spo0A* and *abrB* genes on bacilysin biosynthesis in *Bacillus subtilis*. *Biochim Biophys Acta* 2003; **1626**: 51–56.
157. Strauch MA, Bobay BG, Cavanagh J, Yao F, Wilson A, Le Breton Y. Abh and AbrB control of *Bacillus subtilis* antimicrobial gene expression. *J Bacteriol* 2007; **189**: 7720–7732.
158. Straight PD, Fischbach MA, Walsh CT, Rudner DZ, Kolter R. A singular enzymatic megacomplex from *Bacillus subtilis*. *PNAS* 2007; **104**: 305–310.
159. Chumsakul O, Takahashi H, Oshima T, Hishimoto T, Kanaya S, Ogasawara N, et al. Genome-wide binding profiles of the *Bacillus subtilis* transition state regulator AbrB and its homolog Abh reveals their interactive role in transcriptional regulation. *Nucleic Acids Res* 2011; **39**: 414–428.
160. Chu F, Kearns DB, McLoon A, Chai Y, Kolter R, Losick R. A novel regulatory protein governing biofilm formation in *Bacillus subtilis*. *Mol Microbiol* 2008; **68**: 1117–1127.
161. Harwood CR, Mouillon JM, Pohl S, Arnau J. Secondary metabolite production and the safety of industrially important members of the *Bacillus subtilis* group. *FEMS Microbiol Rev* . 2018. Oxford University Press. , **42**: 721–738
162. Ongena M, Jourdan E, Adam A, Paquot M, Brans A, Joris B, et al. Surfactin and fengycin lipopeptides of *Bacillus subtilis* as elicitors of induced systemic resistance in plants. *Environ Microbiol* 2007; **9**: 1084–1090.
163. Pi H, Helmann JD. Sequential induction of Fur-regulated genes in response to iron limitation in *Bacillus subtilis*. *PNAS* 2017; **114**: 12785–12790.
164. Ferreiro MD, Gallegos MT. Distinctive features of the Gac-Rsm pathway in plant-associated *Pseudomonas*. *Environ Microbiol* 2021; **23**: 5670–5689.
165. Cheng X, de Bruijn I, van der Voort M, Loper JE, Raaijmakers JM. The Gac regulon of *Pseudomonas fluorescens* SBW25. *Environ Microbiol Rep* 2013; **5**: 608–619.
166. Lapouge K, Schubert M, Allain FHT, Haas D. Gac/Rsm signal transduction pathway of γ-proteobacteria: From RNA recognition to regulation of social behaviour. *Mol Microbiol* 2008; **67**: 241–253.
167. Song H, Li Y, Wang Y. Two-component system GacS/GacA, a global response regulator of bacterial physiological behaviors. *Engineering Microbiology* 2023; **3**: 100051.
168. Christiansen L, Alanin KS, Phippen CBW, Olsson S, Stougaard P, Hennessy RC. Fungal-Associated Molecules Induce Key Genes Involved in the Biosynthesis of the Antifungal Secondary Metabolites Nunamycin and Nunapeptin in the Biocontrol Strain *Pseudomonas fluorescens* In5. *Appl Environ Microbiol* 2020; **86**: e01284-20.
169. Broder UN, Jaeger T, Jenal U. LadS is a calcium-responsive kinase that induces acute-to-chronic virulence switch in *Pseudomonas aeruginosa*. *Nat Microbiol* 2016; **2**: 1–11.
170. Cheng X, Pu L, Fu S, Xia A, Huang S, Ni L, et al. Engineering Gac/Rsm Signaling Cascade for Optogenetic Induction of the Pathogenicity Switch in *Pseudomonas aeruginosa*. *ACS Synth Biol* 2021; **10**: 1520–1530.

171. Shang L, Yan Y, Zhan Y, Ke X, Shao Y, Liu Y, et al. A regulatory network involving Rpo, Gac and Rsm for nitrogen-fixing biofilm formation by *Pseudomonas stutzeri*. *NPJ Biofilms Microbiomes* 2021; **7**.

172. Zhang B, Zhang Y, Liang F, Ma Y, Wu X. An Extract Produced by *Bacillus* sp. BR3 Influences the Function of the GacS/GacA Two-Component System in *Pseudomonas syringae* pv. *tomato* DC3000. *Front Microbiol* 2019; **10**: 2005.

173. Peng J, Chen G, Xu X, Wang T, Liang H. Iron facilitates the RetS-Gac-Rsm cascade to inversely regulate protease IV (piv) expression via the sigma factor PvdS in *Pseudomonas aeruginosa*. *Environ Microbiol* 2020; **22**: 5402–5413.

174. Frangipani E, Visaggio D, Heeb S, Kaever V, Cámara M, Visca P, et al. The Gac/Rsm and cyclic-di-GMP signalling networks coordinately regulate iron uptake in *Pseudomonas aeruginosa*. *Environ Microbiol* 2014; **16**: 676–688.

175. Zehr JP, Jenkins BD, Short SM, Steward GF. Nitrogenase gene diversity and microbial community structure: A cross-system comparison. *Environ Microbiol* 2003; **5**: 539–554.

176. Elkoca E, Kantar F, Sahin F. Influence of nitrogen fixing and phosphorus solubilizing bacteria on the nodulation, plant growth, and yield of chickpea. *J Plant Nutr* 2008; **31**: 157–171.

177. Setten L, Soto G, Mozzicafreddo M, Fox AR, Lisi C, Cuccioloni M, et al. Engineering *Pseudomonas protegens* Pf-5 for Nitrogen Fixation and its Application to Improve Plant Growth under Nitrogen-Deficient Conditions. *PLoS One* 2013; **8**: e63666.

178. Yousuf J, Thajudeen J, Rahiman M, Krishnankutty S, P. Alikunj A, Mohamed MH. Nitrogen fixing potential of various heterotrophic *Bacillus* strains from a tropical estuary and adjacent coastal regions. *J Basic Microbiol* 2017; **57**: 922–932.

179. Çakmakçi R, Kantar F, Sahin F. Effect of N2-fixing bacterial inoculations on yield of sugar beet and barley. *Journal of Plant Nutrition and Soil Science* 2001; **164**: 527–531.

180. Saeid A, Prochownik E, Dobrowolska-Iwanek J. Phosphorus solubilization by *Bacillus* species. *Molecules* 2018; **23**: 2897.

181. Andreolli M, Zapparoli G, Angelini E, Lucchetta G, Lampis S, Vallini G. *Pseudomonas protegens* MP12: A plant growth-promoting endophytic bacterium with broad-spectrum antifungal activity against grapevine phytopathogens. *Microbiol Res* 2019; **219**: 123–131.

182. Trapet P, Avoscan L, Klinguer A, Pateyron S, Citerne S, Chervin C, et al. The *Pseudomonas fluorescens* siderophore pyoverdine weakens *Arabidopsis thaliana* defense in favor of growth in iron-deficient conditions. *Plant Physiol* 2016; **171**: 675–693.

183. Singh P, Kumar R, Khan A, Singh A, Srivastava A. Bacillibactin siderophore induces iron mobilisation responses inside aerobic rice variety through YSL15 transporter. *Rhizosphere* 2023; **27**: 100724.

184. Ryu C-M, Farag MA, Hu C-H, Reddy MS, Wei H-X, Paré PW, et al. Bacterial volatiles promote growth in Arabidopsis. *PNAS* 2003; **100**: 4927–4932.

185. Zhang H, Kim MS, Krishnamachari V, Payton P, Sun Y, Grimson M, et al. Rhizobacterial volatile emissions regulate auxin homeostasis and cell expansion in Arabidopsis. *Planta* 2007; **226**: 839–851.
186. Li Q, Li H, Yang Z, Cheng X, Zhao Y, Qin L, et al. Plant growth-promoting rhizobacterium *Pseudomonas* sp. CM11 specifically induces lateral roots. *New Phytologist* 2022; **235**: 1575–1588.
187. Singh P, Singh RK, Zhou Y, Wang J, Jiang Y, Shen N, et al. Unlocking the strength of plant growth promoting *Pseudomonas* in improving crop productivity in normal and challenging environments: a review. *J Plant Interact* 2022; **17**: 220–238.
188. Lin Q, Li M, Wang Y, Xu Z, Li L. Root exudates and chemotactic strains mediate bacterial community assembly in the rhizosphere soil of *Casuarina equisetifolia L*. *Front Plant Sci* 2022; **13**: 988442.
189. Vora SM, Joshi P, Belwalkar M, Archana G. Root exudates influence chemotaxis and colonization of diverse plant growth promoting rhizobacteria in the pigeon pea – maize intercropping system. *Rhizosphere* 2021; **18**: 100331.
190. Liu Y, Shu X, Chen L, Zhang H, Feng H, Sun X, et al. Plant commensal type VII secretion system causes iron leakage from roots to promote colonization. *Nat Microbiol* 2023.
191. Pomerleau M, Charron-Lamoureux V, Léonard L, Grenier F, Rodrigue S, Beauregard PB. Adaptative Laboratory Evolution reveals biofilm regulating genes as key players in *B. subtilis* root colonization. *BioRxiv* 2023.
192. Zeriouh H, de Vicente A, Pérez-García A, Romero D. Surfactin triggers biofilm formation of *Bacillus subtilis* in melon phylloplane and contributes to the biocontrol activity. *Environ Microbiol* 2014; **16**: 2196–2211.
193. Pérez-Lorente AI, Molina-Santiago C, de Vicente A, Romero D. Sporulation Activated via σ W Protects *Bacillus* from a Tse1 Peptidoglycan Hydrolase Type VI Secretion System Effector. *Microbiol Spectr* 2023; e05045-22.
194. Molina-Santiago C, Pearson JR, Navarro Y, Berlanga-Clavero MV, Caraballo-Rodriguez AM, Petras D, et al. The extracellular matrix protects *Bacillus subtilis* colonies from *Pseudomonas* invasion and modulates plant co-colonization. *Nat Commun* 2019; **10**: 1919.
195. Tao C, Li R, Xiong W, Shen Z, Liu S, Wang B, et al. Bio-organic fertilizers stimulate indigenous soil *Pseudomonas* populations to enhance plant disease suppression. *Microbiome* 2020; **8**: 137.
196. Khabbaz SE, Zhang L, Cáceres LA, Sumarah M, Wang A, Abbasi PA. Characterisation of antagonistic *Bacillus* and *Pseudomonas* strains for biocontrol potential and suppression of damping-off and root rot diseases. *Annals of Applied Biology* 2015; **166**: 456–471.

197. Blake C, Christensen MN, Kovacs AT. Molecular aspects of plant growth promotion and protection by *Bacillus subtilis*. *Molecular Plant-Microbe Interactions* 2021; **34**: 15–25.

198. Preston GM. Plant perceptions of plant growth-promoting *Pseudomonas*. *Philosophical Transactions of the Royal Society B* 2004; **359**: 907–918.

199. Nalli Y, Singh S, Gajjar A, Mahizhaveni B, Nynar V, Dusthackeer A, et al. Bacillibactin class siderophores produced by the endophyte *Bacillus subtilis* NPROOT3 as antimycobacterial agents. *Lett Appl Microbiol* 2022; **76**: ovac026.

200. Dimopoulou A, Theologidis I, Benaki D, Koukounia M, Zervakou A, Tzima A, et al. Direct Antibiotic Activity of Bacillibactin Broadens the Biocontrol Range of Bacillus amyloliquefaciens MBI600. *mSphere* 2021; **6**: e00376-21.

201. Getzke F, Hassani MA, Crüsemann M, Malisic M, Zhang P, Ishigaki Y, et al. Cofunctioning of bacterial exometabolites drives root microbiota establishment. *PNAS* 2023; **120**: e2221508120.

202. Carrillo C, Teruel JA, Aranda FJ, Ortiz A. Molecular mechanism of membrane permeabilization by the peptide antibiotic surfactin. *Biochim Biophys Acta Biomembr* 2003; **1611**: 91–97.

203. Bais HP, Fall R, Vivanco JM. Biocontrol of *Bacillus subtilis* against Infection of Arabidopsis Roots by *Pseudomonas syringae* Is Facilitated by Biofilm Formation and Surfactin Production. *Plant Physiol* 2004; **134**: 307–319.

204. Bakker PAHM, Pieterse CMJ, van Loon LC. Induced systemic resistance by fluorescent *Pseudomonas* spp. *Phytopathology* 2007; **97**: 239–243.

205. Wang S, Zheng Y, Gu C, He C, Yang M, Zhang X, et al. *Bacillus cereus* AR156 activates defense responses to *Pseudomonas syringae* pv. *tomato* in *Arabidopsis thaliana* similarly to flg22. *Molecular Plant-Microbe Interactions* 2018; **31**: 311–322.

206. Niu D-D, Liu H-X, Jiang C-H, Wang Y-P, Wang Q-Y, Jin H-L, et al. The Plant Growth-Promoting Rhizobacterium Bacillus cereus AR156 Induces Systemic Resistance in Arabidopsis thaliana by Simultaneously Activating Salicylate-and Jasmonate/Ethylene-Dependent Signaling Pathways. *Molecular Plant-Microbe Interactions* 2011; **24**: 533–542.

207. Niu D, Wang X, Wang Y, Song X, Wang J, Guo J, et al. *Bacillus cereus* AR156 activates PAMP-triggered immunity and induces a systemic acquired resistance through a NPR1-and SA-dependent signaling pathway. *Biochem Biophys Res Commun* 2016; **469**: 120–125.

208. Li J, Chai Z, Yang H, Li G, Wang D. First report of *Pseudomonas marginalis* pv. *marginalis* as a cause of soft rot of potato in China. *Australas Plant Dis Notes* 2007; **2**: 71–73.

209. Liao C-H, McCallus DE, Fett WF, Kang Y-G. Identification of gene loci controlling pectate lyase production and soft-rot pathogenicity in *Pseudomonas marginalis*. *Can J Microbiol* 1997; **43**: 425–431.

210. Yang M, Mavrodi D V., Mavrodi O V., Thomashow LS, Weller DM. Exploring the Pathogenicity of *Pseudomonas brassicacearum* Q8r1-96 and Other Strains of the *Pseudomonas fluorescens* Complex on Tomato. *Plant Dis* 2020; **104**: 1026–1031.
211. Kůdela V, Krejzar V, Pánková I. *Pseudomonas corrugata* and *Pseudomonas marginalis* Associated with the Collapse of Tomato Plants in Rockwool Slab Hydroponic Culture. *Plant Protection Science* 2010; **46**: 1–11.
212. Belimov AA, Dodd IC, Safronova VI, Hontzeas N, Davies WJ. *Pseudomonas brassicacearum* strain Am3 containing 1-aminocyclopropane-1- carboxylate deaminase can show both pathogenic and growth-promoting properties in its interaction with tomato. *J Exp Bot* 2007; **58**: 1485–1495.
213. Weeraratne N, Stodart BJ, Venturi V, Hofte M, Hua GKH, Ongena M, et al. Syringopeptin contributes to the virulence of *Pseudomonas fuscovaginae*, based on *sypA* biosynthesis mutant analysis. *Phytopathology* 2020; **110**: 780–789.
214. Kitten T, Kinscherf TG, McEvoy JL, Willis DK. A newly identified regulator is required for virulence and toxin production in *Pseudomonas syringae*. *Mol Microbiol* 1998; **28**: 917–929.
215. Bassarello C, Lazzaroni S, Bifulco G, Lo Cantore P, Iacobellis NS, Riccio R, et al. Tolaasins A-E, five new lipodepsipeptides produced by *Pseudomonas tolaasii*. *J Nat Prod* 2004; **67**: 811–816.
216. Licciardello G, Caruso A, Bella P, Gheleri R, Strano CP, Anzalone A, et al. The LuxR regulators PcoR and RfiA co-regulate antimicrobial peptide and alginate production in *Pseudomonas corrugata*. *Front Microbiol* 2018; **9**: 521.
217. Levit GS, Hossfeld U. Ernst Haeckel in the history of biology. *Current Biology* . 2019. Cell Press. , **29**: R1276–R1284
218. Darwin C. On the origin of species by means of natural selection, First. 1859. W. Clowes and Sons, London.
219. Pijnenborg R, Vercruysse L. Thomas Huxley and the rat placenta in the early debates on evolution. *Placenta* 2004; **25**: 233–237.
220. Konstantinidis KT, Tiedje JM. Prokaryotic taxonomy and phylogeny in the genomic era: advancements and challenges ahead. *Curr Opin Microbiol* . 2007. , **10**: 504–509
221. Maughan H, Van der Auwera G. *Bacillus* taxonomy in the genomic era finds phenotypes to be essential though often misleading. *Infection, Genetics and Evolution* . 2011. , **11**: 789–797
222. Henz SR, Huson DH, Auch AF, Nieselt-Struwe K, Schuster SC. Whole-genome prokaryotic phylogeny. *Bioinformatics* 2005; **21**: 2329–2335.
223. Meier-Kolthoff JP, Carbasse JS, Peinado-Olarte RL, Göker M. TYGS and LPSN: A database tandem for fast and reliable genome-based classification and nomenclature of prokaryotes. *Nucleic Acids Res* 2022; **50**: D801–D807.

224. Yoon SH, Hur CG, Kang HY, Kim YH, Oh TK, Kim JF. A computational approach for identifying pathogenicity islands in prokaryotic genomes. *BMC Bioinformatics* 2005; **6**: 184.

225. Russel J, Røder HL, Madsen JS, Burmølle M, Sørensen SJ. Antagonism correlates with metabolic similarity in diverse bacteria. *PNAS* 2017; **114**: 10684–10688.

226. Machado D, Maistrenko OM, Andrejev S, Kim Y, Bork P, Patil KR, et al. Polarization of microbial communities between competitive and cooperative metabolism. *Nat Ecol Evol* 2021; **5**: 195–203.

227. Stefanic P, Kraigher B, Lyons NA, Kolter R, Mandic-Mulec I. Kin discrimination between sympatric *Bacillus subtilis* isolates. *PNAS* 2015; **112**: 14042–14047.

228. Schoustra SE, Dench J, Dali R, Aaron SD, Kassen R. Antagonistic interactions peak at intermediate genetic distance in clinical and laboratory strains of *Pseudomonas aeruginosa*. *BMC Microbiol* 2012; **12**: 40.

229. Naughton HR, Alexandrou MA, Oakley TH, Cardinale BJ. Phylogenetic distance does not predict competition in green algal communities. *Ecosphere* 2015; **6**: 116.

230. Koeppel AF, Wu M. Species matter: The role of competition in the assembly of congeneric bacteria. *ISME Journal* 2014; **8**: 531–540.

231. Vetsigian K, Jajoo R, Kishony R. Structure and evolution of *Streptomyces* interaction networks in soil and in silico. *PLoS Biol* 2011; **9**: e1001184.

232. Schlatter DC, Song Z, Vaz-Jauri P, Kinkel LL. Inhibitory interaction networks among coevolved *Streptomyces* populations from prairie soils. *PLoS One* 2019; **14**: e0223779.

233. Turlin E, Débarbouillé M, Augustyniak K, Gilles AM, Wandersman C. *Staphylococcus aureus* FepA and FepB Proteins Drive Heme Iron Utilization in *Escherichia coli*. *PLoS One* 2013; **8**: e56529.

234. Barton LE, Quicksall AN, Maurice PA. Siderophore-Mediated Dissolution of Hematite (α-Fe2O3): Effects of Nanoparticle Size. *Geomicrobiol J* 2012; **29**: 314–322.

235. Kessler N, Kraemer SM, Shaked Y, Schenkeveld WDC. Investigation of Siderophore-Promoted and Reductive Dissolution of Dust in Marine Microenvironments Such as Trichodesmium Colonies. *Front Mar Sci* 2020; **7**: 45.

236. Raaijmakers JM, Van Der Sluis L, Koster M, Bakker PAHM, Weisbeek PJ, Schippers B. Utilization of heterologous siderophores and rhizosphere competence of fluorescent *Pseudomonas* spp. *Can J Microbiol* 1995; **41**: 126–135.

237. Grandchamp GM, Caro L, Shank EA, Stabb E V. Pirated Siderophores Promote Sporulation in *Bacillus subtilis*. *Appl Environ Microbiol* 2017; **83**: e03293-16.

238. Noinaj N, Guillier M, Barnard TJ, Buchanan SK. TonB-dependent transporters: Regulation, structure, and function. *Annu Rev Microbiol* 2010; **64**: 43–60.

239. Ye L, Matthijs S, Bodilis J, Hildebrand F, Raes J, Cornelis P. Analysis of the draft genome of *Pseudomonas fluorescens* ATCC17400 indicates a capacity to take up iron from a wide range of sources, including different exogenous pyoverdines. *BioMetals* 2014; **27**: 633–644.

240. Matthijs S, Brandt N, Ongena M, Achouak W, Meyer JM, Budzikiewicz H. Pyoverdine and histicorrugatin-mediated iron acquisition in *Pseudomonas thivervalensis*. *BioMetals* 2016; **29**: 467–485.
241. Hartney SL, Mazurier S, Kidarsa TA, Quecine MC, Lemanceau P, Loper JE. TonB-dependent outer-membrane proteins and siderophore utilization in *Pseudomonas fluorescens* Pf-5. *BioMetals* 2011; **24**: 193–213.
242. Matthijs S, Laus G, Meyer JM, Abbaspour-Tehrani K, Schäfer M, Budzikiewicz H, et al. Siderophore-mediated iron acquisition in the entomopathogenic bacterium *Pseudomonas entomophila* L48 and its close relative *Pseudomonas putida* KT2440. *BioMetals* 2009; **22**: 951–964.
243. Cornelis P, Bodilis J. A survey of TonB-dependent receptors in fluorescent pseudomonads. *Environ Microbiol Rep* 2009; **1**: 256–262.
244. Dingemans J, Ye L, Hildebrand F, Tontodonati F, Craggs M, Bilocq F, et al. The deletion of TonB-dependent receptor genes is part of the genome reduction process that occurs during adaptation of *Pseudomonas aeruginosa* to the cystic fibrosis lung. *Pathog Dis* 2014; **71**: 26–38.
245. Butaite E, Baumgartner M, Wyder S, Kümmerli R. Siderophore cheating and cheating resistance shape competition for iron in soil and freshwater *Pseudomonas* communities. *Nat Commun* 2017; **8**: 414.
246. Miethke M, Kraushaar T, Marahiel MA. Uptake of xenosiderophores in *Bacillus subtilis* occurs with high affinity and enhances the folding stabilities of substrate binding proteins. *FEBS Lett* 2013; **587**: 206–213.
247. Abergel RJ, Zawadzka AM, Hoette TM, Raymond KN. Enzymatic hydrolysis of trilactone siderophores: Where chiral recognition occurs in enterobactin and bacillibactin iron transport. *J Am Chem Soc* 2009; **131**: 12682–12692.
248. Galet J, Deveau A, Hôtel L, Frey-Klett P, Leblond P, Aigle B. *Pseudomonas fluorescens* pirates both ferrioxamine and ferricoelichelin Siderophores from *Streptomyces ambofaciens*. *Appl Environ Microbiol* 2015; **81**: 3132–3141.

Research manuscripts

Study 1

Mark Lyng, Ákos T. Kovács

Microbial ecology: Metabolic heterogeneity and the division of labor in multi-cellular structures

Current Biology 2022; 32:14, R771-R773,

https://doi.org/10.1016/j.cub.2022.06.008

necessarily do just 'one thing' in the brain, but that its role likely spans multiple functions including motivation, motor control (including action selection and inhibition), arousal, and reward encoding. Future studies will determine whether the functional heterogeneity of dopamine is defined by anatomical or projection specificity, as suggested by Lammel *et al.*[6] and others[7], by the density and distribution of different dopamine receptors throughout the brain, by interactions with other neurotransmitters and neuromodulators, and/or by some other, as-yet-undetermined factor. We believe that future studies that parse the roles of receptor subtypes in these effects might be particularly fruitful, given evidence that dopamine D1 and D2 receptors exert opposing effects on approach/avoidance behaviour[8], conditioned place preference[9] and nicotine ingestion and withdrawal[10].

Finally, future studies that continue to elucidate the role of dopamine in backwards conditioning could have important clinical implications. While Seitz *et al.*[2] used appetitive outcomes to show that backward-paired cues bias responding towards actions earning alternative rewards, studies using aversive outcomes show that backward conditioning may imbue cues with desirable associations. For example, studies of wheel running in rodents show that although forward flavour–running pairings generate a conditioned taste aversion, flavours consumed *after* running are relatively more preferred[11], and a conditioned place preference develops for neutral contexts exposed after running[12]. It has also been suggested that foods consumed after chemotherapy sessions may be less likely to become aversive than those consumed before[13]. Thus, in addition to the potential implications of this work for pathologies such as schizophrenia noted by Seitz *et al.*[2], if dopamine activity is necessary for the formation of aversive as well as appetitive backwards associations, it is also possible that these useful backwards associations could be facilitated through the use of pharmaceuticals that target dopamine function.

DECLARATION OF INTERESTS

The authors declare no competing interests.

REFERENCES

1. Schultz, W., Dayan, P., and Montague, P.R. (1997). A neural substrate of prediction and reward. Science *275*, 1593–1599.
2. Seitz, B.M., Hoang, I.B., DiFazio, L.E., Blaisdell, A.P., and Sharpe, M.J. (2022). Dopamine errors drive excitatory and inhibitory components of backward conditioning in an outcome-specific manner. Curr. Biol. *32*, 3210–3218.
3. Sutton, R.S., and Barto, A.G. (1998). Reinforcement Learning: An Introduction (MIT Press).
4. Waelti, P., Dickinson, A., and Schultz, W. (2001). Dopamine responses comply with basic assumptions of formal learning theory. Nature *412*, 43–48.
5. Maes, E.J.P., Sharpe, M.J., Usypchuk, A.A., Lozzi, M., Chang, C.Y., Gardner, M.P.H., Schoenbaum, G., and Iordanova, M.D. (2020). Causal evidence supporting the proposal that dopamine transients function as temporal difference prediction errors. Nat. Neurosci. *23*, 176–178.
6. Lammel, S., Lim, B.K., and Malenka, R.C. (2014). Reward and aversion in a heterogeneous midbrain dopamine system. Neuropharmacology *76*, 351–359.
7. Lerner, T.N., Shilyansky, C., Davidson, T.J., Evans, K.E., Beier, K.T., Zalocusky, K.A., Crow, A.K., Malenka, R.C., Luo, L., Tomer, R., *et al.* (2015). Intact-brain analyses reveal distinct information carried by SNc dopamine subcircuits. Cell *162*, 635–647.
8. Nguyen, D., Alushaj, E., Erb, S., and Ito, R. (2019). Dissociative effects of dorsomedial striatum D1 and D2 receptor antagonism in the regulation of anxiety and learned approach-avoidance conflict decision-making. Neuropharmacology *146*, 222–230.
9. White, N.M., Packard, M.G., and Hiroi, N. (1991). Place conditioning with dopamine D1 and D2 agonists injected peripherally or into nucleus accumbens. Psychopharmacology *103*, 271–276.
10. Grieder, T.E., George, O., Tan, H., George, S.R., Le Foll, B., Laviolette, S.R., and van der Kooy, D. (2012). Phasic D1 and tonic D2 dopamine receptor signaling double dissociate the motivational effects of acute nicotine and chronic nicotine withdrawal. Proc. Natl. Acad. Sci. USA *109*, 3101–3106.
11. Salvy, S.J., Pierce, W.D., Heth, D.C., and Russell, J.C. (2004). Taste avoidance induced by wheel running: effects of backward pairings and robustness of conditioned taste aversion. Physiol. Behav. *82*, 303–308.
12. Lett, B.T., Grant, V.L., Koh, M.T., and Smith, J.F. (2001). Wheel running simultaneously produces conditioned taste aversion and conditioned place preference in rats. Learn. Motivat. *32*, 129–136.
13. Jacobsen, P.B., Bovbjerg, D.H., Schwartz, M.D., Andrykowski, M.A., Futterman, A.D., Gilewski, T., Norton, L., and Redd, W.H. (1993). Formation of food aversions in cancer patients receiving repeated infusions of chemotherapy. Behav. Res. Therap. *31*, 739–748.

Microbial ecology: Metabolic heterogeneity and the division of labor in multicellular structures

Mark Lyng[1,2] and Ákos T. Kovács[1,2,*]
[1]Bacterial Interactions and Evolution Group, DTU Bioengineering, Technical University of Denmark, Kgs Lyngby 2800, Denmark
[2]Twitter: @MarkLyng5 (M.L.), @EvolvedBiofilm (Á.T.K.)
*Correspondence: atkovacs@dtu.dk
https://doi.org/10.1016/j.cub.2022.06.008

Many bacterial species are capable of differentiating to create phenotypic heterogeneity. Using the aggregate-forming marine bacterium *Vibrio splendidus*, a new study reveals how this organism differentiates to form spherical structures with a motile, carbon-storing core and a non-motile shell.

Contrary to long-standing assumptions about the simplicity of bacterial communities, we now know that many are capable of forming complex multicellular structures, such as biofilms, with distinct subpopulations.

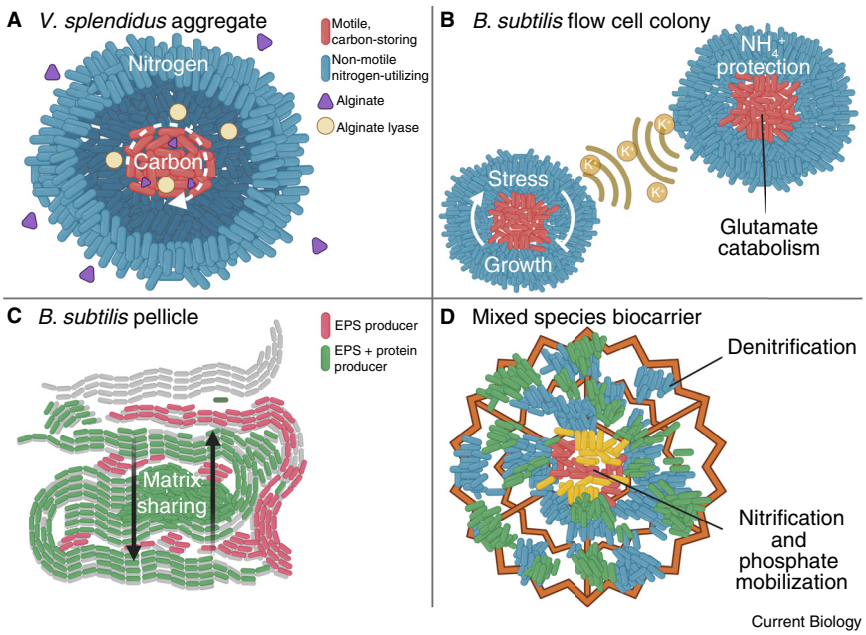

Figure 1. Metabolic heterogeneity in spatially structured microbial assemblies.
(A) *Vibrio splendidus* 12B01 assembles into spherical aggregates in the presence of alginate, where the core is composed of motile cells that rearrange themselves to make alginate lyase available as a public good to the entire population, while simultaneously storing carbon. (Adapted from Schwartzman *et al.*[3] and Ebrahimi *et al.*[4].) (B) *Bacillus subtilis* microcolonies oscillate in metabolism accumulating stress during growth at the periphery, which is alleviated at a threshold, allowing for the core cells to catabolize glutamate to ammonia, which diffuses out to the fast-growing periphery. The oscillation is mediated by potassium ions to regulate metabolism even between two separate colonies. (Adapted from Liu *et al.*[7], Prindle *et al.*[8], and Liu *et al.*[9].) (C) *B. subtilis* floating pellicle biofilms produce matrix components that are shared as public goods. The population exhibits a transcriptional heterogeneity, dividing matrix producers into one of three categories: those cells that produce both exopolysaccharides and the amyloid protein TasA, those that produce only exopolysaccharides, and those that produce neither. (Adapted from Dragoš *et al.*[6].) (D) A mixed-species biocarrier from a wastewater treatment plant reveals spatial distribution of genera, dividing the biofilm into an outer layer responsible for denitrification and an inner structure responsible for nitrification and phosphate mobilization. (Adapted from Villard *et al.*[11].) This figure was created with BioRender.com.

Biofilms offer an opportunity to dissect the fundamental principles underlying how and why this complex multicellularity arises. Multicellular bacterial communities often enjoy environmental advantages, mostly provided by the extracellular matrix secreted by cells in the biofilm. However, matrix components cannot stand alone and owe much of their effectiveness to the communal assembly of individual cells[1]. Nevertheless, assembly of cells leads to an increased concentration of extracellular polysaccharides, proteins, and DNA that confers novel properties otherwise impossible for individual cells to achieve. These properties often manifest themselves through a division of labor, where costly public goods are secreted by producers for the benefit of the entire population and provide a fitness advantage to the community that would be unattainable by an individual cell. This division in production mainly occurs because cells in biofilms can differentially regulate their gene expression, driven mainly by changes in the microenvironment, leading to phenotypic heterogeneity[2].

A prime example of how phenotypic heterogeneity can lead to the emergence of multicellular complexity is reported by Schwartzman and colleagues[3] in this issue of *Current Biology* (Figure 1A). Here, the authors work with *Vibrio splendidus* (12B01), a marine bacterium that grows on alginate as a carbon source and forms multicellular particles. Using this model, Schwartzman *et al.* show how this bacterium differentiates from isoclonal single cells to heterogeneous aggregates with specialized metabolic compartments in the presence of alginate. The authors demonstrate how these aggregates develop over time from individual cells — first to small, differentiated aggregates and later to larger spheres approximately 40 μm (or larger) in diameter with a motile core and a non-motile outer shell that eventually ruptures to free core-based cells, becoming a hollow shell.

By separating aggregates at different developmental stages and performing transcriptomics on the cells within each fraction, the authors reveal how the outer-shell-residing cells express the genes involved in production of adhesion structures, whereas cells in the core upregulate genes associated with carbon storage, nitrogen assimilation, and alginate catabolism, prompting the authors to hypothesize that the core must be experiencing nitrogen limitation. Using fluorescence microscopy and staining for carbon storage with Nile Red, the authors were able to test this hypothesis and show how the core cells store carbon when they are subjected to nitrogen limitation. Interestingly, the transcription of extracellular matrix genes was not increased in cells harvested from the aggregates. Thus, Schwartzman and colleagues have elegantly demonstrated how isoclonal populations differentiate to form specialized compartments within multicellular aggregates, adding to the growing body of literature showing how phenotypic heterogeneity in bacteria is almost exclusively coupled to spatial organization.

Two observations especially stand out from this publication: first, the compartmentalization facilitates rearrangement of cells within the core; secondly, the inner core is nitrogen-limited and carbon-storing. The Cordero lab previously investigated this same strain of *V. splendidus* and found that, even though it was a weak degrader of alginate not expected to produce aggregates larger than 10 μm (based on mathematical modeling), the bacterium surpassed the initial mathematical model by rearranging the cells within the core, allowing some aggregates to grow to sizes larger than 50 μm[4]. How was this achieved? The mixing of the cells within the core facilitated the distribution of the public-good enzyme alginate lyase, allowing the aggregate to overcome

diffusion limitations of both substrate and enzyme.

Sharing of public goods is crucial for bacterial multicellularity, although in some microbes, motility is completely lost upon the switch to multicellularity, preventing active rearrangement. Instead, closely associated cells differentiate to produce separate public goods to share with their immediate neighbors[5,6]. This has been observed, for example, with *Bacillus subtilis*, which produces biofilms with heterogeneous expression of matrix-associated genes (Figure 1C), and with *Pseudomonas aeruginosa*, which was recently shown to produce biofilms with high degrees of heterogeneity, wherein subpopulations of cells specialize to metabolize nutrients based on local concentration gradients.

Clearly, different organisms exhibit distinct patterns of spatial organization, be it free-floating aggregates or surface-associated biofilms. From Schwartzman *et al.*[3], as well as other studies, it seems likely that the spatial organization influences phenotypic differentiation where the multicellular structures either contain cells that are all producers but rearrange themselves to share public goods with the entire population or comprise locally differentiated clusters of producers. The multicellular fate of a population is likely influenced by many factors including the strength of producers, the surrounding environment, and the size of the multicellular structure. Whereas *V. splendidus* assembles into relatively small aggregates, *P. aeruginosa* biofilms often cover surfaces spanning hundreds of thousands of cell lengths, rendering it infeasible to use free-floating cells to move nutrients from one end to the other.

Large structures may instead use long-distance signals to regulate the physiological states of cells, both within biofilms and between biofilms. This is the case for *B. subtilis* biofilms formed in microfluidic chambers that oscillate in growth and metabolism to periodically reduce starvation of cells in the inner core[7]. This oscillation was shown to be a response to nitrogen limitation and was coordinated by potassium ions that even led to electrical signaling, facilitating a form of electrical communication between separate biofilms[8,9].

An interesting common thread can be noted between the *V. splendidus* alginate-degrading particles and the *B. subtilis* biofilms: nitrogen limitation at the center of the multicellular community. Schwartzman *et al.*[3] found that nitrogen for biomass production was abundant in the outer shell but limited in the core. Similarly, in the *B. subtilis* studies[7–9] the inner core was shown to degrade the nitrogen source (glutamate) into ammonia, which was then transferred from the core to the periphery of the biofilm (Figure 1B). Although not explicitly stated, there seems to be a general tendency for multicellular microbes to leave catabolism to the cells in the inner parts of the population and then transfer the metabolic products to the outer parts of the biofilm to increase biomass at the frontiers. This fits nicely with the current paradigm of multicellularity of biofilms having the outer periphery of cells die to protect the inner core. Based on the findings by Schwartzman *et al.*[3], one might speculate that carbon storage in spatially structured bacterial assemblies is then a general strategy utilized in the event of dispersal or for protection of the metabolically robust core.

The studies discussed up until this point all investigate single-species populations. However, in most natural settings, biofilms are mixed-species communities, sometimes with high degrees of taxonomic diversity. With high diversity, one might ask if these generalities still hold true. In one study, the authors found that mixing cross-feeding overproducers of histidine and tryptophan led to a high degree of intermixing during growth on solid medium[10]. When non-cooperating auxotrophs were introduced to the community, they were excluded from the colony, resulting in segmented colonies where cooperators and non-cooperators were spatially segregated. When the three strains were cultivated in liquid culture, the productivity of the community decreased as a result of the fitness cost associated with overproducing amino acids while having a non-cooperator taking a share of the public goods.

Thus, the spatial organization of mixed-species communities determines the distribution of metabolically specialized cells. This was also recently shown in a natural wastewater treatment system where biocarriers with mixed-species biofilms were disrupted into spatial fractions from the outer layer to the inner structure[11] (Figure 1D). Metagenomic analysis of the fractions revealed differential abundances of genera in the different fractions of the biofilm, which contained complementary nitrogen-metabolizing genes. As such, the authors hypothesized that the outer layer of the biofilm, comprised of *Flavobacterium*, was responsible for a part of the denitrification pathway, whereas the cells in the inner structure, belonging to *Phyllobacteriaceae*, *Intrasporangiaceae*, and *Betaproteobacteria*, were responsible for the rest of denitrification, as well as nitrification and phosphate mobilization.

It appears then that there may be a general trend in the metabolic division of labor of multicellular aggregates. A trend that may even surpass taxonomy and manifest in mixed species structures. It will be exciting to see if future studies of single- and mixed-species microbial assemblies further converge on the same principles.

DECLARATION OF INTERESTS

The authors declare no competing interests.

REFERENCES

1. Lyons, N.A., and Kolter, R. (2015). On the evolution of bacterial multicellularity. Curr. Opin. Microbiol. *24*, 21–28.
2. Cooper, G.A., Frost, H., Liu, M., and West, S.A. (2021). The consequences of group structure and efficiency benefits for the evolution of division of labour. eLife *10*, 71968.
3. Schwartzman, J.A., Ebrahimi, A., Chadwick, G., Sato, Y., Roller, B.R.K., Orphan, V.J., and Cordero, O.X. (2022). Bacterial growth in multicellular aggregates leads to the emergence of complex life cycles. Curr. Biol. *32*, 3059–3069.
4. Ebrahimi, A., Schwartzman, J., and Cordero, O.X. (2019). Multicellular behaviour enables cooperation in microbial cell aggregates. Philos. Trans. R. Soc. B *374*, 20190077.
5. Dar, D., Dar, N., Cai, L., and Newman, D.K. (2021). Spatial transcriptomics of planktonic and sessile bacterial populations at single-cell resolution. Science *373*, eabi4882.
6. Dragoš, A., Kiesewalter, H., Martin, M., Hsu, C.Y., Hartmann, R., Wechsler, T., Eriksen, C., Brix, S., Drescher, K., Stanley-Wall, N., *et al.* (2018). Division of labor during biofilm matrix production. Curr. Biol. *28*, 1903–1913.

7. Liu, J., Prindle, A., Humphries, J., Gabalda-Sagarra, M., Asally, M., Lee, D.Y.D., Ly, S., Garcia-Ojalvo, J., and Süel, G.M. (2015). Metabolic co-dependence gives rise to collective oscillations within biofilms. Nature *523*, 550–554.

8. Prindle, A., Liu, J., Asally, M., Ly, S., Garcia-Ojalvo, J., and Süel, G.M. (2015). Ion channels enable electrical communication in bacterial communities. Nature *527*, 59–63.

9. Liu, J., Martinez-Corral, R., Prindle, A., Lee, D.-Y.D., Larkin, J., Gabalda-Sagarra, M., Garcia-Ojalvo, J., and Süel, G.M. (2017). Coupling between distant biofilms and emergence of nutrient time-sharing. Science *356*, 638–642.

10. Pande, S., Kaftan, F., Lang, S., Svato, A., Germerodt, S., and Kost, C. (2016). Privatization of cooperative benefits stabilizes mutualistic cross-feeding interactions in spatially structured environments. ISME J. *10*, 1413–1423.

11. Villard, D., Saltnes, T., Sørensen, G., Angell, I.L., Eikås, S., Johansen, W., and Rudi, K. (2022). Spatial fractionation of phosphorus accumulating biofilm: stratification of polyphosphate accumulation and dissimilatory nitrogen metabolism. Biofouling *38*, 162–172.

Corollary discharge: Linking saccades and memory circuits in the human brain

Julio Martinez-Trujillo
Departments of Physiology and Pharmacology, and Psychiatry, Schulich School of Medicine and Dentistry, Western Institute for Neuroscience, Western University, London, ON, Canada
Correspondence: julio.martinez@robarts.ca
https://doi.org/10.1016/j.cub.2022.06.006

A new study has found that, in primates with highly specialized visual systems, a corollary discharge of motor commands to make exploratory saccades arises in the midbrain, propagates to the thalamus, and then reaches hippocampal circuits in the depths of the temporal lobe where it shapes the making of memories.

In systems neurophysiology, a corollary discharge is a signal copy of commands originating in motor regions of the nervous system that reaches sensory brain areas carrying information about incoming actions[1]. The corollary discharge makes it possible to distinguish whether signals activating sensory receptors are generated by external forces, such as an object touching us, or by our own actions, for example when we touch the object. Indeed, disfunction of corollary discharge signals has been suggested to be a factor in schizophrenia, a human brain disease in which self-monitoring functions are impaired[2]. In this issue of *Current Biology*, Katz *et al.*[3] report evidence that a corollary discharge signal reaches the human hippocampus where it influences long-term memory formation.

In organisms with highly evolved visual systems, such as humans and other primates, which explore their environment through gaze shifts, a corollary discharge of motor commands that drive eye muscles enables perceptual stability. Consider that saccades are made at a rate of three to four per second, and with every saccade the eyeball carries the retina at speeds greater than 150 degrees per second. Without a corollary discharge that inhibits visual processing while the retina is in motion, saccades would produce retinal smear impairing perceptual stability, comparable to the effect of fast camera motion on a photograph[4]. The corollary discharge signal can also be used to fill the trans-saccadic gap in visual perception by producing re-mapping of receptive fields in visual areas[5]. In non-human primates, a corollary discharge of saccade commands originates in the superior colliculus of the midbrain, travels to the thalamus, and then propagates to various levels of the visuomotor processing hierarchy[5] (Figure 1A). One issue that has been a matter of recent debate is whether the corollary discharge also serves other brain functions.

Some studies have proposed that in humans and other primates, the corollary discharge signal accompanying saccades impacts memory formation[6]. The rationale is that in primates with high-resolution foveal vision, goal-directed saccades select behaviorally relevant information in a visual scene[7]. Behaviorally relevant information is most likely to enter the deepest levels of the visual hierarchy including the hippocampus and be stored as long-term memories to be used in the future for guiding behavior.

Katz *et al.*[3] recorded from single neurons in the medial temporal lobe of human subjects with epilepsy who had been implanted with microwire electrodes[8]. Subjects performed a visual search task on stationary images presented on a computer screen while their eye movements were measured using video-based eye tracking. Subjects searched for an odd target object in a scene and then associated the object with the scene elements for future recall. This task requires the formation of long-term associative memories, which requires the integrity of hippocampal circuits[9].

The authors found that, during the encoding phase, 20% of recorded single neuron responses in the hippocampus were modulated before and around the time of saccades. Most neurons showed response suppression and were in their majority broad spiking. In mammalian cortex, including the hippocampus, most neurons are excitatory, generally pyramidal cells that fire broad action potentials[10,11], so the authors inferred

Study 2

Mark Lyng, Ákos T. Kovács

Frenemies of the soil: *Bacillus* and *Pseudomonas* interspecies interactions

Trends in Microbiology 2023; 31:8, 845-857,
https://doi.org/10.1016/j.tim.2023.02.003

Trends in Microbiology

CellPress OPEN ACCESS

Review

Frenemies of the soil: *Bacillus* and *Pseudomonas* interspecies interactions

Mark Lyng[1,@] and Ákos T. Kovács[1,2,@,*]

Bacillus **and** ***Pseudomonas*** **ubiquitously occur in natural environments and are two of the most intensively studied bacterial genera in the soil. They are often coisolated from environmental samples, and as a result, several studies have experimentally cocultured bacilli and pseudomonads to obtain emergent properties. Even so, the general interaction between members of these genera is virtually unknown. In the past decade, data on interspecies interactions between natural isolates of** ***Bacillus*** **and** ***Pseudomonas*** **has become more detailed, and now, molecular studies permit mapping of the mechanisms behind their pairwise ecology. This review addresses the current knowledge about microbe–microbe interactions between strains of** ***Bacillus*** **and** ***Pseudomonas*** **and discusses how we can attempt to generalize the interaction on a taxonomic and molecular level.**

Highlights

Outcomes of pairwise interactions between bacilli and pseudomonads do not correlate with species-level taxonomy.

Most interaction pairs of *Bacillus* and *Pseudomonas* engage in net negative interactions that stabilize into coexistence.

Strains from both genera are ubiquitous and often coisolated from soil. Understanding why this is the case may translate to other microbial interactions and deepen our insight into microbial ecology in general.

Bacillus and *Pseudomonas* in microbial ecology

Most of the biomass of the earth is made up of microbial life that drives countless natural and biotechnological processes [1]. The environmental distribution of microbes is determined by microbial ecology, that is, the **ecological interaction** (see Glossary) of microbes with their environment, plants, animals, and each other. For a long time, intermicrobial relations were neglected in favor of understanding how individual microbes affected their hosts and surrounding environment. This has been most common for plant–microbe interactions, in which the bacterial genera *Bacillus* and *Pseudomonas* are heavily represented. While the ability of both genera to suppress plant pathogens was appreciated, little attention was paid to how they affect the rest of the microbiome. Additionally, although both genera are environmentally ubiquitous and often coisolated [2–7], it remains ambiguous whether the two genera generally engage in positive or negative interactions. In the past few decades, this problem has come closer to being solved, and not only do we now have genomic, transcriptional, and metabolic information on the interspecies interactions of many bacilli and pseudomonads, but studies are also starting to map the molecular mechanisms behind intermicrobial interactions.

Therefore, the aim of this review is to provide an overview of the current knowledge of interspecies interactions between *Bacillus* spp. and *Pseudomonas* spp. pairwise and in more complex communities and environments with an emphasis on phylogeny and molecular mechanisms.

Most reported *Pseudomonas–Bacillus* interactions represent competition

The environmental ubiquity of the *Pseudomonas* and *Bacillus* genera provides natural opportunities for individual strains to come into contact and coexist [2–4]. The fact that *Pseudomonas* and *Bacillus* are often coisolated suggests that species of these genera generally settle into a stable coexistence (i.e., they are, in principle, compatible) [5–7]. Indeed, interactions between members of the two genera range from mutualism to competition depending on media, bioactive compound potential, and – to a lesser extent – phylogeny (Figure 1). However, the majority of the currently reported cocultures of bacilli and pseudomonads interacting directly with each other

[1]Bacterial Interactions and Evolution group, DTU Bioengineering, Technical University of Denmark, Kgs Lyngby 2800, Denmark
[2]Institute of Biology, Leiden University, Leiden, The Netherlands

*Correspondence: a.t.kovacs@biology.leidenuniv.nl (Á.T. Kovács).
@Twitter: @MarkLyng5 (M. Lyng) and @EvolvedBiofilm (Á.T. Kovács).

© 2023 The Authors. Published by Elsevier Ltd. This is an open access article under the CC BY license (http://creativecommons.org/licenses/by/4.0/).

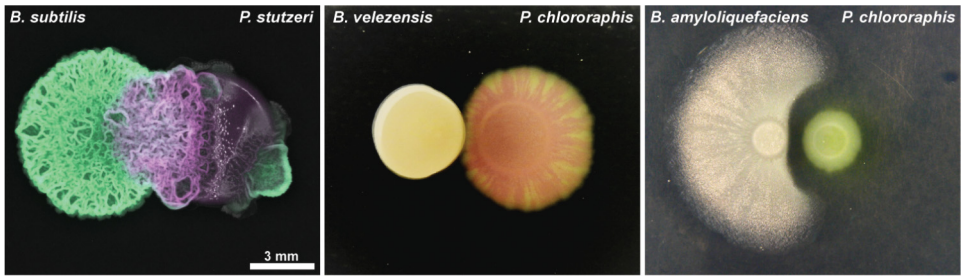

Figure 1. *Bacillus–Pseudomonas* interactions range from mutualism to competition. The pairwise ecology of bacilli and pseudomonads is highly dependent on media and secreted molecules and less dependent on phylogeny. Left: mutualistic coculture with *Bacillus subtilis* 3610 (green) spotted next to *Pseudomonas stutzeri* XL272 (magenta) on tryptic soy agar and incubated at 37°C for 72 h. Scale bar: 3 mm. Center: neutral coculture with *Bacillus velezensis* GA1 spotted next to *Pseudomonas chlororaphis* JV497 on casamino acid agar and incubated at 30°C for 24 h. Adapted from [25]. Right: competitive coculture with *Bacillus amyloliquefaciens* FZB42 spotted next to *P. chlororaphis* PCL1606 on King's B agar and incubated at 30°C for 24 h. Adapted from [22].

reveal either competition or amensalism mediated by bioactive natural products (Table 1; see Box 1 for an overview of how interactions are studied). It is important to recognize that the vast majority of published interactions between bacilli and pseudomonads are from cocultures of isolates originating from plants (either the phyllosphere or rhizosphere) and soil (Table 2). Pairwise interactions with microbes from these environments generally follow the distribution obtained by Kehe *et al*. (2021) [8], although they similarly cocultured soil isolates and not isolates from other niches. Although, the number of *Bacillus–Pseudomonas* interactions is sparse, interactions with pairs from other niches do not follow a similar distribution, possibly due to the diverse levels of nutrient availability in other niches. Still, negative interactions seem to be common when coculturing bacterial species in pairs [8,9], but the debate is currently heavy on whether these findings fail to reflect natural systems which are often much more complex than cultivations in the laboratory. Natural environments harbor multitudes of species, all engaging in a vast network of higher-order interactions [10]. Indeed, what may seem like a negative interaction in a pairwise system, can equilibrate into a competitive balance where numerous species coexist [11,12] or when intraspecific competition is greater than interspecific competition [13], though it remains to be experimentally proven if that is the case for *Bacillus–Pseudomonas* interactions as well. An example of stable competition is observed in the case of the THOR tri-species **synthetic community** (**SynCom**), where a *Bacillus cereus* isolate was found to contain the 'hitchhikers' *Pseudomonas koreensis* and *Flavobacterium johnsonii* [7]. This community synergistically increases biofilm formation when all three species are present, even though *P. koreensis* chemically restricts the growth of *F. johnsonii*, as *B. cereus* limits the concentration of the koreenceine antibiotic from *P. koreensis*. Intriguingly, the interactions in this SynCom are highly temperature-sensitive; a seemingly positive effect at one temperature becomes negative at a different temperature [14].

Studies reporting a net negative interaction between *Bacillus* and *Pseudomonas* therefore might potentially conceal a coexistence when abundances equilibrate in the long term. In addition to this complexity, interaction outcomes seem to lack conservation at the species level, resulting in interplays between pseudomonads and bacilli as diverse as the genera themselves (Table 1). Rather, interactions associated with the metabolomic arsenal of the interacting strains and strains of identical species, but with differing natural product potential, can yield distinct interaction outcomes [15]. This arsenal is mostly composed of bioactive secondary metabolites, but also by other – less obvious – molecules, proteins, and pseudo-organelles. Only some of these molecules

Glossary

2,4-diacetylphloroglucinol (DAPG): a plant-growth-promoting polyketide produced by certain pseudomonads of the *P. fluorescens* group.
Autoinducer II (AI2): a signaling molecule involved in quorum sensing.
Cyclic lipopeptides (CLPs): a group of nonribosomal peptides often exhibiting bioactivity.
Ecological interactions: relationships between pairs of organisms are described by the effect of the relationship on each partner; that is, positive (+), neutral (0), or negative (–). Ecological interactions are divided into mutualism (+/+), competition (–/–), predation/parasitism (+/–), commensalism (+/0), and amensalism (–/0).
Elongation factor G (FusA): a prokaryotic elongation factor involved in protein translation.
***N*-acylhomoserine lactone (AHL):** a signaling molecule involved in quorum sensing.
Plant-growth-promoting rhizobacterium (PGPR): a bacterial strain associated with plant growth promotion.
***Pseudomonas* quionolone signal (PQS):** a *Pseudomonas*-specific quorum sensing system.
Quorum sensing: a bacterial signaling system dependent on local signaling molecule concentrations.
Synthetic community (SynCom): a combined population of microbial species, the composition of which has been designed synthetically.
Type VI secretion system (T6SS): a needle-like pseudo-organelle used by some bacterial strains to inject toxins into competitors.
White-line-inducing principle (WLIP): a CLP encoded by some *Pseudomonas* spp.

Table 1. Outcome of pairwise cocultures with *Bacillus* and *Pseudomonas*[a]

Net Interaction	Direction	*Bacillus* sp.	*Pseudomonas* sp.	Effector	Refs
Negative	Amensalism against *Bacillus*	*B. cereus*	*Pseudomonas.* sp.	Unknown antagonist	[12]
		B. cereus	*P. fluorescens*	Unknown antagonist	[76]
		B. subtilis	*P. chlororaphis*	T6SS effector	[20,21]
		B. thuringiensis	*P. fluorescens*	Unknown antagonist	[93]
		B. velezensis	*P. sessilinigenes*	Lipopeptide	[25]
		B. velezensis	*P. kilonensis*	Lipopeptide	[25]
		B. velezensis	*P. chlororaphis*	Lipopeptide	[25]
		B. subtilis	*P. protegens*	DAPG	[24]
		B. subtilis	*P. putida*	DAPG	[24]
	Amensalism against *Pseudomonas*	*Bacillus.* sp.	*P. fluorescens*	Pr. Metabolism	[66]
		B. stratosphericus	*P. syringae*	Unknown antagonist	[94]
		B. subtilis	*P. syringae*	Lipopeptide	[95]
		B. subtilis	*P. aeruginosa*	Quorum quencher	[68]
	Competition	*B. amyloliquefaciens*	*P. chlororaphis*	Bacillaene and unknown antagonist	[22]
		B. thuringiensis	*P. fluorescens*	Pr. Metabolism	[11]
		B. velezensis	*P. protegens*	Lipopeptide	[25]
		B. velezensis	*P. tolaasii*	Lipopeptide	[25]
		B. cabrialesii	*P. syringae*	Unknown antagonist	[15]
		B. subtilis	*P. syringae*	Unknown antagonist	[15]
		B. velezensis	*P. syringae*	Unknown antagonist	[15]
Neutral	Neutralism	*B. aerius*	*P. monteilii*		[6]
		B. aerius	*P. aeruginosa*		[6]
		B. cereus	*P. fluorescens*		[89]
		B. pumilus	*P. monteilii*		[6]
		B. pumilus	*P. aeruginosa*		[6]
		B. subtilis	*P. putida*		[33]
		B. subtilis	*P. monteilii*		[6]
		B. subtilis	*P. aeruginosa*		[6]
		B. thuringiensis	*P. fluorescens*		[96]
		B. velezensis	*P. protegens*		[25]
		B. velezensis	*P. lactis*		[25]
		B. velezensis	*P. chlororaphis*		[25]
		B. velezensis	*P. mosselii*		[25]
Positive	Mutualism	*B. cereus*	*P. koreensis*	Pr. Metabolism	[7,14,67]
		B. cereus	*P. fluorescens*	Pr. Metabolism	[77–80]
		B. flexus	*P. azotoformans*	Pr. Metabolism	[86]
		B. velezensis	*P. stutzeri*	Pr. Metabolism	[73]

[a]Pr. Metabolism: An interaction characterized by resource competition and not bioactive secondary metabolites.

Box 1. Experimental coculture setups

Research of the interactions between microbes has generally followed quite similar experimental setups (Figure I). For growth kinetics, partners are coinoculated into a medium of interest and cultivated planktonically to determine synergy in growth rate, carrying capacity, or total live colony-forming units (CFUs). In planktonic cocultures, the direction and strength of an interaction is often derived from the carrying capacity of each pair compared to monoculture growth. An increased abundance of both partners is interpreted as mutualism, while a decreased abundance of both implies competition. In cases where a study aims to determine the effect of a natural product, the focal species is inoculated into a medium containing either a concentrated crude extract from the producer or the purified effector molecule. This approach has been useful in determining minimal inhibitory concentrations and in providing evidence for whether an effector molecule is secreted at concentrations that are bioactive against the focal strain. However, planktonic cultures often do not represent natural systems; thus, a favored and appropriate alternative would be to culture strains on solid agar where interacting molecules can diffuse through the agar at concentrations that mimic natural systems more closely. Many bacterial species activate transcription of biofilm-related genes on solid media and differentiate into spatial heterogeneity, increasing the accuracy (and complexity) of the interaction system. Solid medium interaction assays typically involve culturing strains in close proximity as macrocolonies or on top of each other as variations of the Burkholder plate assay. Experiments like these are valuable for insight on how molecules secreted in ecologically relevant concentrations affect a partner, and the experimenter uses inhibition zones or growth-free 'halos' to infer competition. For information on natural product bioactivity, variations of the Kirby–Bauer disc assay are a common choice, where the size of a growth-free 'halo' correlates with bioactivity; however, a researcher must interpret the strength of bioactivity in the context of the tested concentration which often is comparable to natural concentrations. For especially intricate hypotheses, researchers often establish a complex model biofilm system imitating the natural environment where the interacting strains are likely to meet. This can be achieved through substrate mimicking, host colonization, etc.

While antagonism and agonism are often identifiable through coculturing, the effector molecules and molecular mechanisms are not. Therefore, researchers use a multi-omics approach comprising transcriptomics and metabolomics. RNA-sequencing is used to analyze the transcriptomic responses to effector molecules or interaction partners, while chromatography and mass spectrometry are utilized for identification of effector and response molecules. In recent years, developments in mass spectrometry imaging have made it possible to visualize the spatial localization of metabolites during interspecies interactions, allowing for novel hypotheses regarding the distribution of metabolites in addition to the quantity.

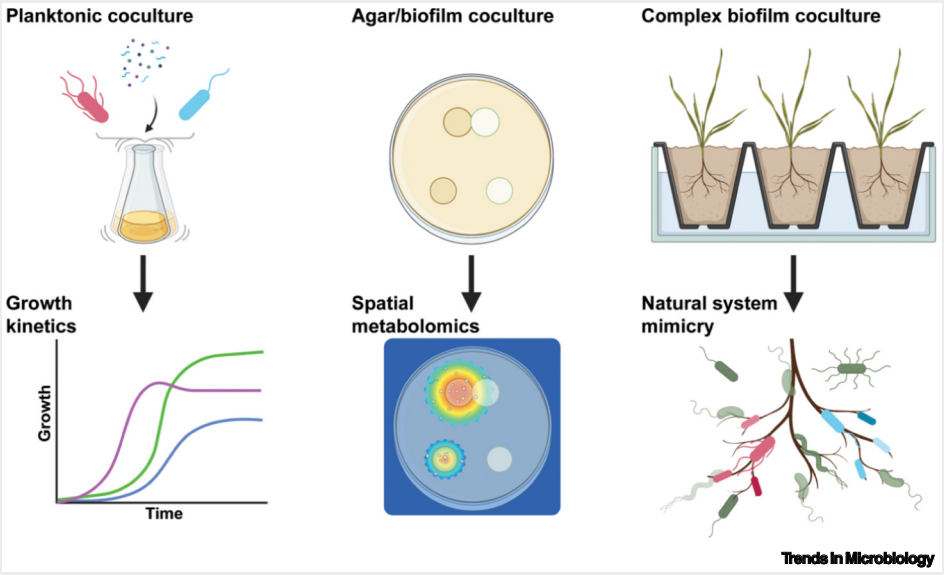

Figure I. Experimental coculture setups. Pairwise interactions are typically assessed via three experimental setups: planktonic cocultures, agar cocultures, and complex biofilm cocultures. Each methodology seeks to understand different aspects of a pairwise interaction from growth kinetics to spatial metabolomics to higher-order interactions in natural systems. Figure created with BioRender.com.

Table 2. Niches of isolates and the outcomes of pairwise interactions[a]

Isolation niche	Positive	Neutral	Negative	Total (*n*)
Plant	13% (4)	20% (6)	67% (20)	30
Soil	10% (1)	40% (4)	50% (5)	10
Animal	0% (0)	70% (7)	30% (3)	10
Marine	0% (0)	0% (0)	100% (4)	4
Laboratory standard	50% (1)	0% (0)	50% (1)	2
Other	50% (4)	0% (0)	50% (4)	8
Combined	15% (10)	26% (17)	58% (38)	65

[a]Sixty-five interactions (cocultures or challenges with cultured media) were summarized based on the isolation environment of the interacting pairs. Interactions with pairs from different origins were excluded except in cases with standard laboratory strains. In these cases, the niche is denoted as that of the isolate.

are conserved among members of a species and even fewer within members of a genus. Instead, many are likely inherited through horizontal gene transfer, possibly originating from a distantly related organism [16]. Few studies report interactions mediated by primary metabolism, though all positive interactions reported in Table 1 are products of cross-feeding or other ways to share resources. This finding may be biased by the underwhelming number of competition assays examining mechanisms such as resource competition.

With the current body of literature on *Bacillus–Pseudomonas* interactions, it is impossible to accurately predict the outcome of a pairwise contact from the phylogeny of the interacting partners. In addition, recent evidence shows that phylogeny might not be the best predictor for pairwise interactions [17], and therefore, the undergoing intensification in research on bioactive compound potential could provide a stronger understanding on *Bacillus–Pseudomonas* ecology.

Physical interactions

The literature investigating interactions between *Bacillus* and *Pseudomonas* has generally focused on how secreted chemicals from one strain affect the interacting partner (Box 1). As such, the number of examples describing physical cell-to-cell interactions are scarce.

Several species of *Pseudomonas* are well known for carrying a **type VI secretion system** (**T6SS**) [18,19], which works as a toxin-injecting syringe, activated upon cell-to-cell contact with competitive species. When cocultured next to *Bacillus subtilis*, *Pseudomonas chlororaphis* uses a T6SS to compete for space, triggering *B. subtilis* cells to undergo sporulation as a defense mechanism [20]. This is most evident in situations where *Bacillus* is unable to produce biofilm matrix components, which it employs as a defensive barrier. The effector toxin was recently defined as Tse1, a peptidoglycan hydrolase, whose gene is located in a T6SS gene cluster that is shared across a number of Gram-negative bacteria [21]. Interestingly, T6SS might be a last line of defense, provided that chemical inhibitors prove ineffective against a competitor allowing for cell-to-cell contact. Close-by macrocolonies of *Bacillus amyloliquefaciens* and *P. chlororaphis* result in a distinct zone of inhibition with no physical contact between colonies. In this case, *P. chlororaphis* downregulates T6SS gene expression in favor of the type II secretion system and production of several secondary metabolites [22].

Chemical interactions

Both *Pseudomonas* spp. and *Bacillus* spp. are well known for their massive arsenal of secondary metabolites (Box 2). Many secondary metabolites display antimicrobial activity, though some are used to gain colonization advantages in competitive niches without killing other microbes.

Box 2. Secondary metabolites

Secondary metabolites (also known as natural products) are non-essential compounds produced by an organism to confer a selective advantage. Two molecular families dominate the secondary metabolite group: nonribosomal peptides and polyketides. The functions of these metabolites range from toxic antagonism [97] to signaling molecules [98,99], cellular differentiators [24], or entries into novel nutritional niches [100].

In pseudomonads, production of secondary metabolites is controlled by the global Gac/Rsm regulon which is responsible for regulating the expression of approximately 10% of *Pseudomonas* genes [101]. Though the signaling pathway is activated by the sensor kinase GacS, it is currently unknown which environmental stimulus causes the initial activation. In bacilli, secondary metabolite regulation is more decentralized, with specific regulons for different classes of compounds [102].

Notable examples are the cyclic lipopeptides (CLPs): surfactin, iturins, and fengycin/plipastatin from *Bacillus*, and viscosin, tolaasin, and syringopeptin from *Pseudomonas* which are known for their bioactivity against fungi and/or other bacteria. In addition, the *Pseudomonas* polyketide 2,4-diacetylphlorogucinol (DAPG), produced by some members of the *P. fluorescens* group, is of great interest due to its apparent plant-growth-promoting and antimicrobial activities. Secondary metabolism of *Bacillus* is reviewed more extensively in [102,103], and of *Pseudomonas* in [104].

In the case of interactions between *Bacillus* and *Pseudomonas*, a general view suggests that *Pseudomonas* spp. are most often offensive (i.e., they produce bactericidal or bacteriostatic molecules) [20,22–24], while *Bacillus* spp. more often defend themselves (i.e., they neutralize offensive molecules or prevent being overtaken by a competitor) [25–27] (Figure 2).

Several studies have demonstrated the antimicrobial effect of secreted molecules through variations of the disk diffusion assay (Box 1). This approach allowed researchers to identify saponins and alkaloids (specifically phenetyl acetamide) produced by *B. cereus, Bacillus thuringiensis,* and *B. subtilis* that inhibit *Pseudomonas aeruginosa* [28,29], while **2,4-diacetylphloroglucinol** (**DAPG**), pyocyanin, and several bacteriocins from *Pseudomonas protegens*, *Pseudomonas putida*, and *P. aeruginosa* have been able to inhibit *B. subtilis*, *Bacillus licheniformis*, *B. cereus*, and *B. thuringiensis* [24,30–33]. While these studies are valuable in identifying effector molecules and their range of effect, their contribution to ecological or mechanistic insight is sparse as they did not report the concentrations of the molecules in the environments where they were produced.

Pseudomonas cyclic lipopeptides are deadly (and) specific

The **cyclic lipopeptides** (**CLPs**) comprise one of the most structurally diverse groups of secondary metabolites produced by both bacilli and pseudomonads [34]. *Bacillus* spp. are

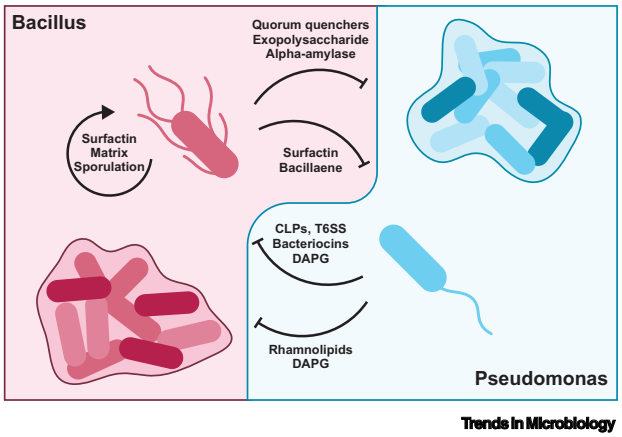

Figure 2. Pseudomonads are offensive, bacilli are defensive. *Pseudomonas* and *Bacillus* use a range of bioactive compounds to interact with each other, mainly in net negative relations. Especially *Pseudomonas* cyclic lipopeptides (CLPs) and 2,4-diacetylphloroglucinol (DAPG) directly antagonize multiple *Bacillus* spp. In cell-to-cell contact, *Pseudomonas* utilizes type VI secretion systems (T6SS) to puncture *Bacillus* and inject toxins intracellularly. *Bacillus* spp. rarely directly antagonize *Pseudomonas*. Instead, they either sequester offensive molecules, produce protective matrix, or undergo sporulation to preserve part of the population. However, bacilli do contain multiple molecules to prevent or disrupt biofilm formation of pseudomonads.

primarily known for surfactin, iturins, and fengycins, while *Pseudomonas* spp. carry the potential for producing up to 14 distinct groups of CLPs [35].

The bioactivity of *Pseudomonas* CLPs is specific to their molecular structure, and mainly CLPs from the viscosin, tolaasin, and syringopeptin groups have been demonstrated to inhibit growth of bacilli. Syringopeptin 22A, syringopeptin 25A, corpeptin, tolaasin, and **WLIP** (**'white-line-inducing principle'**) all inhibit *Bacillus megaterium* [36–38], while massetolide A, syringomycin E, orfamide A, arthrofacin, and entolysin B do not [39,40]. Even within CLP groups, bioactivity varies. Though massetolide A is unable to antagonize *B. megaterium*, massetolide E, from *Pseudomonas lurida*, strongly inhibits *B. thuringiensis* [39]. Within the viscosin group, a hierarchy of effect has been established on the antagonism of *B. subtilis* and *B. cereus* with pseudodesmin being the most active, closely followed by viscosinamide and finally viscosin and WLIP showing almost no inhibition [41].

The lipopeptides of *Bacillus* – fengycin, iturin, and surfactin – are all well known for their bioactivities. Fengycin and iturin are generally regarded as antifungal [42], and accordingly demonstrate very weak activity against *Pseudomonas.* Concentrations must reach more than 200 μg/ml, at which point fengycin kills *P. aeruginosa* cells by altering the cell topography, causing leakage of the intracellular content [43]. More examples exist of surfactin bioactivity against pseudomonads, and against *Pseudomonas fluorescens,* it is bactericidal down to 25 μg/ml, inhibiting tomato root colonization [42]. Though best known for enhancing motility during swarming [44] and sliding [43,45], surfactin produced by *Bacillus velezensis* also functions as a chemical trap to sequester the *Pseudomonas sessilinigenes* cyclic lipopeptide sessilin [25]. This reduces the toxicity of sessilin to a level where *B. velezensis* is not eradicated in a coculture. Interestingly, this chemical interplay is specific to sessilin and does not carry over to other *Pseudomonas* CLPs.

Bacillus defends itself by producing biofilm matrix and committing to sporulation

Both *B. subtilis* and *B. amyloliquefaciens* have been shown to defend themselves against competitors using biofilm matrix components and, as a last resort, by inducing sporulation to preserve part of the population [20,22]. In several reported cocultures, bacilli have entered sporulation with no evidence that *Pseudomonas* is able to destroy *Bacillus* endospores. To date, only a single study has provided evidence of *Bacillus* directly inhibiting the growth of pseudomonads with bacillaene produced by *B. amyloliquefaciens* that interacts with *P. chlororaphis* **elongation factor G** (**FusA**) inhibiting protein synthesis without killing *Pseudomonas* [22]. More examples exist that report indirect inhibition of *Pseudomonas* by priming plant systemic resistance, for example with *B. cereus* instigating *Arabidopsis thaliana* systemic resistance against *P. syringae* pv. *tomato* both dependently and independently of salicylic acid, jasmonic acid, and ethylene signaling [46–48].

Bacillus biofilm formation can be inhibited by *Pseudomonas* species of the *fluorescens* and *protegens* subgroups through the production of the antimicrobial secondary metabolite DAPG [24]. Although DAPG-producing pseudomonads are often applied in biocontrol, the compound antagonizes more than just plant pathogens. DAPG at high concentrations suppresses the growth of *B. subtilis*, while subinhibitory concentrations reduce biofilm formation and delay sporulation [24]. The mechanism is unknown but speculated to be due to an interaction with Spo0A, the global regulator of sporulation in *Bacillus*. Interestingly, a combination of *B. subtilis* with DAPG-producing pseudomonads still led to synergistic biocontrol [49]. Additionally, *Bacillus* surface-associated biofilm can be prevented and dispersed by the rhamnolipid biosurfactants of *Pseudomonas* [50–52]. The current consensus suggests an altered surface hydrophobicity without experimental proof so far [53]. However, as most studies assess biofilm functionality *in vitro*, the ecological relevance of biofilm requires further testing.

Bacillus carries a vast arsenal of quorum quenchers

Bacillus spp. have demonstrated the ability to prevent competitors from establishing themselves, particularly by disrupting or inhibiting their biofilm formation. Isolates of *Bacillus pumilus, Bacillus paralicheniformis, B. subtilis,* and *B. thuringiensis* have all demonstrated some sort of *Pseudomonas* **quorum sensing** inhibition [16,26,54–57]. At this point, *Bacillus* isolates have been experimentally shown to quench quorum sensing systems that depend on ***N*-acylhomoserine lactones** (**AHLs**) and ***Pseudomonas* quinolone signal** (**PQS**), but not **autoinducer II (AI2)**-dependent cell–cell communication. Interestingly, supplementation of AI2 seems to inhibit initiation of the sporulation process in *B. velezensis* [58]. Particularly, the lactonase AiiA has been shown to degrade both short-, medium-, and long-chain AHLs, thus disrupting quorum sensing and downstream effects in *P. aeruginosa* and plant pathogenic pseudomonads [54,56,59]. AiiA was originally discovered in endophytic *B. thuringiensis* isolates [56]; however, additional research revealed conservation of lactonase activity in the entire *B. cereus* group. Noor and colleagues reported that 22 out of 64 *B. subtilis* soil isolates carry homologs of AiiA, conserved with 84.4% amino acid identity [57]. A second lactonase, YtnP, was identified in a soil isolate of *B. paralicheniformis* and shown to degrade AHLs from multiple Gram-negative strains, including *P. aeruginosa, Pseudomonas extremeorientalis,* and *Pseudomonas lini* [55]. Similarly, *B. pumilus* disrupts quorum sensing by producing an acylase that enzymatically deacetylates AHLs [26], while a marine *Bacillus* sp. isolate produces a non-enzymatic antagonist of AHL without enzymatically changing the *Pseudomonas* autoinducers [60]. None of the identified quorum quenchers exhibit direct growth inhibition against any tested *Pseudomonas* spp. strains.

Recently, *B. subtilis* isolates were shown to encode Stigmatellin Y: an orthosteric antagonist for quinolones in PQS quorum sensing [16,61]. It is speculated that StigY is not conserved in *Bacillus* spp. but rather was horizontally transferred from *Stigmatella aurantiaca*. Other than quorum quenching, some bacilli use specialized exopolysaccharides to reduce the surface hydrophobicity of Gram-negatives and thus suppress adherence and biofilm formation [62].

Certain bacilli are also capable of degrading already established *Pseudomonas* biofilm, as experimentally demonstrated by exopolysaccharide degradation by α-amylase and through an unknown mechanism facilitated by an antimicrobial protein [52,63,64]. However, it is likely that the concentration required for biofilm degradation far surpasses that produced in natural systems. Importantly, these studies recognize the potential of quorum quenching as a treatment option via these *Bacillus* effector molecules, but no experimental test has been reported to prove that quenching occurs in natural settings or even within *in vitro* cocultures.

Transcriptional responses are unique to a coculture partner

An unresolved question in microbial ecology is whether an interaction is caused by a specific response or is simply the passive consequence of microbes being in the vicinity of molecules secreted by other microbes. Additionally, if a strain responds to the presence of an unrelated neighbor, is its metabolism regulated based on the specific interaction partner or is it simply a general response to any microbe or stress condition [65]?

For *Pseudomonas*, evidence of specificity is derived from transcriptomic and gene essentiality studies, where proximal macrocolonies with different neighboring organisms led to distinct transcriptional and gene essentiality profiles [66]. Although differential expression and conditional essentiality are shared between all organisms, most genes are highly dependent on the specific organism. Interestingly, patterns diverge when coculturing one *Pseudomonas* strain next to different bacilli, suggesting that the metabolome of the interacting *Bacillus* strongly influences the response of *Pseudomonas* [20,22], though this, too, may be species- or even strain-specific

[67]. Although fewer examples exist of *Bacillus* transcriptomic responses to *Pseudomonas*, there is evidence that *B. subtilis* alters its metabolome in response to secreted molecules from *P. aeruginosa*, increasing its antibiofilm activity [68]. A recent study using the THOR SynCom also demonstrated that, in the three-species community, *B. cereus* was the member that modulated its expression of biosynthetic gene clusters primarily when cocultured with *P. koreensis*. The metabolome and transcriptome of *P. koreensis* were not altered dramatically in coculture with *B. cereus*, and both *B. cereus* and *P. koreensis* were unresponsive towards *F. johnsonii* [67]. Additionally, *P. chlororaphis* has been shown to produce antagonistic molecules that select for specific genetic variants of *B. amyloliquefaciens* [22].

How these interaction patterns fit together is difficult to conclude based on the current literature. Nevertheless, a candidate regulatory system that is likely involved in interspecies interactions of *Pseudomonas* is the main controller of secondary metabolism, the Gac/Rsm two-component system (or its orthologs – see [69]). In addition to secondary metabolism, Gac/Rsm controls several primary metabolic lifestyles such as motility, quorum sensing, and biofilm formation. Generally, GacS activation results in an increased production of offensive and defensive molecules, secreted or retained intracellularly [70–72].

On secondary metabolism-inducing King's B agar, *P. chlororaphis* GacS was reported to be essential for antagonism against *B. amyloliquefaciens* in a transposon library screen, but transcriptomic analysis of the same interaction revealed no differential expression [22]. When competing *P. fluorescens* Pf0-1 with *Bacillus* sp. V102 on a carbon-limited water-agar medium, *gacS* and *gacA* were also not found to be differentially expressed, though several other two-component systems were transcribed at increased levels in coculture compared to monoculture [66]. In a similar setup, competition of *P. protegens* against *B. subtilis* and several other soil microbes demonstrated that *P. protegens* GacS was not essential in interactions with *B. subtilis* but was essential in coculture with another *Pseudomonas* strain and even disadvantageous in interactions with fungal plant pathogens [23]. Future comprehensive molecular ecology studies will hopefully reveal the emerging and common patterns in *Bacillus–Pseudomonas* interactions.

Mutually beneficial coexistence

Only few *Bacillus–Pseudomonas* coculture studies have been reported with the aim of identifying and understanding positive interactions. This could explain the abundance of net negative interactions and the lack of direct positive interactions. In recent years, however, the field has started to report studies providing evidence for commensalism and even mutualism.

An important recent study supports the coexistence of bacilli and pseudomonads: Sun and colleagues [73] inoculated cucumber roots with the **plant-growth-promoting rhizobacterium** (**PGPR**) *B. velezensis* SQR9 and found that, in particular, *Pseudomonas* spp. were enriched in the rhizosphere compared to non-inoculated controls. With a combination of transcriptomics, metabolomics, and molecular biology, a mutualistic relationship was ultimately identified between *B. velezensis* and a *Pseudomonas stutzeri* soil isolate potentially facilitated by cross-feeding of branched amino acids. Similarly, combinations of bacilli and pseudomonads increase the growth of the plant *Cannabis sativa* by up to 70%, with *Bacillus* spp. being the main modulator of the soil microbiome while *Pseudomonas* spp. are more associated with plant growth promotion [74]. Apparently, *Bacillus* arrives first and subsequently recruits *Pseudomonas* via metabolic byproducts. However, only few studies reporting synergy have also evaluated the compatibility of the consortium members, instead concentrating primarily on the application efficiency and thus lack specific insights on the distribution and the interaction of the mixed species. As such, it is impossible to deduce the net outcome of the pairwise interaction and whether synergy

stems from positive or negative interactions. Some of these studies show positive interactions and subsequent synergy [75], while others report competition and synergy [76]. For instance, in a series of coculture studies with *B. cereus* and *P. fluorescens,* initial planktonic cocultures revealed antagonism by *P. fluorescens* against *B. cereus* [76]. In biofilm reactors, inhibition was absent, and instead, biofilm matrix formation increased synergistically with more protein present in the coculture biofilm [77,78]. Interestingly, despite the synergistic increase in biofilm formation, coculture biofilm could be removed more efficiently with a quaternary ammonium disinfectant [79,80]. The complexity of such interactions means that one should be careful oversimplifying and attempting to generalize pairwise interactions.

Applicability of *Bacillus–Pseudomonas* cocultures

With their status as plant-growth-promoting rhizobacteria, *Bacillus* and *Pseudomonas* have been studied extensively for their potential as alternatives to chemical fertilizers and pesticides. Species from either genus have been successfully applied as growth promoters and biopesticides, but several studies have also shown how consortia of bacilli and pseudomonads act in synergy to produce emergent properties not possible by any of the partners in isolation. Such synergy has led to the control of *Cephalysporium* in maize [81], of *Fusarium* in beans [82], and blight in cucumber, radish, and cotton [49,83]. As with interactions between *Bacillus* and *Pseudomonas*, secondary metabolites are the main mediators of biocontrol, and the cocultivation of species has resulted in additive effects of metabolites produced in monocultures, but also in novel compounds produced only in coculture. In the case of plant growth promotion, synergy may again stem from additive effects of molecules produced by each microbe [84], or the enhanced ability of cocultures to establish themselves on plants compared to pure cultures [85], allowing higher production of effector molecules [5,49,81–87].

Pairs of bacilli and pseudomonads clearly can create biotechnological value, and it will be interesting to see if future formulations will be able to outcompete chemical alternatives.

Concluding remarks

Research into pairwise interactions between *Bacillus* and *Pseudomonas* still leaves much unanswered (see Outstanding questions). With our current understanding, a reductionistic approach using selected single isolates of each genus is insufficient, as we cannot draw clear conclusions and identify overarching patterns. One thing that most research agrees on is that interspecies interactions are more complex than net negative or positive associations.

Thus, the simple hypothesis that successfully applied biotechnological consortia must in general engage in mutualism is flawed. If the scope is limited to look only for isolates that grow synergistically, we risk overlooking emergent properties evident in competitive interactions that settle into a stable equilibrium. It is well known that resource competition is a strong selective pressure that determines species coexistence [88]. Indeed, several examples exist of *Bacillus* and *Pseudomonas* being capable of specifically controlling the differentiation and metabolism of each other independently of secreted molecule toxicity [24,68,73]. However, pairwise interactions do not necessarily translate to higher-order interactions in multispecies consortia. Rather, several examples exist of bacilli and pseudomonads that outcompete each other in dual species coculture but stabilize into coexistence in a more diverse community [67,89]. Importantly, pairwise interactions between *Pseudomonas* and *Bacillus* have greatly contributed to our understanding of the effects of secondary metabolites on model soil bacteria and the relevance of pairwise interactions in biotechnology. However, it is exceedingly rare to find studies reporting concentrations (or even the presence) of effector molecules in natural environments. This is largely due to the complexity of *in situ* quantification. Though examples exist, they currently rely on relatively simple substrates (e.g., the

Outstanding questions

Why are bacilli and pseudomonads so often coisolated?

How do pairwise interactions between *Bacillus* and *Pseudomonas* affect natural microbiomes?

How can knowledge of *Bacillus–Pseudomonas* dynamics be applied in the development of biotechnologically relevant culture formulations?

What are the concentrations of effector molecules in natural systems?

phyllosphere) [90,91], and it has not yet been possible to quantify secondary metabolites directly from soil. An undergoing development in mimicking natural systems and detecting molecules from complex systems [92] means that future studies could potentially report biological functions in the context of naturally occurring concentrations, an important advance in understanding chemical microbial ecology.

Acknowledgments

The authors would like to thank Carlos N. Lozano Andrade and Clara Gaja Corbera for insightful discussions during the preparation of this review. We would also like to extend our gratitude to Sofija Andric, Marc Ongena, Carlos Molina-Santiago, and Diego Romero for contributing their raw images for Figure 1. Work in the laboratory of Á.T.K. is supported by the Danish National Research Foundation (DNRF137) for the Center for Microbial Secondary Metabolites and the Novo Nordisk Foundation within the INTERACT project of the Collaborative Crop Resiliency Program (NNF19SA0059360). Biofilm-related work in the group of Á.T.K. is supported by a DTU Alliance Strategic Partnership PhD fellowship.

Declaration of interests

No interests are declared.

References

1. Magnabosco, C. *et al.* (2018) The biomass and biodiversity of the continental subsurface. *Nat. Geosci.* 11, 707–717
2. Chiellini, C. *et al.* (2019) *Pseudomonas* strains isolated from different environmental niches exhibit different antagonistic ability. *Ethol. Ecol. Evol.* 31, 399–420
3. Yadav, A.N. *et al.* (2015) Diversity and phylogenetic profiling of niche-specific *Bacilli* from extreme environments of India. *Ann. Microbiol.* 65, 611–629
4. Compant, S. *et al.* (2011) Endophytes of grapevine flowers, berries, and seeds: identification of cultivable bacteria, comparison with other plant parts, and visualization of niches of colonization. *Microb. Ecol.* 62, 188–197
5. Roberts, C. *et al.* (2020) Environmental consortium containing *Pseudomonas* and *Bacillus* species synergistically degrades polyethylene terephthalate plastic. *mSphere* 5, e01151–20
6. Bodawatta, K.H. *et al.* (2020) Great tit (*Parus major*) uropygial gland microbiomes and their potential defensive roles. *Front. Microbiol.* 11, 1735
7. Lozano, G.L. *et al.* (2019) Introducing THOR, a model microbiome for genetic dissection of community behavior. *mBio* 10, e02846–18
8. Kehe, J. *et al.* (2021) Positive interactions are common among culturable bacteria. *Sci. Adv.* 7, eabi7159
9. Palmer, J.D. and Foster, K.R. (2022) Bacterial species rarely work together. *Science* 376, 581–582
10. Ludington, W.B. (2022) Higher-order microbiome interactions and how to find them. *Trends Microbiol.* 30, 618–621
11. Monmeyran, A. *et al.* (2021) Four species of bacteria deterministically assemble to form a stable biofilm in a millifluidic channel. *NPJ Biofilms Microbiomes* 7, 64
12. Chakraborty, B. *et al.* (2016) Deciphering a survival strategy during the interspecific competition between *Bacillus cereus* MSM-S1 and *Pseudomonas* sp. MSM-M1. *R. Soc. Open Sci.* 3, 160438
13. Leinweber, A. *et al.* (2017) Cheating fosters species co-existence in well-mixed bacterial communities. *ISME J.* 11, 1179–1188
14. Burman, E. and Bengtsson-Palme, J. (2021) Microbial community interactions are sensitive to small changes in temperature. *Front. Microbiol.* 12, 672910
15. Zhou, L. *et al.* (2021) Antimicrobial activity screening of rhizosphere soil bacteria from tomato and genome-based analysis of their antimicrobial biosynthetic potential. *BMC Genomics* 22, 29
16. Boopathi, S. *et al.* (2022) *Bacillus subtilis* BR4 derived stigmatellin Y interferes Pqs-PqsR mediated quorum sensing system of *Pseudomonas aeruginosa*. *J. Basic Microbiol.* 62, 801–814
17. Nestor, E. *et al.* (2023) Interactions between culturable bacteria are predicted by individual species' growth *mSystems* 8, e00836-22
18. Boyer, F. *et al.* (2009) Dissecting the bacterial type VI secretion system by a genome wide *in silico* analysis: what can be learned from available microbial genomic resources? *BMC Genomics* 10, 104
19. Bernal, P. *et al.* (2018) Type VI secretion systems in plant-associated bacteria. *Environ. Microbiol.* 20, 1–15
20. Molina-Santiago, C. *et al.* (2019) The extracellular matrix protects *Bacillus subtilis* colonies from *Pseudomonas* invasion and modulates plant co-colonization. *Nat. Commun.* 10, 1919
21. Pérez-Lorente, A.I. (2023) Sporulation Activated via σW Protects Bacillus from a Tse1 Peptidoglycan Hydrolase Type VI Secretion System Effector. *Microbiol Spectr* 11, e0504522 https://doi.org/10.1128/spectrum.05045-22
22. Molina-Santiago, C. *et al.* (2021) Chemical interplay and complementary adaptative strategies toggle bacterial antagonism and co-existence. *Cell Rep.* 36, 109449
23. Vick, S.H.W. *et al.* (2021) Delving into defence: identifying the *Pseudomonas protegens* Pf-5 gene suite involved in defence against secreted products of fungal, oomycete and bacterial rhizosphere competitors. *Microb. Genom.* 7, 000671
24. Powers, M.J. *et al.* (2015) Inhibition of cell differentiation in *Bacillus subtilis* by *Pseudomonas protegens*. *J. Bacteriol.* 197, 2129–2138
25. Andrić, S. *et al.* (2021) Lipopeptide interplay mediates molecular interactions between soil *Bacilli* and *Pseudomonads*. *Microbiol. Spectr.* 9, e02038–21
26. Nithya, C. *et al.* (2010) *Bacillus pumilus* of Palk Bay origin inhibits quorum-sensing-mediated virulence factors in Gram-negative bacteria. *Res. Microbiol.* 161, 293–304
27. Andrić, S. *et al.* (2022) Plant-associated *Bacillus* mobilizes its secondary metabolites upon perception of the siderophore pyochelin produced by a *Pseudomonas* competitor. *ISME J.* 17, 263–275
28. Feliatra, F. *et al.* (2021) The potentials of secondary metabolites from *Bacillus cereus* SN7 and *Vagococcus fluvialis* CT21 against fish pathogenic bacteria. *Microb. Pathog.* 158, 105062
29. Vaca, J. *et al.* (2020) Indole alkaloid derivatives as building blocks of natural products from *Bacillus thuringiensis* and *Bacillus velezensis* and their antibacterial and antifungal activity study. *J. Antibiot.* 73, 798–802
30. Baron, S.S. and Rowe, J.J. (1981) Antibiotic action of pyocyanin. *Antimicrob. Agents Chemother.* 20, 814–820
31. Fontoura, R. *et al.* (2009) Purification and characterization of an antimicrobial peptide produced by *Pseudomonas* sp. strain 4B. *World J. Microbiol. Biotechnol.* 25, 205–213

32. Rahman, P.K.S.M. *et al.* (2009) Development of a simple and low cost microbioreactor for high-throughput bioprocessing. *Biotechnol. Lett.* 31, 209–214
33. Ahmad, A. *et al.* (2013) *Pseudomonas putida* strain FStm2 isolated from shark skin: a potential source of bacteriocin. *Probiotics Antimicrob. Proteins* 5, 165–175
34. Raaijmakers, J.M. *et al.* (2006) Cyclic lipopeptide production by plant-associated *Pseudomonas* spp.: diversity, activity, biosynthesis, and regulation. *MPMI* 19, 699–710
35. Geudens, N. and Martins, J.C. (2018) Cyclic lipodepsipeptides from *Pseudomonas* spp. – biological Swiss-army knives. *Front. Microbiol.* 9, 1867
36. Grgurina, I. *et al.* (2002) A new syringopeptin produced by bean strains of *Pseudomonas syringae* pv. *syringae*. *Biochem. Biophys. Acta* 1597, 81–89
37. Bassarello, C. *et al.* (2004) Tolaasins A–E, five new lipodepsipeptides produced by *Pseudomonas tolaasii*. *J. Nat. Prod.* 67, 811–816
38. Rokni-Zadeh, H. *et al.* (2012) Genetic and functional characterization of cyclic lipopeptide white-line-inducing principle (WLIP) production by rice rhizosphere isolate *Pseudomonas putida* RW10S2. *Appl. Environ. Microbiol.* 78, 4826–4834
39. Kissoyan, K.A.B. *et al.* (2019) Natural *C. elegans* microbiota protects against infection via production of a cyclic lipopeptide of the viscosin group. *Curr. Biol.* 29, 1030–1037
40. Reder-Christ, K. *et al.* (2012) Model membrane studies for characterization of different antibiotic activities of lipopeptides from *Pseudomonas*. *Biochim. Biophys. Acta Biomembr.* 1818, 566–573
41. Geudens, N. *et al.* (2016) Membrane interactions of natural cyclic lipodepsipeptides of the viscosin group. *Biochim. Biophys. Acta* 1859, 331–339
42. Kiesewalter, H.T. *et al.* (2021) Genomic and chemical diversity of *Bacillus subtilis* secondary metabolites against plant pathogenic fungi. *mSystems* 6, e00770–20
43. Grau, R.R. *et al.* (2015) A duo of potassium-responsive histidine kinases govern the multicellular destiny of *Bacillus subtilis*. *mBio* 6, e00581–15
44. Kearns, D.B. and Losick, R. (2003) Swarming motility in undomesticated *Bacillus subtilis*. *Mol. Microbiol.* 49, 581–590
45. Jautzus, T. *et al.* (2022) Complex extracellular biology drives surface competition during colony expansion in *Bacillus subtilis*. *ISME J.* 16, 2320–2328
46. Niu, D. *et al.* (2016) *Bacillus cereus* AR156 activates PAMP-triggered immunity and induces a systemic acquired resistance through a NPR1-and SA-dependent signaling pathway. *Biochem. Biophys. Res. Commun.* 469, 120–125
47. Niu, D.-D. *et al.* (2011) The plant growth-promoting rhizobacterium *Bacillus cereus* AR156 induces systemic resistance in *Arabidopsis thaliana* by simultaneously activating salicylate-and jasmonate/ethylene-dependent signaling pathways. *Mol. Plant-Microbe Interact.* 24, 533–542
48. Wang, S. *et al.* (2018) *Bacillus cereus* AR156 activates defense responses to *Pseudomonas syringae* pv. *tomato* in *Arabidopsis thaliana* similarly to flg22. *Mol. Plant-Microbe Interact.* 31, 311–322
49. Khabbaz, S.E. *et al.* (2015) Characterisation of antagonistic *Bacillus* and *Pseudomonas* strains for biocontrol potential and suppression of damping-off and root rot diseases. *Ann. Appl. Biol.* 166, 456–471
50. Diaz De Rienzo, M.A. and Martin, P.J. (2016) Effect of mono and di-rhamnolipids on biofilms pre-formed by *Bacillus subtilis* BBK006. *Curr. Microbiol.* 73, 183–189
51. Vasileva-Tonkova, E. *et al.* (2011) The effect of rhamnolipid biosurfactant produced by *Pseudomonas fluorescens* on model bacterial strains and isolates from industrial wastewater. *Curr. Microbiol.* 62, 427–433
52. Dusane, D.H. *et al.* (2010) Rhamnolipid mediated disruption of marine *Bacillus pumilus* biofilms. *Colloids Surf. B Biointerfaces* 81, 242–248
53. Díaz De Rienzo, M.A. *et al.* (2016) Antibacterial properties of biosurfactants against selected Gram-positive and -negative bacteria. *FEMS Microbiol. Lett.* 363, fnv224
54. Anandan, K. and Vittal, R.R. (2019) Quorum quenching activity of AiiA lactonase KMMI17 from endophytic *Bacillus thuringiensis KMCL07* on AHL- mediated pathogenic phenotype in *Pseudomonas aeruginosa*. *Microb. Pathog.* 132, 230–242
55. Djokic, L. *et al.* (2022) Novel quorum quenching YtnP lactonase from *Bacillus paralicheniformis* reduces *Pseudomonas aeruginosa* virulence and increases antibiotic efficacy *in vivo*. *Front. Microbiol.* 13, 906312
56. Dong, Y.-H. *et al.* (2000) AiiA, an enzyme that inactivates the acylhomoserine lactone quorum-sensing signal and attenuates the virulence of *Erwinia carotovora*. *PNAS* 97, 3526–3531
57. Noor, A.O. *et al.* (2022) Biodiversity of N-acyl homoserine lactonase (aiiA) gene from *Bacillus subtilis*. *Microb. Pathog.* 166, 105543
58. Xiong, Q. *et al.* (2021) Quorum sensing signal autoinducer-2 inhibits sporulation of *Bacillus* by interacting with 2 RapC and functions across species. *bioRxiv* Posted November 2, 2021. https://doi.org/10.1101/2021.11.02.466875
59. Dong, Y.H. *et al.* (2002) Identification of quorum-quenching N-acyl homoserine lactonases from *Bacillus* species. *Appl. Environ. Microbiol.* 68, 1754–1759
60. Musthafa, K.S. *et al.* (2011) Antipathogenic potential of marine *Bacillus* sp. SS4 on N-acyl-homoserine- lactone-mediated virulence factors production in *Pseudomonas aeruginosa* (PAO1). *J. Biosci.* 36, 55–67
61. Boopathi, S. *et al.* (2017) Stigmatellin Y – an anti-biofilm compound from *Bacillus subtilis* BR4 possibly interferes in PQS–PqsR mediated quorum sensing system in *Pseudomonas aeruginosa*. *Bioorg. Med. Chem. Lett.* 27, 2113–2118
62. Sayem, S.A. *et al.* (2011) Anti-biofilm activity of an exopolysaccharide from a sponge-associated strain of *Bacillus licheniformis*. *Microb. Cell Factories* 10, 74
63. Vaikundamoorthy, R. *et al.* (2018) Development of thermostable amylase enzyme from *Bacillus cereus* for potential antibiofilm activity. *Bioorg. Chem.* 77, 494–506
64. Hamza, F. *et al.* (2018) Efficacy of cell free supernatant from *Bacillus licheniformis* in protecting *Artemia salina* against *Vibrio alginolyticus* and *Pseudomonas gessardii*. *Microb. Pathog.* 116, 335–344
65. Comforth, D.M. and Foster, K.R. (2013) Competition sensing: the social side of bacterial stress responses. *Nat. Rev. Microbiol.* 11, 285–293
66. Garbeva, P. *et al.* (2011) Transcriptional and antagonistic responses of *Pseudomonas fluorescens* Pf0-1 to phylogenetically different bacterial competitors. *ISME J.* 5, 973–985
67. Chevrette, M.G. *et al.* (2022) Microbiome composition modulates secondary metabolism in a multispecies bacterial community. *PNAS* 119, e2212930119
68. Boopathi, S. *et al.* (2022) Investigation of interspecies crosstalk between probiotic *Bacillus subtilis* BR4 and *Pseudomonas aeruginosa* using metabolomics analysis. *Microb. Pathog.* 166, 105542
69. Lapouge, K. *et al.* (2008) Gac/Rsm signal transduction pathway of γ-proteobacteria: From RNA recognition to regulation of social behaviour. *Mol. Microbiol.* 67, 241–253
70. Cheng, X. *et al.* (2013) The Gac regulon of *Pseudomonas fluorescens* SBW25. *Environ. Microbiol. Rep.* 5, 608–619
71. Frangipani, E. *et al.* (2014) The Gac/Rsm and cyclic-di-GMP signalling networks coordinately regulate iron uptake in *Pseudomonas aeruginosa*. *Environ. Microbiol.* 16, 676–688
72. Cheng, X. *et al.* (2016) Role of the GacS sensor kinase in the regulation of volatile production by plant growth-promoting *Pseudomonas fluorescens* SBW25. *Front. Plant Sci.* 7, 1706
73. Sun, X. *et al.* (2022) *Bacillus velezensis* stimulates resident rhizosphere *Pseudomonas stutzeri* for plant health through metabolic interactions. *ISME J.* 16, 774–787
74. Comeau, D. *et al.* (2021) Interactions between *Bacillus* spp., *Pseudomonas* spp. and *Cannabis sativa* promote plant growth. *Front. Microbiol.* 12, 715758
75. Ansari, F.A. and Ahmad, I. (2019) Fluorescent *Pseudomonas* -FAP2 and *Bacillus licheniformis* interact positively in biofilm mode enhancing plant growth and photosynthetic attributes. *Sci. Rep.* 9, 4547
76. Simões, M. *et al.* (2008) Antagonism between *Bacillus cereus* and *Pseudomonas fluorescens* in planktonic systems and in biofilms. *Biofouling* 24, 339–349
77. Lemos, M. *et al.* (2014) The effects of surface type on the removal of *Bacillus cereus* and *Pseudomonas fluorescens* single and dual species biofilms. *Food Bioprod. Process.* 93, 234–241

78. Simões, L.C. *et al.* (2011) The effects of glutaraldehyde on the control of single and dual biofilms of *Bacillus cereus* and *Pseudomonas fluorescens*. *Biofouling* 27, 337–346
79. Gomes, I.B. *et al.* (2021) The effects of chemical and mechanical stresses on *Bacillus cereus* and *Pseudomonas fluorescens* single-and dual-species biofilm removal. *Microorganisms* 9, 1174
80. Kim, U. *et al.* (2022) Detection of *Bacillus cereus* and *Pseudomonas fluorescens* in dual-species biofilm via real-time PCR and eradication using grapefruit seed extract. *LWT Food Scie. Technol.* 165, 113679
81. Ghazy, N. and El-Nahrawy, S. (2021) Siderophore production by *Bacillus subtilis* MF497446 and *Pseudomonas koreensis* MG209738 and their efficacy in controlling *Cephalosporium maydis* in maize plant. *Arch. Microbiol.* 203, 1195–1209
82. Kalantari, S. *et al.* (2018) Improvement of bean yield and Fusarium root rot biocontrol using mixtures of *Bacillus*, *Pseudomonas* and *Rhizobium*. *Trop. Plant Pathol.* 43, 499–505
83. Salaheddin, K. *et al.* (2010) Management of bacterial blight of cotton using a mixture of *Pseudomonas fluorescens* and *Bacillus subtilis*. *Plant Protect. Sci.* 46, 41–50
84. Bautista-Cruz, A. *et al.* (2019) Phosphate-solubilizing bacteria improve *Agave angustifolia* Haw. growth under field conditions. *J. Sci. Food Agric.* 99, 6601–6607
85. Kumar, M. *et al.* (2016) Synergistic effect of *Pseudomonas putida* and *Bacillus amyloliquefaciens* ameliorates drought stress in chickpea (*Cicer arietinum* L.). *Plant Signal. Behav.* 11, e1071004
86. Aravinthan, A. *et al.* (2016) Synergistic growth of *Bacillus* and *Pseudomonas* and its degradation potential on pretreated polypropylene. *Prep. Biochem. Biotechnol.* 46, 109–115
87. Gómez-Guzmán, A. *et al.* (2017) Evaluation of nutrients removal (NO_3-N, NH_3-N and PO_4-P) with *Chlorella vulgaris, Pseudomonas putida, Bacillus cereus* and a consortium of these microorganisms in the treatment of wastewater effluents. *Water Sci. Technol.* 76, 49–56
88. Bernhardt, J.R. *et al.* (2020) The evolution of competitive ability for essential resources. *Philos. Trans. R. Soc. B Biol. Sci.* 375, 20190247
89. Baliarda, A. *et al.* (2021) Dynamic interspecies interactions and robustness in a four-species model biofilm. *Microbiologyopen* 10, e1254
90. Zeriouh, H. *et al.* (2014) Surfactin triggers biofilm formation of *Bacillus subtilis* in melon phylloplane and contributes to the biocontrol activity. *Environ. Microbiol.* 16, 2196–2211
91. Cuellar-Gaviria, T.Z. *et al.* (2021) Role of *Bacillus tequilensis* EA-CB0015 cells and lipopeptides in the biological control of black Sigatoka disease. *Biol. Control* 155, 104523
92. Lozano-Andrade, C.N. *et al.* (2022) Establishment of a transparent soil system to study *Bacillus subtilis* chemical ecology. *bioRxiv* Posted January 10, 2022. https://doi.org/10.1101/2022.01.10.475645
93. Rojas-Ruiz, N.E. *et al.* (2015) Analysis of *Bacillus thuringiensis* population dynamics and its interaction with *Pseudomonas fluorescens* in soil. *Jundishapur J. Microbiol.* 8, e27953
94. Durairaj, K. *et al.* (2017) Potential for plant biocontrol activity of isolated *Pseudomonas aeruginosa* and *Bacillus stratosphericus* strains against bacterial pathogens acting through both induced plant resistance and direct antagonism. *FEMS Microbiol. Lett.* 364, fnx225
95. Bais, H.P. *et al.* (2004) Biocontrol of *Bacillus subtilis* against infection of *Arabidopsis* roots by *Pseudomonas syringae* is facilitated by biofilm formation and surfactin production. *Plant Physiol.* 134, 307–319
96. Vidal-Quist, J.C. *et al.* (2013) *Bacillus thuringiensis* colonises plant roots in a phylogeny-dependent manner. *FEMS Microbiol. Ecol.* 86, 474–489
97. Foster, K.R. and Bell, T. (2012) Competition, not cooperation, dominates interactions among culturable microbial species. *Curr. Biol.* 22, 1845–1850
98. Romero, D. *et al.* (2011) Antibiotics as signal molecules. *Chem. Rev.* 111, 5492–5505
99. Straight, P.D. *et al.* (2006) Interactions between *Streptomyces coelicolor* and *Bacillus subtilis*: role of surfactants in raising aerial structures. *J. Bacteriol.* 188, 4918–4925
100. Vaz Jauri, P. *et al.* (2013) Subinhibitory antibiotic concentrations mediate nutrient use and competition among soil *Streptomyces*. *PLoS One* 8, e81064
101. Ferreiro, M.D. and Gallegos, M.T. (2021) Distinctive features of the Gac-Rsm pathway in plant-associated *Pseudomonas*. *Environ. Microbiol.* 23, 5670–5689
102. Kaspar, F. *et al.* (2019) Bioactive secondary metabolites from *Bacillus subtilis*: a comprehensive review. *J. Nat. Prod.* 82, 2038–2053
103. Sansinenea, E. and Ortiz, A. (2011) Secondary metabolites of soil *Bacillus* spp. *Biotechnol. Lett.* 33, 1523–1538
104. Gross, H. and Loper, J.E. (2009) Genomics of secondary metabolite production by *Pseudomonas* spp. *Nat. Prod. Rep.* 26, 1408–1446

Study 3

Mark Lyng, Birta Þórisdóttir, Sigrún H. Sveinsdóttir, Morten L. Hansen, Gergely Maróti, Lars Jelsbak, Ákos T. Kovács

Taxonomy of *Pseudomonas* spp determines interactions with *Bacillus subtilis*

To be submitted 2023; deposited to *bioRxiv*

https://doi.org/10.1101/2023.07.18.549276

Taxonomy of *Pseudomonas* spp determines interactions with *Bacillus subtilis*

Mark Lyng[1], Birta Þórisdóttir[1], Sigrún H. Sveinsdóttir[1], Morten L. Hansen[2], Gergely Maróti[3], Lars Jelsbak[2], Ákos T. Kovács[1,4]*

[1]Bacterial Interactions and Evolution group, DTU Bioengineering, Technical University of Denmark, Kgs Lyngby 2800, Denmark

[2]Microbiome Interactions and Engineering, DTU Bioengineering, Technical University of Denmark, Kgs. Lyngby 2800, Denmark

[3]Institute of Plant Biology, Biological Research Center, ELKH, 6726 Szeged, Hungary

[4]Institute of Biology Leiden, Leiden University, 2333BE Leiden, The Netherlands

*Correspondence: a.t.kovacs@biology.leidenuniv.nl (A.T.K.)

Abstract

Bacilli and pseudomonads are among the most well-studied microorganisms commonly found in soil, and frequently co-isolated. Despite this, no systematic approach has been employed to assess the pairwise compatibility of members from these genera. Here, we screened 720 fluorescent soil isolates for their effects on *Bacillus subtilis* pellicle formation in two types of media and found a predictor for interaction outcome in *Pseudomonas* taxonomy. Interactions were context-dependent and both medium composition and culture conditions strongly influenced interactions. Negative interactions were associated with *Pseudomonas capeferrum, Pseudomonas entomophila* and *Pseudomonas protegens,* and 2,4-diacetylphloroglucinol was confirmed as a strong (but not exclusive) inhibitor of *B. subtilis*. Non-inhibiting strains were closely related to *Pseudomonas trivialis* and *Pseudomonas lini*, but in this case, cocultures with increased *B. subtilis* pellicle formation were spatially segregated. Our study is the first to propose an overall negative outcome from pairwise interactions between *B. subtilis* and fluorescent pseudomonads, hence cocultures comprising members from these groups are likely to require additional microorganisms for coexistence.

Keywords: *Bacillus subtilis*, *Pseudomonas*, microbial ecology, biofilm, competition, secondary metabolite

Introduction

Plant growth-promoting rhizobacteria (PGPR) possess great potential to replace traditional fertilisers and pesticides as a more sustainable alternative. In particular, isolates from *Bacillus* and *Pseudomonas* genera have been studied extensively due to their abilities to inhibit plant pathogens, induce plant systemic resistance, increase the growth rate of plants, and alleviate environmental stress (*Bacillus* reviewed in [1] and *Pseudomonas* reviewed in [2]). Several studies combined isolates from the two genera and observed a synergistic increase in a trait of interest, be it plant growth or protection [3–7]. However, few studies have investigated the cause of synergy, hence little information is available on the pairwise compatibility of *Bacillus* and *Pseudomonas*, and whether environmental isolates engage in antagonism or symbiosis.

Bacillus subtilis is one of the most well-studied model organisms in biology, serving as a prototypical example of biofilm formation and plant root colonisation. Several strains have demonstrated antagonism towards other microorganisms, especially plant pathogenic fungi [8]. Such interactions are mainly mediated by secreted bioactive secondary metabolites, of which *B. subtilis* produces a diverse arsenal. Of note is plipastatin that shows antifungal properties [9,10], while surfactin and bacillaene display more broad antimicrobial properties [11,12]. Positive interactions between *Bacillus* and *Pseudomonas* have also been observed, such as intraspecies division of labour [13] and interspecies cross-feeding [14].

Pseudomonas is a genus of numerous species comprising at least 166 type strains that are found in soil, plant rhizospheres, marine habitats and animal hosts [15–18]. The impact of *Pseudomonas* spp. on human society ranges from human and plant pathogenicity to bioremediation, biocontrol and biostimulation [19–22]. Interestingly, there is a fine line between pathogenic and beneficial *Pseudomonas* spp. that mainly depends on the arsenal of secondary metabolites produced by a given strain [23,24]. Similarly, compatibility with *Bacillus* spp. also seems to rely mainly on a relatively small collection of secondary metabolites and defence mechanisms [25]. Understanding the frequency of positive and negative interactions between *Bacillus* and diverse *Pseudomonas* spp., as well as the underlying mechanisms of such interactions would be of great interest to agricultural biotechnology relying on mixed consortia of species from the two genera.

Here, we cocultured 720 soil isolates selected for fluorescent *Pseudomonas* properties with the undomesticated type-strain *B. subtilis* DK1042 (hereafter DK1042) under floating biofilm (pellicle)-inducing conditions and used a spinning disc-based medium-throughput screen to quantify DK1042 biofilms. Using two types of media, we demonstrate that although positive interactions with superior pellicle abundance were rare in both types of media, interactions were highly medium-dependent. By taxonomically characterising isolates at the species level, we determined that DK1042 was least likely to be compatible with species closely related to type strains of *Pseudomonas capeferrum, Pseudomonas entomophila* and *Pseudomonas protegens*, and most likely to be compatible with *Pseudomonas lini* and *Pseudomonas trivialis*. We found that *Pseudomonas* antagonism towards DK1042 is mainly due to the

presence of specific biosynthetic gene clusters (BGCs), and that 2,4-diactylphloroglucinol (DAPG) is a major (though not exclusive) inhibitor of DK1042 against both pellicles and colonies.

Results

Pseudomonads negatively affect *B. subtilis*

Relationships between *B. subtilis* and fluorescent pseudomonads range from antagonism to co-existence and, potentially, to synergistic growth, but no systematic investigation of interaction outcomes between the two has been performed. To address this, we performed pairwise coculture of DK1042 and each of 720 *Pseudomonas* soil isolates in 96-well plates and measured DK1042 biomass using an Opera High-Content screening spinning disc platform (Fig. 1a). We screened the library against DK1042 *amyE*::$P_{hyperspank}$-*mKate2* constitutively expressing the fluorophore mKate2, and recorded the three-dimensional volume occupied by *Bacillus* as a proxy for cell abundance. Each isolate was cocultured three times with DK1042 both in rich Tryptic Soy Broth (TSB) medium and diluted biofilm-inducing lysogeny broth medium supplemented with glycerol and manganese (0.1× LBGM), and biovolume in coculture was compared with that in monocultures as $\log_2$(Fold Change) (Fig. 1b).

The distribution of $\log_2$(FC) differed substantially between media types, suggesting that many neutral interactions in rich media become negative in diluted media, in line with stronger resource competition in nutrient-poor media among microorganisms [26]. Examining the biovolume for each isolate (Fig. S2a) revealed that isolates from site P9 were more likely to antagonise DK1042 while isolates from the P8 site more often resulted in a high DK1042 biovolume. This also differed between media types, as cocultures in TSB had a higher degree of within-sample variance in biovolume measurements and therefore also in calculated $\log_2$(FC) values (Fig. S2b and S2c). We divided each isolate into three categories based on median $\log_2$(FC) and found that most interactions (regardless of medium) were neutral (Fig. 2a), while only a very small number of isolates had a positive effect on DK1042 (Fig. 1b). These results indicate that fluorescent pseudomonads very rarely stimulate *B. subtilis* cell abundance in TSB or 0.1× LBGM, and that inhibition of *B. subtilis* by *Pseudomonas* spp. is strongly influenced by medium composition.

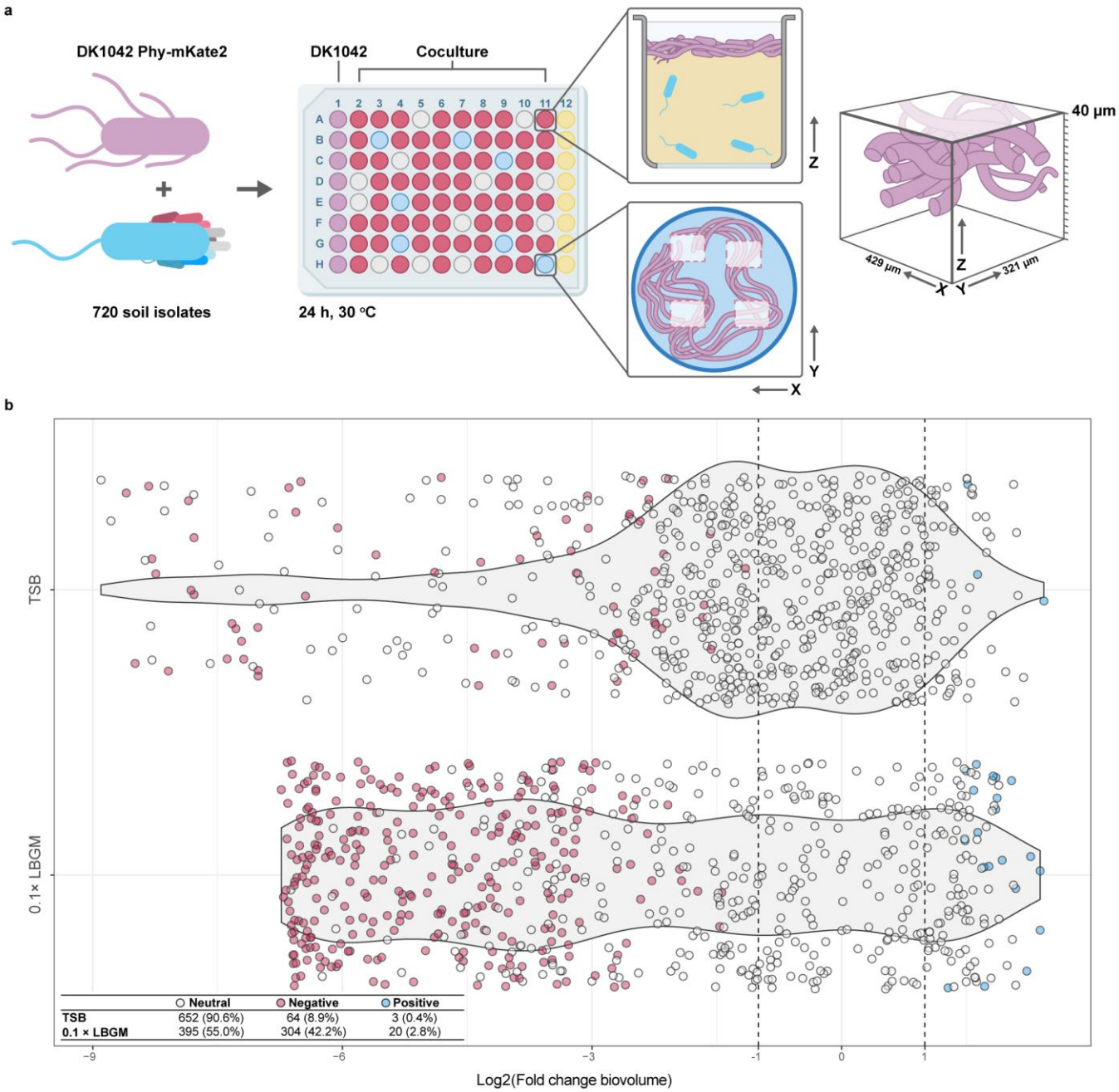

Fig. 1. Pseudomonads negatively affect *B. subtilis*. a: DK1042 constitutively expressing mKate2 was mixed pairwise with 720 fluorescent soil isolates and cultured for 24 h at 30°C in a microplate format. Monocultures of DK1042 (purple wells) were used for comparison of pellicle formation, and wells with non-inoculated medium (yellow wells) were used to control for contamination. Each well was imaged in four positions with a Perkin Elmer Opera QEHS, acquiring images in the Z-direction every 2 µm to obtain a cube with height 40 µm. Media was removed prior to microscopy. **b:** DK1042 biovolumes were compared between co- and monoculture to yield $\log_2$(Fold Change). Points represent medians of three replicates. Neutral, negative and positive categories were assigned based on median and interquartile range.

Pseudomonas taxonomy predicts interaction outcome

To determine the taxonomic distribution of isolates, we sequenced amplicons of the *rpoD* gene from pools of isolates corresponding to their screening category (neutral, negative and positive; Fig. 2 and Dataset S1).

The species diversity of each category demonstrates how the categorisation based on *B. subtilis* pellicle formation selectively distributes specific phyla into separate categories (Permutational Analysis of Variance, p <0.001, Fig. S3). The total library of 720 isolates was mainly comprised of *P. capeferrum*, *Pseudomonas helmanticensis*, *Pseudomonas koreensis* and *P. protegens* (Fig. 2c and Table 1). A similar distribution occured in the neutral category, while negative and positive strains differed significantly in species abundance. The pool of negative isolates contained more strains associated with the *P. putida*

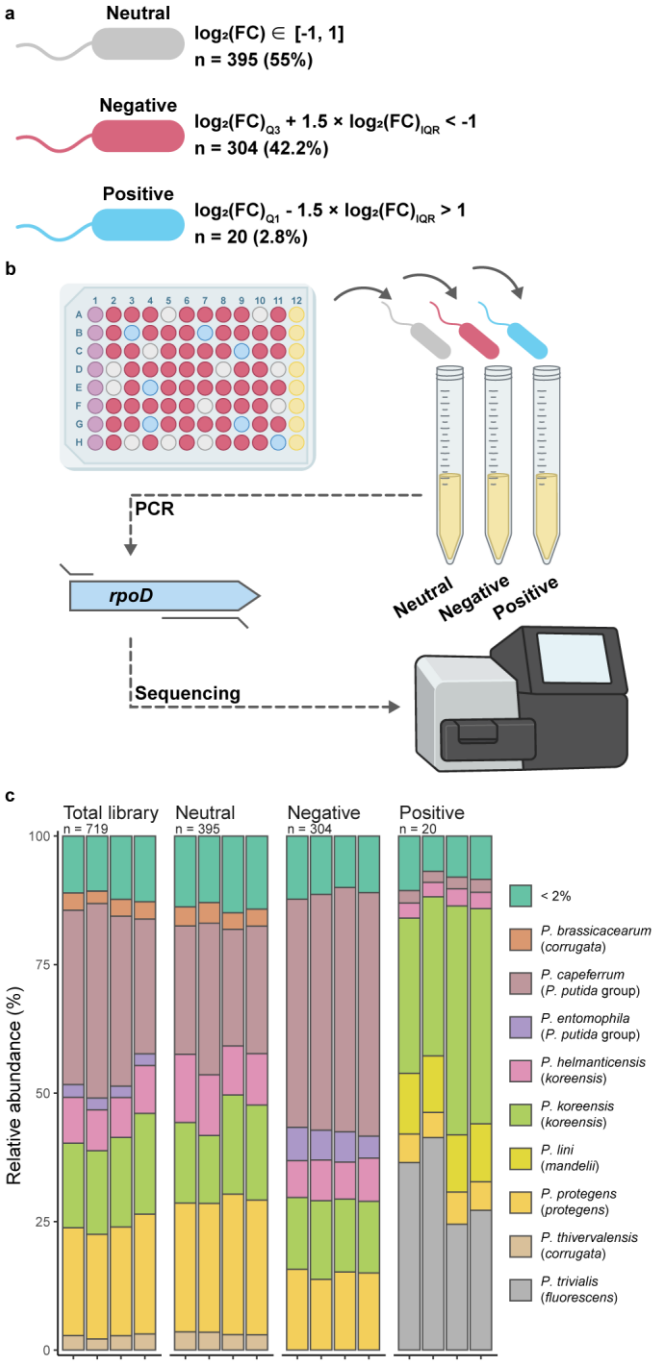

Fig. 2. Screening categories enriched for species-specific taxa. a: Fluorescent isolates were assigned a category based on median and interquartile range, such that negatives resulted in DK1042 $\log_2$(FC) <-1 and positives in $\log_2$(FC) >1. n and percentages are from screening in 0.1× LBGM. **b:** Isolates were grown in precultures and pooled in equal cell numbers according to their categorisation to taxonomically characterise each category at the species level via *rpoD* amplicon sequencing. **c:** Relative abundance of *Pseudomonas* spp. in each category. Parentheses indicate groups or *P. fluorescens* subgroups (see Table 1 for details on taxonomy). Taxons comprising <2% of a pool were merged.

group compared with the total library, but no single species was significantly depleted from this category. Differential abundance analysis revealed that the pool of positive isolates contained fewer isolates from the *Pseudomonas putida* group, and the *P. protegens*, *Pseudomonas corrugata* and *P. koreensis* subgroups, compared with the total library (Table 1). By contrast, *P. trivialis* and members of the *Pseudomonas mandelii* subgroup were enriched. As the pool of positive strains only contained 20 isolates, the statistical power in determining differential abundance was quite low. Therefore, caution should be applied when inferring from statistical tests in this group, hence we refer to isolates henceforth as "inhibiting" (negative) or "non-inhibiting" (neutral and positive).

Table 1: Significantly differentially abundant species in screening categories compared with the total library

***fluorescens* subgroup**[a]	***Pseudomonas* sp.**	**Neutral (log_2FC)**	**Negative (log_2FC)**	**Positive (log_2FC)**
asplenii	*P. asplenii*	1.363*	-0.235	-0.153
corrugata	*P. thivervalensis*	-0.028	-0.090	-0.921*
	P. brassicacearum	-0.066	-0.263	-1.123*
fluorescens	*P. trivialis*	**-0.292**	**-0.381**	**2.900****
	P. cedrina	-1.607*	0.646	-1.110
	P. libanensis	-0.084	-0.038	-1.124*
	P. lurida	0.153	-1.097	-1.196*
gesaardii	*P. brenneri*	-1.176	1.048	-1.261*
koreensis	*P. helmanticensis*	0.063	0.173	-0.884*
	P. granadensis	0.341	-1.736*	-1.134
	P. moraviensis	0.031	-0.267	-1.244*
mandelii	*P. lini*	**-0.048**	**-0.425**	**2.623****
	P. migulae	-0.510	-0.348	1.829*
	P. frederiksbergensis	-0.163	-1.292	1.574**
	P. mandelii	0.088	1.007*	0.396
protegens	*P. protegens*	**-0.015**	**-0.090**	**-1.215****
P. putida[b]	*P. mosselii*	-0.935	1.213**	-0.830
	P. soli	-1.558*	0.856	-1.443*
	P. entomophila	-2.064**	1.138*	-2.294**
	P. capeferrum	**-0.452**	**0.627**	**-2.493****

[a] As described in [15].

[b] Not a subgroup of *P. fluorescens*.

* Differentially abundant from the total library with FDR-adjusted *p*-value <0.05. ** FDR-adjusted *p*-value <0.01.

Bold indicates predictions.

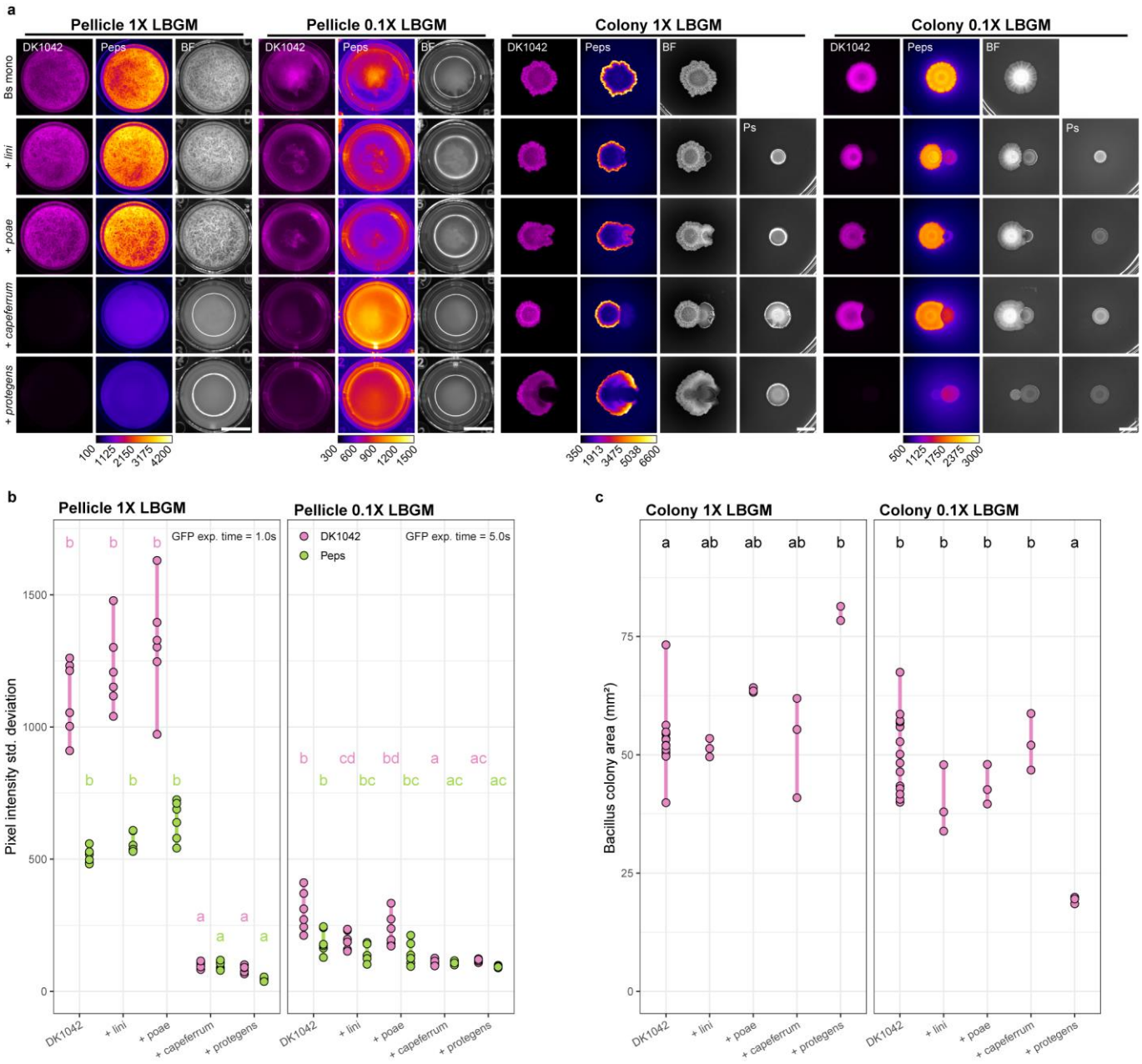

Fig. 3. Screening prediction of inhibitors and non-inhibitors. a: Cocultures of DK1042 with four reference strains that were independent from the soil isolate library were used to assess the validity of interaction prediction resulting from screening *Pseudomonas* soil isolates. Cultures were grown at 30°C for 24 h (pellicles) or 72 h (colonies). Cultures were prepared with DK1042 reporting expression of the *epsA–O* operon using GFP. Scale bar = 5 mm. **b:** Pellicle wrinkle formation represented by the standard deviation in pixel intensity (i.e. high standard deviation equals stronger wrinkle formation). n = 6 independent experiments. **c:** Colony area of DK1042 spotted as monoculture or neighbouring the four *Pseudomonas* reference strains. n = 3 independent cocultures. Grouping letters are from ANOVA with Tukey-Kramer's post-hoc test. Identical letters within each plot indicate a statistically significant grouping (p <0.05).

To test the predictions resulting from screening, we obtained four *Pseudomonas* strains closely related to species that were implicated in different interaction patterns, and cocultured them with DK1042 in liquid and solidified 1× LBGM and 0.1× LBGM media (Fig. 3). As predicted, *P. capeferrum* and *P. protegens* both inhibited pellicle formation (even in 1× LBGM), while neither *P. lini* nor *Pseudomonas poae* (in place of *P. trivialis*) reduced pellicle abundance or winkle formation (as measured via pixel standard deviation; Fig. 3b). However, on solid media, no pseudomonad was able to reduce the colony size of DK1042 on 1× LBGM, but on diluted 0.1× LBGM *P. protegens* strongly antagonised DK1042

(Fig. 3c). Thus, *Pseudomonas* antagonism of DK1042 not only depends on medium constituents, but also on mode of growth.

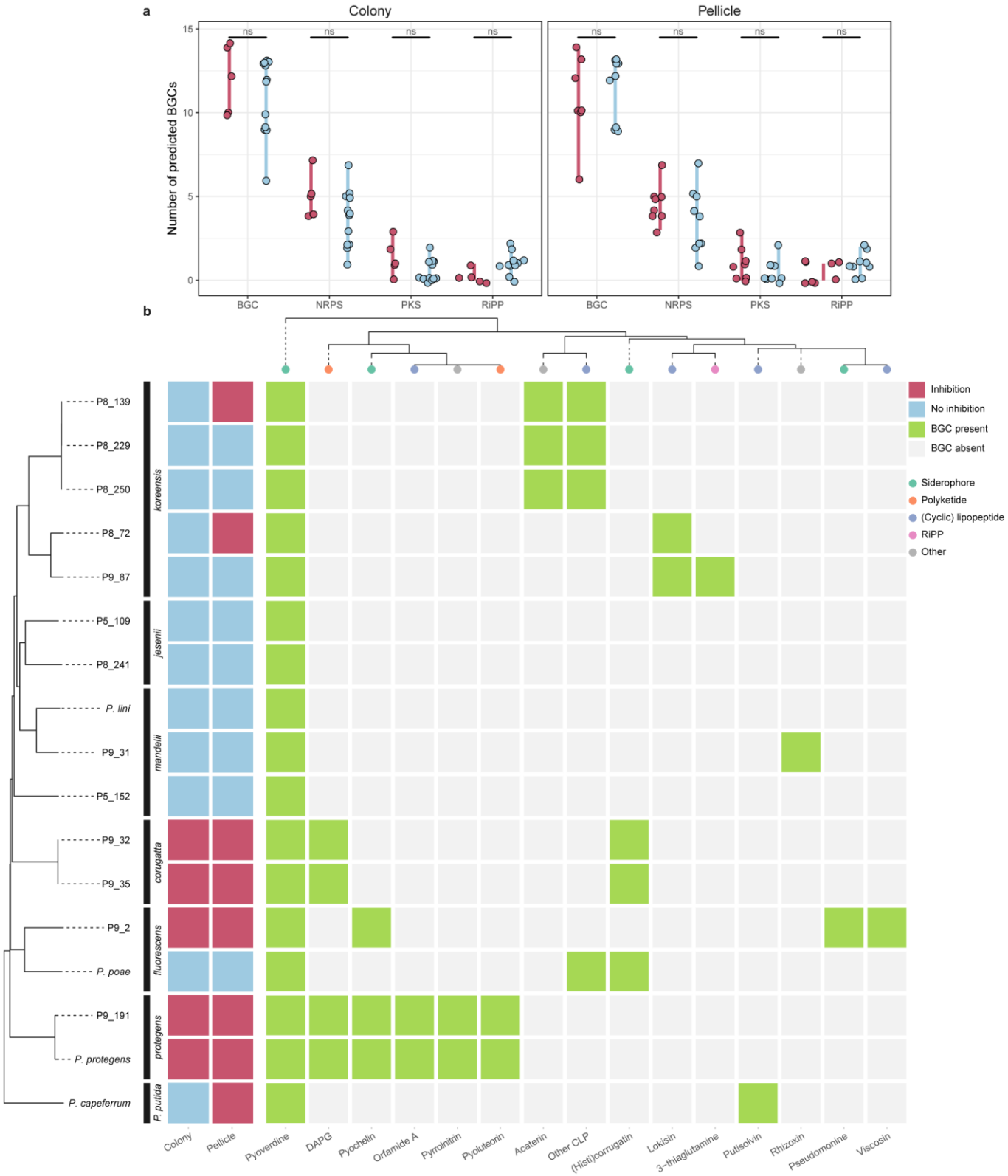

Fig. 4. Specific BGCs (not abundance) predict interaction outcome. Thirteen isolates were whole-genome sequenced and compared with the four reference strains. **a:** AntiSmash predictions of biosynthetic gene clusters (BGCs) and BGC subgroups grouped by inhibition potential in colony or pellicle cocultures. Statistical tests were pairwise Student's t-tests adjusted for multiple testing with the false discovery rate method. ns, not significant (adj. p >0.05). **b:** *Pseudomonas*-related natural product machinery encoded within each strain. Strain phylogeny is based on whole-genome sequence identity as described in TYGS [76].

BGC abundance does not determine interaction outcome

Pseudomonas secondary metabolites are often implicated in *Bacillus-Pseudomonas* antagonism [12,27,28], therefore we sequenced the genomes of 13 candidate isolates and predicted BGCs and BGC subgroups using antiSMASH (Fig. 4). Interestingly, there was no significant difference in the abundance of encoded BGCs between inhibiting and non-inhibiting isolates (Fig. 4a). Therefore, we examined each genome for the presence of BGCs with known products (Fig. 4b). As expected, all isolates carried a version of pyoverdine, a fluorescent siderophore, but many non-inhibitory isolates were negative for most other biosynthetic gene clusters compared with inhibiting isolates. Isolates from *P. mandelii* and *Pseudomonas jesenii* subgroups collectively encoded only one BGC with a predicted product (rhizoxin, originally isolated from *Paraburkholderia rhizoxinica* [29]). By contrast, colony-inhibiting isolates from *P. corrugata* and *P. protegens* subgroups both carried genes encoding 2,4-diacetylphloroglucinol(DAPG)-producing enzymes, while *P. protegens* additionally encoded enzymes for producing pyochelin, orfamide A, pyrrolnitrin, and pyoluteorin.

Non-inhibiting isolates are spatially segregated from DK1042

While the main biofilm mode of *B. subtilis* in liquid culture involves growth at the air-liquid interface [30], *Pseudomonas* spp. are usually observed colonising submerged surfaces in laboratory environments, although examples of *Pseudomonas* pellicle formation do exist [31,32]. The presence of pellicles in cocultures with non-inhibiting isolates therefore suggests three potential scenarios: either non-inhibiting pseudomonads are outcompeted by *B. subtilis*, are growing with *B. subtilis* in the pellicle, or are spatially isolated from *B. subtilis* on the submerged surface of the microtiter plates. To determine which of these scenarios occurred with DK1042, we fluorescently labelled a non-inhibitor (P9_31), cocultured it statically with DK1042 in liquid 1× LBGM and 0.1× LBGM, and imaged the entire depth of the well (Fig. 5). In both media, P9_31 was spatially segregated to the submerged surface, even when DK1042 was mostly present in the pellicle. Interestingly, while cultivation in 1× LBGM resulted in a pellicle

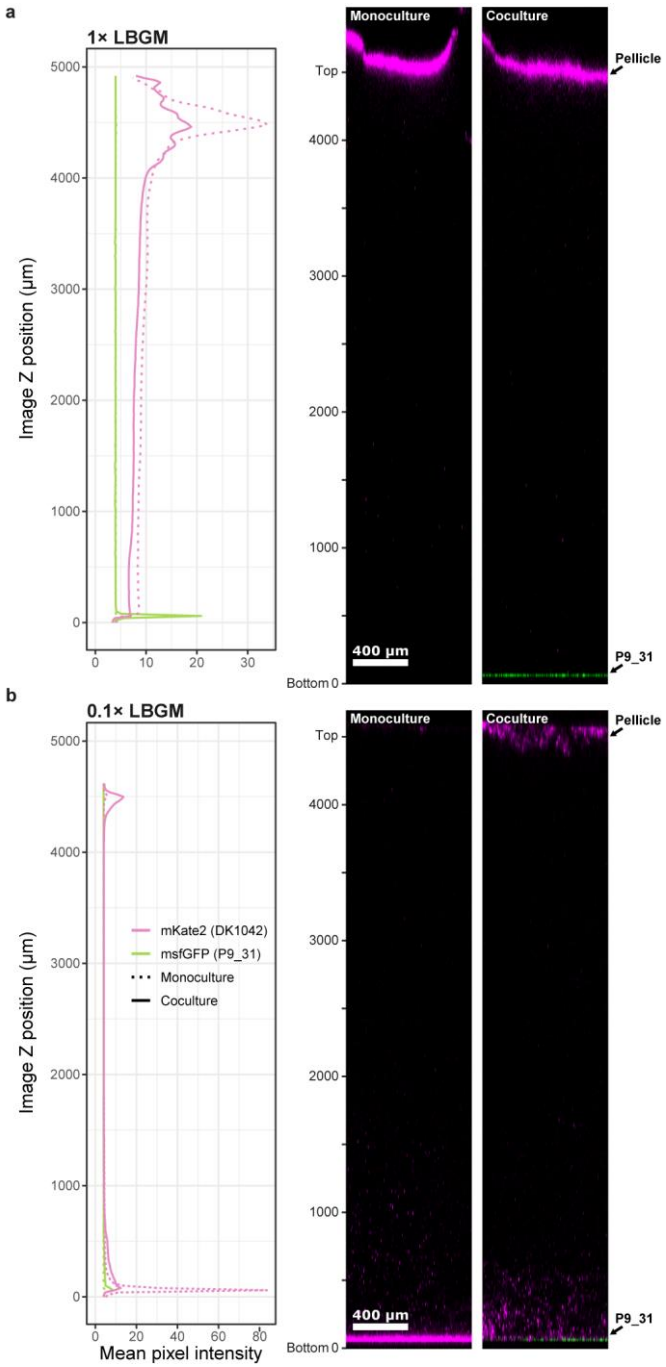

Fig. 5. Non-inhibiting *Pseudomonas* is not present in the pellicle. Coculture of DK1042 (magenta) with non-inhibiting isolate P9_31 (green) in 1× LBGM (**a**) and 0.1× LBGM (**b**). Confocal laser scanning microscopy was employed to acquire Z-slices every 20 µm spanning the entire depth of a well. Plots show the mean pixel intensity of each strain over the depth of the well. Pixel intensities cannot be compared between 1× LBGM and 0.1× LBGM.

both with and without P9_31, cultivation in 0.1× LBGM required P9_31 for pellicle formation, even though the *Pseudomonas* isolate was present at the bottom of the well and not in the pellicle.

DAPG is a biomarker for *B. subtilis* inhibition

Four of five colony-inhibiting isolates were found to contain the conserved *phl* BGC operon known to produce DAPG [33]. From 61 cocultures on solid 0.1× LBGM, 11 isolates resulted in markedly reduced

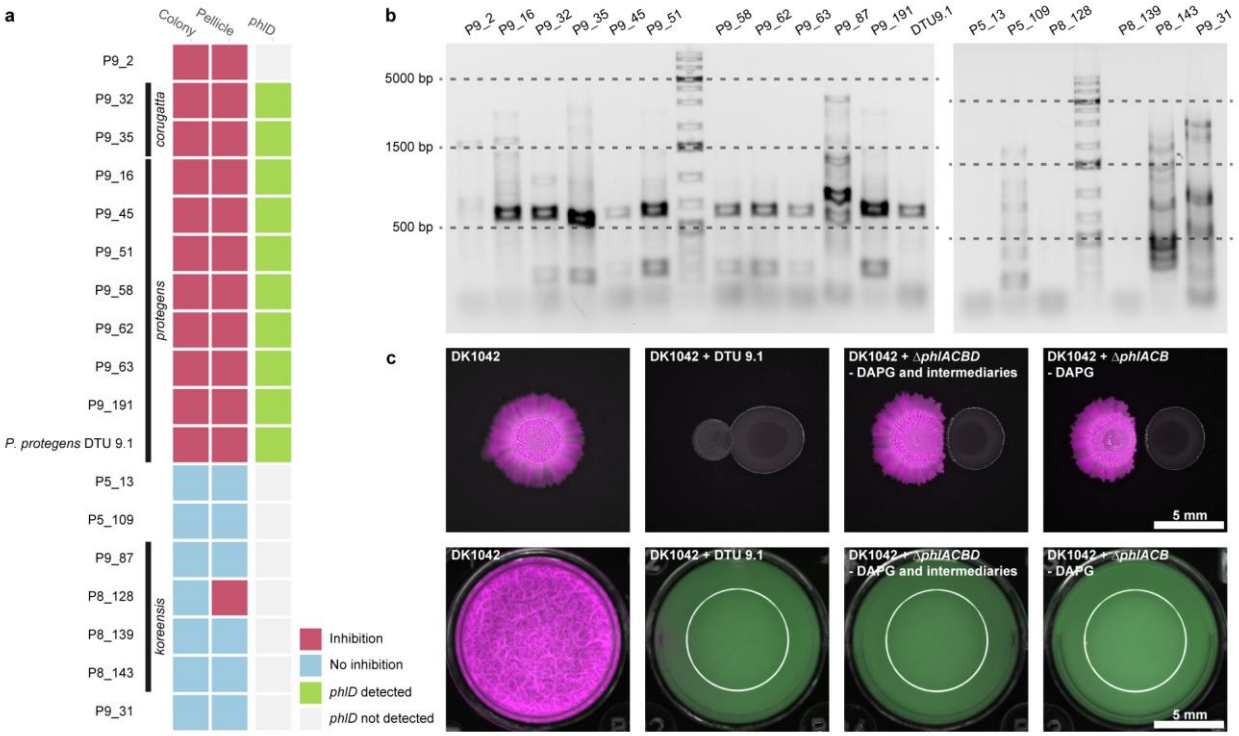

Fig. 6. 2,4-Diacetylphloroglucinol (DAPG) is a major (but not exclusive) antagonistic metabolite. a: Inhibition potential of a selection of isolates and the presence/absence of *phlD* as determined by PCR (**b**). *phlD* was amplified with primers yielding a product of ~630 bp. Ladder is GeneRuler 1 kb Plus DNA Ladder (Thermo Fisher Scientific). **c:** Cocultures of DK1042 and *P. protegens* DTU 9.1 and *phl*-mutant derivatives of DTU 9.1. Δ*phlACB* cannot produce DAPG. Δ*phlACBD* additionally cannot produce phloroglucinol, monoacetylated phloroglucinol, chlorinated phloroglucinol (PG-Cl/PG-Cl_2) or pyoluteorin.

DK1042 colony growth (Fig. 6a). A PCR screen of the main biosynthetic gene for DAPG, *phlD*, revealed that 10 of 11 colony-inhibiting isolates carried *phlD* (Fig. 6b). By contrast, 0 of 7 non-inhibiting strains tested positive for *phlD*. To determine if DAPG or any intermediate products from the PhlA–D BGC operon, we cocultured *P. protegens* DTU9.1 and mutants lacking *phlACB* ($DAPG^-$) or *phlACBD* ($phloroglucinol^-$, monoacetylated $phloroglucinol^-$, $DAPG^-$, chlorinated $phloroglucinol^-$ and $pyoluteorin^-$) with DK1042 in liquid 1× LBGM and on solid 0.1× LBGM (Fig. 6c). Disrupting the production of DAPG in DTU9.1 markedly improved DK1042 fitness in colonies but not in pellicles. Thus, DAPG is a strong inhibitor of *B. subtilis* growth in colonies and pellicles, but not the only inhibiting factor.

Discussion

In this study, we propose a generalisation of *Bacillus subtilis-Pseudomonas* interactions based on *Pseudomonas* taxonomy. Our results suggest that fluorescent pseudomonads are very likely to inhibit the *B. subtilis* pellicle, particularly in 0.1× LBGM. Many studies have demonstrated how nutrient sources determine the outcome of pairwise interactions[14,26,34,35]. Most of our pairwise interactions were negative, fitting the current paradigm. Large-scale pairwise interaction studies have demonstrated that most pairwise interactions are negative, and that the direction of interaction depends on carbon source complexity[26,36,37]. It is interesting, however, that such a large proportion of our interactions proved to

be negative or neutral. Granted, our setup only shows the interaction outcome of one of the two participants, hence we cannot differentiate between mutualism (+/+) and parasitism (+/-). Even so, Kehe et al. (2021) reported that for 23% of their >180,000 pairwise interactions at least one participant benefitted from coculturing[26], while we report only 2.8% positive interactions, making interactions between *B. subtilis* and fluorescent pseudomonads less likely to be positive compared with average interactions among culturable microorganisms.

This could be due to our decision to coculture under pellicle-inducing conditions. DK1042 proved less durable in liquid broth compared with solid agar. It is likely that both the pseudomonads and DK1042 have different metabolic profiles under the two conditions, and that antagonistic molecules are produced in one setting and not the other. Alternatively, the concentration gradients could be more homogeneous under liquid conditions; for example, DK1042 may be unable to reach adequate cell density for biofilm activation before being growth-inhibited. It is likely that a similar screen performed on solid agar media would result in fewer examples of *Pseudomonas*-mediated antagonism.

Predicting interactions from phylogeny is arguably a cornerstone of ecology. Charles Darwin proposed what would become the competition-relatedness hypothesis, stating that closely related species are more likely to compete due to niche overlap[38]. Indeed, relatedness has consistently correlated with competitiveness, though some find that there is a competitive "peak" at intermediate relatedness[39,40]. Bacilli and pseudomonads are phylogenetically distant, belonging to distinct phyla, though metabolically similar enough that syntrophy between isolates has been reported[14]. As such, the competition-relatedness hypothesis states that members of these genera should generally compete. Additionally, these are organisms with large genomes and the potential to produce several antimicrobial compounds. Such organisms cluster into highly competitive communities in metabolic simulations[41]. Additionally, members of *Bacillus* and *Pseudomonas* are frequently co-isolated, suggesting frequent encounters and possible co-evolution. Interactions between *Streptomyces* soil isolates have argued that local evolution is a stronger contributor to interaction outcomes than phylogeny[42,43]. Interactions from a single grain of soil were dramatically different even across isolates with almost identical 16S rDNA sequences, and comparisons between three soil sites found interaction network distributions to differ significantly, again irrespective of phylogenetic distance. In a recent preprint, Pomerleau *et al.* (2023) demonstrated how adaptive laboratory co-evolution of *B. subtilis* with fluorescent pseudomonads increases *B. subtilis* competitive potential[44]. Thus, it is plausible that competitive interactions between bacilli and pseudomonads stem from co-evolution. Predicting interactions from taxonomy requires a certain degree of conservation within taxonomic units. Indeed, with *Pseudomonas* genomes, accessory genes have been found to evolve with core genes, suggesting little horizontal gene transfer, and thus conservation across *Pseudomonas* phylogeny[45,46]. Recently, phylogenetic distance was demonstrated to correlate positively with predictive ability in pairwise interactions, and interactions are conserved within a taxonomic unit but vary between units[34]. We propose that *Pseudomonas* constitutes a taxonomic unit with high phylogenetic predictability, at least in interactions with *Bacillus*. This

predictability provides potential for future bioformulations. Both *P. trivialis* and *P. lini* have been implicated in biocontrol and biostimulation[47–49], and their compatibility with *B. subtilis* therefore implicates them as candidates for beneficial *Bacillus-Pseudomonas* consortia. Future studies should investigate how mixed cultures function in the rhizosphere and in more diverse communities.

Positive interactions between *Bacillus* and *Pseudomonas* have been reported before, but never with a fluorescent isolate. Sun et al. (2021) molecularly characterised a mutualistic relationship between *Bacillus velezensis* and *Pseudomonas stutzeri* (now *Stutzerimonas degradans*) [14], and described how *B. velezensis* arrives first and subsequently recruits *Pseudomonas* spp. This interaction gave rise to a mixed biofilm of homogeneously distributed *B. velezensis* and *S. degradans*, which we did not observe. Rather, we observed spatial segregation to the air-liquid interface (DK1042) and the liquid-surface interface (P9_31), though still with enhanced pellicle density in 0.1× LBGM. One could speculate that P9_31 secretes a metabolite that can be distributed throughout the medium and that influences *Bacillus* pellicle formation.

We found several antagonistic species, and, like others before us [50,51], experimentally demonstrated the influence of DAPG produced by *Pseudomonas* as a key antagonistic metabolite. However, species without the biosynthetic potential to produce DAPG were also characterised as antagonistic, herein members of the *P. putida* group (*P. entomophila* and *P. capeferrum*) and the *P. fluorescens* subgroup. Previous studies demonstrated how cyclic lipopeptide-producing pseudomonads can inhibit *Bacillus* spp. [52], and given their potential to produce one or more cyclic lipopeptides, the isolates presented here likely share a similar antagonistic property mediated by bioactive specialised metabolites.

Understanding cocultures of *Bacillus* and *Pseudomonas* is pertinent to their applicability in biotechnology. Especially within agriculture, plant growth-promoting rhizobacteria are being investigated as alternatives to traditional fertilisers and pesticides. Both *B. subtilis* and many fluorescent pseudomonads are characterised as plant growth-promoting, and several products based on members of either genus are currently available [53,54]. Interestingly, several studies report having successfully combined bacilli and pseudomonads and achieved some form of synergy [4,55]. Our results suggest that this synergy likely does not stem from increased *Bacillus* growth. This does not contradict the aforementioned studies, which do not report on synergistic growth of members, but on outcomes of other parameters (often plant growth with or without stress). One study even reported biocontrol synergy from a mixture of *B. subtilis* and *P. protegens* [56], which suggests either that continued growth of both participants is not required for synergy, or that higher-order interactions abolish DAPG-mediated antagonism of *B. subtilis*.

Both species may not be required to be present at the same time. If the hypothesis proposed by Sun and colleagues that *Bacillus* recruits *Pseudomonas* to the rhizosphere is correct, it is possible that *Pseudomonas* is the effector of biocontrol, eradicating *Bacillus* in the process. However, the fact that many studies have isolated members of both genera from the rhizosphere provides evidence supporting

co-existence of the two. Our pairwise interactions then suggest that other factors underpin *Bacillus* and *Pseudomonas* compatibility.

Although future studies are needed to probe the entire breadth of *Pseudomonas* phylogeny and how it enables interaction predictions, our work demonstrates the relevance in doing so.

Methods

Culturing and genetic modification

A library of 720 soil isolates was acquired from soil samples taken from pristine grassland in Dyrehaven Lyngby, Denmark, by plating solubilised soil on King's B agar (KB; 20 g/L peptone, 1% v/v glycerol, 8.1 mmol/L K_2HPO_4, 6.08 mmol/L $MgSO_4 \cdot 7H_2O$) supplemented with 40 µg/mL ampicillin, 13 µg/mL chloramphenicol and 100 µg/mL cycloheximide. Plates were incubated at 30°C for 5 days, and colonies were assessed for fluorescence and placed into lysogeny broth (LB; Lennox, Carl Roth, Karlsruhe, Germany) in 96-well microtiter plates. We labelled the isolation sites as P5 (n = 237 isolates), P8 (n = 279) and P9 (n = 224), where P5 and P9 came from short grass, while P8 came from long grass.

DK1042 and soil isolates were routinely cultured in tryptone soy broth (CASO broth; Sigma-Aldrich, Darmstadt, Germany), LB, LB supplemented with 1% glycerol and 0.1 mM $MnCl_2$ (1× LBGM), and a 10× dilution of LBGM (0.1× LBGM) at 30°C. Solid media was supplemented with 1.5% (w/v) agar. Antibiotics were added as appropriate in the following final concentrations: gentamycin (Gm) 50 µg/mL, ampicillin (Amp) 100 µg/mL, chloramphenicol (Cm) 10 µg/mL, nalidixic acid (NalAc) 20 µg/mL.

Pseudomonas soil isolates were fluorescently tagged by inserting constitutively expressed msfGFP into the attTn7 site as described previously [57].

High-content screening

Precultures of isolates and *B. subtilis* DK1042 Phy-mKate2 were mixed in equal volumes in 96-well imaging microtiter plates (PerkinElmer, Waltham, MA, USA) in TSB or 0.1× LBGM (Fig. 1a). Isolates were adjusted to a final dilution of 100-fold and DK1042 to a final OD_{600} = 0.01. One column contained DK1042 monocultures and one column non-inoculated medium (blank control). Pellicles were incubated at 30°C for 24 h, before removing the supernatant underneath the pellicle and scanning the plate in an Opera QEHS high-content screening microscope (PerkinElmer) equipped with a UAPO20×W3/340 objective with NA = 0.7.

Focal height was adjusted using monoculture samples, and each plate was scanned by imaging four random locations per well, acquiring 21 Z-slices in increments of 2.0 µm from the bottom. Samples were excited with a 561 nm laser collecting emission light through a 690/70 nm filter for mKate2 fluorescence. Laser power was set to 100 µW and samples were excited for 800 ms.

Opera flex-files were imported into FIJI (2.1.0/1.53f51) [58] using BioFormats and segmented by applying a 5×5 mean convolution kernel to remove noise, a 3D median filter with radius Z = 2.0 µm to remove single cells or objects only present in one slice, and applying the built-in ImageJ Remove Background function with a rolling ball size of 100 px. Images were then thresholded using the MaxEnthropy algorithm [59] based on the pixel intensities in the entire volume (Fig. S1).

Biovolume was calculated using BiofilmQ [60] by importing the segmented images and sectioning the segmentation into 8 µm cubes. Objects smaller than 8 μm^3 were filtered out and the total biovolume from each image stack was determined.

Subsequent analysis was carried out in Rstudio (2022.02.3-b492) [61] within R (4.1.1) [62] with the Tidyverse framework (1.3.1) [63]. Log_2(FoldChange) was calculated between the coculture biovolume of each isolate and the monoculture biovolume in the corresponding plate. Assuming that each participant in a biofilm is theoretically able to occupy 1/k of the space (where k is the number of participants), we divided the biovolume from the monoculture by k to take this lack of space into account.

Isolates were divided into three categories (neutral, negative, or positive) based on the median and interquartile range of three biological replicates (Fig. 2a).

rpoD-targeted amplicon sequencing

To determine the taxonomic composition of the screen output, we employed a targeted amplicon sequencing approach using the species-specific gene *rpoD* as previously demonstrated [64].

Precultures of isolates were adjusted to OD = 0.5 and pooled by equal volume according to their category. Genomic DNA was extracted twice from 100 µL of each pool using a Bacterial & Yeast Genomic DNA Purification Kit (EURx, Gdańsk, PL) following the manufacturer's instructions, yielding 1000−1500 ng of DNA in 50 µL. DNA was also extracted from a pool of all 720 isolates and as a negative control, nuclease-free H_2O was used in place of a bacterial pool. From each DNA extraction, 10 ng was used as template in two PCR amplification experiments using TEMPase hotstart polymerase (Ampliqon, Odense, DK) and barcoded primer pairs (Table S1), resulting in two PCR mixtures from each of two genomic DNA extractions. A final 25 µL PCR experiment consisted of TEMPase mastermix (1×), forward primer (320 nmol/L), reverse primer (320 nmol/L), $MgCl_2$ (1.75 mmol/L), template gDNA and nuclease-free H_2O. The reaction was initiated with 15 min at 95°C to denature the DNA and activate the TEMPase polymerase, followed by 35 cycles of 30 s denaturation (95°C), 30 s annealing (53°C), 30 s elongation (70°C), and a final 5 min elongation step at 70°C. Read length was assessed by DNA agarose gel electrophoresis (1% w/v) and amplicons were purified from the PCR mix using a NucleoSpin Gel and PCR Clean-up kit (Macherey-Nagel, Düren, DE) following manufacturer's instructions.

DNA purities and concentrations were assessed using a Denovix spectrophotometer (DeNovix, Wilmington, DE, USA) and a Qubit 2.0 fluorimeter (Thermo Fisher Scientific, Waltham, MA, USA)

and a Qubit High Sensitivity kit, respectively. Optical density ratios (260/280 and 260/230) measured 2.0 ± 0.20 and concentrations ranged from 20 to 68 ng/µL. Amplicon DNA (360 ng) from each sample was pooled to a total of 10 µg DNA and sent to Seqomics Biotechnology Ltd. for sequencing on a MiSeq platform (Illumina, San Diego, CA, USA) using a MiSeq Reagent Kit v3 (600-cycle).

The resulting reads were quality-checked and demultiplexed using CutAdapt V4.0 [65]. FastP V0.23.2 [66] was used with default settings for quality filtering. Mapping and post-mapping filtering was performed using the bowtier.sh script from Lauritsen *et al*. 2021 [64]. In brief, paired reads were aligned with bowtie2 to a custom database of 160 *rpoD* genes. The resulting SAM-file was then filtered for only concordant pairs mapped with a quality >10 using samtools. In Rstudio, a permutational multivariate ANOVA was performed to test for between-sample clustering. Amplicon reads were normalized with DESeq2 [67] before calculating relative abundances. Differential abundance analysis was carried out using ANCOM-BC [68] with uncorrected read counts and multiple testing was corrected with the false discovery rate (FDR) method [69].

In addition, Sanger sequencing of the *rpoD* gene was used for individual routine taxonomic identification of isolates with primers PsEG30F and PsEG790R [64].

Pairwise interactions

On agar, DK1042 *amyE*::$P_{hyperspank}$-*mKate2 sacA*::P_{eps}-*gfp* and a candidate isolate were spotted 5.0 mm apart on agar surfaces using 2 µL of culture at an OD_{600} of 1.0. Prior to spotting, plates were dried for 30 min in a lateral flow hood then incubated at 30°C for 72 h.

In broth, the DK1042 *amyE*::$P_{hyperspank}$-*mKate2 sacA*::P_{eps}-*gfp* strain and a candidate isolate were mixed 1:1 volumetrically in 1 mL liquid LBGM in 24-well microtiter plates at a final OD_{600} of 0.01 and incubated for 24 h at 30°C.

Example *Pseudomonas* strains were *P. lini* 1.6, *P. poae* DSM 14936 [70], *Pseudomonas kermanshahensis* F8 (previously *P. capeferrum*) [71] and *P. protegens* DTU 9.1 [71].

Stereomicroscopy

Colonies and pellicles were imaged with a Carl Zeiss Axio Zoom.V16 stereomicroscope (Carl Zeiss, Oberkochen, Baden-Württemberg, Germany) equipped with a CL 9000 LED light source (Carl Zeiss) and an AxioCam 503 monochromatic camera (Carl Zeiss). The stereoscope was equipped with a PlanApo Z 0.5x/0.125 FWD 114 mm, and the filter sets 38 HE eGFP (ex: 470/40, em: 525/50) and 63 HE mRFP (ex: 572/25, em: 629/62). Exposure time was optimised for contrast but kept constant under identical conditions (i.e. media types or biofilm type).

Image processing and analysis was performed in FIJI. Contrast in fluorescence channels was adjusted identically on a linear scale to allow for visual comparisons between images with equal exposure time. Reporter fluorescence intensity was measured by segmenting the colony of interest with the Triangle

thresholding algorithm [72] based on mKate2 signal and measuring relative eGFP intensity per area within the resulting region of interest outlining the entire colony. For pellicles, circles were manually fitted to include only the well. Standard deviation of the pixel intensity was measured and reported as a proxy for pellicle wrinkles.

Confocal microscopy

DK1042 was cultured with isolate P9_31 in 1× LBGM or 0.1× LBGM in 24-well imaging microtiter plates (PerkinElmer). Wells were imaged on a Leica SP8 confocal microscope (Leica Microsystems, Wetzlar, Germany) equipped with an HC PL Fluotar 10x/0.30 air objective and lasers exciting at 488 nm and 552 nm. Photomultiplier tubes were adjusted to acquire photons at wavelengths of 493–581nm (msfGFP) and 586–779nm, and gain was adjusted for optimal contrast, but kept constant for each media type. Images were acquired with 8 bits and size 512px × 512px × 247px (XYZ – voxel size: 1.78 µm × 1.78 µm × 20.00 µm) averaging over four lines.

Genome mining

Whole-genome sequencing was performed as described previously [57]. Assembled genomes were annotated with Bakta (V1.6.1) [73] and a BGC presence/absence matrix was created with antiSMASH (V7.0.0) [74] using its relaxed mode performing KnownClusterBlast, ClusterBlast, SubClusterBlast and MIBiG cluster comparison, and ActiveSiteFinder, RREFinder and TFBS analysis. Results were manually curated using the *Pseudomonas* Genome Database [75] as reference. PCR screening for *phlD* was performed with primers B2BF (5'-ACCCACCGCAGCATCGTTTATGAGC) and BPR4 (5'-CCGCCGGTATGGAAGATGAAAAAGTC), yielding a 630 bp product.

Data availability

Analysis scripts and processed data have been deposited at Github (https://github.com/marklyng/screen_repository). *rpoD* amplicon sequencing data have been deposited at the Sequence Read Archive under BioProject ID PRJNA985909.

Acknowledgements

This project was funded by a DTU Alliance Strategic Partnership PhD fellowship, by the Danish National Research Foundation (DNRF137) for the Center for Microbial Secondary Metabolites, and the Novo Nordisk Foundation within the INTERACT project of the Collaborative Crop Resiliency Program (NNF19SA0059360), and the "Imaging microbial language in bio-control (IMLiB)" infrastructure grant (NNF19OC0055625).

References

1. Blake, C., Christensen, M.N., and Kovacs, A.T. (2021). Molecular aspects of plant growth promotion and protection by *Bacillus subtilis*. Molecular Plant-Microbe Interactions *34*, 15–25. 10.1094/MPMI-08-20-0225-CR.

2. Singh, P., Singh, R.K., Zhou, Y., Wang, J., Jiang, Y., Shen, N., Wang, Y., Yang, L., and Jiang, M. (2022). Unlocking the strength of plant growth promoting *Pseudomonas* in improving crop productivity in normal and challenging environments: a review. J Plant Interact *17*, 220–238. 10.1080/17429145.2022.2029963.

3. Comeau, D., Balthazar, C., Novinscak, A., Bouhamdani, N., Joly, D.L., and Filion, M. (2021). Interactions Between *Bacillus* spp., *Pseudomonas* spp. and *Cannabis sativa* Promote Plant Growth. Front Microbiol *12*, 715758. 10.3389/fmicb.2021.715758.

4. Bautista-Cruz, A., Antonio-Revuelta, B., del Carmen Martínez Gallegos, V., and Báez-Pérez, A. (2019). Phosphate-solubilizing bacteria improve *Agave angustifolia* Haw. growth under field conditions. J Sci Food Agric *99*, 6601–6607. 10.1002/jsfa.9946.

5. Balthazar, C., Cantin, G., Novinscak, A., Joly, D.L., and Filion, M. (2020). Expression of Putative Defense Responses in Cannabis Primed by Pseudomonas and/or Bacillus Strains and Infected by Botrytis cinerea. Front Plant Sci *11*. 10.3389/fpls.2020.572112.

6. Kalantari, S., Marefat, A., Naseri, B., and Hemmati, R. (2018). Improvement of bean yield and Fusarium root rot biocontrol using mixtures of *Bacillus, Pseudomonas* and *Rhizobium*. Trop Plant Pathol *43*, 499–505. 10.1007/s40858-018-0252-y.

7. Ghazy, N., and El-Nahrawy, S. (2021). Siderophore production by *Bacillus subtilis* MF497446 and *Pseudomonas koreensis* MG209738 and their efficacy in controlling *Cephalosporium maydis* in maize plant. Arch Microbiol *203*, 1195–1209. 10.1007/s00203-020-02113-5.

8. Kiesewalter, H.T., Lozano-Andrade, C.N., Wibowo, M., Strube, M.L., Maróti, G., Snyder, D., Jørgensen, T.S., Larsen, T.O., Cooper, V.S., Weber, T., et al. (2021). Genomic and Chemical Diversity of Bacillus subtilis Secondary Metabolites against Plant Pathogenic Fungi. mSystems *6*, e00770-20.

9. Asaka, O., and Shoda, M. (1996). Biocontrol of *Rhizoctonia solani* Damping-Off of Tomato with *Bacillus subtilis* RB14. Appl Environ Microbiol *62*, 4081–4085.

10. Ongena, M., Jacques, P., Touré, Y., Destain, J., Jabrane, A., and Thonart, P. (2005). Involvement of fengycin-type lipopeptides in the multifaceted biocontrol potential of *Bacillus subtilis*. Appl Microbiol Biotechnol *69*, 29–38. 10.1007/s00253-005-1940-3.

11. Bais, H.P., Fall, R., and Vivanco, J.M. (2004). Biocontrol of *Bacillus subtilis* against Infection of Arabidopsis Roots by *Pseudomonas syringae* Is Facilitated by Biofilm Formation and Surfactin Production. Plant Physiol *134*, 307–319. 10.1104/pp.103.028712.

12. Molina-Santiago, C., Vela-Corcía, D., Petras, D., Díaz-Martínez, L., Pérez-Lorente, A.I., Sopeña-Torres, S., Pearson, J., Caraballo-Rodríguez, A.M., Dorrestein, P.C., de Vicente, A., et al. (2021). Chemical interplay and complementary adaptative strategies toggle bacterial antagonism and co-existence. Cell Rep *36*, 109449. 10.1016/j.celrep.2021.109449.

13. Dragoš, A., Kiesewalter, H., Martin, M., Hsu, C.Y., Hartmann, R., Wechsler, T., Eriksen, C., Brix, S., Drescher, K., Stanley-Wall, N., et al. (2018). Division of Labor during Biofilm Matrix Production. Current Biology *28*, 1903-1913.e5. 10.1016/j.cub.2018.04.046.

14. Sun, X., Xu, Z., Xie, J., Hesselberg-Thomsen, V., Tan, T., Zheng, D., Strube, M.L., Dragoš, A., Shen, Q., Zhang, R., et al. (2022). *Bacillus velezensis* stimulates resident rhizosphere *Pseudomonas stutzeri* for plant health through metabolic interactions. ISME Journal *16*, 774–787. 10.1038/s41396-021-01125-3.

15. Hesse, C., Schulz, F., Bull, C.T., Shaffer, B.T., Yan, Q., Shapiro, N., Hassan, K.A., Varghese, N., Elbourne, L.D.H., Paulsen, I.T., et al. (2018). Genome-based evolutionary history of *Pseudomonas* spp. Environ Microbiol *20*, 2142–2159. 10.1111/1462-2920.14130.

16. Chiellini, C., Lombardo, K., Mocali, S., Miceli, E., and Fani, R. (2019). *Pseudomonas* strains isolated from different environmental niches exhibit different antagonistic ability. Ethol Ecol Evol *31*, 399–420. 10.1080/03949370.2019.1621391.

17. Crone, S., Vives-Flórez, M., Kvich, L., Saunders, A.M., Malone, M., Nicolaisen, M.H., Martínez-García, E., Rojas-Acosta, C., Catalina Gomez-Puerto, M., Calum, H., et al. (2020). The environmental occurrence of *Pseudomonas aeruginosa*. APMIS *128*, 220–231. 10.1111/apm.13010.

18. Peix, A., Ramírez-Bahena, M.H., and Velázquez, E. (2018). The current status on the taxonomy of *Pseudomonas* revisited: An update. Infection, Genetics and Evolution *57*, 106–116. 10.1016/j.meegid.2017.10.026.

19. Raaijmakers, J.M., and Weller, D.M. (1998). Natural Plant Protection by 2,4-Diacetylphloroglucinol-Producing *Pseudomonas* spp. in Take-All Decline Soils. Mol Plant Microbe Interact *11*, 144–152.

20. Xin, X.F., Kvitko, B., and He, S.Y. (2018). *Pseudomonas syringae*: What it takes to be a pathogen. Nat Rev Microbiol *16*, 316–328. 10.1038/nrmicro.2018.17.

21. Qin, S., Xiao, W., Zhou, C., Pu, Q., Deng, X., Lan, L., Liang, H., Song, X., and Wu, M. (2022). *Pseudomonas aeruginosa*: pathogenesis, virulence factors, antibiotic resistance, interaction with host, technology advances and emerging therapeutics. Signal Transduct Target Ther *7*, 1–27. 10.1038/s41392-022-01056-1.

22. Joshi, M.N., Dhebar, S. v., Dhebar, S. v., Bhargava, P., Pandit, A., Patel, R.P., Saxena, A., and Bagatharia, S.B. (2014). Metagenomics of petroleum muck: Revealing microbial diversity and depicting microbial syntrophy. Arch Microbiol *196*, 531–544. 10.1007/s00203-014-0992-0.

23. Trantas, E.A., Sarris, P.F., Pentari, M.G., Mpalantinaki, E.E., Ververidis, F.N., and Goumas, D.E. (2015). Diversity among *Pseudomonas corrugata* and *Pseudomonas mediterranea* isolated from tomato and pepper showing symptoms of pith necrosis in Greece. Plant Pathol *64*, 307–318. 10.1111/ppa.12261.

24. Xin, X.F., Kvitko, B., and He, S.Y. (2018). *Pseudomonas syringae*: What it takes to be a pathogen. Nat Rev Microbiol *16*, 316–328. 10.1038/nrmicro.2018.17.

25. Lyng, M., and Kovács, Á.T. (2023). Frenemies of the soil: *Bacillus* and *Pseudomonas* interspecies interactions. Trends Microbiol, TIMI2204. 10.1016/j.tim.2023.02.003.

26. Kehe, J., Ortiz, A., Kulesa, A., Gore, J., Blainey, P.C., and Friedman, J. (2021). Positive interactions are common among culturable bacteria. Sci Adv *7*, eabi7159.

27. Andrić, S., Rigolet, A., Argüelles Arias, A., Steels, S., Hoff, G., Balleux, G., Ongena, L., Höfte, M., Meyer, T., and Ongena, M. (2022). Plant-associated Bacillus mobilizes its secondary metabolites upon perception of the siderophore pyochelin produced by a Pseudomonas competitor. ISME J. 10.1038/s41396-022-01337-1.

28. Andrić, S., Meyer, T., Rigolet, A., Prigent-Combaret, C., Höfte, M., Balleux, G., Steels, S., Hoff, G., De Mot, R., Mccann, A., et al. (2021). Lipopeptide Interplay Mediates Molecular Interactions between Soil *Bacilli* and *Pseudomonads*. Microbiol Spectr *9*, e02038-21. https://doi.org/10.1128/spectrum.02038-21.

29. Partida-Martinez, L.P., and Hertweck, C. (2005). Pathogenic fungus harbours endosymbiotic bacteria for toxin production. Nature *437*, 884–888. 10.1038/nature03997.

30. Vlamakis, H., Chai, Y., Beauregard, P., Losick, R., and Kolter, R. (2013). Sticking together: Building a biofilm the Bacillus subtilis way. Nat Rev Microbiol *11*, 157–168. 10.1038/nrmicro2960.

31. Zhu, J., Yan, Y., Wang, Y., and Qu, D. (2019). Competitive interaction on dual-species biofilm formation by spoilage bacteria, *Shewanella baltica* and *Pseudomonas fluorescens*. J Appl Microbiol *126*, 1175–1186. 10.1111/jam.14187.

32. Farias, G.A., Olmedilla, A., and Gallegos, M.T. (2019). Visualization and characterization of *Pseudomonas syringae* pv. tomato DC3000 pellicles. Microb Biotechnol *12*, 688–702. 10.1111/1751-7915.13385.

33. Almario, J., Bruto, M., Vacheron, J., Prigent-Combaret, C., Moënne-Loccoz, Y., and Muller, D. (2017). Distribution of 2,4-diacetylphloroglucinol biosynthetic genes among the *Pseudomonas* spp. Reveals unexpected Polyphyletism. Front Microbiol *8*, 1–9. 10.3389/fmicb.2017.01218.

34. Nestor, E., Toledano, G., and Friedman, J. (2023). Interactions between Culturable Bacteria Are Predicted by Individual Species' Growth. mSystems *8*, e00836-22. 10.1128/msystems.00836-22.

35. Baichman-Kass, A., Song, T., and Friedman, J. (2023). Competitive interactions between culturable bacteria are highly non-additive. Elife *12*, e83398. 10.7554/eLife.

36. Foster, K.R., and Bell, T. (2012). Competition, not cooperation, dominates interactions among culturable microbial species. Current Biology *22*, 1845–1850. 10.1016/j.cub.2012.08.005.

37. Palmer, J.D., and Foster, K.R. (2022). Bacterial species rarely work together. Science (1979) *376*, 581–582. 10.1126/science.abn5093.

38. Darwin, C. (1859). On the origin of species by means of natural selection First. J. Murray, ed. (W. Clowes and Sons).

39. Schoustra, S.E., Dench, J., Dali, R., Aaron, S.D., and Kassen, R. (2012). Antagonistic interactions peak at intermediate genetic distance in clinical and laboratory strains of *Pseudomonas aeruginosa*. BMC Microbiol *12*, 40. 10.1186/1471-2180-12-40.

40. Russel, J., Røder, H.L., Madsen, J.S., Burmølle, M., and Sørensen, S.J. (2017). Antagonism correlates with metabolic similarity in diverse bacteria. PNAS *114*, 10684–10688. 10.1073/pnas.1706016114.

41. Machado, D., Maistrenko, O.M., Andrejev, S., Kim, Y., Bork, P., Patil, K.R., and Patil, K.R. (2021). Polarization of microbial communities between competitive and cooperative metabolism. Nat Ecol Evol *5*, 195–203. 10.1038/s41559-020-01353-4.

42. Vetsigian, K., Jajoo, R., and Kishony, R. (2011). Structure and evolution of *Streptomyces* interaction networks in soil and in silico. PLoS Biol *9*, e1001184. 10.1371/journal.pbio.1001184.

43. Schlatter, D.C., Song, Z., Vaz-Jauri, P., and Kinkel, L.L. (2019). Inhibitory interaction networks among coevolved *Streptomyces* populations from prairie soils. PLoS One *14*, e0223779. 10.1371/journal.pone.0223779.

44. Pomerleau, M., Charron-Lamoureux, V., Léonard, L., Grenier, F., Rodrigue, S., and Beauregard, P.B. (2023). Adaptative Laboratory Evolution reveals biofilm regulating genes as key players in *B. subtilis* root colonization. BioRxiv. 10.1101/2023.07.04.547689.

45. Pacheco-Moreno, A., Stefanato, F.L., Ford, J.J., Trippel, C., Uszkoreit, S., Ferrafiat, L., Grenga, L., Dickens, R., Kelly, N., Kingdon, A.D.H., et al. (2021). Pan-genome analysis identifies intersecting roles for *Pseudomonas* specialized metabolites in potato pathogen inhibition. Elife *10*, e71900. 10.7554/eLife.71900.

46. Garrido-Sanz, D., Meier-Kolthoff, J.P., Göker, M., Martín, M., Rivilla, R., and Redondo-Nieto, M. (2016). Genomic and genetic diversity within the *Pseudomonas fluorescens* complex. PLoS One *11*, e0150183. 10.1371/journal.pone.0150183.

47. Mejri, D., Gamalero, E., and Souissi, T. (2013). Formulation development of the deleterious rhizobacterium *Pseudomonas trivialis* X33d for biocontrol of brome (*Bromus diandrus*) in durum wheat. J Appl Microbiol *114*, 219–228. 10.1111/jam.12036.

48. Abd El-Aziz, F.E.Z.A., and Bashandy, S.R. (2019). Dose-dependent effects of *Pseudomonas trivialis* rhizobacteria and synergistic growth stimulation effect with earthworms on the common radish. Rhizosphere *10*, 100156. 10.1016/j.rhisph.2019.100156.

49. Egamberdieva, D., Berg, G., Lindström, K., and Räsänen, L.A. (2013). Alleviation of salt stress of symbiotic *Galega officinalis L.* (goat's rue) by co-inoculation of *Rhizobium* with root-colonizing *Pseudomonas*. Plant Soil *369*, 453–465. 10.1007/s11104-013-1586-3.

50. Powers, M.J., Sanabria-Valentín, E., Bowers, A.A., and Shank, E.A. (2015). Inhibition of cell differentiation in *Bacillus subtilis* by *Pseudomonas protegens*. J Bacteriol *197*, 2129–2138. 10.1128/JB.02535-14.

51. Getzke, F., Hassani, M.A., Crüsemann, M., Malisic, M., Zhang, P., Ishigaki, Y., Böhringer, N., Jiménez Fernández, A., Wang, L., Ordon, J., et al. (2023). Cofunctioning of bacterial exometabolites drives root microbiota establishment. PNAS *120*, e2221508120. 10.1073/pnas.2221508120.

52. Geudens, N., and Martins, J.C. (2018). Cyclic lipodepsipeptides from *Pseudomonas* spp. - Biological Swiss-Army knives. Front Microbiol *9*, 1867. 10.3389/fmicb.2018.01867.

53. Fira, D., Dimkić, I., Berić, T., Lozo, J., and Stanković, S. (2018). Biological control of plant pathogens by *Bacillus* species. J Biotechnol *285*, 44–55. 10.1016/j.jbiotec.2018.07.044.

54. Höfte, M. (2021). The use of *Pseudomonas* spp. as bacterial biocontrol agents to control plant diseases. In Microbial bioprotectants for plant disease management, pp. 301–374. 10.19103/as.2021.0093.11.

55. Kumar, M., Mishra, S., Dixit, V., Kumar, M., Agarwal, L., Chauhan, P.S., and Nautiyal, C.S. (2016). Synergistic effect of *Pseudomonas putida* and *Bacillus amyloliquefaciens* ameliorates drought stress in chickpea (*Cicer arietinum L.*). Plant Signal Behav *11*, e1071004. 10.1080/15592324.2015.1071004.

56. Khabbaz, S.E., Zhang, L., Cáceres, L.A., Sumarah, M., Wang, A., and Abbasi, P.A. (2015). Characterisation of antagonistic *Bacillus* and *Pseudomonas* strains for biocontrol potential and suppression of damping-off and root rot diseases. Annals of Applied Biology *166*, 456–471. 10.1111/aab.12196.

57. Lyng, M., Jørgensen, J.P.B., Schostag, M.D., Jarmusch, S.A., Aguilar, D.K.C., Lozano-Andrade, C.-L.N., and Kovács, Á.T. (2023). Competition for iron shapes metabolic antagonism between *Bacillus subtilis* and *Pseudomonas*. BioRxiv. 10.1101/2023.06.12.544649.

58. Schindelin, J., Arganda-Carreras, I., Frise, E., Kaynig, V., Longair, M., Pietzsch, T., Preibisch, S., Rueden, C., Saalfeld, S., Schmid, B., et al. (2012). Fiji: An open-source platform for biological-image analysis. Nat Methods *9*, 676–682. 10.1038/nmeth.2019.

59. Wong, A.K., and Sahoo, P. (1989). A Gray-Level Threshold Selection Method Based on Maximum Entropy Principle. IEEE *19*, 866–871. 10.1109/21.35351.

60. Hartmann, R., Jeckel, H., Jelli, E., Singh, P.K., Vaidya, S., Bayer, M., Rode, D.K.H., Vidakovic, L., Díaz-Pascual, F., Fong, J.C.N., et al. (2021). Quantitative image analysis of microbial communities with BiofilmQ. Nat Microbiol *6*, 151–156. 10.1038/s41564-020-00817-4.

61. RStudio Team (2019). RStudio: Integrated Development for R.

62. R Core Team (2021). R: A language and environment for statistical computing.

63. Wickham, H., Averick, M., Bryan, J., Chang, W., McGowan, L., François, R., Grolemund, G., Hayes, A., Henry, L., Hester, J., et al. (2019). Welcome to the Tidyverse. J Open Source Softw *4*, 1–6. 10.21105/joss.01686.

64. Lauritsen, J.G., Hansen, M.L., Bech, P.K., Jelsbak, L., Gram, L., and Strube, M.L. (2021). Identification and Differentiation of *Pseudomonas* Species in Field Samples Using an *rpoD* Amplicon Sequencing Methodology. mSystems *6*, 1–14.

65. Martin, M. (2011). Cutadapt removes adapter sequences from high-throughput sequencing reads. EMBnet J *17*, 10–12. 10.14806/ej.17.1.200.

66. Chen, S., Zhou, Y., Chen, Y., and Gu, J. (2018). Fastp: An ultra-fast all-in-one FASTQ preprocessor. Bioinformatics *34*, i884–i890. 10.1093/bioinformatics/bty560.

67. Love, M.I., Huber, W., and Anders, S. (2014). Moderated estimation of fold change and dispersion for RNA-seq data with DESeq2. Genome Biol *15*, 1–21. 10.1186/s13059-014-0550-8.

68. Lin, H., and Peddada, S. Das (2020). Analysis of compositions of microbiomes with bias correction. Nat Commun *11*, 3514. 10.1038/s41467-020-17041-7.

69. Benjaminit, Y., and Hochberg, Y. (1995). Controlling the False Discovery Rate: a Practical and Powerful Approach to Multiple Testing. J. R. Statist. Soc. B *57*, 289–300. 10.1111/j.2517-6161.1995.tb02031.x.

70. Behrendt, U., Ulrich, A., and Schumann, P. (2003). Fluorescent pseudomonads associated with the phyllosphere of grasses; *Pseudomonas trivialis* sp. nov., *Pseudomonas poae* sp. nov. and *Pseudomonas congelans* sp. nov. Int J Syst Evol Microbiol *53*, 1461–1469. 10.1099/ijs.0.02567-0.

71. Hansen, M.L., Wibowo, M., Jarmusch, S.A., Larsen, T.O., and Jelsbak, L. (2022). Sequential interspecies interactions affect production of antimicrobial secondary metabolites in *Pseudomonas protegens* DTU9.1. ISME Journal *16*, 2680–2690. 10.1038/s41396-022-01322-8.

72. Zack, G.W., Rogers, W.E., and Latt, S.A. (1977). Automatic measurement of sister chromatid exchange frequency. The Journal of Histochemistry and Cytochemistry *25*, 741–753. 10.1177/25.7.70454.

73. Schwengers, O., Jelonek, L., Dieckmann, M.A., Beyvers, S., Blom, J., and Goesmann, A. (2021). Bakta: Rapid and standardized annotation of bacterial genomes via alignment-free sequence identification. Microb Genom *7*, 000685. 10.1099/MGEN.0.000685.

74. Blin, K., Shaw, S., Augustijn, H.E., Reitz, Z.L., Biermann, F., Alanjary, M., Fetter, A., Terlouw, B.R., Metcalf, W.W., Helfrich, E.J.N., et al. (2023). antiSMASH 7.0: new and improved predictions for detection, regulation, chemical structures and visualisation. Nucleic Acids Res *gkad344*. 10.1093/nar/gkad344.

75. Winsor, G.L., Griffiths, E.J., Lo, R., Dhillon, B.K., Shay, J.A., and Brinkman, F.S.L. (2016). Enhanced annotations and features for comparing thousands of *Pseudomonas* genomes in the *Pseudomonas* genome database. Nucleic Acids Res *44*, D646–D653. 10.1093/nar/gkv1227.

76. Meier-Kolthoff, J.P., Carbasse, J.S., Peinado-Olarte, R.L., and Göker, M. (2022). TYGS and LPSN: A database tandem for fast and reliable genome-based classification and nomenclature of prokaryotes. Nucleic Acids Res *50*, D801–D807. 10.1093/nar/gkab902.

Study 4

Mark Lyng, Johan P. B. Jørgensen, Morten D. Schostag, Scott A. Jarmusch, Diana K. C. Aguilar, Carlos N. Lozano-Andrade, Ákos T. Kovács

Competition for iron shapes metabolic antagonism between *Bacillus subtilis* and *Pseudomonas*

in review at ISME Journal 2023; deposited to *bioRxiv*
https://doi.org/10.1101/2023.06.12.544649

Competition for iron shapes metabolic antagonism between *Bacillus subtilis* and *Pseudomonas*

Mark Lyng[1], Johan P. B. Jørgensen[1], Morten D. Schostag[2], Scott A. Jarmusch[3], Diana K. C. Aguilar[1], Carlos N. Lozano-Andrade[1], and Ákos T. Kovács[1,4]

[1]Bacterial Interactions and Evolution group, DTU Bioengineering, Technical University of Denmark, Kgs Lyngby 2800, Denmark

[2]Bacterial Ecophysiology & Biotechnology, DTU Bioengineering, Technical University of Denmark, Kgs Lyngby 2800, Denmark

[3]Natural Product Discovery, DTU Bioengineering, Technical University of Denmark, Kgs Lyngby 2800, Denmark

[4]Institute of Biology Leiden, Leiden University, Leiden, The Netherlands

*email: a.t.kovacs@biology.leidenuniv.nl

Abstract

Siderophores have long been implicated in sociomicrobiology as determinants of bacterial interrelations. For plant-associated genera like *Bacillus* and *Pseudomonas*, siderophores are well known for their biocontrol functions. Here, we explored the functional role of the *Bacillus subtilis* siderophore bacillibactin in an antagonistic interaction with *Pseudomonas marginalis*. The presence of bacillibactin strongly influenced the outcome of the interaction in an iron-dependent manner. The bacillibactin producer *B. subtilis* restricts colony spreading of *P. marginalis* by repressing the transcription of histidine kinase-encoding gene *gacS*, thereby abolishing production of secondary metabolites such as pyoverdine and viscosin. By contrast, lack of bacillibactin restricted *B. subtilis* colony growth in a mechanism reminiscent of a siderophore tug-of-war for iron. Our analysis revealed that the *Bacillus-Pseudomonas* interaction is conserved across fluorescent *Pseudomonas* spp., expanding our understanding of the interplay between two genera of the most well-studied soil microbes.

Keywords: iron; siderophore; bacillibactin; *Bacillus subtilis*; *Pseudomonas*; GacSA

INTRODUCTION

Interactions between bacteria is of huge relevance to how microbial ecology can be manipulated for biotechnological benefit. In natural environments, bioavailable iron is often scarce and because it is an essential mineral to virtually all life, many organisms have evolved to scavenge iron using high-affinity metal chelators [1]. Metal chelators are a main driver of antagonism between microorganisms both in sequestering metal ions from competing organisms, and through bioactive toxicity directly inhibiting or even killing competitors [2, 3].

The catecholate siderophore bacillibactin (BB) produced by members of the *Bacillus* genus is an example of an iron chelator that performs multiple functions. In *Bacillus subtilis*, it is the main iron acquisition metabolite with high affinity for ferric iron, Fe(III) [4]. BB is synthesised through a non-ribosomal peptide synthetase pathway encoded by the *dhbA–F* operon and is exported to acquire Fe(III) before being taken up again by the FeuABC-YusV ABC transporter system [5–8]. Once intracellular, BB-Fe is hydrolysed by BesA to release iron ions for use in enzymatic reactions and in transcriptional regulation through the ferric uptake regulator Fur [7].

However, the *dhbA–F* operon also plays an essential role in *Bacillus* biofilm formation. The *ΔdhbA* mutant lacks dehydrogenation of (2S,3S)-2,3-dihydroxy-2,3-dihydrobenzoate to 2,3-dihydroxybenzoate (DHB) and therefore is unable to produce pellicle biofilms in biofilm-promoting defined medium MSgg due to an inability to perform extracellular electron transport with ferric iron captured by DHB [9]. Additionally, BB from *Bacillus amyloliquefaciens* has even been suggested to exhibit direct bioactivity against the plant-pathogenic *Pseudomonas syringae* pv. *tomato*, though without direct experimental evidence [10], and recent studies have demonstrated antibacterial properties of BB isomers [11, 12].

Bacillus and *Pseudomonas* are bacterial genera with high environmental impacts. They are environmentally ubiquitous and often co-isolated, especially within the context of crops, where they function as biostimulants and biocontrol agents, but also, in the case of *Pseudomonas*, as phytopathogens [13]. Both genera contain members capable of producing bioactive natural products that antagonise competing microbes [14–16], and both can alter the local microbiome [17, 18]. Such abilities have immense

implications in areas such as agriculture, where microbiome composition is consistently correlated with plant health and disease outcome [19, 20], and therefore considered an environmentally friendly agricultural practice.

Pairwise interactions between bacilli and pseudomonads might therefore play a crucial role in determining plant growth, health, and local microbiome composition. Studies investigating such pairwise interactions are revealing more detail, outlining the molecular mechanisms, and determining the degree to which interactions and their effector molecules are conserved [21–25]. However, despite these advances, the large bioactive potential of *Bacillus* and *Pseudomonas* makes mapping the overarching interaction mechanisms challenging, and a consensus has not been reached on the general interactions between members of these two genera. Some studies investigated the role of iron and siderophores in interactions between them, identifying *Pseudomonas* siderophores pyoverdine (Pvd) and pyochelin as signalling molecules for *Bacillus velezensis* [21] and pulcherriminic acid as an iron sequestering agent in interactions between *B. subtilis* and *Pseudomonas protegens* [26].

Here, we investigated the functional role of *B. subtilis* BB in antagonising *Pseudomonas*. Using a macrocolony competition assay, we observed that *B. subtilis* DK1042 (hereafter DK1042) was unable to restrict the colony size of *Pseudomonas marginalis* PS92 (hereafter PS92) when lacking the complete BB biosynthetic pathway, and that products of DhbA–F enzymes can be secreted and shared among *B. subtilis* cells. The interaction depended on iron in the media, but transcriptomic analysis revealed no iron starvation response in cocultures. Instead, the PS92 Gac/Rsm signalling system, herein Pvd biosynthesis, was strongly downregulated transcriptionally and metabolically when cocultured alongside DK1042. Finally, the specific interaction of DK1042 and the consequence of lacking BB were found to be conserved among fluorescent pseudomonads.

METHODS

Culturing

B. subtilis DK1042 (the naturally competent derivative of 3610) and *Pseudomonas marginalis* PS92 were routinely cultured in lysogeny broth (LB; Lennox, Carl Roth, 10 g/L tryptone, 5 g/L yeast extract and 5 g/L NaCl), LB supplemented with 1% (v/v) glycerol and 0.1 mM $MnCl_2$ (LBGM), or King's B medium (KB; 20 g/L peptone, 1% glycerol (v/v), 8.1 mM K_2HPO_4, 6.08 mM $MgSO_4 \cdot 7H_2O$) at 30°C. Colonies were grown on media solidified with 1.5% agar (w/v). $FeCl_3$, ammonium ferric citrate and 2,2'-bipyridine (BPD) were added to autoclaved agar at varying concentrations. Antibiotics were added in the following final concentrations: 50 μg/mL gentamycin (Gm), 100 μg/mL ampicillin (Amp), 5 μg/mL chloramphenicol (Cm), 10 μg/mL Kanamycin (Km).

Pairwise interactions on agar

DK1042 and PS92 were routinely spotted 5 mm apart on agar surfaces using 2 μL culture at an optical density at 600 nm (OD_{600}) of 1.0. Prior to spotting, plates were dried for 30 min in a lateral flow hood then incubated at 30°C. When spotting cocultures, each species was adjusted to an OD_{600} of 1.0 and the two strains were then mixed in equal volumes. For mixed *B. subtilis* cultures, wild-type (WT) and mutant strains were mixed 1:1, 1:10, or 1:100, based on OD_{600}.

Stereomicroscopy

Interactions for stereomicroscopy were assessed using DK1042 carrying *amyE::*$P_{hyperspank}$*-mKate2* and PS92 carrying *attTn7::msfGFP*. Colonies were imaged with a Carl Zeiss Axio Zoom V16 stereomicroscope equipped with a Zeiss CL 9000 LED light source and an AxioCam 503 monochromatic camera (Carl Zeiss, Jena, Germany). The stereoscope was equipped with a PlanApo Z 0.5×/0.125 FWD 114 mm, and filter sets 38 HE eGFP (ex: 470/40, em: 525/50) and 63 HE mRFP (ex: 572/25, em: 629/62). Exposure time was optimised for appropriate contrast.

Image processing and analysis were performed using FIJI (2.1.0/1.53f51) [27]. Contrast in fluorescence channels was adjusted identically on a linear scale. Colony area was measured by segmenting the colony of interest using Otsu's algorithm [28] based on fluorescence (msfGFP or mKate2 for *Pseudomonas* or *Bacillus*, respectively).

Genetic modification

DK1042 mutants were created through homologous recombination using the *B. subtilis* single gene deletion library [29]. In brief, genomic DNA from a donor *B. subtilis* 168 mutant was extracted using a EURx Bacterial & Yeast Genomic DNA Purification Kit (EURex, Gdansk, Poland) following the manufacturer's instructions, and 100–200 ng genomic DNA was added to DK1042 grown to OD_{600} ~0.5 in 400 µL at 37°C in competence medium (80 mM K_2HPO_4, 38.2 mM KH_2PO_4, 20 g/L glucose, 3 mM tri-Na citrate, 45 µM ferric NH_4 citrate, 1 g/L casein hydrolysate, 2 g/L K-glutamate, 0.335 µM $MgSO_4 \cdot 7H_2O$, 0.005 % [w/v] tryptophan). Cells were incubated with DNA at 37°C for 3 h before 100 µL of the transformation mix was spread onto LB agar supplemented with kanamycin and incubated at 37°C for 16–24 h. Mutants were validated by colony PCR with primers designed to anneal 50–150 bp up- and downstream of the gene of interest (Table S1).

PS92 attTn7::*msfGFP* was constructed by conjugation with pBG42 as described by Zobel *et al.* (2015) [30]. In brief, cultures of *Escherichia coli λpir* CC118/pBG42 (donor - Gm^R), *E. coli* HB101/pRK600 (helper, Cm^R), *E. coli λpir* CC118/pTNS2 (transposase-carrying, Amp^R) and PS92 (recipient) were started in LB medium supplemented with appropriate antibiotics and incubated overnight. Each culture was washed thrice in 0.9% NaCl before being mixed equally based on OD_{600}. The mix was spotted onto LB without antibiotics and incubated overnight at 30°C. Resultant colonies were resuspended in 0.9% NaCl and plated on Pseudomonas Isolation Agar (45.03 g/L; Millipore, Burlington, Massachusetts, United States) supplemented with Gm to select for positive *Pseudomonas* conjugants.

Mass spectrometry imaging

Pairwise interaction colonies were grown on 10 mL agar plates incubated for 72 h before being excised, dried, and sprayed for matrix-assisted laser desorption ionization-mass spectrometry imaging (MALDI-MSI). Agar was adhered to MALDI IntelliSlides (Bruker, Billerica, Massachusetts, USA) using a 2-Way Glue Pen (Kuretake Co., Ltd., Nara-Shi, Japan). Slides were covered by spraying 1.5 mL of 2,5-dihydrobenzoic acid (40 mg/mL in ACN/MeOH/H_2O [70:25:5, v/v/v]) in a nitrogen atmosphere and dried overnight in a desiccator prior to MSI acquisition. Samples were then subjected to timsTOF flex using a Bruker Daltonik GmbH mass spectrometer for MALDI MSI acquisition in positive MS scan

mode with a 40 µm raster width and a mass range of 100−2000 Da. Calibration was performed using red phosphorus. The settings in timsControl were as follows: Laser: imaging 40 µm, Power Boost 3.0%, scan range 46 µm in the XY interval, laser power 70%; Tune: Funnel 1 RF 300 Vpp, Funnel 2 RF 300 Vpp, Multipole RF 300 Vpp, isCID 0 eV, Deflection Delta 70 V, MALDI plate offset 100 V, quadrupole ion energy 5 eV, quadrupole loss mass 100 m/z, collision energy 10 eV, focus pre TOF transfer time 75 µs, pre-pulse storage 8 µs. After data acquisition, data were analysed using SCiLS software (version 2021b Pro).

Images were prepared from data normalised to the root-mean square. Images from each m/z value were expanded to be of equal size by adding pixels with NaN values if necessary. Linear scaling of pixel intensity was performed across images displaying the same m/z values. NaN is presented as 0 in the final images.

Liquid chromatography mass spectrometry (LC-MS)

B. subtilis DK1042 was inoculated into 20 mL LB in a 100 mL flask and grown overnight. The culture was adjusted to OD_{600} = 1.0 and 1 mL was spread on each of 150 LBGM agar plates and incubated at 30°C for 72 h. Extraction and subsequent LC-MS analysis were performed as previously described [31].

Whole-genome sequencing and genome comparisons

Pseudomonas genomes were sequenced and assembled using a hybrid approach with Oxford Nanopore and Illumina sequencing. From a culture grown in LB overnight, genomic DNA was extracted using an EURx Bacterial & Yeast Genomic DNA Purification Kit following the manufacturer's instructions. Short read library preparation and sequencing were performed at Novogene Co., Ltd. on an Illumina NovaSeq PE150 platform. Long-read library preparation was performed using an SQK-RBK004 Oxford Nanopore Rapid Barcoding kit, libraries were sequenced on a fresh Oxford Nanopore MinION Mk1B 9.4 flow cell for 12 h, and base called simultaneously with Guppy in MinKNOW (Oxford Nanopore Technologies, Oxford United Kingdom) using the default r941_min_hac_g507 model.

Genomes were assembled using Trycycler (V0.5.3) [32] when the long read sequencing depth was adequate for subsetting or Unicycler (V0.5.0) [33] in all other cases. Adapters were removed using Porechop (0.2.4 https://github.com/rrwick/Porechop) and reads were filtered with Filtlong (V0.2.1

https://github.com/rrwick/Filtlong). Default Trycycler and Unicycler workflows were applied to assemble genomes (see Supplementary Methods for details). Completeness and contamination were assessed using CheckM (V1.1.3) [34] and whole-genome taxonomy was determined with AutoMLST [35] and the TYGS database (V342) [36].

Assembled genomes were annotated with Bakta (V1.6.1) [37] and a gene presence/absence matrix was created with Panaroo (V1.3.2) [38] using its moderate mode and a CD-HIT amino acid identity threshold at 40%.

Transcriptomics

Colonies were collected with a 10 µL loop and placed in RNAse-free screw-cap tubes to sample either the interaction zone (~2 mm into each colony for pairwise interactions) or the entire colony (for monocultures). The collected biomass was solubilised in RNAProtect and frozen in liquid nitrogen before being stored at -80°C prior to RNA purification, for no more than 3 days.

RNA was extracted using a Qiagen RNeasy PowerMicrobiome RNA extraction kit (QIAGEN N.V., Venlo, The Netherlands) via combined bead beating and phenol-chloroform extraction (see Supplementary Methods for details). Ribosomal RNA depletion, library preparation and sequencing were performed at Novogene Co., Ltd. on an Illumina NovaSeq PE150 platform.

Read abundances were determined using Kallisto (0.48.0) [39]. The genome of PS92 was annotated with Bakta (V1.6.1) [37] while the genome of *B. subtilis* DK1042 (Acc: CP020102 and CP020103) was retrieved from GenBank. Genomes were converted into a fasta-formatted transcript file with gffread (v0.11.7) [40] then combined into a Kallisto index.

RNA sequencing (RNA-seq) datasets were trimmed and filtered with FastP, and reads were quantified by mapping every sample to the combined index file (consisting of transcripts from both species), with 100 bootstrap replicates. Differential expression analysis was performed with DESeq2 (v1.34.0) [41] in Rstudio (2022.02.3-b492) [42] running R (4.1.1) [43] with the Tidyverse framework (1.3.1) [44].

Pathway analysis was performed by functionally annotating the transcriptome of each species using eggNOG-mapper V2 (online browser version) with default parameters [45]. Differentially expressed pathways were investigated using KEGG Mapper Reconstruct [46], and manually using the databases Subtiwiki [47] and The *Pseudomonas* Genome Database [48] as references.

Data availability

Analysis scripts and processed data have been deposited at Github (https://github.com/mark-lyng/dhb_story).

Genome assemblies have been deposited at NCBI (accession numbers are listed in Table S1).

Raw sequence reads (long- and short-gDNA reads and RNA) have been deposited at the Sequencing Read Archive (SRA; https://www.ncbi.nlm.nih.gov/sra) with BioProject ID PRJNA956831.

Raw microscopy images have been deposited at Dryad (https://datadryad.org/; DOI https://doi.org/10.5061/dryad.vq83bk3zc).

MSI data have been deposited at Metaspace [49] under project ID https://metaspace2020.eu/project/lyng-2023

LC-MS data have been deposited at GNPS-MassIVE under MSV000092142.

RESULTS

BB is involved in mutual antagonism between DK1042 and PS92

Molina-Santiago and colleagues previously described that on solid KB medium (a growth medium for *Pseudomonas*-produced Pvd detection), DK1042 surrounds and restricts the growth of *Pseudomonas chlororaphis* PCL1606, unlike on various other media used in their experiments [24]. Therefore, we tested a soil-isolated *Pseudomonas* species (designated PS92) and revealed an interaction phenotype comparable to that of PCL1606. Since antagonism was apparent on KB medium, which induces Pvd production in *Pseudomonas*, and not on LB medium (Fig. S1a), we hypothesised that BB, the catechol siderophore of *B. subtilis*, is involved in this interaction. To evaluate the effect of BB in the interaction between DK1042 and PS92, we cultured fluorescently labelled versions of the two species together in close-proximity macro colonies on solid agar medium. Spots (2 µL) of each culture were placed 5 mm apart and grown at 30°C for 3 days (Fig. 1a and Video S1). We compared WT DK1042 and the single gene disruption mutant (Δ*dhbA*) lacking the ability to produce DHB and BB.

By measuring the areas of colonies, we determined that the growth of PS92 cocultured next to DK1042 was restricted and after 72 h; the area of monoculture colonies was approximately twice that of the area of coculture colonies (Fig. 1b). The Δ*dhbA* mutant did not surround nor restrict the growth of PS92, but rather, was itself restricted approximately two-fold. The restriction in area is reflected in the number of colony-forming units from colonies in each interaction, showing a 16-fold reduction in cells in PS92 colonies grown next to DK1042 and a 10^3-fold reduction in cells from Δ*dhbA*-mutant colonies grown next to PS92 (Fig. 1c). When coculturing the strains in liquid medium, we observed inhibition of PS92 in KB broth regardless of whether the coculture was with DK1042 or Δ*dhbA*. Neither DK1042 nor Δ*dhbA* was antagonised by PS92, demonstrating that the observed antagonism is specific to solid media (Fig. S1d and S1e). We also observed that the interaction occurs on LBGM but not on MSgg, and that glycerol is likely implicated in the antagonism (Fig. S2).

In previous studies, BB production was reported to be linked to iron stress conditions [10]. As both LB and KB contain sources of natural iron from tryptone or yeast extract, low BB production could be expected on both types of media. LC-MS was used to compare BB production from DK1042 inoculated

in liquid and solid LB and KB, revealing a 10-fold increase in BB concentration on solid KB compared to solid LB (Fig. 1d), while virtually undetectable in liquid media (Fig. S3). The dependency on *dhbA* for antagonism and defence coupled with the exclusive production on solid KB suggests a BB-mediated regulation in DK1042. However, a previous study showed that in *B. subtilis* biofilms, BB but not DHB is dispensable in air-liquid interface pellicle biofilms [9]. Thus, we tested whether BB or any precursor from the *dhbA-F* pathway influenced the pairwise interaction (Fig. 2a) and found all mutants unable to antagonise PS92 (Fig. 2b), suggesting that BB, and not an intermediate, must be present for antagonism.

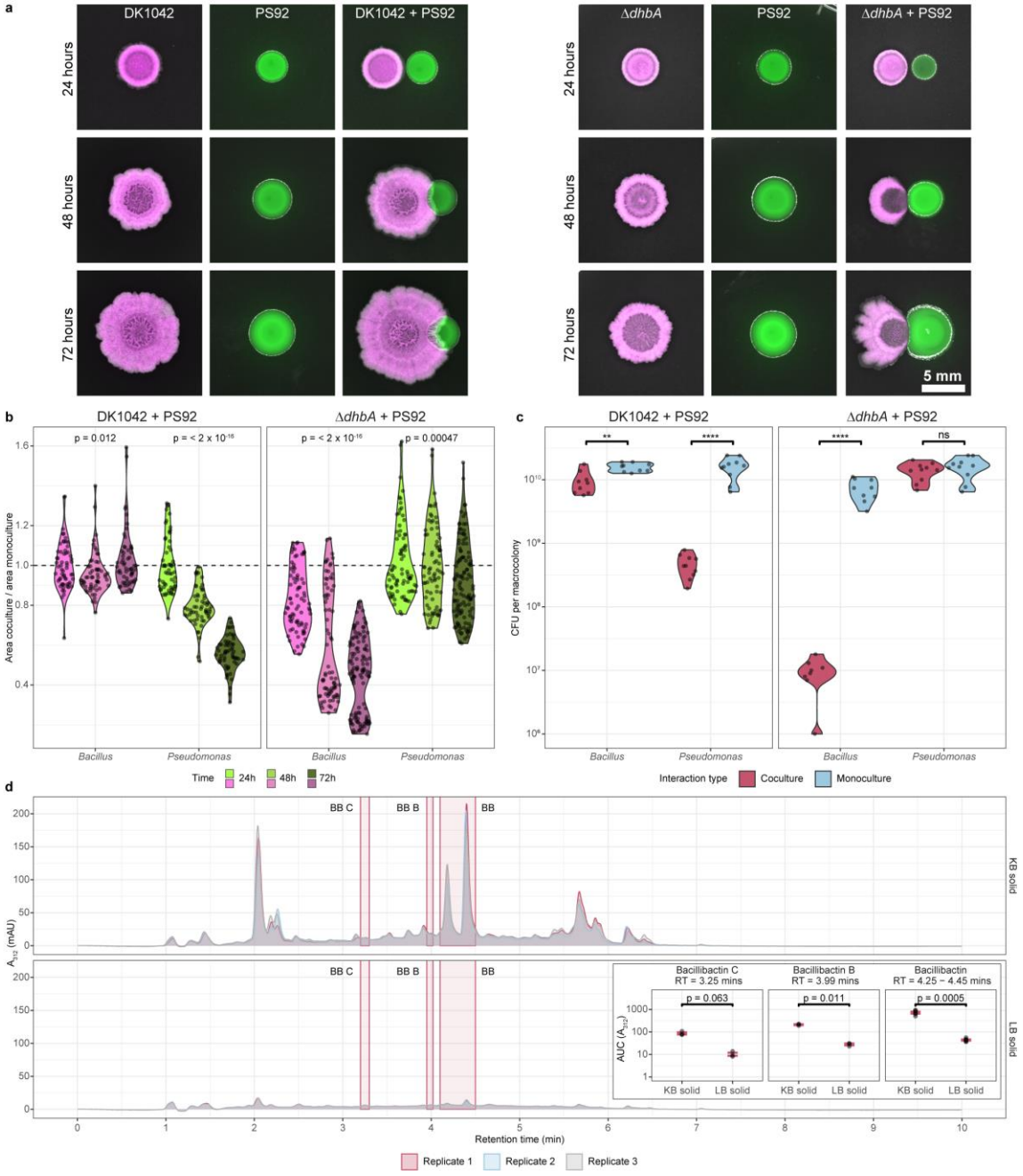

Fig 1 Antagonism is DhbA-dependent a: DK1042 (mKate2, magenta) and PS92 (msfGFP, green) were cocultured on KB agar with 5 mm between colony centres and imaged every 24 h. Scale = 5 mm. **b:** Coculture colony area was normalised against monoculture colony area and plotted for each partner (x-axis) in the two interactions (facets). The dashed line indicates coculture = monoculture. The *p*-value was calculated by analysis of variance (ANOVA) within groups (n = 40 colonies from two independent experiments). **c:** Colony-forming units were determined from the macrocolonies in coculture and monoculture. Significance stars are from Student's t-tests (n = 10 colonies from two independent experiments; ***p* <0.01, *****p* <0.0001; ns: not significant. **d:** Ultra-violet quantification of LC-MS on DK1042 monocultures at λ = 312 nm. Bacillibactin and isomers in KB (above) and LB (below). BB, Bacillibactin; BB B, Bacillibactin B; BB C, Bacillibactin C. Inset: Peak area under the curve (AUC) of bacillibactin and isomers in KB and LB. Labels are *p*-values from Student's t-test (n = 3 independent experiments).

Bacillibactin precursors are 'common goods'

Since DHB has been shown to function as a siderophore in biofilms [50], we hypothesised that it could be used as a 'common good' and taken up by Δ*dhbA* mutant cells. Therefore, we mixed mutants disrupted in early biosynthesis (Δ*dhbA* and Δ*dhbB*), late biosynthesis (*ΔdhbE* and *ΔdhbF*), and mutants disrupted in both early and late biosynthesis (Δ*dhbA* and Δ*dhbF*) that should be able to complement each other through Δ*dhbF* supplying DHB to Δ*dhbA*, which then completes the synthesis of BB. Only the mixture of Δ*dhbA* and Δ*dhbF* was able to antagonise and restrict the growth of PS92 on solid KB medium (Fig. 2c), which not only demonstrates the ability of the mutants to complement each other, but also confirms that BB, and not DHB, is responsible for the antagonistic interaction between DK1042 and PS92. This was further corroborated by mixing DK1042 with Δ*dhbA* (unable to produce DHB) or Δ*dhbF* (unable to synthesise the non-ribosomal peptide) using 1:1, 1:10 and 1:100 ratios, respectively, and spotted mixtures next to PS92 (Fig. S4). Both mutants were rescued by the WT strain, even at a ratio of 1:100, and expansion of PS92 colonies was restricted independently of which mutant was used in the mixture or the ratio of the mixed strains. This indicates that the critical components of the DhbA-F pathway can be secreted and shared between members in a population.

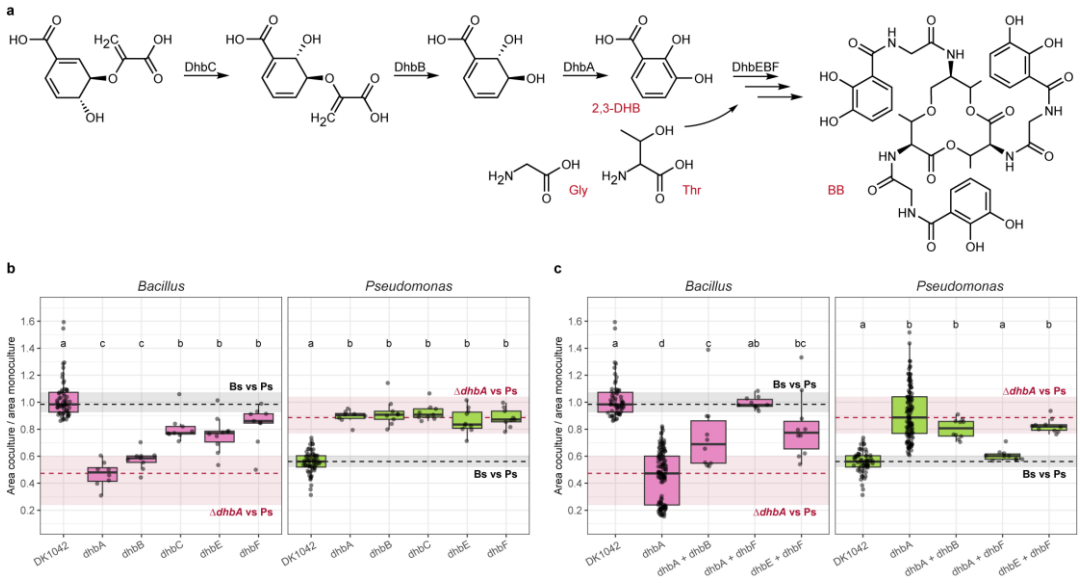

Fig 2 Bacillibactin precursors are 'common goods'. a: Bacillibactin (BB) is produced by the biosynthetic enzymes DhbACEBF from chorismate to 2,3-dihydroxybenzoate (2,3-DHB), which is then used as a starting unit by the non-ribosomal synthase complex DhbEBF to cyclize three monomers of 2,3-DHB using glycine (Gly) and threonine (Thr) linkers. **b:** Relative colony areas of PS92 (green) and individual Δ*dhbA–F* gene deletion mutants (magenta). **c:** Relative colony areas of PS92 (green) and combinations of Δ*dhbA–F* gene deletion mutants (magenta). Black dashed lines and grey rectangles denote the mean relative colony size in the DK1042 + PS92 interaction (lines = mean, rectangles = min and max). Red dashed lines and rectangles denote similarly for the Δ*dhbA* + PS92 interaction. Grouping letters are from ANOVA with Tukey-Kramer's Post-hoc test. Identical letters within each plot indicate a statistically significant grouping (p <0.05, n >8, from three independent experiments).

Excess iron abolishes antagonism

Given that BB is the main siderophore of *B. subtilis*, we hypothesised that the antagonism was driven by iron in the media. To test this hypothesis, we cocultured DK1042 and PS92 on KB agar supplemented with varying concentrations of the ferrous iron chelator BPD (Fig. 3a) or with excess ferric iron either as ferric citrate, which is not transported into the cell via the BB and FeuABC-YusV machinery (Fig. 3b), or as $FeCl_3$ from which iron is readily bound to DHB and BB (Fig. 3c) [6, 9]. Curiously, sequestration of Fe(II) and addition of Fe(III) resulted in increased coculture colony size for the Δ*dhbA* mutant. Sequestering ferrous iron did not lead Δ*dhbA* to regain the ability to restrict PS92 size, but, independently of concentration, both the addition of $FeCl_3$ and ferric citrate did, even though Δ*dhbA* should be unable to utilise $FeCl_3$ [51]. Similarly, the Δ*besA* mutant unable to release iron from BB was also complemented by any iron-related change to the medium. However, the Δ*feuA* mutant did not respond

to $FeCl_3$ (as expected), but could be complemented by ferric citrate in a dose-dependent manner. Though the iron concentration added to the medium in these experiments was relatively high, these results suggest that the interaction, both defensive and offensive, is iron-dependent.

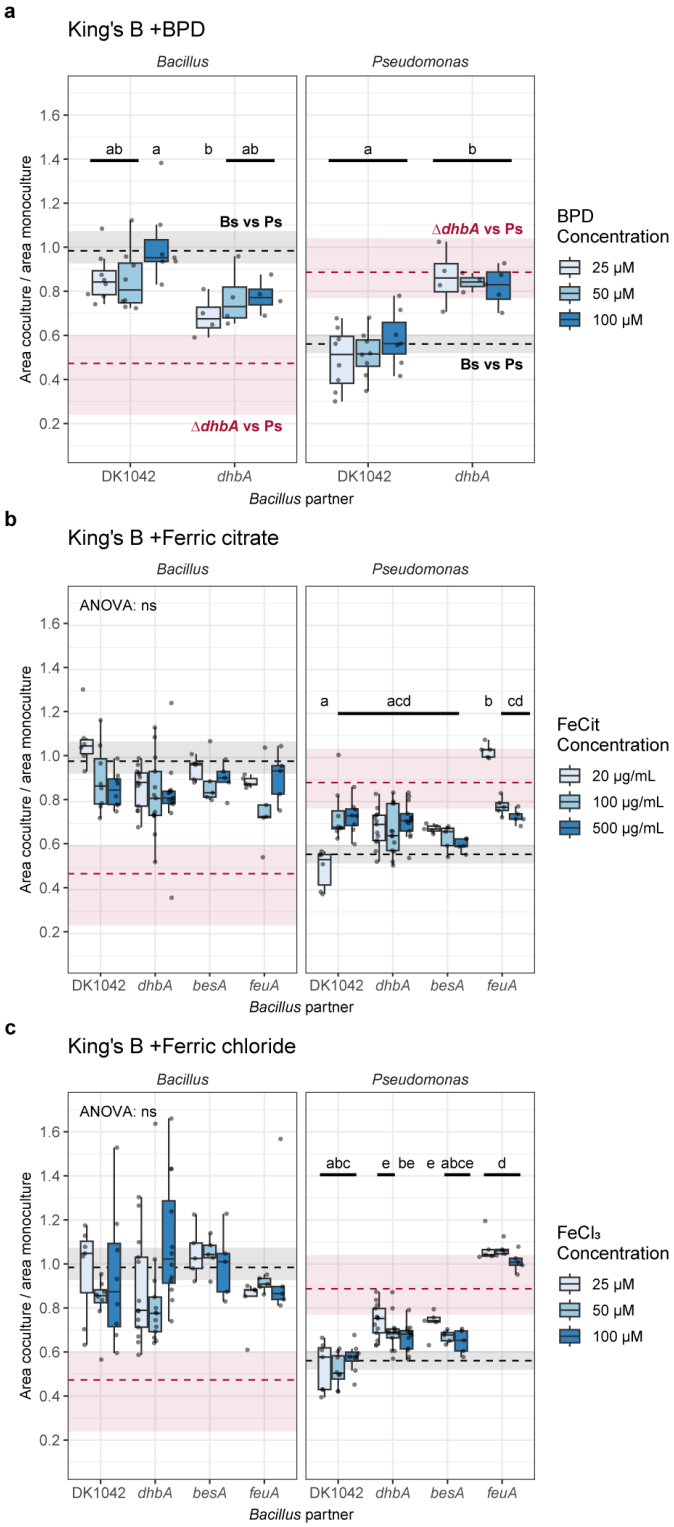

Fig 2 Excess iron restores mutant bacilli offensive and defensive attributes. *Bacillus* and *Pseudomonas* relative colony areas on KB with increasing concentrations of **a:** Fe(II) chelator 2,2-bipryidine

(BPD), **b:** ferric citrate (FeCit) and **c:** ferric chloride ($FeCl_3$). PS92 was spotted next to DK1042 or mutants deficient in the bacillibactin biosynthesis and uptake pathway. Dashed lines and rectangles are median, 1st and 3rd quartiles for PS92 colonies spotted next to Δ*dhbA* (red) and DK1042 (grey) on non-supplemented KB. Grouping letters are from ANOVA with Tukey-Kramer's Post-hoc test. Identical letters within each plot indicate a statistically significant grouping (p <0.05, n ≥4 colonies from two independent experiments).

DK1042 heavily alters the PS92 transcriptome

To better understand the transcriptional landscape present in each strain as a result of cocultivation, we extracted total RNA from colonies cultured in monoculture or with an interaction partner. This allowed us to identify transcriptional differences between DK1042 and Δ*dhbA* both in monoculture and coculture, but also between each individual strain in monoculture compared to coculture to ascertain how a neighbouring partner alters the transcription of a focal strain (Fig. S5). Transcriptomic analysis revealed that the PS92 transcriptome was heavily altered by DK1042 (1036 differentially regulated genes at $\log_2$(FC) >|2| and adjusted p <0.01) but not by Δ*dhbA* (9 differentially regulated genes). Approximately 4–8% of the transcriptomes of DK1042 and Δ*dhbA* (364 and 172 differentially regulated genes, respectively) were differentially regulated by the presence of PS92, but comparison of cocultures revealed that 1002 transcripts were differentially regulated between the two strains in coculture. In monoculture, 395 transcripts were differentially regulated between DK1042 and Δ*dhbA*.

Δ*dhbA* downregulates sporulation and biofilm formation

When coculturing DK1042 with PS92, a large number of genes related to sporulation and germination were upregulated in DK1042 (Fig. 4a), though not differentially regulated in the Δ*dhbA* mutant in coculture compared with its monoculture. However, comparing the levels of transcription between DK1042 and Δ*dhbA* reveals that lack of *dhbA* strongly downregulated sporulation and germination pathways, independently of whether it was cocultured with PS92.

Elimination of DHB and BB production affected several genes related to biofilm formation and sporulation in the *epsA-O*, *tapA-tasA-sipW*, *spsA-L*, *cot* and *spoII*, *III*, *IV*, *V* and *VI* operons, an effect reported previously [9, 51]. In addition, the transcription level of the *sinI* gene was higher in monoculture for Δ*dhbA* compared with DK1042, though not in coculture. In coculture, lack of *dhbA* upregulated the

transcription of the biofilm repressor gene *abrB*. Together, this suggests that the Δ*dhbA* mutant did not form a biofilm or undergo sporulation either in coculture or in monoculture.

Repression of sporulation and biofilm formation was further corroborated by the downregulation of genes involved in utilisation of glutamine, manganese, and glycerol. Manganese and glutamine/glutamate utilisation are well known for their role in the Spo0A sporulation pathway that drives both biofilm formation and sporulation [52–55], while manganese homeostasis was very recently shown to be tightly interlinked with iron homeostasis [56].

Interestingly, the transcriptome of the Δ*dhbA* mutant did not display signs of iron starvation, with the exception of a slight repression in the transcription of *fur*. The *dhb*, *feu*, *yusV*, *besA*, and *yvm* genes were not differentially regulated in the Δ*dhbA* mutant compared with DK1042, except the *dhbA* transcript level which was deleted in the genome of the mutant and therefore transcriptionally absent in the mutant. Additionally, genes involved in production of known bioactive secondary metabolites were not differentially regulated in *Bacillus*, regardless of mutation or coculture partner.

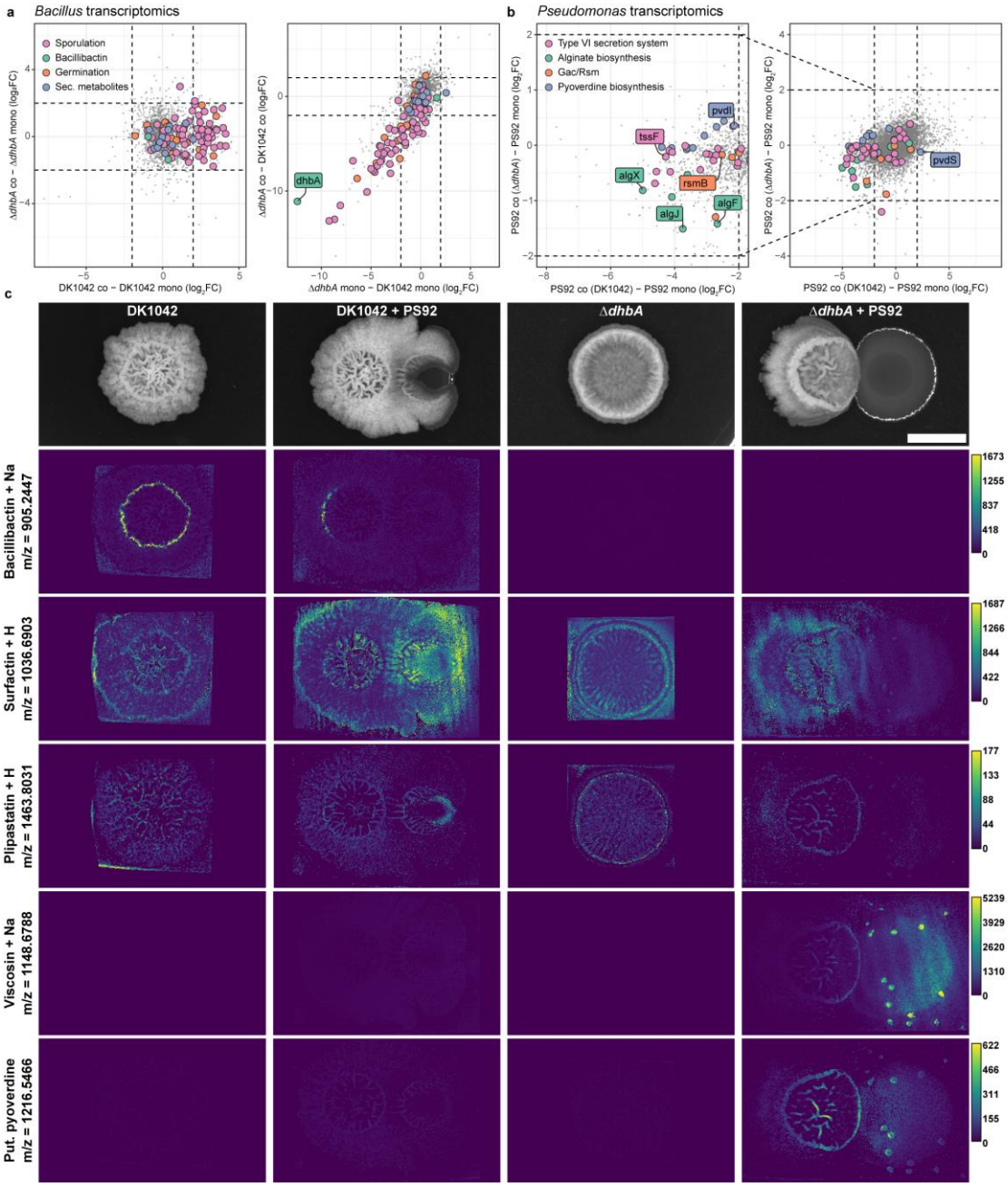

Fig 3 DK1042 alters PS92 transcriptome and metabolome via *gacS* a: Δ*dhbA* downregulates genes related to sporulation and germination independently of having PS92 as its interaction partner. DK1042-upregulated genes of the same category only when in coculture with PS92. Dashed lines indicate log2(FC) = |2|. **b:** Several biosynthetic pathways related to the Gac/Rsm two-component system were significantly downregulated (log_2(FC) <-2 and adjusted *p*-value <0.01) in coculture with DK1042, except for the alternative sigma factor *pvdS*. **c:** Mass spectrometry imaging reveals the presence/absence of select metabolites as well as their spatial localisation in the interactions. Scale bar = 5 mm. Grey values are root mean squared intensity across all samples, and lookup tables were scaled identically across each metabolite. NaN pixels were set to zero. Metabolites were annotated with metaspace using the 2019 Natural Product Atlas database. m/z = 1216.5466 was manually annotated as a pyoverdine structure.

PS92 downregulates Gac/Rsm and iron acquisition in coculture with DK1042

When cocultured with DK1042, PS92 underwent downregulation of biosynthetic genes responsible for production of several secondary metabolites (Fig. 4b and Dataset S1). All biosynthetic genes involved in Pvd, alginate and viscosin production were repressed along with a Type VI secretion system (T6SS) subtype i3, while genes responsible for type II and III secretion and reactive oxygen neutralisation were upregulated. Similar changes have previously been observed in the closely related *P. fluorescence* SBW25 when removing the histidine kinase *gacS* (OrthoANIu similarity between SBW25 and PS92 = 99.06%) [57]. The Gac/Rsm pathway is a conserved two-component system found in many γ-proteobacteria and known to positively regulate biofilm formation and secondary metabolism in most pseudomonads and induce virulence factors in plant pathogenic species. Indeed, PS92 *gacS* (FNPKGJ_17835) was downregulated 4-fold in PS92 when cocultured with DK1042 but not when cocultured with Δ*dhbA*.

Unexpectedly, while Pvd biosynthetic genes were downregulated, the iron starvation sigma factor-encoding gene *pvdS* (FPNKGJ_22055) had a higher transcript level in coculture with DK1042. Pvd is the primary siderophore in SBW25 [58], though other iron-chelating molecules are encoded in the genomes of both SBW25 [57] and PS92. A biosynthetic gene cluster encoding the production machinery for a corrugatin-like molecule (FNPKGJ_15100-15175) was similarly repressed, although not below the threshold of $\log_2$(FC) <-2. Upregulation of *pvdS* suggests that PS92 is starved for iron in coculture with DK1042, but with downregulation of the iron acquisition systems it is unclear whether the consequence of coculture is iron starvation, repression of the Gac/Rsm pathway, or a combination of both.

We found further evidence for repression of the Gac/Rsm system in mass spectrometry imaging of cocultures showing that several molecules produced by genes under control of the Gac/Rsm system were absent from cocultures with DK1042 but present in monoculture colonies and cocultures with Δ*dhbA* (Fig. 4c). The presence of viscosin in all cultures except coculture with DK1042 on KB prompted us to test if viscosin was the antagonistic molecule against Δ*dhbA*. In lieu of a PS92 Δ*viscA* gene deletion mutant, we obtained a *P. fluorescens* SBW25 Δ*viscA* mutant with an identical interaction with DK1042, but found that *ΔviscA* was still able to antagonise Δ*dhbA*, similarly to the WT strain (Fig. S6).

Antagonism depends on bacillibactin

Based on the transcriptome data for DK1042, we screened multiple gene disruption mutants for their antagonistic effect against PS92 (Fig. 5). Effects of mutations ranged from deficiency in production of biofilm matrix (*epsA-O*, *tasA*) and secondary metabolites (*srfAA*, *pksL*, *sfp*, *cypX*, *yvmC*) to lacking sensor kinases (*kinA-E*) or being unable to undergo sporulation (*spo0A*). Interestingly, only three mutants were significantly unable to antagonise PS92 (Δ*sfp*, Δ*feuA* and Δ*glpK*). Thus, neither sporulation nor biofilm formation are essential for antagonism, and likewise, typical secondary metabolites with antimicrobial properties such as surfactin and bacillaene had no effect on the restriction of PS92 colony area (although this was suggested from the mass spectrometry imaging). The inability of Δ*feuA* to antagonise suggests that iron uptake by BB is essential for restriction of PS92 colony size, but the fitness of the Δ*feuA* mutant was rather low even in monoculture (**Fig. S7**), which could result in low metabolic output in general. The antagonistic activity of the Δ*besA* mutant suggests that Fe(III) from BB is not required for antagonism, and that BB itself may inhibit PS92.

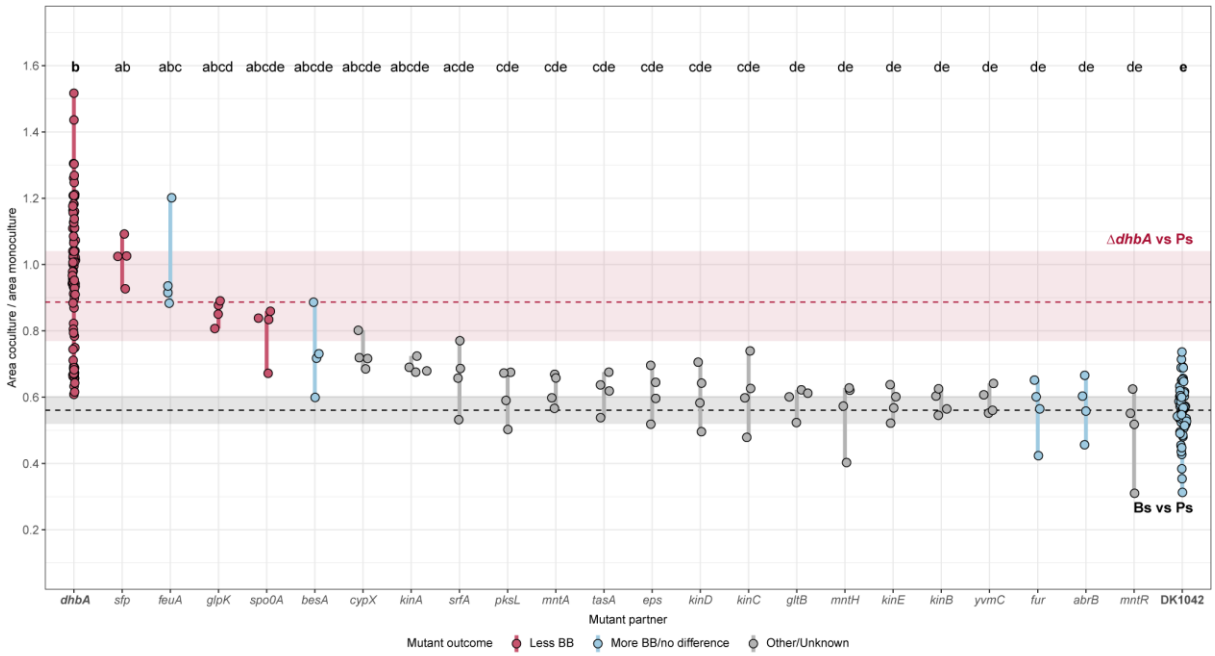

Fig 4 *Pseudomonas* colony size restriction is related to *sfp* and *feuA*: PS92 colony size was measured in cocultures next to *Bacillus* gene deletion mutants deficient in multiple aspects of cell physiology. Colonies spotted next to mutants lacking *sfp, feuA* and *glpK* were significantly larger than those spotted next to DK1042 relative to monoculture colony size, while not being significantly smaller than colonies spotted next to Δ*dhbA*. Other mutants related to biofilm formation, metal homeostasis and bioactive secondary metabolites were not diminished in their restriction of PS92. Dashed lines and rectangles are median, 1st and 3rd quartiles for PS92 colonies spotted next to Δ*dhbA* (red) and DK1042 (grey).

Grouping letters are from ANOVA with Tukey-Kramer's Post-hoc test. Identical letters within each plot indicate a statistically significant grouping (p <0.05, n = 4 biologically independent colonies). *dhbA* and DK1042 represent pooled data from multiple experiments (n >80).

Interaction is conserved across fluorescent *Pseudomonas* isolates

To determine if the iron-related antagonism is specific to DK1042 and PS92, we cocultured DK1042 and Δ*dhbA* on KB agar with a collection of 16 fluorescent *Pseudomonas* soil isolates for which genomes had been sequenced (Fig. 6). Thus, we could qualitatively compare the interaction outcome with the genomic presence of biosynthetic pathways. Multiple isolates were restricted in colony size by DK1042 and not by Δ*dhbA*. Most isolates also seemed to influence the size and/or morphology of Δ*dhbA*, except XL272 (previously *Pseudomonas stutzeri*, now *Stutzerimonas degradans*) which is the only isolate lacking the Gac/Rsm-controlled biosynthetic machineries producing pyoverdine and alginate. A few isolates belonging to *Pseudomonas corrugata* and *protegens* subgroups were able to inhibit both DK1042 and Δ*dhbA*, which may be attributed to their potential for producing 2,4-diacetylphloroglucinol and pyoluteorin [59]. Strains from other *Pseudomonas fluorescens* subgroups were all restricted in colony growth in the presence of BB-producing *B. subtilis*, demonstrating the conservation of this antagonism across species.

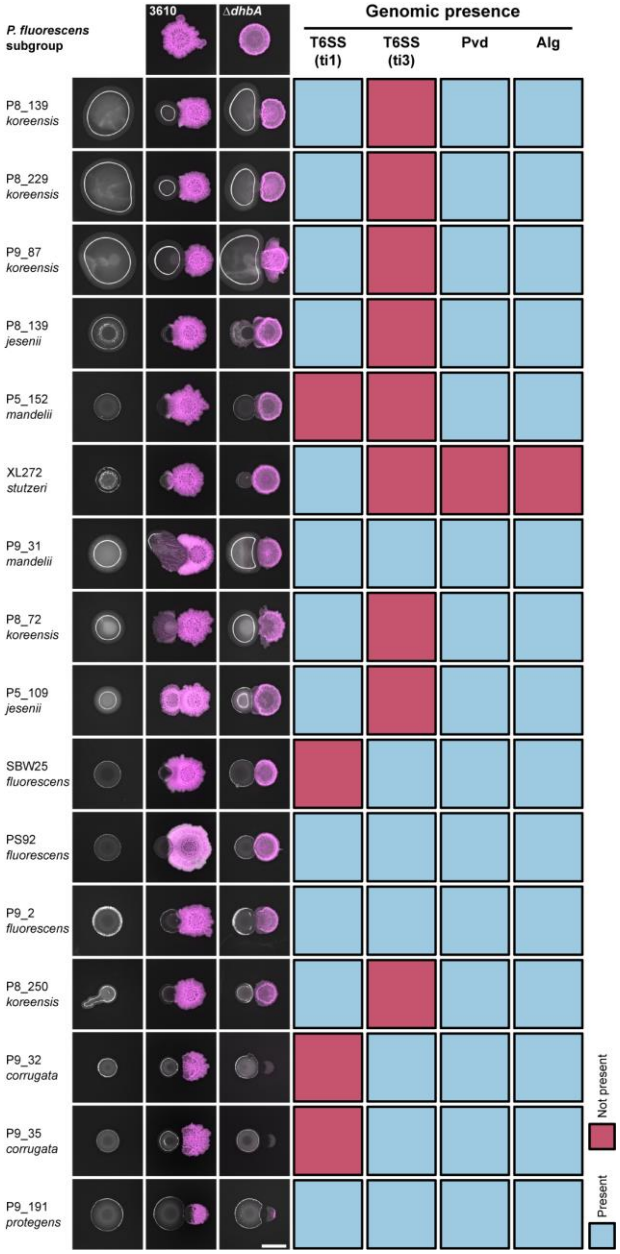

FIG 5 Antagonism is conserved across *Pseudomonas* spp. Fluorescent *Pseudomonas* soil isolates were cultured next to DK1042 or Δ*dhbA* on KB agar and their genomes were assessed for the presence of Gac/Rsm-related biosynthetic genes. Presence of >80% of PS92 genes at 40% amino acid identity was scored as 'present' (blue) while any less was scored as 'not present' (red). Isolates are presented as their strain ID and the closest related *P. fluorescens* subgroup as described by Hesse et al. (2016) based on whole-genome alignments. T6SS, Type VI Secretion system; ti1, Type i1; ti3, Type i3; Pvd, Pyoverdine; Alg, Alginate.

DISCUSSION

In this study, we report a novel molecular interaction conserved between *B. subtilis* and multiple *Pseudomonas* spp. We show that the interaction is dependent on iron and BB, and that a lack of BB on KB

agar results in both diminished offense and defence. The consequence of the BB-mediated antagonism is a restriction of *Pseudomonas* colony spreading and a reduction both in transcription and production of several products related to the Gac/Rsm system, which over time allows *Bacillus* to overgrow a *Pseudomonas* colony.

Bacillus defence is especially affected by iron availability. Iron homeostasis, biofilm formation, and sporulation are tightly interlinked in *B. subtilis*, and DhbA is essential for structured biofilm formation and proper sporulation due to the high iron demands of these lifestyles [9, 51, 60]. Surprisingly, matrix and sporulation as defensive measures in microbial ecology have received little attention [61], though the relation to T6SS has been investigated [24, 62]. Defence appears to take precedence for *Bacillus* in the interaction, and a biofilm- and sporulation-deficient mutant may be too antagonised by PS92 to produce the necessary effector for growth restriction. This could explain our observations with Δ*feuA* which requires large quantities of supplemented iron for proper fitness. Additionally, a biofilm-proficient strain lacking the antagonistic molecule may block PS92 growth through spatial competition [63–65], though it will be unable to restrict colony spreading chemically.

Another possibility could be that BB is a stronger iron chelator than Pvd, sequestering Fe(III) away from *Pseudomonas* and thereby inducing iron starvation. When *Bacillus* is unable to produce BB the tide turns, and Pvd from *Pseudomonas* sequesters Fe(III) away from *Bacillus*. Pvd production on KB has been shown in several pseudomonads to be highly dependent on iron-content, where iron-binding Fur represses Pvd production through repression of *pvdS* [58]. This could explain how Δ*dhbA*, Δ*besA* and Δ*feuA* are rescued by iron supplementation even in the form of ferric chloride. With this mechanism, strong iron starvation responses are likely in both *Bacillus* and *Pseudomonas*, but in Δ*dhbA* iron homeostasis was not significantly upregulated in coculture with PS92. On the other hand, *pvdS* in PS92 was significantly upregulated, which is indicative of iron starvation, but without the complementary upregulation of the rest of the pyoverdine biosynthetic genes. In *P. aeruginosa* Gac/Rsm is known to positively regulate pyoverdine biosynthetic gene transcription trough PvdS [66, 67], and a similar phenotype has been described in *P. fluorescens* SBW25 [57]. Recently, both pyoverdine and, to a larger extent, pyochelin were shown to be sensed by *B. velezensis*, instigating mobilisation of secondary metabolites [21]. Although sensing of pyochelin occurs independently of iron and BB, pyoverdine was

shown to increase the production of BB. PS92 does not contain a gene cluster encoding the synthetic machinery for any type of pyochelin, and thus, pyochelin sensing presumably does not occur in the interaction between DK1042 and PS92.

Our results suggest *Bacillus*-mediated repression of *gacS*, a phenomenon with precedent from interaction between a *Bacillus* sp. isolate and *Pseudomonas syringae* pv. tomato DC3000 [68], though neither previous nor our experiments reveal if *gacS* repression is directly caused by DK1042 or by a sensory mechanism in PS92. Currently, there is no consensus on exactly which ligand triggers the Gac signal cascade [69], though it is expected that secreted products resulting from the activated pathway itself are at least partly responsible [70]. However, in *Pseudomonas* GacS is activated and inhibited by LadS and RetS, respectively, which in turn are activated by calcium ions (LadS) and mucin glycans or temperature (RetS) [71–73]. It is also hypothesised that the Gac/Rsm pathway functions via an alternative quorum sensing pathway, and that induction is achieved at higher cell densities [70]. This might explain why *gacS* was downregulated in PS92 spotted next to DK1042, where the colony is indeed restricted in size and at a lower cell density. Unfortunately, large-scale purification and chemical synthesis of BB was unsuccessful, hence we could not probe the antagonistic properties of BB directly.

Siderophores have long been implicated in microbial interactions, particularly in iron-scarce environments. In infections, pyoverdine and enterobactin are essential for *P. aeruginosa* and *E. coli*, respectively, not only due to iron requirements in a complex environment, but also in polymicrobial interactions as interspecies competitive factors [74]. Siderophores are also thought to play a role in biocontrol of plant pathogens by both *Pseudomonas* and *Bacillus*, but a thorough examination of the literature reveals that *Bacillus* and *Pseudomonas* siderophores have only rarely been directly implicated in interspecies interactions *in planta* [13]. Most evidence originated in the previous millennium where *Pseudomonas* siderophores proved to be determinants of microbial interactions through iron sequestration [75, 76]. Others have since inferred biocontrol potential from the ability to produce siderophores without experimentally determining the consequence of losing siderophore production [10, 77]. Our study systematically investigated the significance of BB and its effects on transcription and metabolite production in microbial interactions. Although we demonstrated the importance of BB on rich media, our study complements and expands the previously established role of BB in biocontrol. Our *P. marginalis*

isolate proved non-pathogenic against lettuce, cabbage and spinach, hence we were unable to determine if BB-mediated antagonism occurs in the phyllosphere as well as on agar surfaces. Other studies have successfully transferred biocontrol properties from *in vitro* to *in planta* [78], but the medium dependency of the antagonism between DK1042 and PS92 might render it difficult to apply to agriculture. Regardless, understanding the molecular mechanism underlying the antagonism could allow the environment to be tailored specifically to the intended interaction. Future studies should investigate the apparent tug-of-war between BB and Pvd, as well as the hypothesis that BB represses Gac sensing in fluorescent pseudomonads.

ACKNOWLEDGEMENTS

The authors thank Lars Jelsbak and Morten Lindquist Hansen for contributing *Pseudomonas* soil isolates for this study, and the DTU Metabolomics Core for MSI and LC-MS instrumentation. This project was funded by a DTU Alliance Strategic Partnership PhD fellowship, by the Danish National Research Foundation (DNRF137) for the Center for Microbial Secondary Metabolites, and the Novo Nordisk Foundation within the INTERACT project of the Collaborative Crop Resiliency Program (NNF19SA0059360) and for the "Imaging microbial language in biocontrol (IMLiB)" infrastructure grant (NNF19OC0055625).

AUTHOR CONTRIBUTIONS

ML and ÁTK designed the study; ML, JPBJ, and SAJ collected and analyzed data; MDS, DKCA, and CNLA contributed with methodology or preliminary data; ML and ÁTK wrote first draft of paper with edits from all authors.

COMPETING INTERESTS

The authors declare no competing interests.

REFERENCES

1. Andrews SC, Robinson AK, Rodríguez-Quiñones F. Bacterial iron homeostasis. *FEMS Microbiol Rev*. 2003; **27**: 215–237
2. Kramer J, Özkaya Ö, Kümmerli R. Bacterial siderophores in community and host interactions. *Nat Rev Microbiol*. 2020; **18**: 152–163
3. Rehm K, Vollenweider V, Gu S, Friman V-P, Kümmerli R, Wei Z, et al. Chryseochelins—structural characterization of novel citrate-based siderophores produced by plant protecting *Chryseobacterium* spp. *Metallomics* 2023; **15**: mfad008.
4. Dertz EA, Stintzi A, Raymond KN. Siderophore-mediated iron transport in *Bacillus subtilis* and *Corynebacterium glutamicum*. *Journal of Biological Inorganic Chemistry* 2006; **11**: 1087–1097.
5. Miethke M, Schmidt S, Marahiel MA. The major facilitator superfamily-type transporter YmfE and the multidrug-efflux activator Mta mediate bacillibactin secretion in *Bacillus subtilis*. *J Bacteriol* 2008; **190**: 5143–5152.
6. Ollinger J, Song KB, Antelmann H, Hecker M, Helmann JD. Role of the Fur regulon in iron transport in *Bacillus subtilis*. *J Bacteriol* 2006; **188**: 3664–3673.
7. Miethke M, Klotz O, Linne U, May JJ, Beckering CL, Marahiel MA. Ferri-bacillibactin uptake and hydrolysis in *Bacillus subtilis*. *Mol Microbiol* 2006; **61**: 1413–1427.
8. May JJ, Wendrich TM, Marahiel MA. The *dhb* Operon of *Bacillus subtilis* Encodes the Biosynthetic Template for the Catecholic Siderophore 2,3-Dihydroxybenzoate-Glycine-Threonine Trimeric Ester Bacillibactin. *Journal of Biological Chemistry* 2001; **276**: 7209–7217.
9. Qin Y, He Y, She Q, Larese-Casanova P, Li P, Chai Y. Heterogeneity in respiratory electron transfer and adaptive iron utilization in a bacterial biofilm. *Nat Commun* 2019; **10**: 1–12.
10. Dimopoulou A, Theologidis I, Benaki D, Koukounia M, Zervakou A, Tzima A, et al. Direct Antibiotic Activity of Bacillibactin Broadens the Biocontrol Range of Bacillus amyloliquefaciens MBI600. *mSphere* 2021; **6**: e00376-21.

11. Chakraborty K, Kizhakkekalam VK, Joy M, Chakraborty RD. Bacillibactin class of siderophore antibiotics from a marine symbiotic *Bacillus* as promising antibacterial agents. *Appl Microbiol Biotechnol* 2022; **106**: 329–340.

12. Nalli Y, Singh S, Gajjar A, Mahizhaveni B, Nynar V, Dusthackeer A, et al. Bacillibactin class siderophores produced by the endophyte *Bacillus subtilis* NPROOT3 as antimycobacterial agents. *Lett Appl Microbiol* 2022; **76**: ovac026.

13. Lyng M, Kovács ÁT. Frenemies of the soil: *Bacillus* and *Pseudomonas* interspecies interactions. *Trends Microbiol* 2023; https://doi.org/10.1016/j.tim.2023.02.003.

14. Gross H, Loper JE. Genomics of secondary metabolite production by *Pseudomonas* spp. *Nat Prod Rep* 2009; **26**: 1408–1446.

15. Kaspar F, Neubauer P, Gimpel M. Bioactive Secondary Metabolites from *Bacillus subtilis*: A Comprehensive Review. *J Nat Prod* 2019; **82**: 2038–2053.

16. Cesa-Luna C, Geudens N, Girard L, De Roo V, Maklad HR, Martins JC, et al. Charting the Lipopeptidome of Nonpathogenic *Pseudomonas*. *mSystems* 2023; **8**: e00988-22.

17. Sun X, Xu Z, Xie J, Hesselberg-Thomsen V, Tan T, Zheng D, et al. *Bacillus velezensis* stimulates resident rhizosphere *Pseudomonas stutzeri* for plant health through metabolic interactions. *ISME Journal* 2022; **16**: 774–787.

18. Liu Y, Xu Z, Xun W, Štefanič P, Yang T, Miao Y, et al. Plant beneficial bacterium promotes plant growth by altering social networks of bacteria in the rhizosphere. *Res Sq* 2023; https://doi.org/10.21203/rs.3.rs-2491444/v1

19. Trivedi P, Leach JE, Tringe SG, Sa T, Singh BK. Plant–microbiome interactions: from community assembly to plant health. *Nat Rev Microbiol* 2020; **18**: 607–621.

20. Wei Z, Gu Y, Friman V-P, Kowalchuk GA, Xu Y, Shen Q, et al. Initial soil microbiome composition and functioning predetermine future plant health. *Sci Adv* 2019; **5**: eaaw075.

21. Andrić S, Rigolet A, Argüelles Arias A, Steels S, Hoff G, Balleux G, et al. Plant-associated Bacillus mobilizes its secondary metabolites upon perception of the siderophore pyochelin produced by a Pseudomonas competitor. *ISME J* 2022; **17:** 263–275

22. Andrić S, Meyer T, Rigolet A, Prigent-Combaret C, Höfte M, Balleux G, et al. Lipopeptide Interplay Mediates Molecular Interactions between Soil *Bacilli* and *Pseudomonads*. *Microbiol Spectr* 2021; **9**: e02038-21.

23. Molina-Santiago C, Vela-Corcía D, Petras D, Díaz-Martínez L, Pérez-Lorente AI, Sopeña-Torres S, et al. Chemical interplay and complementary adaptative strategies toggle bacterial antagonism and co-existence. *Cell Rep* 2021; **36**: 109449.

24. Molina-Santiago C, Pearson JR, Navarro Y, Berlanga-Clavero MV, Caraballo-Rodriguez AM, Petras D, et al. The extracellular matrix protects *Bacillus subtilis* colonies from *Pseudomonas* invasion and modulates plant co-colonization. *Nat Commun* 2019; **10**: 1919.

25. Pérez-Lorente AI, Molina-Santiago C, de Vicente A, Romero D. Sporulation Activated via σ W Protects *Bacillus* from a Tse1 Peptidoglycan Hydrolase Type VI Secretion System Effector. *Microbiol Spectr* 2023; e05045-22.

26. Charron-Lamoureux V, Haroune L, Pomerleau M, Hall L, Orban F, Leroux J, et al. Pulcherriminic acid modulates iron availability and protects against oxidative stress during microbial interactions. *Nat Commun* 2023; **14**: 2536.

27. Schindelin J, Arganda-Carreras I, Frise E, Kaynig V, Longair M, Pietzsch T, et al. Fiji: An open-source platform for biological-image analysis. *Nat Methods* 2012; **9**: 676–682.

28. Otsu N. A Threshold Selection Method from Gray-Level Histograms. *IEEE* 1979; **SMC-9**: 62–66.

29. Koo BM, Kritikos G, Farelli JD, Todor H, Tong K, Kimsey H, et al. Construction and Analysis of Two Genome-Scale Deletion Libraries for *Bacillus subtilis*. *Cell Syst* 2017; **4**: 291–305.

30. Zobel S, Benedetti I, Eisenbach L, De Lorenzo V, Wierckx N, Blank LM. Tn7-Based Device for Calibrated Heterologous Gene Expression in *Pseudomonas putida*. *ACS Synth Biol* 2015; **4**: 1341–1351.

31. Kiesewalter HT, Lozano-Andrade CN, Wibowo M, Strube ML, Maróti G, Snyder D, et al. Genomic and Chemical Diversity of Bacillus subtilis Secondary Metabolites against Plant Pathogenic Fungi. *mSystems* 2021; **6**: e00770-20.

32. Wick RR, Judd LM, Cerdeira LT, Hawkey J, Méric G, Vezina B, et al. Trycycler: consensus long-read assemblies for bacterial genomes. *Genome Biol* 2021; **22**: 1–17.

33. Wick RR, Judd LM, Gorrie CL, Holt KE. Unicycler: Resolving bacterial genome assemblies from short and long sequencing reads. *PLoS Comput Biol* 2017; **13**: e1005595.

34. Parks DH, Imelfort M, Skennerton CT, Hugenholtz P, Tyson GW. CheckM: Assessing the quality of microbial genomes recovered from isolates, single cells, and metagenomes. *Genome Res* 2015; **25**: 1043–1055.

35. Alanjary M, Steinke K, Ziemert N. AutoMLST: An automated web server for generating multi-locus species trees highlighting natural product potential. *Nucleic Acids Res* 2019; **47**: W276–W282.

36. Meier-Kolthoff JP, Göker M. TYGS is an automated high-throughput platform for state-of-the-art genome-based taxonomy. *Nat Commun* 2019; **10**: 2182.

37. Schwengers O, Jelonek L, Dieckmann MA, Beyvers S, Blom J, Goesmann A. Bakta: Rapid and standardized annotation of bacterial genomes via alignment-free sequence identification. *Microb Genom* 2021; **7**: 000685.

38. Tonkin-Hill G, MacAlasdair N, Ruis C, Weimann A, Horesh G, Lees JA, et al. Producing polished prokaryotic pangenomes with the Panaroo pipeline. *Genome Biol* 2020; **21**: 180.

39. Bray NL, Pimentel H, Melsted P, Pachter L. Near-optimal probabilistic RNA-seq quantification. *Nat Biotechnol* 2016; **34**: 525–527.

40. Pertea M, Pertea G. GFF Utilities: GffRead and GffCompare. *F1000Res* 2020; **9**: 1–19.

41. Love MI, Huber W, Anders S. Moderated estimation of fold change and dispersion for RNA-seq data with DESeq2. *Genome Biol* 2014; **15**: 550.

42. RStudio Team. RStudio: Integrated Development for R. 2019. Boston, MA.

43. R Core Team. R: A language and environment for statistical computing. 2021. Vienna, Austria.

44. Wickham H, Averick M, Bryan J, Chang W, McGowan L, François R, et al. Welcome to the Tidyverse. *J Open Source Softw* 2019; **4**: 1–6.

45. Cantalapiedra CP, Herņandez-Plaza A, Letunic I, Bork P, Huerta-Cepas J. eggNOG-mapper v2: Functional Annotation, Orthology Assignments, and Domain Prediction at the Metagenomic Scale. *Mol Biol Evol* 2021; **38**: 5825–5829.

46. Kanehisa M, Sato Y, Kawashima M. KEGG mapping tools for uncovering hidden features in biological data. *Protein Science* 2022; **31**: 47–53.

47. Pedreira T, Elfmann C, Stülke J. The current state of *Subti*Wiki, the database for the model organism *Bacillus subtilis*. *Nucleic Acids Res* 2022; **50**: D875–D882.

48. Winsor GL, Griffiths EJ, Lo R, Dhillon BK, Shay JA, Brinkman FSL. Enhanced annotations and features for comparing thousands of *Pseudomonas* genomes in the *Pseudomonas* genome database. *Nucleic Acids Res* 2016; **44**: D646–D653.

49. Palmer A, Phapale P, Chernyavsky I, Lavigne R, Fay D, Tarasov A, et al. FDR-controlled metabolite annotation for high-resolution imaging mass spectrometry. *Nat Methods* 2016; **14**: 57–60.

50. Miethke M, Klotz O, Linne U, May JJ, Beckering CL, Marahiel MA. Ferri-bacillibactin uptake and hydrolysis in *Bacillus subtilis*. *Mol Microbiol* 2006; **61**: 1413–1427.

51. Rizzi A, Roy S, Bellenger J-P, Beauregard PB. Iron Homeostasis in *Bacillus subtilis* Requires Siderophore Production and Biofilm Formation. *Appl Environ Microbiol* 2019; **85**: e02439-18.

52. Mhatre E, Troszok A, Gallegos-Monterrosa R, Lindstädt S, Hölscher T, Kuipers OP, et al. The impact of manganese on biofilm development of *Bacillus subtilis*. *Microbiology (United Kingdom)* 2016; **162**: 1468–1478.

53. Shemesh M, Chaia Y. A combination of glycerol and manganese promotes biofilm formation in *Bacillus subtilis* via histidine kinase KinD signaling. *J Bacteriol* 2013; **195**: 2747–2754.

54. Kimura T, Kobayashi K. Role of glutamate synthase in biofilm formation by *Bacillus subtilis*. *J Bacteriol* 2020; **202**: e00120-20.

55. Hassanov T, Karunker I, Steinberg N, Erez A, Kolodkin-Gal I. Novel antibiofilm chemotherapies target nitrogen from glutamate and glutamine. *Sci Rep* 2018; **8**: 7097.

56. Steingard CH, Pinochet-Barros A, Wendel BM, Helmann JD. Iron homeostasis in *Bacillus subtilis* relies on three differentially expressed efflux systems. *Microbiology (United Kingdom)* 2023; **169**: 001289.

57. Cheng X, de Bruijn I, van der Voort M, Loper JE, Raaijmakers JM. The Gac regulon of *Pseudomonas fluorescens* SBW25. *Environ Microbiol Rep* 2013; **5**: 608–619.

58. Moon CD, Zhang XX, Matthijs S, Schäfer M, Budzikiewicz H, Rainey PB. Genomic, genetic and structural analysis of pyoverdine-mediated iron acquisition in the plant growth-promoting bacterium *Pseudomonas fluorescens* SBW25. *BMC Microbiol* 2008; **8**: 7.

59. Powers MJ, Sanabria-Valentín E, Bowers AA, Shank EA. Inhibition of cell differentiation in *Bacillus subtilis* by *Pseudomonas protegens*. *J Bacteriol* 2015; **197**: 2129–2138.

60. Pelchovich G, Omer-Bendori S, Gophna U. Menaquinone and iron are essential for complex colony development in *Bacillus subtilis*. *PLoS One* 2013; **8**: e79488.

61. Arnaouteli S, Bamford NC, Stanley-Wall NR, Kovács ÁT. *Bacillus subtilis* biofilm formation and social interactions. *Nat Rev Microbiol* 2021; **19**: 600–614.

62. Toska J, Ho BT, Mekalanos JJ. Exopolysaccharide protects *Vibrio cholerae* from exogenous attacks by the type 6 secretion system. *PNAS* 2018; **115**: 7997–8002.

63. Rosenberg G, Steinberg N, Oppenheimer-Shaanan Y, Olender T, Doron S, Ben-Ari J, et al. Not so simple, not so subtle: The interspecies competition between *Bacillus simplex* and *Bacillus subtilis* and its impact on the evolution of biofilms. *NPJ Biofilms Microbiomes* 2016; **2**: 15027.

64. Lloyd DP, Allen RJ. Competition for space during bacterial colonization of a surface. *J R Soc Interface* 2015; **12:** 20150608.

65. Jautzus T, van Gestel J, Kovács ÁT. Complex extracellular biology drives surface competition during colony expansion in *Bacillus subtilis*. *ISME Journal* 2022; **16**: 2320–2328.

66. Frangipani E, Visaggio D, Heeb S, Kaever V, Cámara M, Visca P, et al. The Gac/Rsm and cyclic-di-GMP signalling networks coordinately regulate iron uptake in *Pseudomonas aeruginosa*. *Environ Microbiol* 2014; **16**: 676–688.

67. Peng J, Chen G, Xu X, Wang T, Liang H. Iron facilitates the RetS-Gac-Rsm cascade to inversely regulate protease IV (piv) expression via the sigma factor PvdS in *Pseudomonas aeruginosa*. *Environ Microbiol* 2020; **22**: 5402–5413.

68. Zhang B, Zhang Y, Liang F, Ma Y, Wu X. An Extract Produced by *Bacillus* sp. BR3 Influences the Function of the GacS/GacA Two-Component System in *Pseudomonas syringae* pv. *tomato* DC3000. *Front Microbiol* 2019; **10**: 2005.

69. Sobrero PM, Valverde C. Comparative Genomics and Evolutionary Analysis of RNA-Binding Proteins of the CsrA Family in the Genus *Pseudomonas*. *Front Mol Biosci* 2020; **7**: 127.

70. Lapouge K, Schubert M, Allain FHT, Haas D. Gac/Rsm signal transduction pathway of γ-proteobacteria: From RNA recognition to regulation of social behaviour. *Mol Microbiol* 2008; **67**: 241–253.

71. Wang BX, Wheeler KM, Cady KC, Lehoux S, Cummings RD, Laub MT, et al. Mucin Glycans Signal through the Sensor Kinase RetS to Inhibit Virulence-Associated Traits in *Pseudomonas aeruginosa*. *Current Biology* 2021; **31**: 90–102.

72. Broder UN, Jaeger T, Jenal U. LadS is a calcium-responsive kinase that induces acute-to-chronic virulence switch in *Pseudomonas aeruginosa*. *Nat Microbiol* 2016; **2**: 16184.

73. Humair B, González N, Mossialos D, Reimmann C, Haas D. Temperature-responsive sensing regulates biocontrol factor expression in *Pseudomonas fluorescens* CHA0. *ISME Journal* 2009; **3**: 955–965.

74. Oliveira F, Rohde H, Vilanova M, Cerca N. The Emerging Role of Iron Acquisition in Biofilm-Associated Infections. *Trends Microbiol* 2021; **29**: 772–775.

75. Loper JE, Buyer JS. Siderophores in Microbial Interactions on plant surfaces. *Molecular Plant-Microbe Interactions* 1991; **4**: 5–13.

76. Raaijmakers JM, Van Der Sluis L, Koster M, Bakker PAHM, Weisbeek PJ, Schippers B. Utilization of heterologous siderophores and rhizosphere competence of fluorescent *Pseudomonas* spp. *Can J Microbiol* 1995; **41**: 126–135.

77. Yu X, Ai C, Xin L, Zhou G. The siderophore-producing bacterium, Bacillus subtilis CAS15, has a biocontrol effect on Fusarium wilt and promotes the growth of pepper. *Eur J Soil Biol* 2011; **47**: 138–145.

78. Zeriouh H, de Vicente A, Pérez-García A, Romero D. Surfactin triggers biofilm formation of *Bacillus subtilis* in melon phylloplane and contributes to the biocontrol activity. *Environ Microbiol* 2014; **16**: 2196–2211.